Improvement of Malignant Glioma Treatment

Preclinical evaluation of adenoviral gene therapy and PRRT

The described research in this thesis was performed at the Departments of Nuclear Medicine and Neurology, Erasmus MC, Rotterdam, The Netherlands.

ISBN: 978-90-8559-327-0

© 2007 S.M. Verwijnen

All rights reserved. No part of this thesis may be reproduced, stored in a retrieval of any nature, or transmitted in any form by any means, electronic, mechanical, photocopying, recording or otherwise, without the permission of the author.

Printed by: Optima Grafische Communicatie, Rotterdam, The Netherlands.
Cover: R. Nusselder, S. van Dijk and Optima

Improvement of Malignant Glioma Treatment:

Preclinical evaluation of adenoviral gene therapy and PRRT

Verbeteren van de behandeling van maligne gliomas:

Pre-klinische evaluatie van adenovirale gentherapie en PRRT

Proefschrift

ter verkrijging van de graad van doctor aan de
Erasmus Universiteit Rotterdam
op gezag van de rector magnificus

Prof.dr. S.W.J. Lamberts
en volgens besluit van het College voor Promoties.

De openbare verdediging zal plaatsvinden op
woensdag 12 december 2007 om 15.45 uur

door

Suzanne Martine Verwijnen
geboren te Dordrecht

ERASMUS UNIVERSITEIT ROTTERDAM

Promotiecommissie

Promotoren	Prof.dr.ir. M. de Jong
	Prof.dr. P.A.E. Sillevis Smitt
Overige leden	Prof.dr. E.P. Krenning
	Prof.dr. R.C. Hoeben
	Prof.dr. P.H. Elsinga

"Als we wisten wat we deden, heette het geen onderzoek"
Albert Einstein (1879-1955)

Contents

Chapter 1: Introduction

1.1 Aim and scope of the thesis 11

1.2 General introduction 19

1.3 Improvement strategies for peptide receptor scintigraphy and radionuclide therapy 37
M. de Visser, S.M. Verwijnen et al., in press CBR

Chapter 2: Molecular imaging of adenoviral gene transfer

2.1 Molecular imaging and treatment of malignant gliomas following adenoviral transfer of the Herpes Simplex virus-thymidine kinase gene and the somatostatin receptor subtype 2 gene 73
S.M. Verwijnen et al, CBR, 2004; 19(1):111-120

2.2 Molecular imaging after adenoviral gene transfer visualizes sst_2 and HSV1-tk expression 89
S.M. Verwijnen et al., submitted

2.3 Locoregional delivery of adenoviral vectors 111
M. ter Horst, S.M. Verwijnen et al., JNM, 2006;47:1-7

2.4 Directly radiolabeled adenoviruses show viral distribution *in vivo* following intratumoral injection. 127
S.M. Verwijnen et al., submitted

Chapter 3: Receptor targeting using radiolabeled peptides

3.1 Receptor expression on human brain tumor tissues 149
S.M. Verwijnen et al., submitted

3.2 Oral versus intravenous administration of lysine: equal effectiveness in reduction of renal uptake of [^{111}In-DTPA^{0}] octreotide 161
S.M. Verwijnen et al., JNM, 2005; 46 (12):2057-2060

Chapter 4: Radiation sensitivity of pancreatic tumor cells *in vitro*

4.1 Low dose rate irradiation by ^{131}I versus high dose rate external beam irradiation in the rat pancreatic tumor cell line CA20948 S.M. Verwijnen et al., CBR, 2004; 19(3):285-292 175

Chapter 5: Summary, general discussion and conclusions

5.1 Summary, general discussion and conclusions 193

5.2 Samenvatting en conclusies 205

List of abbreviations 219

Dankwoord 223

Curriculum Vitae 231

Publicatielijst 233

Color figures 235

1

Introduction

1.1 Aim and scope of the thesis

Glioblastoma multiforme (GBM) is the most aggressive type of malignant glioma (WHO grade 4). Patients suffering from a GBM have a median survival of less than a year after diagnosis despite the recent developments in neurosurgery, radiotherapy and chemotherapy. This poor prognosis has led to the investigation of new treatment modalities. Locoregional treatment modalities are potentially attractive for GBMs because these tumors are generally confined to the central nervous system and only rarely metastasize outside the nervous system. Examples of such locoregional treatment modalities are gene therapy and peptide receptor radionuclide therapy (PRRT).

As will be discussed in chapter 1.2, after successful gene therapy treatment experiments in animal models, the clinical results of GBM gene therapy have been disappointing, showing the need for improvement of this modality.

PRRT could also be beneficial for GBM patients since small radiolabeled peptide molecules can migrate from the injection site to the tumor, and target to their corresponding receptor on the cell membrane of these cells. At this moment, however, it is not clear which peptide receptors are expressed on human GBM tissues.

The goal of this thesis was to identify bottlenecks limiting the efficacy of glioma gene therapy using molecular imaging techniques. In addition, we explored the possibility of PRRT treatment for GBM patients.

Investigating Ad5.tk.sst$_2$ for glioblastoma imaging and treatment

Chapter 2 of this thesis investigates different aspects of the use of Ad5.tk.sst$_2$ for gene therapy of GBM in a preclinical setting. Ad5.tk.sst$_2$ is a genetically modified serotype 5 adenovirus, which is replication deficient due to the insertion of the HSV-tk and sst$_2$ genes in the E1 region of the genome (see figure 1). As will be shown in chapter 1.2, Ad5.tk.sst$_2$ can be used for infecting tumor cells, thereby expressing two transgenes in these cells: HSV-tk and sst$_2$ (see figure 2 and [1]). In **chapter 2.1**, we aimed to investigate expression of the viral genes after *in vitro* infection of several rat and human glioblastoma cell lines. We also compared uptake of the radiolabeled ligands ^{125}I-FIRU and [^{111}In-DOTA^{0},Tyr^{3}]octreotate used for detecting HSV-tk and sst$_2$ expression, respectively, in cells infected with Ad5.tk.sst$_2$.

As will be explained in chapter 1.2, molecular imaging techniques have become increasingly interesting for gene therapy modalities. Therefore, we aimed to image HSV-tk and sst$_2$ expression following Ad5.tk.sst$_2$ infection *in vivo* in U87MG-bearing mice (**chapter 2.2**). We again used FIRU, radiolabeled with ^{123}I, and octreotate, radiolabeled with ^{99m}Tc, for gene expression imaging with an animal SPECT/CT camera. We aimed to image simultaneous and longitudinal gene expression *in vivo*.

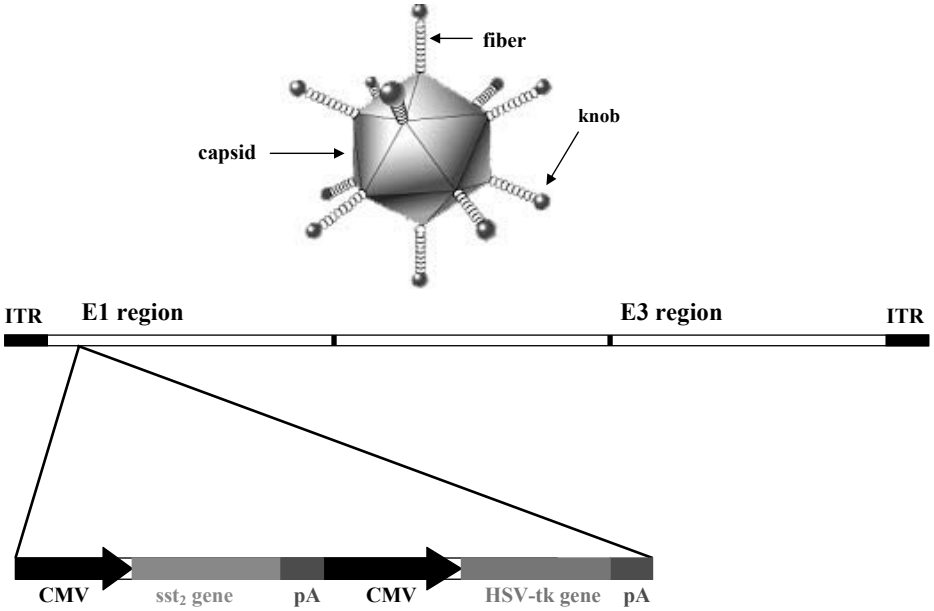

Figure 1: Construction of replication deficient Ad5.tk.sst_2 used in this thesis for GBM gene therapy. Both genes are under control of the constitutive cytomegalovirus (CMV) promoter. Figure adapted from [53].

In **chapter 2.3** we compared convection enhanced delivery (CED) with multiple injections (MI) and single injection (SI) to improve intratumoral biodistribution of adenoviral vectors in human U87MG glioblastoma tumor-bearing mice. It has been hypothesized that large molecules diffuse better through tumor tissue when they are infused slowly, compared to one or several bolus injections. We therefore injected replication-deficient Ad5.tk.sst_2 in U87MG using CED, MI or SI and investigated the transduced areas via sst_2 receptor expression in *ex vivo* autoradiographic images.

In addition to imaging gene expression, it would also be of interest to follow viral vectors directly after injection, rather than to wait until receptor expression has occurred. Therefore, Ad5.tk.sst_2 was radiolabeled with ^{99m}Tc using Isolink™, a carbonyl radiolabeling agent (Mallinckrodt Medical B.V.) (**chapter 2.4**). We investigated the infectivity of the virus after radiolabeling *in vitro* and *in vivo* in U87MG tumor cells. $^{99m}Tc(CO_3)$-Ad5.tk.sst_2 viruses were also imaged after *in vivo* tumor injection using gamma camera and animal SPECT/CT imaging techniques.

PRRT as treatment option for GBM patients

As mentioned, PRRT might be an interesting adjuvant treatment option for patients with GBM, which will especially be attractive when the radiolabeled peptide

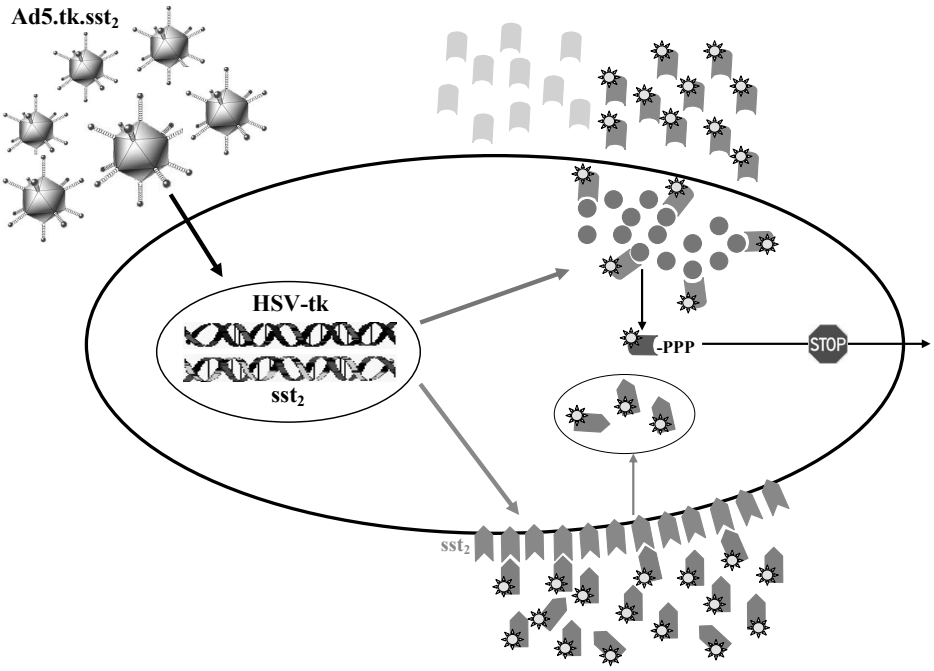

Figure 2: Schematic representation of the events following infection with Ad5.tk.sst_2. After entry of the virus into the host cell, the viral genome enters the nucleus where the genome is transcribed (arrow 1). HSV-tk enzymes (arrow 2) and somatostatin subtype 2 receptors (sst_2, arrow 3) are subsequently formed. Ganciclovir (GCV) or radiolabeled FIRU (*I-FIRU) molecules enter the cell and are phosphorylated by HSV-tk enzymes (arrow 4) and subsequently trapped in the cell (indicated by the STOP-sign). Radiolabeled octreotate binds the sst_2 receptor and is transported into the cell in a lysosome (arrow 5). Using FIRU or octreotate compounds radiolabeled with γ-emitting radionuclides enables the visualization of the viral infected cells. In addition, introduction of GCV or octreotate radiolabeled with a β-particle emitting radionuclide enables the treatment of these cells. Figure adapted from [54].

molecules could be local-regionally introduced into the tumor, as shown by Kneifel et al. [2]. We therefore examined in chapter 3 the receptor expression status of several samples of GBM, meningioma and metastatic lesions in the brain, all of human origin in a pilot study to identify one or more candidate receptor targets for PRRT (**chapter 3.1**). Samples of normal brain tissue were also investigated for receptor expression, since a high uptake of peptide analogs in background tissue would make PRRT less interesting.

As will be discussed in chapter 1.2, the kidneys are one of the dose-limiting organs in PRRT treatments using radiolabeled ss analogs conjugated with DTPA or DOTA, due to the renal clearance of these radiolabeled peptides. Damage to the kidneys can be avoided by the infusion of positively charged amino acids such as lysine and arginine. Ideally, a solution of lysine/arginine is administered to the patient prior to PRRT during a 4-10 hour infusion, which is a labor intensive procedure. In a

preclinical study we explored whether orally administered lysine could also reduce renal uptake of [^{111}In-DTPA^{0}]octreotide compared to intravenously injected lysine (**chapter 3.2**).

In **chapter 4** we investigated the radiation sensitivity of the rat pancreatic cell line CA20948. This cell line expresses a large number of different peptide receptors on the cell membrane (e.g. sst_2/sst_5, neurokinine 1 (NK-1), cholecystokinin 2 (CCK_2), gastrin releasing peptide (GRP)) and is therefore widely used in preclinical studies for PRS and PRRT. Response of tumor cells to treatment with radiolabeled peptides *in vitro* and *in vivo* is dependent on their radiosensitivity. Usually, radiosensitivity is measured using external beam radiotherapy (XRT). However, it is to be expected that the response after XRT is not representative for the response to treatment with radiolabeled peptides. Therefore, we compared the response of CA20948 *in vitro* after high-dose-rate XRT and lower-dose-rate radionuclide therapy (RT) using ^{131}I.

References

1. Zinn, K.R., Chaudhuri, T.R., Buchsbaum, D.J., Mountz, J.M. and Rogers, B.E. Simultaneous evaluation of dual gene transfer to adherent cells by gamma-ray imaging. *Nucl Med Biol*, 2001 28(2): 135-144.
2. Kneifel, S., Cordier, D., Good, S., Ionescu, M.C., Ghaffari, A., Hofer, S., *et al.* Local targeting of malignant gliomas by the diffusible peptidic vector 1,4,7,10-tetraazacyclododecane-1-glutaric acid-4,7,10-triacetic acid-substance p. *Clin Cancer Res*, 2006 12(12): 3843-3850.

1.2 General introduction

Molecular Imaging

Molecular imaging is a relatively new, multidisciplinary field, which gives a visual representation of biological processes at the (sub)cellular level in living organisms. Especially in the preclinical field molecular imaging is a very welcome new tool, while working with specialized animal imaging equipment. Previously, differences between pathological and normal tissue was assessed by identifying macro- and microscopic changes at physical, physiological or metabolic level, rather than showing molecular events playing a role in disease in intact animals. With the molecular imaging techniques performed these days in animal models, it is possible to:

- assess the functions of a protein/substance throughout the body, as compared to one organ or cell type only;
- show temporal and spatial biodistribution of a substance in an intact living organism;
- visualize functions and interactions of particular genes in a subject;
- image repetitively to determine changes or stability in one animal over time (longitudinal imaging);
- quantitatively assess the biological process under investigation, without necessarily obtaining *in vitro* or *ex vivo* data;
- shift data from the animal to the human situation more easily.

The images produced with animal imaging technologies display a virtual slice of the animal that identifies internal anatomical structures and/or information about the function of organs.

The roots of molecular imaging lie in nuclear medicine, since from early on this discipline used radiolabeled tracers injected into patients to show uptake or metabolism in specific organs. One example is the tumor visualization and treatment of patients with well-differentiated thyroid carcinoma: radioactive iodine, e.g. ^{123}I (emitting γ-rays) and ^{131}I (emitting high-energy β-particles), is specifically taken up by the thyroid after systemic injection. ^{125}I is used to show (pathological) uptake in the thyroid, while the β-particles of ^{131}I induces damage to the cancer cells, which leads to a decrease in tumor mass [1, 2].

After the discovery of overexpression of somatostatin receptors (sst) on various tumor types in the 1980s [3], it was found that these tumors could be visualized after systemic injection of radiolabeled sst analogs [4]. Visualization or peptide receptor scintigraphy (PRS) is being performed using peptide analogs radiolabeled with γ-emitting radionuclides (e.g. ^{99m}Tc, ^{111}In, ^{125}I), which can be detected using planar gamma cameras or single photon emission computed tomography (SPECT) instrumentation. When radiolabeled with β-particle emitting radionuclides (e.g. ^{90}Y, ^{177}Lu, ^{64}Cu, ^{188}Re), these peptides can be used for peptide receptor radionuclide therapy

(PRRT), which is very successful for the treatment of neuroendocrine tumors and also other tumor types (reviewed in chapter 1.3).

Advantages of SPECT include the use of radionuclides with longer half-lives, which allows to follow processes with slow kinetics [5]. In addition, these radionuclides are widely available since they are not required to be produced on site, and they are relatively cheap. Another advantage is that SPECT radionuclides have a broad energy spectrum and therefore multiple tracers can be used simultaneously [5].

Another nuclear medicine technique is positron emission tomography (PET), which detects positron-emitting radionuclides (e.g. ^{11}C, ^{15}O, ^{18}F, ^{68}Ga, ^{124}I). The most popular tracer for PET is [^{18}F]fluoro-2-deoxyglucose (^{18}FDG), which demonstrates elevated glucose consumption by (tumor) cells, and is used clinically for the accurate staging and restaging of cancer, planning of radiotherapy, and predicting response or lack of response in the early stages of treatment. One of the advantages of PET over SPECT imaging is that PET-radionuclides can be used for imaging of many compounds without altering the chemical structure. For example, $H_2{}^{15}O$ is chemically identical to H_2O and will therefore not behave differently after injection. For SPECT this is only possible when using iodine labeled compounds (e.g. ^{123}I, ^{125}I, ^{131}I). Other SPECT-radionuclides, such as ^{111}In and ^{177}Lu, require labeling via a chelator, thereby changing the chemical structure of the compound and subsequently changing its behavior *in vivo* [6]. A second advantage of PET imaging compared to SPECT is the relatively higher sensitivity and resolution, although with "pinhole" SPECT the spatial resolution is increased to the sub-millimeter range [7]. Unfortunately, the improved resolution achieved with pinhole SPECT compromised the sensitivity. A third advantage of PET is the better possibility to quantify radioactivity in a region of interest.

In this thesis, computed tomography was used for anatomical imaging of animals. CT images are obtained when tissues differentially absorb X-rays which pass through the body [8]. CT images acquire anatomical information with high resolution, in a relatively short acquisition time. Unfortunately, CT has a relatively poor soft tissue contrast, making it necessary to administer contrast agents to define specific organs. At present, CT is not a molecular imaging technique by itself, but is used for anatomical information in complementary to other imaging modalities. The relatively low costs and short acquisition time are the main advantages of this technique. However, the radiation dose to the animal might be considerable, which will limit longitudinal imaging of an animal.

Besides SPECT, PET and CT, other molecular imaging techniques include optical imaging (OI), magnetic resonance imaging (MRI) and ultrasonography (US) and nowadays these are also highly integrated in (pre)clinical investigations [9-12]. These techniques were not used in the experiments presented in this thesis and

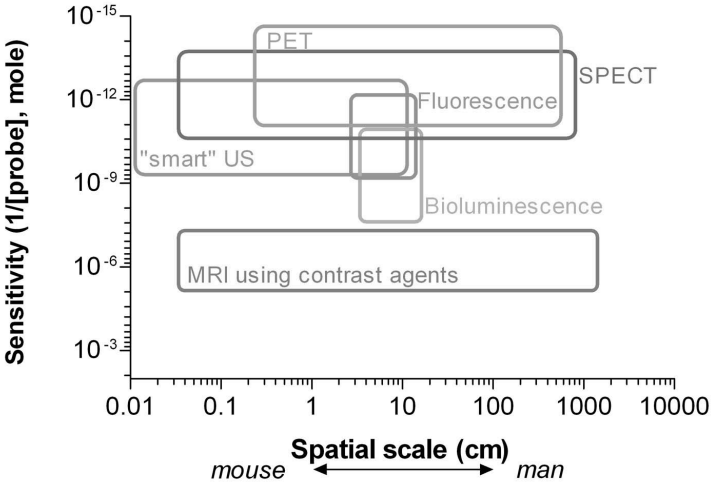

Figure 1: The sensitivity and spatial resolution of molecular imaging modalities (adapted from [5]). Sensitivity refers to the amount of probe that is required *in vivo* to bring forth a high enough signal. "Smart" US refers to high frequency ultrasound using contrast agents.

will therefore not be discussed. Each molecular imaging modality is characterized by different resolutions and sensitivities for imaging morphology or functions in a living subject. Combinations of imaging modalities that integrate the strengths of two or more modalities may improve diagnostics, therapeutic monitoring, and preclinical research. Figure 1 shows the spatial resolution and the sensitivity for tracer detection of each molecular imaging modality.

Gene Therapy

Gene therapy can be defined as the introduction of nucleic acids into cells with the intention to alter the course of a medical condition or disease. In most cases, these nucleic acids are DNA molecules encoding proteins. Viral and non-viral vehicles form the two major means, by which these DNA molecules are entered into a cell. Viral vectors have the advantage that they are designed to transfer their genetic material into human cells. However, they can also trigger an immune response, making them less interesting for repeated administrations. Certain viruses integrate their genetic material into the host genome resulting in stable gene transfer and long-term gene expression, upon cell division. In addition, when the transfected cell divides, it passes this new genetic material over to its descendants. However, integration of viral DNA into the host genome can also cause deleterious side effects such as insertional oncogenesis [13]. Non-viral vectors are less immunogenic and do

Table 1: Main features, advantages and disadvantages of various viral and non-viral vectors for gene therapy of gliomas.

Viral vector	Main features	Advantage / Disadvantage
Adenovirus (AV)	double-stranded DNA diameter: 80-90 nm 10 kb transgene cap.	Advantage: infect both dividing and quiescent cells with high efficiency; no integration into the host genome (no genetic alteration) Disadvantage: elicits a strong immune response; limited duration of transgene expression
Retrovirus (RV)	double-stranded RNA diameter: 100 nm 7.5 kb transgene cap.	Advantage: low immunogenicity Disadvantage: random integration into the host genome; insertional oncogenesis; use of packaging cells; only transduction of dividing cells
Adeno-associated virus (AAV)	single-stranded DNA diameter: 20 nm 4.7 kb transgene cap.	Advantage: transduction of non-dividing cell; sustained gene expression; low immune response (non-pathogenic); site-specific integration into host genome (chromosome 19) Disadvantage: limited transgene capacity; low transduction efficiency depending on cell type; difficult to produce
Herpes Simplex virus (HSV)	double-stranded DNA diameter: 125 nm 30 kb transgene cap.	Advantage: high sensitivity to antiherpic agents (provides safety); can be produced with high titers; large transgene capacity; no integration into the host genome Disadvantage: genetic manipulation of the virus is difficult; high immunogenicity in patients
Reovirus	double-stranded RNA diameter: 60 nm	Advantage: only replicates in cells in which a Ras signaling pathway is activated, no integration into host genome Disadvantage: genetic manipulation of the virus is difficult
Lentivirus (LV)	double-stranded RNA diameter: 80-100 nm 30 kb transgene cap	Advantage: high-efficiency infection of dividing and non-dividing cells; long-term stable expression Disadvantage: Random integration into the host genome; insertional oncogenesis; recombination resulting in replication competent lentivirus
Non-viral vector	**Main features**	**Advantage / Disadvantage**
Naked DNA and Cationic Lipids	DNA molecules delivered by direct injection (naked DNA) or packed in lipids.	Advantage: simple large scale production ; no limit to the size of genes to be delivered; low host immunogenicity and toxicity; no generation of infectious form or mutagenic changes Disadvantage: low *in* vivo transduction efficiency resulting in low levels of transgene expression

not integrate into the host genome; however, the gene transfer efficiency is much lower compared to viral vectors, especially *in vivo*. Table 1 shows an overview of the different viral and non-viral vectors currently applied and their advantages and disadvantages when used in glioma gene therapy modalities.

After a vector has been designed, constructed and produced in large quantities, the subsequent gene transfer can be performed *ex vivo* (cells are removed to be modified and transplanted back in the recipient) or *in vivo* (direct injection of the vector into the recipient).

As can be seen from figure 2, two-thirds of all clinical gene therapy trials worldwide aim to treat malignant diseases. In these trials, a wide variety of cancer types are treated, including melanoma (15%), prostate cancer (10%), breast cancer (7%),

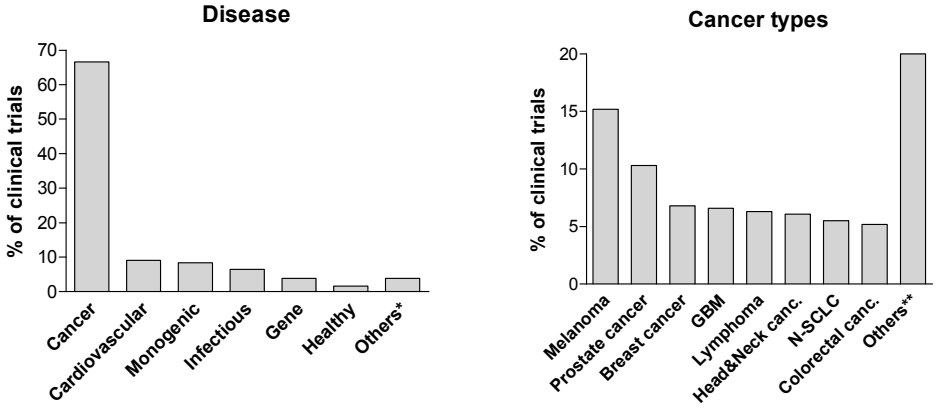

Figure 2: The world wide clinical gene therapy trials from 1989 to 2007 divided by disease, cancer type, vector system, gene type, transferred gene and country in which the trial was conducted. This figure is adapted from http://www.wiley.co.uk/genmed/clinical/, which was last updated in January 2007.

GBM (7%) and lymphoma (6%). Gene therapy trials for GBM were conducted with retroviruses (RV) in 40% of the cases, with herpes simplex virus (HSV) in 23% and in 17% with adenoviruses (AV), while 12% was performed with non-viral vectors, such as naked DNA and lipids. The most widely applied gene in GBM directed gene therapy trials include Herpes Simplex Virus-thymidine kinase (HSV-tk); 38% of these trials were conducted with the use of this gene. The application of HSV-tk will be further discussed in chapter 1.3.

Although there are many publications of successful *in vivo* gene therapy experiments for cancer treatment in animal models, the translation to the clinic remains more complex than initially anticipated. The efficiency of gene therapy for cancer treatment in the clinic needs to be improved, e.g. by the development of tissue specific vectors, prolonging the duration of gene expression, increasing distribution of vectors and prodrugs in the tumor and decreasing immunogenicity of the vector [14]. These improvement strategies will be discussed in more detail in the paragraph "Viral gene therapy for GBM".

Clinical gene therapy trials have generated the need for *in vivo* imaging of both vector and target (e.g. cellular receptor used for viral binding and/or entry) distribution, as well as *in vivo* imaging of the resulting transgene expression. Molecular imaging can be highly interesting to visualize the location, spread and persistence of a vector in animal experiments as well as in patients. In addition, these techniques allow the non-invasive follow-up of gene expression over time.

Glioblastoma Multiforme

Primary brain tumors are a diverse group of neoplasms arising from different cells of the central nervous system (CNS). Gliomas present histological features of glial cells, such as astrocytes, oligodendrocytes, and ependymal cells. Malignant or high-grade diffuse gliomas are classified by the World Health Organization (WHO) as either grade III anaplastic astrocytoma, anaplastic oligodendroglioma, or anaplastic oligoastrocytoma, or as grade IV glioblastoma multiforme (GBM). At least 80% of malignant gliomas are GBMs, the most aggressive type of primary brain tumor.

The annual incidence of malignant glioma varies between 3-7 per 100,000 people per year [15, 16]. Although brain tumors account for only 2% of all cancers and are about one-fifth as common as breast or lung cancer, these neoplasms result in a disproportionate share of cancer morbidity and mortality [17]. The overall median survival from time of diagnosis in GBM patients is less then one year and fewer than 5% of the patients survive five years or more [18]. A recent randomized trial, comparing the survival of GBM patients treated with radiotherapy alone or radiotherapy with adjuvant temozolomide chemotherapy, showed that the two-year survival in this selected group of GBM patients improved significantly from 10.4% to 26.5%, respectively [19]. In addition, minimal additional toxicity was observed.

GBMs are diffusely infiltrative tumors that display invasion into the cerebral parenchyma. Their highly infiltrative nature prevents curative surgical resection and complicates effective delivery of many kinds of therapy. However, metastasis of GBM outside the CNS is extremely rare and despite their infiltrative growth pattern, 80% of GBMs recur within a 2-3 cm margin from the original tumor. The poor prognosis, treatment outcome and low overall survival show the need for new treatment modalities for GBMs. The non-metastatic growth pattern and high rate of local recurrences of GBM has led to the development and investigation of new loco-regional treatment strategies, including gene therapy and convection enhanced delivery of immunotoxins [20, 21].

Viral gene therapy for GBM

GBM is an attractive tumor type for viral gene therapy due to the poor prognosis of the patients and the almost complete lack of distant metastases. Roughly 7% of the clinical gene therapy trials that were conducted between 1989 and 2007 included GBM (see figure 2b). Many different vectors and transgenes have been used for the treatment of malignant gliomas in phase I and II clinical trials world wide, as depicted in figure 3. An overview of the gene therapy trials in GBM patients and

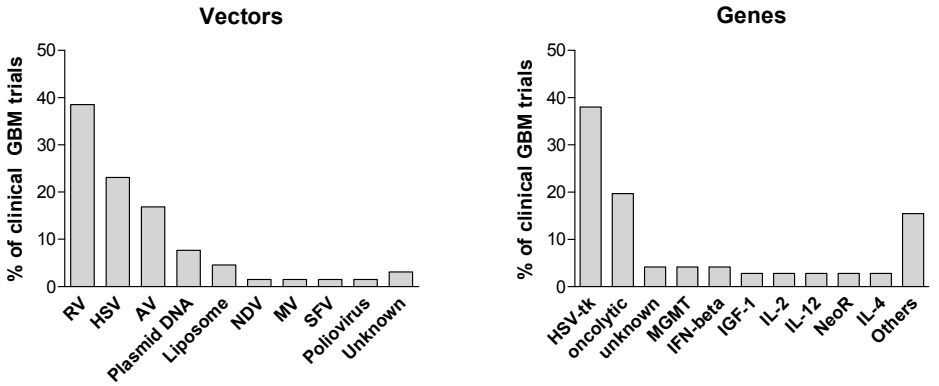

Figure 3: Vectors and genes used in clinical trials for GBM patients. This figure is adapted from http://www.wiley.co.uk/genmed/clinical/.

their results is presented in table 2. The most frequently used vector and transgene in these trials were RV and HSV-tk, respectively. In addition, oncolytic or (conditionally) replicating viruses, including HSV, AV and reovirus, are becoming increasingly important [22].

RV vectors were the first to be developed and investigated in clinical gene therapy trials for GBM. An important finding of these phase I-II trials was that the intratumoral administration of RV producing cells was safe [23-25]. A randomized phase III trial was then conducted in 248 patients with newly diagnosed GBM [26]. Patients received either standard therapy (surgery and radiotherapy) or standard therapy plus additional HSV-tk gene transfer. Unfortunately, the addition of gene therapy to standard treatment did not improve progression-free or overall survival time.

Several investigators reported on the use of AV vectors in clinical phase I and II gene therapy trials for GBM patients [27-31]. They all showed that AV gene therapy was well tolerated and safe, although Trask et al. showed that the vector dose should not exceed $2x10^{11}$ viral particles (VP). In two patients treated with $2x10^{12}$ VP significant toxicity was observed, although it was not clear whether other factors, such as age, bilateral tumor and possible intra-ventricular injection attributed to the risk for toxicity [27]. Sandmair and co-workers reported a more than 4-fold increase in anti-adenovirus antibodies in four patients receiving adenovirus, indicating an immune response against the adenoviral particles [28].

A statistically significant survival improvement with AV vectors encoding HSV-tk (Adtk) was seen in the studies of Sandmair et al. and Immonen et al. [28, 31]. The latter was a randomized phase II study treating both primary and recurrent malignant gliomas [31]. Adtk treatment produced a clinically and statistically significant increase in mean survival from 39 to 71 [31]. Thus far, no phase III randomized trial has been conducted with AV vectors.

Table 2: Results reported in clinical trials of gene therapy in patients with GBM.

Author, year	Trial	Vector	Gene	Viral dose	Pts	Response	Surv. (m)
Ram, 1997	I-II	nr-RV	tk	up to 10^9 VPC	15	5 of 15	8 (med)
Klatzmann, 1998	I-II	nr-RV	tk	$6x10^7$-$6x10^8$ VPC	12	4 of 11 (at 4m)	7 (med)
Shand, 1999	I-II	nr-RV	tk	$2x10^7$ VPC	48	6 of 48 (at 6m)	8.6 (med)
Packer, 2000	I	nr-RV	tk	10^8-10^9 VPC	12	1 of 11 (at 24m)	n.s.
Harsh, 2000	I	nr-RV	tk	10^6 VPC (4x)	5	0 of 5	8 (med)
Rainov, 2000	III	nr-RV	tk	up to 10^9 VPC	124	n.s.	12.0 (med)
		std*	-	-	124	n.s.	11.6 (med)
Prados, 2003	I-II	nr-RV	tk	up to 10^9 VPC	30	1 of 30	8.4 (med)
Colombo, 2005	I-II	nr-RV	tk/IL-2		12	6 of 12	25% (12m)
Trask, 2000	I	nr-AV	tk	up to $2x10^{12}$ PFU	13	n.s.	4 (med)
Smitt, 2003	I	nr-AV	tk	up to $4.6x10^{11}$ VP	14	0 of 14	4 (med)
Germano, 2003	I	nr-AV	tk	up to $9x10^{11}$ VP	11	2 of 11	13.5 (mn)
Immonen, 2004	III	nr-AV	tk	$3x10^{10}$ PFU	17	n.s.	14.4
		control	-	-	19	n.s.	8.7
Lang, 2003	I	nr-AV	p53	up to $3x10^{12}$ VPC	15	5 of 15	9.9 (med)
Sandmair, 2000	I-II	nr-RV	tk	up to$2x10^9$ VPC	7	n.s.	7 (med)
		nr-AV	tk	up to $6x10^{10}$ VPC	7	3 of 7 SD	15 (med)
		control	LacZ	-	7	-	8 (med)
Chiocca, 2004	I	onc. AV	-	10^7-10^{10} PFU	24	0 of 24	4.9 (med)
Markert, 2000	I	onc. HSV	G207	up to $3x10^9$ PFU	21	0 of 21	15.9 (mn)
Rampling, 2000	I	onc. HSV	1716	10^3-10^5 PFU	9	2 of 9	14-24 (4 pts)
Papanastassiou, 2002	II	onc. HSV	1716	10^5 PFU	12	n.s.	n.s.
Harrow, 2004	II	onc. HSV	1716	10^5 PFU	12	2 of 12	15-22 (3 pts)
Freeman, 2006	I-II	onc. NDV	OV001	10^8-10^{10} IU/day, 5 days/wk, 1-2 wks	11	1 of 11	7.4 (med)
Jacobs, 2001	-	liposome	tk	-	5	1 of 5	n.s.

* standard therapy.

Abbreviations used: nr = non-replicating, RV = retrovirus, AV = adenovirus, onc. = oncolytic, HSV = herpes simplex virus, NDV = Newcastle disease virus, tk = HSV-thymidine kinase, LacZ = β-galactosidase, VPC = viral producer cells, PFU = plaque forming units, VP = viral particles, IU = infectious units, wk = week, pts = (number of) patients, resp. = response, m = months, SD = stable disease, surv. = survival, med = median, n.s. = not stated, mn = mean, rel. adv. events = related adverse events.

Note: all reports used intratumoral injection.

The interest in the use of oncolytic viral vectors has recently increased. Most oncolytic or replicating vectors in clinical trials have been engineered to replicate selectively in dividing cells (e.g. the HSV mutant HSV1716) or cancer cells (e.g. the AV ONYX-015). This enhances the dose administered to the tumor and infected cells are lysed, thereby eliminating the tumor [32-36]. The results of clinical trials showed that oncolytic gene therapy was safe and well tolerated. Some investigators report evidence that suggest an anti-tumor activity in some patients [33-35].

Despite favorable responses in individual patients, it is clear from the current clinical gene therapy trials that there are a number of obstacles limiting the success of gene therapy in GBM patients. These obstacles include poor spatial distribution of the viral vector following injection into the tumor, poor *in vivo* transduction of glioma cells, poor efficacy of therapeutic genes and/or gene/prodrug combinations, and the host immune response elicited by many viral vectors.

Many studies showed that direct injection of viral particles into the tumor results in a limited viral spread, mostly 5 mm from the injection tract [23, 26, 28, 37, 38] (see table 2). To improve the distribution of the gene therapy vectors in the tumor, manual vector administration can be replaced by convection enhanced delivery (CED) [39-41]. Voges et al. treated eight patients with a HSV-tk expressing liposome that was delivered with CED [42]. They found that intracerebral infusion of large volumes of a liposomal vector is well tolerated with minor side effects. Unfortunately, in the majority of the patients the effects of HSV-tk/GCV treatment was restricted to a relatively small volume around the infusion sites, not indicating improved spatial distribution. Moreover, it was also found that the diffusion of GCV into the tumor varied according to the permeability of the blood-tumor barrier. Simultaneous administration of GCV with a blood-tumor barrier modifier such as the selective B2 bradykinin agonist RMP-7 may result in a significantly higher intra-tumoral prodrug concentration and the subsequent elimination of persisting tumor cells [26].

Another approach to improve the penetration into the tumor is the use of oncolytic or replicating viral vectors, such as HSV, AV and reovirus. These conditionally replicating viruses will induce lysis of glioma cells, while no replication is seen in normal brain tissue [22]. Following glioma cell lysis, the replication-competent viruses could potentially reach distant tumor cells in the infiltrated brain, which were not reached directly after viral inoculation. The effects of oncolytic viruses were examined in clinical trials and were found to be safe [33-36, 43]. Papanastassiou et al. assessed replication of the oncolytic vector HSV1716 after infection of GBM in twelve patients and found replication without causing toxicity [36]. Harrow and co-workers suggested that the injection of the same virus (HSV1716) during resection might increase inflammation events and therefore it might be preferred to perform infection several days post-surgery. However, this would result in two intervention procedures, which is also not favorable for these patients [34]. Chiocca et al. could not demonstrate anti-tumor efficacy using a replication-conditional adenovirus, ONYX-015 [32]. In contrast, a study by Freeman et al. using oncolytic Newcastle disease virus in recurrent GBM showed a complete response in one patient, although this patient became progressive again three months after the complete disappearance of the tumor [33].

Little is known about the actual transduction efficiency in human GBMs, which is rather important since efficient gene delivery is a prerequisite for successful treatment

when performing gene therapy. In the study of Puumalainen and co-workers the gene transfer efficiency varied between <0.01 and 4% with retroviruses and between <0.01 and 11% with adenoviruses [37]. Many strategies have been developed to retarget viruses to receptors that are abundantly and selectively expressed on glioma cells. One approach is the genetic modification of the AV fiber gene to enhance uptake in glioblastoma cells [44].

Finally, the efficiency of gene therapy may be improved by combining different therapeutic genes: For example interleukin 2 (IL-2) in combination with HSV-tk [45] and the combination sst_2 and HSV-tk [46]. In the first paradigm the therapeutic outcome might be enhanced by the proved immunological response to the tumor. The second concept allows prodrug therapy combined with radionuclide therapy using peptide analogs with high affinity for sst_2. In addition, improved prodrug-activating genes with freely diffusible metabolites, such as cytosine deaminase (CD)/5-fluorocytosine (5-FU) system, may offer an advantage over HSV-tk/GCV [26, 47]. It is likely that viral gene therapy in conjunction with other treatments, such as chemotherapeutics and radiation therapy would demonstrate greater efficacy over treatment with viral agents alone [22, 48].

Molecular imaging in gene therapy for GBM

Non-invasive imaging of gene expression will give the possibility to quantify transgene expression, which may predict treatment outcome, as well as gain insight into vector distribution, extent and duration of gene expression. At this moment, there is an inability to non-invasively measure transduction levels or functional enzyme activity in order to correlate this with clinical changes after GCV treatment. Jacobs et al. published a study in which five patients enrolled in a gene therapy procedure using a liposomal vector carrying a HSV-tk gene [49]. They performed a dynamic PET scan using ^{124}I-FIAU, a radioactive nucleoside analog, which is trapped in the same manner by HSV-tk as GCV. They made scans before and after vector application, to investigate specific FIAU-accumulation in the brain of these patients. After vector infusion, GCV was administered and treatment responses were recorded by MRI images as well as PET using ^{18}F-FDG and ^{11}C labeled methionine, which is used to detect solid brain tumors [50]. They showed a specific HSV-tk-related uptake of FIAU at the site of injection in one patient, who also showed a response to treatment. Unfortunately, in the other patients no increased FIAU uptake could be measured; they also failed to respond to treatment. This study shows that non-invasive imaging of HSV-tk gene expression is feasible and highly desirable in order to assess gene transfer. Dempsey et al. reported on eight GBM patients imaged with SPECT using ^{123}I-FIAU prior to and

after application of an oncolytic HSV virus [51]. Unfortunately, no increased uptake of FIAU was determined after viral infection in these patients. A possible explanation for this is that FIAU might not be the ideal tracer for monitoring HSV-tk expression in subjects with intact BBB, as FIAU does not penetrate it [51, 52].

Concluding, different gene therapy strategies for brain tumor patients have been investigated. Their therapeutic success, however, is still very limited and depends highly on the applied vector system [48]. Improvement of viruses and their administration in patients, the implementation of imaging techniques and combination treatment should be further explored to increase therapeutic efficacy. In this thesis, molecular imaging was applied to demonstrate and quantify gene expression after viral infection. We also investigated whether convection enhanced delivery (CED) would increase the viral vector distribution in a GBM tumor model.

References

1. Black, B.M., Woolner, L.B. and Blackburn, C.M. The uptake of radioactive iodine by carcinoma of the thyroid gland: a study of 128 cases. *J Clin Endocrinol Metab*, 1953 13(11): 1378-1390.
2. Tubiana, M., Lacour, J., Monnier, J.P., Bergiron, C., Gerard-Marchant, R., Roujeau, J., *et al.* External radiotherapy and radioiodine in the treatment of 359 thyroid cancers. *Br J Radiol*, 1975 48(575): 894-907.
3. Reubi, J.C. and Landolt, A.M. High density of somatostatin receptors in pituitary tumors from acromegalic patients. *J Clin Endocrinol Metab*, 1984 59(6): 1148-1151.
4. Lamberts, S.W., Bakker, W.H., Reubi, J.C. and Krenning, E.P. Somatostatin receptor imaging *in vivo* localization of tumors with a radiolabeled somatostatin analog. *J Steroid Biochem Mol Biol*, 1990 37(6): 1079-1082.
5. Meikle, S.R., Kench, P., Kassiou, M. and Banati, R.B. Small animal SPECT and its place in the matrix of molecular imaging technologies. *Phys Med Biol*, 2005 50(22): R45-61.
6. de Jong, M., Bakker, W.H., Breeman, W.A., van der Pluijm, M.E., Kooij, P.P., Visser, T.J., *et al.* Hepatobiliary handling of iodine-125-Tyr^3-octreotide and indium-111-DTPA-D-Phe^1-octreotide by isolated perfused rat liver. *J Nucl Med*, 1993 34(11): 2025-2030.
7. Beekman, F. and van der Have, F. The pinhole: gateway to ultra-high-resolution three-dimensional radionuclide imaging. *Eur J Nucl Med Mol Imaging*, 2007 34(2): 151-161.
8. Paulus, M.J., Gleason, S.S., Kennel, S.J., Hunsicker, P.R. and Johnson, D.K. High resolution X-ray computed tomography: an emerging tool for small animal cancer research. *Neoplasia*, 2000 2(1-2): 62-70.
9. Massoud, T.F. and Gambhir, S.S. Molecular imaging in living subjects: seeing fundamental biological processes in a new light. *Genes Dev*, 2003 17(5): 545-580.
10. Winnard, P., Jr. and Raman, V. Real time non-invasive imaging of receptor-ligand interactions *in vivo*. *J Cell Biochem*, 2003 90(3): 454-463.
11. Choy, G., Choyke, P. and Libutti, S.K. Current advances in molecular imaging: noninvasive *in vivo* bioluminescent and fluorescent optical imaging in cancer research. *Mol Imaging*, 2003 2(4): 303-312.
12. Koo, V., Hamilton, P.W. and Williamson, K. Non-invasive *in vivo* imaging in small animal research. *Cell Oncol*, 2006 28(4): 127-139.
13. Hacein-Bey-Abina, S., Von Kalle, C., Schmidt, M., McCormack, M.P., Wulffraat, N., Leboulch, P., *et al.* LMO2-associated clonal T cell proliferation in two patients after gene therapy for SCID-X1. *Science*, 2003 302(5644): 415-419.
14. Weissleder, R. and Mahmood, U. Molecular imaging. *Radiology*, 2001 219(2): 316-333.
15. van der Sanden, G.A., Schouten, L.J. and Coebergh, J.W. Incidence of primary cancer of the central nervous system in southeastern Netherlands during the period 1980-94. Specialists in neuro-oncology in southeastern Netherlands. *Cancer Causes Control*, 1998 9(2): 225-228.
16. Surawicz, T.S., McCarthy, B.J., Kupelian, V., Jukich, P.J., Bruner, J.M. and Davis, F.G. Descriptive epidemiology of primary brain and CNS tumors: results from the Central Brain Tumor Registry of the United States, 1990-1994. *Neuro-oncol*, 1999 1(1): 14-25.
17. Jemal, A., Siegel, R., Ward, E., Murray, T., Xu, J. and Thun, M.J. Cancer statistics, 2007. *CA Cancer J Clin*, 2007 57(1): 43-66.
18. Surawicz, T.S., Davis, F., Freels, S., Laws, E.R., Jr. and Menck, H.R. Brain tumor survival: results from the National Cancer Data Base. *J Neurooncol*, 1998 40(2): 151-160.
19. Stupp, R., Mason, W.P., van den Bent, M.J., Weller, M., Fisher, B., Taphoorn, M.J., *et al.* Radiotherapy plus concomitant and adjuvant temozolomide for glioblastoma. *N Engl J Med*, 2005 352(10): 987-996.
20. Kunwar, S., Prados, M.D., Chang, S.M., Berger, M.S., Lang, F.F., Piepmeier, J.M., *et al.* Direct intracerebral delivery of cintredekin besudotox (IL13-PE38QQR) in recurrent malignant glioma:

a report by the Cintredekin Besudotox Intraparenchymal Study Group. *J Clin Oncol*, 2007 25(7): 837-844.

21. Kneifel, S., Cordier, D., Good, S., Ionescu, M.C., Ghaffari, A., Hofer, S., *et al.* Local targeting of malignant gliomas by the diffusible peptidic vector 1,4,7,10-tetraazacyclododecane-1-glutaric acid-4,7,10-triacetic acid-substance p. *Clin Cancer Res*, 2006 12(12): 3843-3850.
22. Shah, A.C., Benos, D., Gillespie, G.Y. and Markert, J.M. Oncolytic viruses: clinical applications as vectors for the treatment of malignant gliomas. *J Neurooncol*, 2003 65(3): 203-226.
23. Ram, Z., Culver, K.W., Oshiro, E.M., Viola, J.J., DeVroom, H.L., Otto, E., *et al.* Therapy of malignant brain tumors by intratumoral implantation of retroviral vector-producing cells. *Nat Med*, 1997 3(12): 1354-1361.
24. Klatzmann, D., Valery, C.A., Bensimon, G., Marro, B., Boyer, O., Mokhtari, K., *et al.* A phase I/II study of herpes simplex virus type 1 thymidine kinase "suicide" gene therapy for recurrent glioblastoma. Study Group on Gene Therapy for Glioblastoma. *Hum Gene Ther*, 1998 9(17): 2595-2604.
25. Shand, N., Weber, F., Mariani, L., Bernstein, M., Gianella-Borradori, A., Long, Z., *et al.* A phase 1-2 clinical trial of gene therapy for recurrent glioblastoma multiforme by tumor transduction with the herpes simplex thymidine kinase gene followed by ganciclovir. GLI328 European-Canadian Study Group. *Hum Gene Ther*, 1999 10(14): 2325-2335.
26. Rainov, N.G. A phase III clinical evaluation of herpes simplex virus type 1 thymidine kinase and ganciclovir gene therapy as an adjuvant to surgical resection and radiation in adults with previously untreated glioblastoma multiforme. *Hum Gene Ther*, 2000 11(17): 2389-2401.
27. Trask, T.W., Trask, R.P., Aguilar-Cordova, E., Shine, H.D., Wyde, P.R., Goodman, J.C., *et al.* Phase I study of adenoviral delivery of the HSV-tk gene and ganciclovir administration in patients with current malignant brain tumors. *Mol Ther*, 2000 1(2): 195-203.
28. Sandmair, A.M., Loimas, S., Puranen, P., Immonen, A., Kossila, M., Puranen, M., *et al.* Thymidine kinase gene therapy for human malignant glioma, using replication-deficient retroviruses or adenoviruses. *Hum Gene Ther*, 2000 11(16): 2197-2205.
29. Germano, I.M., Fable, J., Gultekin, S.H. and Silvers, A. Adenovirus/herpes simplex-thymidine kinase/ganciclovir complex: preliminary results of a phase I trial in patients with recurrent malignant gliomas. *J Neurooncol*, 2003 65(3): 279-289.
30. Smitt, P.S., Driesse, M., Wolbers, J., Kros, M. and Avezaat, C. Treatment of relapsed malignant glioma with an adenoviral vector containing the herpes simplex thymidine kinase gene followed by ganciclovir. *Mol Ther*, 2003 7(6): 851-858.
31. Immonen, A., Vapalahti, M., Tyynela, K., Hurskainen, H., Sandmair, A., Vanninen, R., *et al.* AdvHSV-tk gene therapy with intravenous ganciclovir improves survival in human malignant glioma: a randomised, controlled study. *Mol Ther*, 2004 10(5): 967-972.
32. Chiocca, E.A., Abbed, K.M., Tatter, S., Louis, D.N., Hochberg, F.H., Barker, F., *et al.* A phase I open-label, dose-escalation, multi-institutional trial of injection with an E1B-Attenuated adenovirus, ONYX-015, into the peritumoral region of recurrent malignant gliomas, in the adjuvant setting. *Mol Ther*, 2004 10(5): 958-966.
33. Freeman, A.I., Zakay-Rones, Z., Gomori, J.M., Linetsky, E., Rasooly, L., Greenbaum, E., *et al.* Phase I/II trial of intravenous NDV-HUJ oncolytic virus in recurrent glioblastoma multiforme. *Mol Ther*, 2006 13(1): 221-228.
34. Harrow, S., Papanastassiou, V., Harland, J., Mabbs, R., Petty, R., Fraser, M., *et al.* HSV1716 injection into the brain adjacent to tumour following surgical resection of high-grade glioma: safety data and long-term survival. *Gene Ther*, 2004 11(22): 1648-1658.
35. Markert, J.M., Medlock, M.D., Rabkin, S.D., Gillespie, G.Y., Todo, T., Hunter, W.D., *et al.* Conditionally replicating herpes simplex virus mutant, G207 for the treatment of malignant glioma: results of a phase I trial. *Gene Ther*, 2000 7(10): 867-874.

36. Papanastassiou, V., Rampling, R., Fraser, M., Petty, R., Hadley, D., Nicoll, J., *et al.* The potential for efficacy of the modified (ICP 34.5(-)) herpes simplex virus HSV1716 following intratumoural injection into human malignant glioma: a proof of principle study. *Gene Ther*, 2002 9(6): 398-406.
37. Puumalainen, A.M., Vapalahti, M., Agrawal, R.S., Kossila, M., Laukkanen, J., Lehtolainen, P., *et al.* Beta-galactosidase gene transfer to human malignant glioma *in vivo* using replication-deficient retroviruses and adenoviruses. *Hum Gene Ther*, 1998 9(12): 1769-1774.
38. Lang, F.F., Bruner, J.M., Fuller, G.N., Aldape, K., Prados, M.D., Chang, S., *et al.* Phase I trial of adenovirus-mediated p53 gene therapy for recurrent glioma: biological and clinical results. *J Clin Oncol*, 2003 21(13): 2508-2518.
39. Bobo, R.H., Laske, D.W., Akbasak, A., Morrison, P.F., Dedrick, R.L. and Oldfield, E.H. Convection-enhanced delivery of macromolecules in the brain. *Proc Natl Acad Sci U S A*, 1994 91(6): 2076-2080.
40. Lieberman, D.M., Laske, D.W., Morrison, P.F., Bankiewicz, K.S. and Oldfield, E.H. Convection-enhanced distribution of large molecules in gray matter during interstitial drug infusion. *J Neurosurg*, 1995 82(6): 1021-1029.
41. Chen, M.Y., Hoffer, A., Morrison, P.F., Hamilton, J.F., Hughes, J., Schlageter, K.S., *et al.* Surface properties, more than size, limiting convective distribution of virus-sized particles and viruses in the central nervous system. *J Neurosurg*, 2005 103(2): 311-319.
42. Voges, J., Reszka, R., Gossmann, A., Dittmar, C., Richter, R., Garlip, G., *et al.* Imaging-guided convection-enhanced delivery and gene therapy of glioblastoma. *Ann Neurol*, 2003 54(4): 479-487.
43. Rampling, R., Cruickshank, G., Papanastassiou, V., Nicoll, J., Hadley, D., Brennan, D., *et al.* Toxicity evaluation of replication-competent herpes simplex virus (ICP 34.5 null mutant 1716) in patients with recurrent malignant glioma. *Gene Ther*, 2000 7(10): 859-866.
44. Tyler, M.A., Ulasov, I.V., Borovjagin, A., Sonabend, A.M., Khramtsov, A., Han, Y., *et al.* Enhanced transduction of malignant glioma with a double targeted Ad5/3-RGD fiber-modified adenovirus. *Mol Cancer Ther*, 2006 5(9): 2408-2416.
45. Colombo, F., Barzon, L., Franchin, E., Pacenti, M., Pinna, V., Danieli, D., *et al.* Combined HSV-TK/IL-2 gene therapy in patients with recurrent glioblastoma multiforme: biological and clinical results. *Cancer Gene Ther*, 2005 12(10): 835-848.
46. Hemminki, A., Zinn, K.R., Liu, B., Chaudhuri, T.R., Desmond, R.A., Rogers, B.E., *et al. In vivo* molecular chemotherapy and noninvasive imaging with an infectivity-enhanced adenovirus. *J Natl Cancer Inst*, 2002 94(10): 741-749.
47. Huber, B.E., Austin, E.A., Richards, C.A., Davis, S.T. and Good, S.S. Metabolism of 5-fluorocytosine to 5-fluorouracil in human colorectal tumor cells transduced with the cytosine deaminase gene: significant antitumor effects when only a small percentage of tumor cells express cytosine deaminase. *Proc Natl Acad Sci U S A*, 1994 91(17): 8302-8306.
48. Rainov, N.G. and Ren, H. Gene therapy for human malignant brain tumors. *Cancer J*, 2003 9(3): 180-188.
49. Jacobs, A., Voges, J., Reszka, R., Lercher, M., Gossmann, A., Kracht, L., *et al.* Positron-emission tomography of vector-mediated gene expression in gene therapy for gliomas. *Lancet*, 2001 358(9283): 727-729.
50. Kracht, L.W., Miletic, H., Busch, S., Jacobs, A.H., Voges, J., Hoevels, M., *et al.* Delineation of brain tumor extent with [^{11}C]L-methionine positron emission tomography: local comparison with stereotactic histopathology. *Clin Cancer Res*, 2004 10(21): 7163-7170.
51. Dempsey, M.F., Wyper, D., Owens, J., Pimlott, S., Papanastassiou, V., Patterson, J., *et al.* Assessment of ^{123}I-FIAU imaging of herpes simplex viral gene expression in the treatment of glioma. *Nucl Med Commun*, 2006 27(8): 611-617.

52. Jacobs, A., Braunlich, I., Graf, R., Lercher, M., Sakaki, T., Voges, J., *et al.* Quantitative kinetics of [^{124}I]FIAU in cat and man. *J Nucl Med*, 2001 42(3): 467-475.
53. Zinn, K.R. and Chaudhuri, T.R. The type 2 human somatostatin receptor as a platform for reporter gene imaging. *Eur J Nucl Med Mol Imaging*, 2002 29(3): 388-399.
54. Zinn, K.R., Chaudhuri, T.R., Buchsbaum, D.J., Mountz, J.M. and Rogers, B.E. Simultaneous evaluation of dual gene transfer to adherent cells by gamma-ray imaging. *Nucl Med Biol*, 2001 28(2): 135-144.

1.3 Improvement strategies for peptide receptor scintigraphy and radionuclide therapy

M. de Visser*, S.M. Verwijnen*, M. de Jong.

** Both authors contributed equally to this manuscript*

in press, Cancer Biotherapy and Radiopharmaceuticals

Summation

Somatostatin receptor-targeting peptides are widely used for imaging and therapy of neuroendocrine tumors. Peptide receptor radionuclide therapy (PRRT) in neuroendocrine tumor patients with radiolabeled somatostatin analogs has resulted in symptomatic improvement, prolonged survival and enhanced quality of life. The side-effects of PRRT are few and mostly mild, certainly when using kidney protective agents. If more widespread use of PRRT is possible, such therapy might become the therapy of first choice in patients with metastasized or inoperable neuroendocrine GEP tumors.

Yet, much profit can be gained from improving the receptor-targeting strategies available and developing new strategies. This review presents an overview of several options to optimize receptor-targeted imaging and radionuclide therapy. These include optimization of peptide analogs, increasing the number of receptors on the tumor site, and combining PRRT with other treatment strategies.

The development of new peptide analogs with increased receptor binding affinity and improved stability might lead to higher accumulation of radioactivity inside tumor cells. Analogs of somatostatin have been widely studied. However, much profit can be gained in improving peptide analogs targeting other tumor related receptors, including gastrin-releasing peptide (GRP) receptors, neurotensin (NT) receptors, cholecystokinin (CCK) receptors, and glucagon-like peptide-1 (GLP-1) receptors. Several peptide analogs targeting these receptors are well on their way to clinical utilization.

Literature shows that it is possible to increase the receptor density on tumor cells using different methods which results in higher binding and internalization rates and thus a higher contrast during peptide-receptor-scintigraphy (PRS). In PRRT treatment, this would enable the administration of higher therapeutic doses to tumors, which might lead to a higher cure rate in patients.

Combinations of radionuclide therapy with other treatment modalities like chemotherapy or pre-treatment with radiosensitizers might increase the impact of the treatment. Furthermore, administration of higher dosages of radioactivity to the patient enabled by combinations of PRRT with strategies reducing the radiation dose to healthy organs will improve the outcome of tumor treatment. Also targeting one or several tumor-specific receptors by using combinations of therapeutic agents, as well as by reducing non-target uptake of radioactivity, will enlarge the therapeutic window of PRRT. Clinical studies will provide more insight in the effects of combining treatment strategies in cancer patients.

Introduction

Radiolabeled receptor-binding peptides are powerful tools for imaging and therapy of tumors expressing peptide binding receptors. Especially analogs of somatostatin are suitable for receptor-targeted localization, staging and treatment of somatostatin receptor (sst)-expressing neuroendocrine tumors [1]. The somatostatin receptor family consists of 5 receptor subtypes: sst_1-sst_5. The majority of neuroendocrine tumors feature a strong overexpression of sst, mainly subtype 2 (sst_2).

The introduction of radiolabeled somatostatin analogs started with the development of the sst-targeting somatostatin analog [^{111}In-DTPA^0]octreotide (Octreoscan®). This analog is being used to visualize sst-receptor positive tumors and their metastases [2, 3]. The therapeutic efficacy of this analog was found promising, although no effects were found in patients with larger tumors and advanced disease [4]. The next generation of modified somatostatin analogs, including [DOTA^0,Tyr^3]octreotide, is being used for somatostatin receptor targeted radionuclide therapy as well. This analog has a higher affinity for sst_2, and has 1,4,7,10-tertraazacyclododecane-N',N'',N''',N''''-tetraacetic acid (DOTA) instead of diethylenetriaminepentaacetic acid (DTPA) as chelator, allowing stable radiolabeling with beta-emitting radionuclides such as ^{90}Y and ^{177}Lu. Several phase-1 and phase-2 peptide-receptor radionuclide therapy (PRRT) trials were performed using [^{90}Y-DOTA^0-Tyr^3]octreotide (^{90}Y-DOTA-TOC; OctreoTher®) [5-9], objective responces in patients with GEP tumors ranged from 9 - 33% [10]. These results were better than those obtained with [^{111}In-DTPA^0] octreotide, despite differences in the [^{90}Y-DOTA^0,Tyr^3]octreotide protocols applied. [^{177}Lu-DOTA^0,Tyr^3]octreotate is a third generation somatostatin analog for PRRT and is being used in our medical center since the year 2000. [DOTA^0,Tyr^3]octreotate differs from [DOTA^0,Tyr^3]octreotide in that the C-terminal threoninol has been replaced with threonine. Compared with [DOTA^0,Tyr^3]octreotide, it shows considerable improvement in binding to sst_2-positive tissues *in vitro* and *in vivo* [11, 12]. [^{177}Lu-DOTA^0,Tyr^3]octreotate represents an important improvement because of the higher absorbed radiation doses that can be achieved to most tumors with about equal radiation doses to dose-limiting organs [13, 14]. ^{90}Y and ^{177}Lu-labeled peptides have greater therapeutic potential compared to ^{111}In-labeled peptides, for their emitted β-particle range exceeds the cell diameter, enabling irradiation of neighboring tumor cells, which is favorable in case of heterogeneous receptor expression. ^{177}Lu, as compared to ^{90}Y, has a lower tissue penetration range which is favorable for treatment of small tumors, whereas ^{90}Y might be more effective in tumors with a larger diameter [15, 16]. In contrast to ^{90}Y, ^{177}Lu also emits low energy γ-rays which directly allows imaging and dosimetry following [^{177}Lu-DOTA^0,Tyr^3]octreotate therapy. Treatment with [^{177}Lu-DOTA^0,Tyr^3]octreotate in patients with GEP tumors resulted in complete

or partial remission in 28% of patients [17]. Median time to progression was more than 36 months in patients who had either stable disease or tumor regression after treatment. In addition, patients treated with [^{177}Lu-DOTA^{0},Tyr^{3}]octreotate indicated a significant improvement of their quality of life [18].

In summary, PRRT with radiolabeled somatostatin analogs is a promising treatment option for patients with inoperable or metastasized neuroendocrine tumors. The side-effects of PRRT are few and mostly mild.

This review discusses several options to optimize receptor-targeted imaging and radionuclide therapy, outlining the efforts to develop optimized radiopharmaceuticals, to increase the target density and combine treatment modalities (see also figure 1):

I. Developing new peptide analogs with increased receptor binding affinity and improved stability might lead to higher accumulation of radioactivity inside tumor cells. Many new nalogs of somatostatin have been developed and widely studied; much profit can also be gained by improving peptide analogs targeting other tumor related receptors, including gastrin-releasing peptide (GRP) receptors, neurotensin (NT) receptors, cholecystokinin (CCK) receptors, and glucagon-like peptide-1 (GLP-1) receptors.
II. Increasing the number of receptors that can be targeted on the tumor cells will result in a higher contrast during peptide-receptor-scintigraphy (PRS), and a higher radiation dose to the tumor during PRRT.

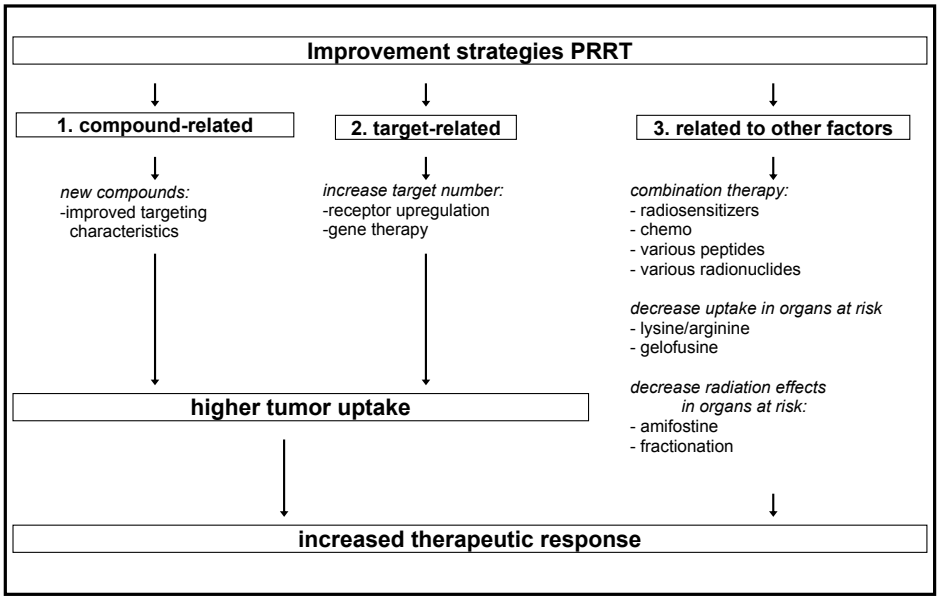

Figure 1: Improvement strategies for peptide receptor radionuclide therapy (PRRT)

III. Combinations of radionuclide therapy with other treatment modalities such as chemotherapy or radiosensitizer pre-treatment might increase treatment impact. Also administration of higher radioactivity doses enabled by combinations of PRRT with strategies reducing the radiation dose to normal organs will improve the outcome of tumor treatment.

I. Development of new peptide analogs

The natural structure of peptides makes them sensitive to peptidases. They are rapidly broken down in blood and other tissues, restricting their potential use as radiopharmaceuticals. Metabolically stable analogs are therefore preferable for clinical application. Strategies to stabilize peptides include the introduction of non-biodegradable peptide bonds, stabilized amino acid derivatives replacing the natural amino acids, and cyclization.

High *in vivo* stability is advantageous but not sufficient for good target-to-non target ratios. Important factors are also long retention time of radioactivity at the tumor site and rapid clearance of radioactivity from non-target tissues and blood. Internalization of radiolabeled peptides by tumor cells may lead to longer retention of radioactivity [19]. Peptide agonists often undergo receptor-mediated endocytosis enabling internalization of the radionuclide into tumor cells, whereas antagonists do most often not internalize [20]. The majority of research efforts to design peptide based radiopharmaceuticals have focused on receptor-agonists. Recently, somatostatin antagonists were shown most suitable for sst-targeting as well [21].

Subtle changes in peptide structures as described above, can have dramatic effects on the receptor-binding capacity and biodistribution of the compound. Attempts to improve the stability of the radiolabeled peptide can at the same time be fatal for its targeting abilities due to loss of receptor-binding affinity. Below we reviewed the most recent efforts to develop new radiolabeled peptides for imaging and therapy of receptor-expressing tumors.

SST receptor-targeting peptides

^{99m}Tc-labeled somatostatin analogs including hydrazinonicotinamide (Hynic)-derivatised ^{99m}Tc-[Hynic-Tyr^3]octreotide, ^{99m}Tc-[Hynic-Tyr^3]octreotate [22-26], and tetraamine-functionalized derivative ^{99m}Tc-[N_4^0,Tyr^3]octreotate (Demotate 1) [27-29], can be regarded as promising new radiopharmaceuticals for sst scintigraphy. Both Hynic- and N_4-derivatized analogs were capable of detecting sst-expressing lesions in patients.

Compared to single-photon emission computed tomography (SPECT) imaging, clinical positron emission tomography (PET) imaging provides a higher spatial resolution and the possibility to more accurately quantitate tumor and normal organ uptake. For PET imaging, peptides can be labeled with positron emitting radionuclides such as ^{68}Ga, ^{18}F, ^{64}Cu, ^{86}Y, ^{89}Zr, and ^{124}I. Several ^{18}F and ^{64}Cu labeled sst analogs have been reported, including Gluc-Lys([^{18}F]FP)-TOCA [30] and ^{64}Cu-TETA-octreotide [31] which both appeared promising for imaging of patients bearing neuroendocrine tumors. In contrast to PET radionuclides that require a cyclotron for production, ^{68}Ga can be produced in-house using a ^{68}Ge/^{68}Ga generator [32]. PET imaging using ^{68}Ga-[DOTA^{0}-Tyr^{3}]octreotide has been shown preferable to SPECT imaging with Octreoscan®, especially in small lesions and tumors with low sst density [33, 34].

The radiolabeled analogs of octreotide and octreotate, including the analogs described above, have high binding-affinity for sst_2 [11], the most frequently expressed subtype in neuroendocrine cancers. In some cancers, however, sst_2 is not or only in low density expressed, whereas other subtype receptors can be present [35, 36]. The heterogeneous and concomitant sst receptor subtype expression strongly pleads for tracers, or combinations of tracers, that can target more than one sst. Ginj et al. evaluated 24 DOTA-somatostatin analogs, all based on octreotide, using a systematic modification at amino acid position 3 [37]. Two analogs, namely [DOTA^{0}-Nal^{3}]octreotide and [DOTA^{0}-BzThi^{3}]octreotide showed high binding affinity for sst_2, sst_3 and sst_5. ^{68}Ga-labeled [DOTA^{0}-Nal^{3}]octreotide has been shown to be a good tracer for primary diagnostic and follow-up studies in patients suspected from or with proven sst-expressing tumors [38].

As mentioned above, peptide agonists internalize into the cell after receptor-binding, which is thought to be essential for good retention of radionuclides in target cells. Ginj et al., however, recently reported promising results in a preclinical study comparing targeting characteristics of sst_2 or sst_3 binding agonists versus antagonists [21]. They found that these antagonists, even though they did not internalize, showed higher accumulation in tumor cells compared to agonists, whereas the receptor affinity of agonists and antagonists was in the same range. In addition, accumulation in non-tumor tissues, exceptfor that in the kidneys, was less for antagonists than for agonists up to 24 hours after injection. These results suggest that antagonists may be better candidates to target tumors than agonists. The authors attribute the superior antagonist accumulation to binding of antagonists to a larger variety of receptor configurations. If the present observation can be translated to other receptors as well, the use of radiolabeled antagonists may considerably improve tumor imaging and PRRT efficacy.

GRP receptor-targeting peptides

Overexpression of GRP receptors has been demonstrated in a large number of human tumors, including prostate and breast tumors [39], which are among the major causes of cancer death worldwide [40]. Bombesin (BN) is a 14 amino acid peptide with high affinity for the GRP receptor, radiolabeled analogs of BN might therefore be useful for GRP receptor-targeted imaging and therapy. First attempts to develop radiolabeled BN analogs for diagnostic imaging aimed at radioiodinated peptides. These compounds were found to be very unstable and iodine was rapidly cleared from the tumor cells [41]. Now, more than 10 years later several ^{111}In and ^{99m}Tc labeled BN analogs have been developed with favorable *in vivo* characteristics for SPECT imaging of GRP receptor-expressing tumors [42-47].

^{99m}Tc-labeled bombesin analogs have a tendency to accumulate in liver and intestines as a result of their high lipophilicity. This high unspecific accumulation of radioactivity interferes with detection of GRP receptor-positive lesions in the abdominal area. Much effort has been put into reducing the lipophilicity of the ^{99m}Tc-labeled BN analogs. Ferro-Flores et al. conjugated the bifunctional chelator HYNIC and the co-ligand EDDA (ethylenediamine-*N,N'*-diacetic acid) to bombesin for the preparation of ^{99m}Tc-EDDA/HYNIC-[Lys^3]-BN. This conjugation resulted in less lipophilic properties of the peptide and consequently lower hepatobiliary and predominantly renal excretion [48]. Furthermore, Garcia Garayoa et al. recently showed that the introduction of a hydrophilic spacer between the peptide sequence and the ^{99m}Tc-binding complex can reduce the high lipophilicity and impove tumor-to-non tumor ratios [49].

Next to tumor diagnosis, staging, and localization, ^{111}In-labeled peptide analogs are often used as surrogates to determine the biodistribution and dosimetry of therapeutic radiopharmaceuticals labeled with radiometals like ^{90}Y. DTPA and DOTA are being used as chelating systems coupled to the BN analogs for this purpose [50]. ^{111}In-DTPA-BN analogs, e.g. [^{111}In-DTPA-Pro^1,Tyr^4]BN [20, 47] were reported to have good tumor uptake and rapid clearance from non-target tissues and blood. Substitution of the DTPA chelator system in [DTPA-Pro^1,Tyr^4]BN by DOTA was previously found to have favorable effects on the receptor-binding characteristics of this radioligand [47]. We recently synthesized a new DTPA-coupled BN analog, [^{111}In-DTPA-ACMpip^5,Tha^6,βAla^{11},Tha^{13},Nle^{14}]BN(5-14) (Cmp 3) with a significantly higher GRP receptor-mediated tumor uptake *in vivo* in animal studies [51]. As ^{111}In-Cmp 3 seems promising for SPECT imaging of GRP receptor-expressing tumors, replacing the DTPA chelator by DOTA would enable therapeutic use of the compound and diagnostic PET imaging.

Most of the recent studies on newly developed BN peptide analogs focus on the DOTA-chelating system for its multipurpose utilization options: SPECT, PET, and

PRRT [19, 52-58]. For example, DOTA-PESIN (DOTA-PEG_4-BN(7-14)) showed to be a very promising new compound. Although it has only a moderate affinity for the GRP receptor, it showed good *in vivo* tumor uptake in animal studies [52]. Clearance of the compound proceeded via kidneys and urinary tract with fast washout from GRP receptor-negative tissues but rather high accumulation in the kidneys. The high kidney retention could not be reduced by lysine.

Another very promising DOTA-BN analog is ^{177}Lu-AMBA [58]. This compound consists of DOTA attached to BN(7-14) by a short linker. ^{177}Lu-AMBA, like DOTA-PESIN, showed in animals high GRP receptor-mediated tumor uptake and favorable tumor-to-background ratios. *In vivo* tumor treatment with ^{177}Lu-AMBA resulted in a significantly prolonged survival of tumor-bearing mice, and decreased tumor growth rate over that of controls. Like DOTA-PESIN, ^{177}Lu-AMBA is excreted via the kidneys, and the relatively high kidney retention cannot be reduced by co-injection of lysine, which is probably due to the lack of lysine residues in these peptide sequences. However, the accumulation of radioactivity in the kidneys is still 50% lower for DTPA- and DOTA-derivatized BN analogs compared to that of somatostatin analogs.

PRRT using BN analogs described above may be promising. Clinical scintigraphy with ^{99m}Tc- and ^{68}Ga-labeled BN analogs clearly delineated tumor lesions, including lymph nodes, and metastases [44, 59, 60]. However, also relatively high uptake in non-target, GRP receptor-positive, tissues such as pancreas and intestines was found which is unfavorable for PRRT. In a pre-clinical study using ^{111}In-Cmp 3 we found that increasing amounts of injected peptide mass in tumor-bearing rats decreased uptake in receptor-positive normal tissues more than that in the tumor. Also pre-injection of excess unlabeled peptide before administration of radiolabeled compound showed to be profitable for tumor uptake compared to that in receptor-expressing normal tissues (figure 2) [61]. These effects were also found with ^{177}Lu-AMBA in tumor bearing mice [58]. Thus, injection of higher peptide mass and/or pre-injection of excess BN may increase tumor-to-non tumor ratios. Taking into account the biologic activity of BN agonists in patients, pre-injection of GRP receptor antagonists might be preferable.

Radiolabeled BN analogs are of particular interest for PRRT of advanced prostate cancer patients who do not respond to hormone therapy. So far, the best treatment strategies available for this group of patients are only marginally effective [62, 63]. However, in a study evaluating GRP receptor-expression in human prostate cancer xenograft models representing the different stages of prostate tumor development, including the shift from androgen-dependent towards androgen-independent tumor growth, we found high GRP receptor density only in androgen–dependent prostate cancer xenografts. These results suggest high GRP receptor expression in the early, androgen-dependent, stages of prostate tumor development and not in later stages.

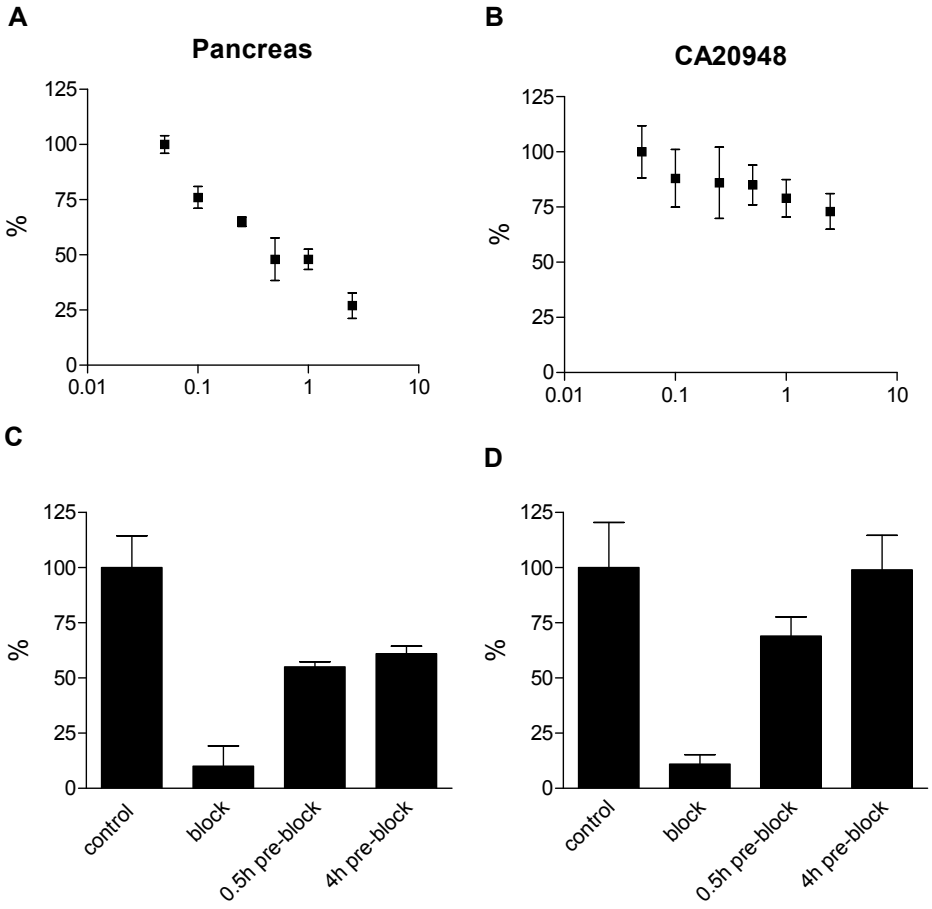

Figure 2: GRP receptor saturation: Uptake of ^{111}In-Cmp 3 in GRP receptor-expressing pancreas (A) and CA20948 tumor (B) in rats (4 hours p.i., lowest peptide mass is set at 100%). Receptor availability: Uptake of 0.1µg ^{111}In-Cmp 3 in rat pancreas (C) and tumor (D) without (control) or with 100µg unlabeled BN either coinjected (block) or pre-injected 0.5 (0.5h pre-block) or 4 hours (4h pre-block) prior to administration of radiolabeled compound (4 hours p.i., control is set at 100%). Injection of a higher peptide mass and/or pre-injection of excess BN affected the uptake in non-target GRP receptor-expressing tissues more than that in tumor.

In addition, simulation of androgen ablation treatment in the animal model (i.e. castration) strongly reduced GRP receptor-expression in androgen-dependent tumors, suggesting that GRP receptor expression in human prostate cancer is androgen-regulated [64]. Studies evaluating GRP receptor-expression on clinical prostate cancer tissue samples are underway to determine whether these results are clinically relevant.

The application of BN peptides in cancer patients is still in its infancy [44, 59, 60]. However, recent developments in the synthesis of new promising BN analogs are encouraging for further utilization in clinical studies.

NT receptor-targeting peptides

Neuroendocrine pancreatic tumors can be successfully localized and treated using radiolabeled somatostatin analogs [65-67]. Exocrine pancreatic cancer, however, does not express a sufficient level of sst for scintigraphic imaging. Reubi et al. reported that 75% of ductal pancreatic carcinomas over-expressed neurotensin (NT) receptors, whereas normal pancreatic tissue, pancreatitis and endocrine pancreatic cancers were NT receptor-negative [68]. Neurotensin is a 13-amino acid peptide localized in both the central nervous system and in peripheral tissues, mainly the gastrointestinal tract [69, 70]. The instability of native neurotensin prompted several groups [71-76] to synthesize neurotensin analogs less susceptible to degradation, while maintaining the binding affinity to NT receptors. Preclinical studies using ^{111}In-labeled DTPA (MP2530) and DOTA (MP2656) linked NT analogs demonstrated that subtle changes as introduction of non-natural amino acids on specific positions can be made in the C-terminal part of the peptide, the crucial part for binding and biological activity, without markedly affecting the binding properties [77]. These NT analogs showed good receptor-mediated uptake in NT receptor expressing HT29 xenografts and were thus promising tools for imaging of exocrine pancreatic tumors. PRRT using these analogs might however be hampered by the relatively high kidney uptake of ^{111}In-NT analogs. Recently, Maes et al. [73] reported a triply-stabilized ^{99m}Tc-labeled NT (NT-XIX) analog with high tumor uptake and reduced kidney uptake which led to a superior tumor-to-kidney ratio compared to ^{111}In-labeled analogs. Also ^{99m}Tc-Demotensin 4, a doubly-stabilized NT analog [72], showed a favorable tumor-to-kidney ratiol. Still, the tumor-to-intestine and tumor-to-liver ratios were considerably higher for ^{111}In-labeled analogs, which is favorable for visualization of pancreatic tumors in patients [78].

Only one clinical evaluation study using a radiolabeled NT analog has been reported [79]. This study included four exocrine pancreatic cancer patients, who were injected with the NT analog: ^{99m}Tc-NT-XI. Scintigraphic imaging showed moderate tumor uptake in one patient whereas the other three patients showed no tumor uptake. Two out of these three patients were found to have a NT receptor-negative tumor.

CCK_2 receptor-targeting peptides

Unlike other neuroendocrine tumors, somatostatin receptor expression is rather low in medullary thyroid cancer (MTC) and is completely absent in clinically aggressive forms of the disease [80, 81]. The presence of cholecystokinin-2 (CCK_2) receptors

was shown in more than 90% of MTCs, and in a high percentage of small cell lung cancers, stromal ovarian cancers, astrocytomas and several other tumor types [82]. On the basis of these findings, Behr et al. [83] evaluated the suitability of radioiodinated gastrin, a specific high affinity ligand for the CCK_2 receptor, for targeting CCK_2 receptor expressing tumors *in vivo*. Their data suggested that gastrin analogs may represent a useful new class of receptor-binding peptides for diagnosis and therapy of a variety of tumor types, including MTC. Reubi et al. [84] developed DTPA-CCK_2 receptor binding CCK analogs, evaluated receptor-binding characteristics and obtained initial preclinical biodistribution data in non tumor-bearing rats. For the DOTA counterpart of the most promising analog [^{111}In-DOTA^0]CCK_8, a high CCK_2 receptor affinity was found. The latter analog could visualize CCK_2 receptor-expressing tumors *in vivo* in rats [85], and also in patients with advanced metastatic MTC [^{111}In-DTPA^0]CCK_8 was able to visualize the tumor lesions [86].

Besides CCK analogs, radiolabeled analogs of minigastrin have also shown to be suitable for CCK_2 receptor-targeting. For example, a clinical study in MTC patients showed that most tumor sites could be visualized with ^{111}In-DTPA-minigastrin [83,

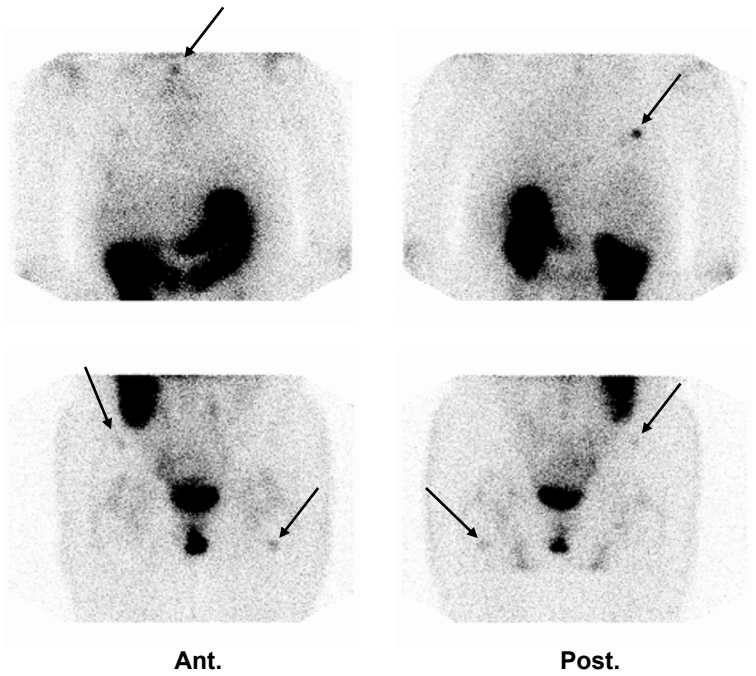

Figure 3: ^{99m}Tc-Demogastrin 2 scintigraphy (3 hours p.i.) in a 44 year old female MTC patient with elevated serum calcitonin. No tumor localization with ultrasound, SRS, CT, MRI and ^{18}FDG-PET. Anterior (Ant) and posterior (Post) images of the thoracic (upper images) and pelvic (lower images) regions showing metastatic lesions (some marked with arrows).

87]. Nock et al. synthesized ^{99m}Tc-labeled N_4-derivatized analogs of minigastrin [88]. Pre-clinical evaluation studies resulted in the selection of [N_4^{0-1},Gly^0,$(D)Glu^1$] minigastrin (Demogastrin 2) as the most promising CCK_2-targeting analog for tumor imaging. The qualities of [^{99m}Tc]Demogastrin 2 could be confirmed in a patient with metastatic MTC; tumor deposits were clearly delineated (see also figure 3).

More recent clinical studies by Gotthardt et al. [89, 90] in patients with metastatic/recurrent MTC compared the results of CCK_2 (gastrin) receptor scintigraphy (GRS), using [^{111}In-$(D)Glu^1$]minigastrin, with somatostatin receptor scintigraphy (SRS), CT and ^{18}F-FDG PET. They found that GRS had a higher tumor detection rate than SRS and ^{18}F-FDG PET. GRS in combination with CT was most effective in the detection of metastatic MTC. Furthermore, GRS in patients bearing neuroendocrine tumors other than MTC detected additional tumor sites that were missed in SRS in 20% of patients. The authors concluded that GRS may become the scintigraphic imaging modality of choice in MTC patients. In conclusion, (pre)clinical studies have shown the suitability of radiolabeled CCK and gastrin analogs for scintigraphy of tumors such as MTC. PRRT using these radioligands is still preliminary but its future is promising.

GLP-1 receptor-targeting peptides

A new promising candidate for *in vivo* tumor targeting is glucagon-like peptide 1 (GLP-1) receptor, a member of the glucagon receptor family [91]. The GLP-1 receptor was recently shown to be highly overexpressed in human endocrine tumors, in particular insulinomas, gastrinomas [92], and pheochromocytomas [93].

Similar to other naturally occurring receptor-binding ligands, native GLP-1 receptor agonists are rapidly degraded in the blood [94, 95]. Therefore, Gotthardt et al. evaluated the more stable GLP-1 selective analog exendin, which showed to have potential for scintigraphic imaging of GLP-1 receptor-expressing tumors [96]. Recently, the exendin analog has been further optimized, which has led to two new, ^{111}In-DTPA-conjugated, Exendin-4 analogs: ^{111}In-DTPA-Lys^{40}-exendin-4 [97] and [Lys^{40}(Ahx-DTPA-^{111}In)NH_2] exendin-4 [98]. Both analogs showed encouraging preclinical characteristics with high GLP-1 receptor-mediated uptake in target tissues and good target-to-background ratios *in vivo* in animal models. In addition, Wicky et al. showed that [Lys^{40}(Ahx-DTPA-^{111}In)NH_2]exendin-4 efficiently repressed insulinoma growth in mice [99]. Kidney toxicity was found the limiting factor in this treatment strategy.

No clinical study using GLP-1 receptor-targeting analogs has been reported so far. For therapeutic purposes, high kidney retention of exendin-4 analogs could be problematic. Nevertheless, when this high accumulation in the kidneys can be overcome, high GLP-1 receptor-expression on tumors, in combination with the favorable *in vivo* characteristics of the recent exendin-4 analogs, gives GLP-1 receptor-targeted PRRT serious potential.

$\alpha_v\beta_3$ *integrin-targeting peptides*

Cell matrix interactions are of fundamental importance for tumor invasion and formation of metastases as well as tumor-induced angiogenesis.

The $\alpha_v\beta_3$ integrin is a transmembrane protein which is preferentially expressed on proliferating endothelial cells [100], whereas it is absent on quiescent endothelial cells. For growth beyond the size of 1-2 mm in diameter, tumors require the formation of new blood vessels. The $\alpha_v\beta_3$ receptors are overexpressed on these newly formed blood vessels of actively growing tumors, and are therefore potential targets for receptor-mediated tumor imaging and therapy and for planning and monitoring of $\alpha_v\beta_3$ targeting treatment strategies.

It was found that the essential amino acid sequence for the binding of extracellular matrix proteins to $\alpha_v\beta_3$ receptors is arginine-glycine-aspartic acid (RGD) [101]. Several studies have been aimed to develope optimized $\alpha_v\beta_3$ targeting compounds. In summary, it was found that cyclic analogs of RGD containing 5 amino acids (RGD sequence + hydrophobic amino acid in position 4 + additional amino acid in position 5) have the highest $\alpha_v\beta_3$ binding affinities [102, 103]. Radiolabeled analogs containing this 5 amino acid sequence have been synthesized and evaluated for their $\alpha_v\beta_3$ targeting characteristics. Among them are DTPA and DOTA conjugated analogs for radiolabeling with ^{111}In, ^{90}Y, ^{177}Lu, ^{68}Ga and ^{64}Cu, enabling SPECT and PET imaging and PRRT [104, 105]. Also ^{18}F-labeled cyclic RGD analogs for PET imaging have been characterized [105-107]. In patients, Beer et al. showed that PET imaging using the RGD analog, ^{18}F-galacto-RGD, can effectively show the level of $\alpha_v\beta_3$ expression in man [108-110].

Dijkgraaf et al. [111] developed multivalent RGD peptides in an attempt to increase receptor-binding affinity. They synthesized and compared the *in vitro* and *in vivo* $\alpha_v\beta_3$ targeting characteristics of DOTA-linked monomeric, dimeric, and tetrameric RGD peptides radiolabeled with ^{111}In. They found enhanced receptor affinity *in vitro* and better tumor uptake *in vivo* for the tetrameric compound compared to its monomeric and dimeric analogs. Alternatively, they synthesized multimeric RGD peptides as dendrimers: macromolecules consisting of multiple perfectly branched monomers. Consistent with their previous results, the tetrameric RGD dendrimer showed enhanced affinity and significantly higher tumor uptake compared to its monomeric and dimeric analogs [112]. The authors ascribe the improved targeting characteristics of the multimer to the enhanced local concentration of RGD units in the vicinity of the receptor (statistical rebinding) and not to binding of the compound to multiple $\alpha_v\beta_3$ receptors. Unfortunately, the kidney retention of the mulitimeric peptides was also increased resulting in unfavorable tumor-to-kidney ratios. Introduction of a linker in between the peptide moiety and the DOTA chelator, in an attempt to improve the target-to-background ratios of the peptide, led to a

marginal enhancement of the tumor-to-kidney ratio only [113]. In a study evaluating the targeting potential of a cyclic RGD analog in an intraperitoneally (i.p.) growing tumor model, Dijkgraaf et al. found that i.p. *vs* i.v injection of the radiolabeled RGD peptide resulted in markedly higher tumor uptake after i.p. administration whereas uptake in the other organs like kidneys were unaffected by the route of administration. PRRT experiments in this model indicated that i.p. growing tumors can be inhibited significantly by i.p. injection of a therapeutic dose of ^{177}Lu-labeled RGD analog [114]. Multimeric RGD peptides are promising tools for *in vivo* imaging of tumor angiogenesis in cancer patients. $\alpha_v\beta_3$ targeted PRRT with these compounds might particularly be used for i.p. growing tumors. Currently, ^{18}F-galacto-RGD is the only $\alpha_v\beta_3$-targeting peptide shown effective for tumor imaging in patients [110].

II. Improving the therapeutic effect: increasing receptor density on target cells

By increasing the receptor density on tumor cells in patients to be treated with radiolabeled peptides, and thereby increasing radioactivity uptake in the tumor, the therapeutic window can be enlarged.

Up-regulation of receptors

During the last three decades several reports have been published concerning hormones and growth factors inducing a higher number of receptors on tumor cells [115-123]. For an overview of references and findings, see table 1. In this review the focus will be on radiation-induced receptor up-regulation.

Up-regulation of peptide receptors on tumor cells after irradiation was first reported by Béhé et al. [124, 125], who showed that a total dose of 4 to 16 Gy of external beam irradiation led to time-dependent up-regulation of both sst_2 and gastrin receptors on AR42J cells, *in vitro* as well as *in vivo*. This phenomenon was also investigated *in vitro* in NCI-H69 small cell lung cancer cells [126]. which were irradiated with a total dose of 4 Gy and the subsequent internalization of [^{177}Lu-DTPA^0,Tyr^3]octreotate was 1.5-3 times increased compared to that in control cells.

Not only the use of external beam radiation, but also low therapeutic doses of radiolabeled peptides were found to induce sst_2 up-regulation. CA20948 rat pancreatic tumor-bearing rats [127, 128] were treated with a relatively low, non-curative dose of either [^{111}In-DTPA^0]octreotide [127] or [^{177}Lu-DOTA^0,Tyr^3]octreotate [128] and sst_2 receptor expression in different phases of tumor response was determined versus base-line (control). Both studies revealed an increased sst_2 density on tumors re-growing after initial therapy-induced regression compared to control: treatment

Table 1: An overview of references concerning receptor up- and down-regulation.

Reference	Cell type	Origin of cell	Modulator	in vitro / in vivo	Effect on expr.
[115] Kimura, 1986	anterior pit. cells†	rat	estradiol	in vitro	up (2-fold)
[116] Presky, 1988	GH_4C_1	rat pit. tumor cells†	SRIF (chronic)	in vitro	up
[117] Kimura, 1989	anterior pit. cells†	rat	estradiol	in vivo	up
[118] Slama, 1992	arcuate nucleus	female rat brain	estradiol	in vivo	up
[119] Vidal, 1994	AR42J	rat panc. tumor cells‡	EGF / Gastrin	in vitro	up
[120]Visser-Wisselaar, 1997	7315b	pituitary tumor cells‡	estradiol	in vitro & in vivo	up (+ up of sst_3)
[121] Froidevaux, 1999	AR42J	rat panc. tumor cells‡	octreotide (continuous)	in vivo	up
[122] Viguerie, 1987	AR42J	rat panc. tumor cells‡	dexamethasone	in vitro	down
[121] Froidevaux, 1999	AR42J	rat panc. tumor cells‡	octreotide	in vitro	down
			octreotide (single injection)	in vivo	down
			octreotide (discontinuous)	in vivo	down
[123] Gunn, 2006	IMR-32	human neuroblastoma	octreotide	in vitro	down
[124] Behe, 2003	AR42J	rat panc. tumor cells‡	external beam irradiation	in vitro & in vivo	up (also gastrin)
[125] Behe, 2004	AR42J	rat panc. tumor cells‡	external beam irradiation	in vivo	up (also gastrin)
[127] Capello, 2005	CA20948	rat panc. tumor cells‡	^{111}In-octreotate (low dose)	in vivo	up (2-fold)
[126] Oddstig, 2006	NCI-H69	small cell lung cancer	x-ray (100 keV)	in vitro	up (1.5-3-fold)
[128] Melis, 2007	CA20948	rat panc. tumor cells‡	^{177}Lu-octreotate (low dose)	in vivo	up (2-5-time)

† pit.=pituitary

‡ panc.=pancreatic

with [^{111}In-DTPA^0]octreotide resulted in a 2-fold increase, while [^{177}Lu-DOTA^0,Tyr^3] octreotate treatment showed a more pronounced effect (2-5-fold increase). This radiation induced up-regulation of receptor expression might be important for improving the response rate in clinical PRRT, although the clinical value has to be determined.

Gene therapy

In general, gene transfer methods can be applied to induce expression of a desired gene in a cell. This concept has been used mostly for the treatment of cancer [129]. By using a vector, either viral or non-viral, a peptide receptor-encoding gene (or several genes) can be transferred into a tumor cell with the aim to enhance the uptake of radiolabeled peptide analogs. Gene therapy approaches in combination with PRRT might have some advantages: first, transduction of receptors is locally achieved (only in the tumor), leading to a higher tumor-to-background ratio. Second, constitutive receptor expression in the tumor is not required, therefore also receptor-negative tumors could theoretically be treated. And third, the therapeutic effect might be enormously increased by performing a dual gene transfer. For example, a "suicide" gene can be co-transferred with the receptor gene into the tumor cell, which can be simultaneously or subsequently used for treatment. On the other hand, patients with metastatic disease are probably difficult to treat with gene therapy, since this requires systemic administration of gene therapy vectors, with all related risks. Therefore, patients with circumscribed tumor lesions would probably benefit from gene therapy strategies, which is the case in ovarian and glioblastoma cancer patients.

Several groups have explored the possibility to increase sst expression on tumors using gene transfer modalities. One of the first studies using the adenoviral vector AdCMVhSSTr2, encoding the human sst_2, was performed in intraperitoneally growing SKOV3.ip1 human ovarian cancer tumor [130]. Biodistribution and gamma camera imaging showed higher uptake of various radiolabeled sst analogs in infected tumors than in control tumors.

Zinn et al. and Hemminki et al. introduced the concept of dual gene transfer using a replication-incompetent adenoviral vector encoding sst_2 and a so-called "suicide gene": the herpes simplex virus type 1 thymidine kinase (HSV1-tk) [131, 132]. This gene encodes the thymidine kinase (tk) enzyme, that unlike mammalian tk, preferentially phosphorylates acycloguanosines, such as acyclovir (ACV) and ganciclovir (GCV), into monophosphate compounds, which are then converted into di- and triphosphates by cellular enzymes. The triphosphates are subsequently trapped inside the cell. Acycloguanosines are so-called "pro-drugs" since only the phosphorylated forms are incorporated as chain-terminating derivatives into the DNA and/or inhibit DNA polymerase activity, eventually leading to cell kill. Moreover, thymidine analogs (e.g. FIAU, FIRU) do not show toxic effects following phosphorylation and can therefore be used for imaging of HSV1-tk expression. Zinn and co-workers showed that expression of both sst_2 and HSV1-tk following AdTKSSTR infection could be measured with ^{99m}Tc-P2045 and radioiodinated FIAU, respectively, in mice bearing an A-427 tumor [133].

In 2002, Hemminki et al. reported the effects of gene transfer and subsequent treatment of s.c. and i.p. SKOV3.ip1 tumors *in vivo*: Mice were infected intra-tumorally with either AdTKSSTR, the infectivity-enhanced counterpart RGDTKSSTR or control virus [134], followed by GCV treatment. The use of the infectivity-enhanced virus RGDTKSSTR resulted in an improved therapeutic effect compared to controls. Sst_2 expression could be detected with ^{99m}Tc-P2045 imaging for 15 days after viral infection, although the uptake of the tracer decreased over time.

Using the same viral vector, our group showed a non-homogeneous uptake of specific sst_2 and HSV1-tk tracers in U87MG human glioma-bearing nude mice intratumorally infected with Ad5.tk.sst_2, using small animal SPECT/CT imaging (manuscript in progress). Herewith a major hurdle of gene therapy was visualized: poor viral spread is not favorable for the therapeutic outcome.

Rogers and co-workers transfected A-427 tumors *in vivo* with an adenovirus expressing sst_2, AdSSTr2. They performed therapy studies in animals, receiving AdSSTr2 and 400-500 µCi [^{90}Y]SMT-487 [135]. Animals that received viral infection plus radiolabeled peptide treatment showed a significantly reducedt tumor quadrupling time compared to control animals.

Dual gene transfer modalities offers the use of two therapeutic pathways: 1) sst_2-targeted therapy with peptides radiolabeled with, for example, a β-particle emitting radionuclide, such as ^{117}Lu or ^{90}Y, 2) suicide therapy with a pro-drug. Both possibilities can have a wide-spread effect: the first can lead to a high tumoricidal effect, since the cross-fire effect of ^{177}Lu and ^{90}Y can cause double stranded, unrepairable DNA breaks, which leads to cell cycle arrest and eventually apoptosis [136]. In addition, non-infected cells are also treated, due to the long particle range of ^{177}Lu and ^{90}Y. In the second pathway, GCV-triphosphate can migrate through gap-junctions to the surrounding cells that might not have been transfected and apoptosis is induced: the co-called "bystander effect" [137]. These two effects are important since homogeneous transduction of a solid tumor has been rarely achieved [138, 139].

The use of molecular imaging in gene therapy experiments offers the opportunity to provide information about, for example, the location of vector delivery and the extent and magnitude of gene transfer and gene expression. Integrating imaging techniques such as SPECT and PET into these gene therapy protocols will make it possible to determine optimal treatment time points following vector administration. Furthermore, imaging will help to optimize treatment protocols for gene therapy modalities.

III. Combination treatment: radiolabeled peptides plus other therapeutic agents

Chemotherapeutics and Radiosensitizers

Recently, investigations have been started to combine PRRT with either chemotherapy or other radiosensitizing agents to increase therapeutic effects in patients with neuroendocrine tumors. Gotthardt et al. performed mono- and combination treatment in nude mice bearing AR42J tumors [140]. They examined [^{177}Lu-DOTA^{0},Tyr^{3}] octreotide (^{177}Lu-DOTATOC) either alone or in combination with doxorubicin (DX) or cisplatinum (CS) during a four-week period. They found that the combination of ^{177}Lu-DOTATOC plus DX was 14% and that of ^{177}Lu-DOTATOC plus CS was 23% more effective than ^{177}Lu-DOTATOC treatment alone, making the combination "PRRT plus chemotherapy" an effective approach to increase therapeutic efficacy in sst expressing tumors.

In patients, the radiosensitizing agent 5-fluorouracil (5-FU) was investigated in combination with high dose ^{111}In-labeled octreotide [141]. In 21 patients with neuroendocrine tumors, the efficacy and toxicity of this combination treatment was evaluated. The authors found that the combination of high dose [^{111}In-DTPA^{0}] octreotide and 5-FU was safe and symptomatic response rates were at least comparable to those reported for [^{111}In-DTPA^{0}]octreotide treatment alone. Stable disease or improvements in hormonal and functional scan abnormalities in patients with previous progression were achieved with the combination treatment. Our group recently started a pilot trial using the oral pro-drug of 5-FU, capecitabine, in combination with [^{177}Lu-DOTA^{0},Tyr^{3}]octreotate in patients with GEP tumors to investigate the feasibility of combination treatment in these patients.

Johnson et al. recently investigated combination treatment of radiolabeled BN analogs with chemotherapy in a pre-clinical setting [56]. They examined the chemotherapeutic agents docetaxel (DC) and estramustine (EMP) in combination with ^{177}Lu labeled DOTA-8-AOC-BBN(7-14)NH_2 (^{177}Lu-BBN) in a PC-3 flank xenograft model. These chemotherapeutics were chosen since they are currently evaluated in clinical trials for the treatment of androgen independent prostate cancer. They work synergistically as microtubule inhibitors and offer an increased cytotoxic effect; they also exhibit radiosensitization properties. The results showed that mice treated with ^{177}Lu-BBN combined with either DC alone or DC + EMP showed a statistically significant longer survival, 107 and 109 days respectively, than the control animals (50 days). Furthermore, combination therapy demonstrated a significant survival advantage compared to the ^{177}Lu-BBN therapy alone. Blood was analyzed during the experiment until 2 weeks after the final therapy administration and no differences in blood cell counts were found.

Unfortunately, kidney damage was not evaluated in these studies. It is of interest to investigate the effect of chemotherapeutics combined with PRRT on radiation uptake in the kidneys and on the long term renal damage. Wild et al. reported therapy studies investigating the combination of the GLP-receptor binding analog [^{111}In-DTPA^{0}]Exendin-4 and the angiogenesis inhibitor PTK in Rip1Tag2 mice. They found that combination therapy resulted in a significantly lower median tumor volume compared to monotherapy. In addition, this study did not reveal renal toxicity in the group that was treated with the combination [142].

An issue that also needs to be addressed is the effect that chemotherapeutic agents might have on receptor expression on the tumor. Fueger and co-workers examined the possible influence of cytotoxic or cytostatic agents on binding characteristics of an sst ligand *in vitro* [143] and they found a reduced expression of high-affinity DOTA-LAN binding sites in response to the incubation with gemcitabine, camptotecin, mitomycin C and doxorubicin. In the case of gemcitabine, sst was again over-expressed after a 4-day recovery period, indicating that the down-regulation of receptor expression can be reversed. However, *in vivo* studies need to be performed to investigate the effect of chemotherapeutic agents on receptor expression, especially when combination treatment is given.

Combining different radionuclides

In preclinical studies, we found that the anti-tumor effect of radiolabeled sst analogs is dependent on tumor size [65, 66]. In a study comparing two radionuclides coupled to sst analogs, we demonstrated that [^{177}Lu-DOTA^{0}-Tyr^{3}]octreotate has a very good tumor cure rate in small tumors of approximately 0.5 cm^2, while larger tumors of about 7-9 cm^2 were better treated with [^{90}Y-DOTA-Tyr^{3}]octreotide [16]. These results agreed with the mathematical model proposed by O'Donoghue et al. [15]. For different radionuclide energies, the model predicts the chance of curation for different tumor diameters: according to this model, radionuclides with lower energies (e.g. ^{177}Lu) are optimal for small tumors and radionuclides with higher energies (e.g. ^{90}Y) are optimal for larger tumors. This indicates that PRRT in patients with sst$_2$-positive tumors of different sizes might have better potential with a combination of radionuclides with higher and lower energy β-particles. However, the feasibility of this combination treatment should be further evaluated in patients, preferably in a randomized clinical trial.

Hybrid molecules: apoptosis-inducing peptides

The receptor-targeted delivery of cytotoxic agents was first proposed to reduce toxicity of chemotherapeutic drugs in patients [144]. In order to achieve this, chemotherapeutic agents were linked to peptide analogs, resulting in the internalization of the

complete molecule into the tumor cell. It is conceivable that these hybrid peptides can be used to improve PRRT, for example in tumors with a low receptor expression or in non-responding receptor-expressing tumor types [145]. Hofland et al. and Nagy et al. have described the development and anti-tumor action of different cytotoxic sst analogs [145, 146]. Recently, new publications showed that the targeted cytotoxic analog AN-238, a conjugate based on the sst analog RC-121 coupled to a derivative of doxorubicin, could offer a more effective therapy than RC-121 treatment alone in mice bearing human melanoma tumors [147] or endometrial tumors [148]. In addition, the combination of targeted cytotoxic conjugates of luteinizing hormone-releasing hormone (LHRH) (AN-207), somatostatin (AN-238) and BN (AN-215) were tested in mice bearing ovarian tumors [149]. Results showed that AN-238 and AN-215 significantly inhibited tumor growth, the combination being equally effective. The authors concluded that combination treatment is feasible and effective with low toxicity risk [149]. Other studies showed that mice bearing human glioblastomas, U118MG and U87MG, could also be effectively treated with these agents. Both AN-215 and AN-238 strongly reduced tumor growth in glioblastoma-bearing mice [150-152]. These studies show that a wide variety of receptor-expressing tumors can be treated with receptor-targeted chemotherapeutic agents, although tumor cure was not achieved yet in these animal studies. It would be of great interest to investigate the effects on tumor growth with these agents radiolabeled with therapeutic radionuclides or combined with PRRT strategies. Meanwhile, clinical trials using these (unlabeled) targeted chemotherapeutic agents are ongoing [145, 148].

Other examples of hybrid peptides are camptothecin conjugated analogs of sst [153, 154] or BN [155, 156]. Several *in vitro* studies have shown increased efficacy of treatment with camptothecin-sst and camptothecin-BN conjugates compared to camptothecin alone [153-156]. This concept was further investigated in mice bearing NCI-H1299 human non-small cell lung tumors, which were treated with the camptothecin-BN conjugate and a camptothecin-BN analog that does not specifically bind the receptor. Tumor growth was significantly reduced after incubation with the camptothecin-BN conjugate, demonstrating the importance of receptor-specific binding and internalization of the conjugate to the tumor cell for therapeutic purposes [155].

Recently, we investigated the hybrid peptide [RGD-DTPA^0]octreotate radiolabeled with ^{111}In [146, 157-159]. Arg-Gly-Asp (RGD) binds the integrin receptor $\alpha_v\beta_3$ and is known as an apoptosis-inducing agent by direct activation of caspase 3 [160]. We found that [RGD-^{111}In-DTPA^0]octreotate predominantly internalizes via the sst_2, probably due to the higher affinity of octreotate for the sst_2 than that of RGD for the $\alpha_v\beta_3$ [157]. Furthermore, when [RGD-^{111}In-DTPA^0]octreotate was compared with either [^{111}In-DTPA^0]RGD or [^{111}In-DTPA^0]octreotate in a clonogenic survival assay using $sst_2/\alpha_v\beta_3$ expressing tumor cells, [RGD-^{111}In-DTPA^0]octreotate showed the highest

tumoricidal effects [158]. Caspase 3 activity assays confirmed that [RGD-^{111}In-DTPA^{0}] octreotate had the most pronounced activation of this executioner protease in the apoptosis pathway. Unfortunately, *in vivo* studies showed that renal uptake of [RGD-^{111}In-DTPA^{0}]octreotate was high, a disadvantage for PRRT [159]. However, caspase-3 activity after incubation with the unlabeled hybrid peptide was higher than after RGD or DTPA-octreotide alone, making unlabeled [RGD-DTPA^{0}]octreotate during or after PRRT interesting as well [159].

Combining different peptides: Multi-receptor targeting

Many cancer types simultaneous overexpress several peptide receptors [92]. There are a number of possible advantages in utilizing multiple radiolabeled ligands for therapeutic application of neuroendocrine tumors: 1) *in vivo* application of multi-receptor targeting selectively increases the radioactivity accumulation in tumors, 2) some of the receptors are not homogeneously expressed, and by multi-receptor targeting it is possible to achieve a higher tumoricidal effect, 3) there is a reduced risk of loss of some peptide receptors during therapy, due to tumor dedifferentiation and the subsequent loss of some peptide receptors [16].

Reubi et al. performed *in vitro* autoradiography on neuroendocrine tumors including ileal carcinoids, bronchial carcinoids, insulinomas, gastrinomas, glucagonomas and vipomas [92]. They found that all neuroendocrine tumors examined expressed two or more receptors; several combinations of peptides are of interest for optimal targeting of neuroendocrine tumors *in vivo*: 1) combination of ligands for the glucagon-like peptide-1 (GLP-1) and CCK_2 receptors for insulinomas, 2) a mixture of sst_2, GLP-1 and GRP radiolabeled ligands for gastrinomas.

Radiation protection in normal organs

Increasing the therapeutic window can also be achieved by reducing radiation toxicity to normal organs. In peptide(sst)-based therapy, the kidney is one of the dose-limiting organs and some clinical studies showed renal toxicity following PRRT ([161-163]). It is therefore favorable to reduce renal radiation, making it feasible to increase the total amount of injected radioactivity.

It has been found that radiolabeled somatostatin analogs are filtered and reabsorbed in the proximal tubules of rat kidneys [164]. Also, in the human kidney radioactivity was mostly concentrated in the cortex and the megalin/cubulin system was found to play an essential role in the reabsorption of octreotide [165, 166]. In addition, it was shown that 18% of the renal uptake of sst_2 targeting peptides can be dedicated to sst-mediated uptake [167].

Standard procedure to reduce renal uptake during PRRT in our institution is a 4-hour infusion of a mixture of lysine and arginine [17]. We investigated whether oral

administration of lysine could also reduce renal uptake [168]. In rats, oral administration of lysine reduced renal uptake with 40%, comparable to reduction found with intravenous administration of lysine [169].

Moreover, other agents, such as gelofusine [170, 171], colchicine [172] and the radioprotective drug amifostine [173], could improve kidney protection strategies currently used in the clinic.

Conclusion

Many tumors overexpress one or more receptors which can be targeted using receptor-specific radiolabeled peptides. So far, sst-targeting peptides are widely used for imaging and therapy of cancer patients. PRRT with ^{177}Lu labeled somatostatin analogs has resulted in symptomatic improvement, prolonged survival and enhanced quality of life of neuroendocrine tumor patients. PRS and PRRT targeting other tumor-specific receptors, such as GRP and CCK receptors, are well on their way to clinical utilization as well.

Literature shows that it is possible to increase the receptor density on tumor cells using different methods. In PRRT treatment, this would enable the administration of higher therapeutic doses to tumors, which might lead to a higher cure rate in patients.

Targeting one or several tumor-specific receptors by combinations of therapeutic agents, as well as by reducing non-target uptake of radioactivity, will enlarge the therapeutic window of PRRT. Clinical studies will provide more insight in the effects of combination treatment strategies in cancer patients.

References

1. Krenning E.P., Teunissen J.J., Valkema R., deHerder W.W., deJong M. and Kwekkeboom D.J. Molecular radiotherapy with somatostatin analogs for (neuro-)endocrine tumors. *J Endocrinol Invest*, 2005 28(11 Suppl): 146-150.
2. Krenning E.P., Kwekkeboom D.J., Bakker W.H., Breeman W.A., Kooij P.P., Oei H.Y., *et al.* Somatostatin receptor scintigraphy with [^{111}In-DTPA-D-Phe^{1}]- and [^{123}I-Tyr^{3}]-octreotide: the Rotterdam experience with more than 1000 patients. *Eur J Nucl Med*, 1993 20(8): 716-731.
3. Kwekkeboom D., Krenning E.P. and de Jong M. Peptide receptor imaging and therapy. *J Nucl Med*, 2000 41(10): 1704-1713.
4. Valkema R., De Jong M., Bakker W.H., Breeman W.A., Kooij P.P., Lugtenburg P.J., *et al.* Phase I study of peptide receptor radionuclide therapy with [In-DTPA]octreotide: the Rotterdam experience. *Semin Nucl Med*, 2002 32(2): 110-122.
5. Bodei L., Cremonesi M., Zoboli S., Grana C., Bartolomei M., Rocca P., *et al.* Receptor-mediated radionuclide therapy with ^{90}Y-DOTATOC in association with amino acid infusion: a phase I study. *Eur J Nucl Med Mol Imaging*, 2003 30(2): 207-216.
6. Valkema R., Pauwels S., Kvols L.K., Barone R., Jamar F., Bakker W.H., *et al.* Survival and response after peptide receptor radionuclide therapy with [^{90}Y-DOTA^{0},Tyr^{3}]octreotide in patients with advanced gastroenteropancreatic neuroendocrine tumors. *Semin Nucl Med*, 2006 36(2): 147-156.
7. Otte A., Herrmann R., Heppeler A., Behe M., Jermann E., Powell P., *et al.* Yttrium-90 DOTATOC: first clinical results. *Eur J Nucl Med*, 1999 26(11): 1439-1447.
8. Waldherr C., Pless M., Maecke H.R., Schumacher T., Crazzolara A., Nitzsche E.U., *et al.* Tumor response and clinical benefit in neuroendocrine tumors after 7.4 GBq ^{90}Y-DOTATOC. *J Nucl Med*, 2002 43(5): 610-616.
9. Chinol M., Bodei L., Cremonesi M. and Paganelli G. Receptor-mediated radiotherapy with Y-DOTA-DPhe-Tyr-octreotide: the experience of the European Institute of Oncology Group. *Semin Nucl Med*, 2002 32(2): 141-147.
10. van Essen M., krenning E.P., de Jong M., Valkema R. and Kwekkeboom D.J. Peptide receptor radionuclide therapy with radiolabelled somatostatin analogues in patients with somatostatin receptor positive tumours. 2007.
11. Reubi J.C., Schar J.C., Waser B., Wenger S., Heppeler A., Schmitt J.S., *et al.* Affinity profiles for human somatostatin receptor subtypes SST1-SST5 of somatostatin radiotracers selected for scintigraphic and radiotherapeutic use. *Eur J Nucl Med*, 2000 27(3): 273-282.
12. de Jong M., Breeman W.A., Bakker W.H., Kooij P.P., Bernard B.F., Hofland L.J., *et al.* Comparison of ^{111}In-labeled somatostatin analogues for tumor scintigraphy and radionuclide therapy. *Cancer Res*, 1998 58(3): 437-441.
13. Esser J.P., Krenning E.P., Teunissen J.J., Kooij P.P., van Gameren A.L., Bakker W.H., *et al.* Comparison of [^{177}Lu-DOTA^{3},Tyr^{3}]octreotate and [^{177}Lu-DOTA^{0},Tyr^{3}]octreotide: which peptide is preferable for PRRT? *Eur J Nucl Med Mol Imaging*, 2006 33(11): 1346-1351.
14. Kwekkeboom D.J., Bakker W.H., Kooij P.P., Konijnenberg M.W., Srinivasan A., Erion J.L., *et al.* [^{177}Lu-DOTA^{0},Tyr^{3}]octreotate: comparison with [^{111}In-DTPA^{0}]octreotide in patients. *Eur J Nucl Med*, 2001 28(9): 1319-1325.
15. O'Donoghue J.A., Bardies M. and Wheldon T.E. Relationships between tumor size and curability for uniformly targeted therapy with beta-emitting radionuclides. *J Nucl Med*, 1995 36(10): 1902-1909.
16. de Jong M., Breeman W.A., Valkema R., Bernard B.F. and Krenning E.P. Combination radionuclide therapy using ^{177}Lu- and ^{90}Y-labeled somatostatin analogs. *J Nucl Med*, 2005 46 Suppl 1: 13S-17S.

17. Kwekkeboom D.J., Teunissen J.J., Bakker W.H., Kooij P.P., de Herder W.W., Feelders R.A., *et al.* Radiolabeled somatostatin analog [^{177}Lu-DOTA^{0},Tyr^{3}]octreotate in patients with endocrine gastroenteropancreatic tumors. *J Clin Oncol*, 2005 23(12): 2754-2762.
18. Teunissen J.J., Kwekkeboom D.J. and Krenning E.P. Quality of life in patients with gastroenteropancreatic tumors treated with [^{177}Lu-DOTA^{0},Tyr^{3}]octreotate. *J Clin Oncol*, 2004 22(13): 2724-2729.
19. Zhang H., Chen J., Waldherr C., Hinni K., Waser B., Reubi J.C., *et al.* Synthesis and evaluation of bombesin derivatives on the basis of pan-bombesin peptides labeled with indium-111, lutetium-177, and yttrium-90 for targeting bombesin receptor-expressing tumors. *Cancer Res*, 2004 64(18): 6707-6715.
20. Breeman W.A., Hofland L.J., de Jong M., Bernard B.F., Srinivasan A., Kwekkeboom D.J., *et al.* Evaluation of radiolabelled bombesin analogues for receptor-targeted scintigraphy and radiotherapy. *Int J Cancer*, 1999 81(4): 658-665.
21. Ginj M., Zhang H., Waser B., Cescato R., Wild D., Wang X., *et al.* Radiolabeled somatostatin receptor antagonists are preferable to agonists for *in vivo* peptide receptor targeting of tumors. *Proc Natl Acad Sci U S A*, 2006 103(44): 16436-16441.
22. Gabriel M., Decristoforo C., Donnemiller E., Ulmer H., Watfah Rychlinski C., Mather S.J., *et al.* An intrapatient comparison of ^{99m}Tc-EDDA/HYNIC-TOC with ^{111}In-DTPA-octreotide for diagnosis of somatostatin receptor-expressing tumors. *J Nucl Med*, 2003 44(5): 708-716.
23. Bangard M., Behe M., Guhlke S., Otte R., Bender H., Maecke H.R., *et al.* Detection of somatostatin receptor-positive tumours using the new ^{99m}Tc-tricine-HYNIC-D-Phe^{1}-Tyr^{3}-octreotide: first results in patients and comparison with ^{111}In-DTPA-D-Phe^{1}-octreotide. *Eur J Nucl Med*, 2000 27(6): 628-637.
24. Hubalewska-Dydejczyk A., Fross-Baron K., Golkowski F., Sowa-Staszczak A., Mikolajczak R. and Huszno B. ^{99m}Tc-EDDA/HYNIC-octreotate in detection of atypical bronchial carcinoid. *Exp Clin Endocrinol Diabetes*, 2007 115(1): 47-49.
25. Hubalewska-Dydejczyk A., Fross-Baron K., Mikolajczak R., Maecke H.R., Huszno B., Pach D., *et al.* ^{99m}Tc-EDDA/HYNIC-octreotate scintigraphy, an efficient method for the detection and staging of carcinoid tumours: results of 3 years' experience. *Eur J Nucl Med Mol Imaging*, 2006 33(10): 1123-1133.
26. Hubalewska-Dydejczyk A., Szybinski P., Fross-Baron K., Mikolajczak R., Huszno B. and Sowa-Staszczak A. ^{99m}Tc-EDDA/HYNIC-octreotate - a new radiotracer for detection and staging of NET: a case of metastatic duodenal carcinoid. *Nucl Med Rev Cent East Eur*, 2005 8(2): 155-156.
27. Gabriel M., Decristoforo C., Maina T., Nock B., vonGuggenberg E., Cordopatis P., *et al.* ^{99m}Tc-N_4-[Tyr^{3}]Octreotate Versus ^{99m}Tc-EDDA/HYNIC-[Tyr^{3}]Octreotide: an intrapatient comparison of two novel Technetium-99m labeled tracers for somatostatin receptor scintigraphy. *Cancer Biother Radiopharm*, 2004 19(1): 73-79.
28. Nikolopoulou A., Maina T., Sotiriou P., Cordopatis P. and Nock B.A. Tetraamine-modified octreotide and octreotate: labeling with ^{99m}Tc and preclinical comparison in AR4-2J cells and AR4-2J tumor-bearing mice. *J Pept Sci*, 2006 12(2): 124-131.
29. Decristoforo C., Maina T., Nock B., Gabriel M., Cordopatis P. and Moncayo R. ^{99m}Tc-Demotate 1: first data in tumour patients-results of a pilot/phase I study. *Eur J Nucl Med Mol Imaging*, 2003 30(9): 1211-1219.
30. Meisetschlager G., Poethko T., Stahl A., Wolf I., Scheidhauer K., Schottelius M., *et al.* Gluc-Lys([^{18}F]FP)-TOCA PET in patients with SSTR-positive tumors: biodistribution and diagnostic evaluation compared with [^{111}In]DTPA-octreotide. *J Nucl Med*, 2006 47(4): 566-573.
31. Anderson C.J., Dehdashti F., Cutler P.D., Schwarz S.W., Laforest R., Bass L.A., *et al.* ^{64}Cu-TETA-octreotide as a PET imaging agent for patients with neuroendocrine tumors. *J Nucl Med*, 2001 42(2): 213-221.

32. Breeman W.A., de Jong M., de Blois E., Bernard B.F., Konijnenberg M. and Krenning E.P. Radiolabelling DOTA-peptides with ^{68}Ga. *Eur J Nucl Med Mol Imaging*, 2005 32(4): 478-485.
33. Kowalski J., Henze M., Schuhmacher J., Macke H.R., Hofmann M. and Haberkorn U. Evaluation of positron emission tomography imaging using [^{68}Ga]-DOTA-D Phe^{1}-Tyr^{3}-Octreotide in comparison to [^{111}In]-DTPAOC SPECT. First results in patients with neuroendocrine tumors. *Mol Imaging Biol*, 2003 5(1): 42-48.
34. Gabriel M., Decristoforo C., Kendler D., Dobrozemsky G., Heute D., Uprimny C., *et al.* ^{68}Ga-DOTA-Tyr^{3}-octreotide PET in neuroendocrine tumors: comparison with somatostatin receptor scintigraphy and CT. *J Nucl Med*, 2007 48(4): 508-518.
35. Kulaksiz H., Eissele R., Rossler D., Schulz S., Hollt V., Cetin Y., *et al.* Identification of somatostatin receptor subtypes 1, 2A, 3, and 5 in neuroendocrine tumours with subtype specific antibodies. *Gut*, 2002 50(1): 52-60.
36. Reubi J.C., Waser B., Schaer J.C. and Laissue J.A. Somatostatin receptor sst_1-sst_5 expression in normal and neoplastic human tissues using receptor autoradiography with subtype-selective ligands. *Eur J Nucl Med*, 2001 28(7): 836-846.
37. Ginj M., Schmitt J.S., Chen J., Waser B., Reubi J.C., de Jong M., *et al.* Design, synthesis, and biological evaluation of somatostatin-based radiopeptides. *Chem Biol*, 2006 13(10): 1081-1090.
38. Wild D., Macke H.R., Waser B., Reubi J.C., Ginj M., Rasch H., *et al.* ^{68}Ga-DOTANOC: a first compound for PET imaging with high affinity for somatostatin receptor subtypes 2 and 5. *Eur J Nucl Med Mol Imaging*, 2005 32(6): 724.
39. Reubi J.C., Wenger S., Schmuckli-Maurer J., Schaer J.C. and Gugger M. Bombesin receptor subtypes in human cancers: detection with the universal radioligand ^{125}I-[D-TYR^{6},beta-ALA^{11}, PHE^{13}, NLE^{14}] bombesin(6-14). *Clin Cancer Res*, 2002 8(4): 1139-1146.
40. Jemal A., Siegel R., Ward E., Murray T., Xu J. and Thun M.J. Cancer statistics, 2007. *CA Cancer J Clin*, 2007 57(1): 43-66.
41. Breeman W.A., de Jong M., Bernard B., Hofland L.J., Srinivasan A., van der Pluijm M., *et al.* Tissue distribution and metabolism of radioiodinated DTPA^{0}, D-Tyr^{1} and Tyr^{3} derivatives of octreotide in rats. *Anticancer Res*, 1998 18(1A): 83-89.
42. Nock B., Nikolopoulou A., Chiotellis E., Loudos G., Maintas D., Reubi J.C., *et al.* [^{99m}Tc] Demobesin 1, a novel potent bombesin analogue for GRP receptor-targeted tumour imaging. *Eur J Nucl Med Mol Imaging*, 2003 30(2): 247-258.
43. Nock B.A., Nikolopoulou A., Galanis A., Cordopatis P., Waser B., Reubi J.C., *et al.* Potent bombesin-like peptides for GRP-receptor targeting of tumors with ^{99m}Tc: a preclinical study. *J Med Chem*, 2005 48(1): 100-110.
44. Van de Wiele C., Dumont F., Vanden Broecke R., Oosterlinck W., Cocquyt V., Serreyn R., *et al.* Technetium-99m RP527, a GRP analogue for visualisation of GRP receptor- expressing malignancies: a feasibility study. *Eur J Nucl Med*, 2000 27(11): 1694-1699.
45. van Bokhoven A., Varella-Garcia M., Korch C., Johannes W.U., Smith E.E., Miller H.L., *et al.* Molecular characterization of human prostate carcinoma cell lines. *Prostate*, 2003 57(3): 205-225.
46. Hoffman T.J., Gali H., Smith C.J., Sieckman G.L., Hayes D.L., Owen N.K., *et al.* Novel series of ^{111}In-labeled bombesin analogs as potential radiopharmaceuticals for specific targeting of gastrin-releasing peptide receptors expressed on human prostate cancer cells. *J Nucl Med*, 2003 44(5): 823-831.
47. Breeman W.A., de Jong M., Erion J.L., Bugaj J.E., Srinivasan A., Bernard B.F., *et al.* Preclinical comparison of ^{111}In-labeled DTPA- or DOTA-bombesin analogs for receptor-targeted scintigraphy and radionuclide therapy. *J Nucl Med*, 2002 43(12): 1650-1656.
48. Ferro-Flores G., Arteaga de Murphy C., Rodriguez-Cortes J., Pedraza-Lopez M. and Ramirez-Iglesias M.T. Preparation and evaluation of ^{99m}Tc-EDDA/HYNIC-[Lys^{3}]-bombesin for imaging gastrin-releasing peptide receptor-positive tumours. *Nucl Med Commun*, 2006 27(4): 371-376.

49. Garcia Garayoa E., Ruegg D., Blauenstein P., Zwimpfer M., Khan I.U., Maes V., *et al.* Chemical and biological characterization of new $Re(CO_3)/[^{99m}Tc](CO_3)$ bombesin analogues. *Nucl Med Biol*, 2007 34(1): 17-28.
50. Reubi J.C., Macke H.R. and Krenning E.P. Candidates for peptide receptor radiotherapy today and in the future. *J Nucl Med*, 2005 46 Suppl 1: 67S-75S.
51. de Visser M., Bernard H.F., Erion J.L., Schmidt M.A., Srinivasan A., Waser B., *et al.* Novel ^{111}In-labelled bombesin analogues for molecular imaging of prostate tumours. *Eur J Nucl Med Mol Imaging*, 2007.
52. Zhang H., Schuhmacher J., Waser B., Wild D., Eisenhut M., Reubi J.C., *et al.* DOTA-PESIN, a DOTA-conjugated bombesin derivative designed for the imaging and targeted radionuclide treatment of bombesin receptor-positive tumours. *Eur J Nucl Med Mol Imaging*, 2007.
53. Yang Y.S., Zhang X., Xiong Z. and Chen X. Comparative *in vitro* and *in vivo* evaluation of two ^{64}Cu-labeled bombesin analogs in a mouse model of human prostate adenocarcinoma. *Nucl Med Biol*, 2006 33(3): 371-380.
54. Smith C.J., Gali H., Sieckman G.L., Hayes D.L., Owen N.K., Mazuru D.G., *et al.* Radiochemical investigations of ^{177}Lu-DOTA-8-Aoc-BBN[7-14]NH_2: an *in vitro/in vivo* assessment of the targeting ability of this new radiopharmaceutical for PC-3 human prostate cancer cells. *Nucl Med Biol*, 2003 30(2): 101-109.
55. Rogers B.E., Bigott H.M., McCarthy D.W., Della Manna D., Kim J., Sharp T.L., *et al.* MicroPET imaging of a gastrin-releasing peptide receptor-positive tumor in a mouse model of human prostate cancer using a ^{64}Cu-labeled bombesin analogue. *Bioconjug Chem*, 2003 14(4): 756-763.
56. Johnson C.V., Shelton T., Smith C.J., Ma L., Perry M.C., Volkert W.A., *et al.* Evaluation of combined ^{177}Lu-DOTA-8-AOC-BBN(7-14)NH_2 GRP receptor-targeted radiotherapy and chemotherapy in PC-3 human prostate tumor cell xenografted SCID mice. *Cancer Biother Radiopharm*, 2006 21(2): 155-166.
57. Biddlecombe G.B., Rogers B.E., Visser M.D., Parry J.J., Jong M.D., Erion J.L., *et al.* Molecular Imaging of Gastrin-Releasing Peptide Receptor-Positive Tumors in Mice Using ^{64}Cu- and ^{86}Y-DOTA-(Pro^1,Tyr^4)-Bombesin(1-14). *Bioconjug Chem*, 2007.
58. Lantry L.E., Cappelletti E., Maddalena M.E., Fox J.S., Feng W., Chen J., *et al.* 177Lu-AMBA: Synthesis and characterization of a selective ^{177}Lu-labeled GRP-R agonist for systemic radiotherapy of prostate cancer. *J Nucl Med*, 2006 47(7): 1144-1152.
59. Van de Wiele C., Dumont F., van Belle S., Slegers G., Peers S.H. and Dierckx R.A. Is there a role for agonist gastrin-releasing peptide receptor radioligands in tumour imaging? *Nucl Med Commun*, 2001 22(1): 5-15.
60. Baum R., Prasad V., Mutloka N., Frischknecht M., Maecke H. and Reubi J. Molecular imaging of bombesin receptors in various tumors by Ga-68 AMBA PET/CT: First results *J Nucl Med*, 2007 48(supplement 2): 79P.
61. de Visser M., van Weerden W.M., Melis M., Krenning E.P. and de Jong M. Radiolabeled bombesin analogs in preclinical studies. *J Nucl Med*, 2007 48, suppl 2: 24P.
62. Mancuso A., Oudard S. and Sternberg C.N. Effective chemotherapy for hormone-refractory prostate cancer (HRPC): present status and perspectives with taxane-based treatments. *Crit Rev Oncol Hematol*, 2007 61(2): 176-185.
63. Oudard S., Banu E., Beuzeboc P., Voog E., Dourthe L.M., Hardy-Bessard A.C., *et al.* Multicenter randomized phase II study of two schedules of docetaxel, estramustine, and prednisone versus mitoxantrone plus prednisone in patients with metastatic hormone-refractory prostate cancer. *J Clin Oncol*, 2005 23(15): 3343-3351.
64. de Visser M., van Weerden W.M., de Ridder C.M., Reneman S., Melis M., Krenning E.P., *et al.* Androgen-dependent expression of the gastrin-releasing Peptide receptor in human prostate tumor xenografts. *J Nucl Med*, 2007 48(1): 88-93.

65. de Jong M., Breeman W.A., Bernard B.F., Bakker W.H., Visser T.J., Kooij P.P., *et al.* Tumor response after [^{90}Y-DOTA^{0},Tyr^{3}]octreotide radionuclide therapy in a transplantable rat tumor model is dependent on tumor size. *J Nucl Med*, 2001 42(12): 1841-1846.
66. de Jong M., Breeman W.A., Bernard B.F., Bakker W.H., Schaar M., van Gameren A., *et al.* [^{177}Lu-DOTA^{0},Tyr^{3}] octreotate for somatostatin receptor-targeted radionuclide therapy. *Int J Cancer*, 2001 92(5): 628-633.
67. De Jong M., Valkema R., Jamar F., Kvols L.K., Kwekkeboom D.J., Breeman W.A., *et al.* Somatostatin receptor-targeted radionuclide therapy of tumors: preclinical and clinical findings. *Semin Nucl Med*, 2002 32(2): 133-140.
68. Reubi J.C., Waser B., Friess H., Buchler M. and Laissue J. Neurotensin receptors: a new marker for human ductal pancreatic adenocarcinoma. *Gut*, 1998 42(4): 546-550.
69. Kuhar M.J. Imaging receptors for drugs in neural tissue. *Neuropharmacology*, 1987 26(7B): 911-916.
70. Ehlers R.A., Kim S., Zhang Y., Ethridge R.T., Murrilo C., Hellmich M.R., *et al.* Gut peptide receptor expression in human pancreatic cancers. *Ann Surg*, 2000 231(6): 838-848.
71. Zhang K., An R., Gao Z., Zhang Y. and Aruva M.R. Radionuclide imaging of small-cell lung cancer (SCLC) using ^{99m}Tc-labeled neurotensin peptide 8-13. *Nucl Med Biol*, 2006 33(4): 505-512.
72. Nock B.A., Nikolopoulou A., Reubi J.C., Maes V., Conrath P., Tourwe D., *et al.* Toward stable N_4-modified neurotensins for NTS1-receptor-targeted tumor imaging with ^{99m}Tc. *J Med Chem*, 2006 49(15): 4767-4776.
73. Maes V., Garcia-Garayoa E., Blauenstein P. and Tourwe D. Novel ^{99m}Tc-labeled neurotensin analogues with optimized biodistribution properties. *J Med Chem*, 2006 49(5): 1833-1836.
74. Garcia-Garayoa E., Maes V., Blauenstein P., Blanc A., Hohn A., Tourwe D., *et al.* Double-stabilized neurotensin analogues as potential radiopharmaceuticals for NTR-positive tumors. *Nucl Med Biol*, 2006 33(4): 495-503.
75. Garcia-Garayoa E., Allemann-Tannahill L., Blauenstein P., Willmann M., Carrel-Remy N., Tourwe D., *et al. In vitro* and *in vivo* evaluation of new radiolabeled neurotensin(8-13) analogues with high affinity for NT1 receptors. *Nucl Med Biol*, 2001 28(1): 75-84.
76. Lugrin D., Vecchini F., Doulut S., Rodriguez M., Martinez J. and Kitabgi P. Reduced peptide bond pseudopeptide analogues of neurotensin: binding and biological activities, and *in vitro* metabolic stability. *Eur J Pharmacol*, 1991 205(2): 191-198.
77. de Visser M., Janssen P.J., Srinivasan A., Reubi J.C., Waser B., Erion J.L., *et al.* Stabilised ^{111}In-labelled DTPA- and DOTA-conjugated neurotensin analogues for imaging and therapy of exocrine pancreatic cancer. *Eur J Nucl Med Mol Imaging*, 2003 30(8): 1134-1139.
78. Emami B., Lyman J., Brown A., Coia L., Goitein M., Munzenrider J.E., *et al.* Tolerance of normal tissue to therapeutic irradiation. *Int J Radiat Oncol Biol Phys*, 1991 21(1): 109-122.
79. Buchegger F., Bonvin F., Kosinski M., Schaffland A.O., Prior J., Reubi J.C., *et al.* Radiolabeled neurotensin analog, ^{99m}Tc-NT-XI, evaluated in ductal pancreatic adenocarcinoma patients. *J Nucl Med*, 2003 44(10): 1649-1654.
80. Reubi J.C., Chayvialle J.A., Franc B., Cohen R., Calmettes C. and Modigliani E. Somatostatin receptors and somatostatin content in medullary thyroid carcinomas. *Lab Invest*, 1991 64(4): 567-573.
81. Kwekkeboom D.J., Reubi J.C., Lamberts S.W., Bruining H.A., Mulder A.H., Oei H.Y., *et al. In vivo* somatostatin receptor imaging in medullary thyroid carcinoma. *J Clin Endocrinol Metab*, 1993 76(6): 1413-1417.
82. Reubi J.C., Schaer J.C. and Waser B. Cholecystokinin(CCK)-A and CCK-B/gastrin receptors in human tumors. *Cancer Res*, 1997 57(7): 1377-1386.

83. Behr T.M., Jenner N., Radetzky S., Behe M., Gratz S., Yucekent S., *et al.* Targeting of cholecystokinin-B/gastrin receptors *in vivo*: preclinical and initial clinical evaluation of the diagnostic and therapeutic potential of radiolabelled gastrin. *Eur J Nucl Med*, 1998 25(4): 424-430.
84. Reubi J.C., Waser B., Schaer J.C., Laederach U., Erion J., Srinivasan A., *et al.* Unsulfated DTPA- and DOTA-CCK analogs as specific high-affinity ligands for CCK-B receptor-expressing human and rat tissues *in vitro* and *in vivo*. *Eur J Nucl Med*, 1998 25(5): 481-490.
85. de Jong M., Bakker W.H., Bernard B.F., Valkema R., Kwekkeboom D.J., Reubi J.C., *et al.* Preclinical and initial clinical evaluation of ^{111}In-labeled nonsulfated CCK8 analog: a peptide for CCK-B receptor-targeted scintigraphy and radionuclide therapy. *J Nucl Med*, 1999 40(12): 2081-2087.
86. Kwekkeboom D.J., Bakker W.H., Kooij P.P., Erion J., Srinivasan A., de Jong M., *et al.* Cholecystokinin receptor imaging using an octapeptide DTPA-CCK analogue in patients with medullary thyroid carcinoma. *Eur J Nucl Med*, 2000 27(9): 1312-1317.
87. Behr T.M., Jenner N., Behe M., Angerstein C., Gratz S., Raue F., *et al.* Radiolabeled peptides for targeting cholecystokinin-B/gastrin receptor-expressing tumors. *J Nucl Med*, 1999 40(6): 1029-1044.
88. Nock B.A., Maina T., Behe M., Nikolopoulou A., Gotthardt M., Schmitt J.S., *et al.* CCK-2/gastrin receptor-targeted tumor imaging with ^{99m}Tc-labeled minigastrin analogs. *J Nucl Med*, 2005 46(10): 1727-1736.
89. Gotthardt M., Behe M.P., Beuter D., Battmann A., Bauhofer A., Schurrat T., *et al.* Improved tumour detection by gastrin receptor scintigraphy in patients with metastasised medullary thyroid carcinoma. *Eur J Nucl Med Mol Imaging*, 2006 33(11): 1273-1279.
90. Gotthardt M., Behe M.P., Grass J., Bauhofer A., Rinke A., Schipper M.L., *et al.* Added value of gastrin receptor scintigraphy in comparison to somatostatin receptor scintigraphy in patients with carcinoids and other neuroendocrine tumours. *Endocr Relat Cancer*, 2006 13(4): 1203-1211.
91. Mayo K.E., Miller L.J., Bataille D., Dalle S., Goke B., Thorens B., *et al.* International Union of Pharmacology. XXXV. The glucagon receptor family. *Pharmacol Rev*, 2003 55(1): 167-194.
92. Reubi J.C. and Waser B. Concomitant expression of several peptide receptors in neuroendocrine tumours: molecular basis for *in vivo* multireceptor tumour targeting. *Eur J Nucl Med Mol Imaging*, 2003 30(5): 781-793.
93. Korner M., Stockli M., Waser B. and Reubi J.C. GLP-1 Receptor Expression in Human Tumors and Human Normal Tissues: Potential for *In Vivo* Targeting. *J Nucl Med*, 2007 48(5): 736-743.
94. Meier J.J. and Nauck M.A. Glucagon-like peptide 1(GLP-1) in biology and pathology. *Diabetes Metab Res Rev*, 2005 21(2): 91-117.
95. Hassan M., Eskilsson A., Nilsson C., Jonsson C., Jacobsson H., Refai E., *et al. In vivo* dynamic distribution of ^{131}I-glucagon-like peptide-1 (7-36) amide in the rat studied by gamma camera. *Nucl Med Biol*, 1999 26(4): 413-420.
96. Gotthardt M., Fischer M., Naeher I., Holz J.B., Jungclas H., Fritsch H.W., *et al.* Use of the incretin hormone glucagon-like peptide-1 (GLP-1) for the detection of insulinomas: initial experimental results. *Eur J Nucl Med Mol Imaging*, 2002 29(5): 597-606.
97. Gotthardt M., Lalyko G., van Eerd-Vismale J., Keil B., Schurrat T., Hower M., *et al.* A new technique for *in vivo* imaging of specific GLP-1 binding sites: First results in small rodents. *Regul Pept*, 2006.
98. Wild D., Behe M., Wicki A., Storch D., Waser B., Gotthardt M., *et al.* [Lys40(Ahx-DTPA-^{111}In)NH_2]exendin-4, a very promising ligand for glucagon-like peptide-1 (GLP-1) receptor targeting. *J Nucl Med*, 2006 47(12): 2025-2033.
99. Wicki A., Wild D., Storch D., Seemayer C., Gotthardt M., Behe M., *et al.* [Lys40(Ahx-DTPA-^{111}In)NH_2]-Exendin-4 Is a Highly Efficient Radiotherapeutic for Glucagon-Like Peptide-1 Receptor-Targeted Therapy for Insulinoma. *Clin Cancer Res*, 2007 13(12): 3696-3705.

100. Brooks P.C. Role of integrins in angiogenesis. *Eur J Cancer*, 1996 32A(14): 2423-2429.
101. Plow E.F., Haas T.A., Zhang L., Loftus J. and Smith J.W. Ligand binding to integrins. *J Biol Chem*, 2000 275(29): 21785-21788.
102. Gurrath M., Muller G., Kessler H., Aumailley M. and Timpl R. Conformation/activity studies of rationally designed potent anti-adhesive RGD peptides. *Eur J Biochem*, 1992 210(3): 911-921.
103. Aumailley M., Gurrath M., Muller G., Calvete J., Timpl R. and Kessler H. Arg-Gly-Asp constrained within cyclic pentapeptides. Strong and selective inhibitors of cell adhesion to vitronectin and laminin fragment P1. *FEBS Lett*, 1991 291(1): 50-54.
104. van Hagen P.M., Breeman W.A., Bernard H.F., Schaar M., Mooij C.M., Srinivasan A., *et al.* Evaluation of a radiolabelled cyclic DTPA-RGD analogue for tumour imaging and radionuclide therapy. *Int J Cancer*, 2000 90(4): 186-198.
105. Chen X., Park R., Tohme M., Shahinian A.H., Bading J.R. and Conti P.S. MicroPET and autoradiographic imaging of breast cancer alpha v-integrin expression using 18F- and ^{64}Cu-labeled RGD peptide. *Bioconjug Chem*, 2004 15(1): 41-49.
106. Cai W., Zhang X., Wu Y. and Chen X. A thiol-reactive 18F-labeling agent, N-[2-(4-^{18}F-fluorobenzamido)ethyl]maleimide, and synthesis of RGD peptide-based tracer for PET imaging of alpha$_v$beta$_3$ integrin expression. *J Nucl Med*, 2006 47(7): 1172-1180.
107. Haubner R., Kuhnast B., Mang C., Weber W.A., Kessler H., Wester H.J., *et al.* [^{18}F]Galacto-RGD: synthesis, radiolabeling, metabolic stability, and radiation dose estimates. *Bioconjug Chem*, 2004 15(1): 61-69.
108. Beer A.J., Haubner R., Sarbia M., Goebel M., Luderschmidt S., Grosu A.L., *et al.* Positron emission tomography using [^{18}F]Galacto-RGD identifies the level of integrin alpha$_v$beta$_3$ expression in man. *Clin Cancer Res*, 2006 12(13): 3942-3949.
109. Beer A.J., Haubner R., Wolf I., Goebel M., Luderschmidt S., Niemeyer M., *et al.* PET-based human dosimetry of ^{18}F-galacto-RGD, a new radiotracer for imaging alpha$_v$beta$_3$ expression. *J Nucl Med*, 2006 47(5): 763-769.
110. Beer A.J., Haubner R., Goebel M., Luderschmidt S., Spilker M.E., Wester H.J., *et al.* Biodistribution and pharmacokinetics of the alpha$_v$beta$_3$-selective tracer ^{18}F-galacto-RGD in cancer patients. *J Nucl Med*, 2005 46(8): 1333-1341.
111. Dijkgraaf I., Kruijtzer J.A., Liu S., Soede A.C., Oyen W.J., Corstens F.H., *et al.* Improved targeting of the alpha$_v$beta$_3$ integrin by multimerisation of RGD peptides. *Eur J Nucl Med Mol Imaging*, 2007 34(2): 267-273.
112. Dijkgraaf I., Rijnders A.Y., Soede A., Dechesne A.C., van Esse G.W., Brouwer A.J., *et al.* Synthesis of DOTA-conjugated multivalent cyclic-RGD peptide dendrimers via 1,3-dipolar cycloaddition and their biological evaluation: implications for tumor targeting and tumor imaging purposes. *Org Biomol Chem*, 2007 5(6): 935-944.
113. Dijkgraaf I., Liu S., Kruijtzer J.A., Soede A.C., Oyen W.J., Liskamp R.M., *et al.* Effects of linker variation on the *in vitro* and *in vivo* characteristics of an ^{111}In-labeled RGD peptide. *Nucl Med Biol*, 2007 34(1): 29-35.
114. Dijkgraaf I., Kruijtzer J.A., Frielink C., Corstens F.H., Oyen W.J., Liskamp R.M., *et al.* Alpha $_v$beta$_3$ integrin-targeting of intraperitoneally growing tumors with a radiolabeled RGD peptide. *Int J Cancer*, 2007 120(3): 605-610.
115. Kimura N., Hayafuji C., Konagaya H. and Takahashi K. 17 beta-estradiol induces somatostatin (SRIF) inhibition of prolactin release and regulates SRIF receptors in rat anterior pituitary cells. *Endocrinology*, 1986 119(3): 1028-1036.
116. Presky D.H. and Schonbrunn A. Somatostatin pretreatment increases the number of somatostatin receptors in GH4C1 pituitary cells and does not reduce cellular responsiveness to somatostatin. *J Biol Chem*, 1988 263(2): 714-721.

117. Kimura N., Hayafuji C. and Kimura N. Characterization of 17-beta-estradiol-dependent and -independent somatostatin receptor subtypes in rat anterior pituitary. *J Biol Chem*, 1989 264(12): 7033-7040.
118. Slama A., Videau C., Kordon C. and Epelbaum J. Estradiol regulation of somatostatin receptors in the arcuate nucleus of the female rat. *Neuroendocrinology*, 1992 56(2): 240-245.
119. Vidal C., Rauly I., Zeggari M., Delesque N., Esteve J.P., Saint-Laurent N., *et al.* Up-regulation of somatostatin receptors by epidermal growth factor and gastrin in pancreatic cancer cells. *Mol Pharmacol*, 1994 46(1): 97-104.
120. Visser-Wisselaar H.A., Van Uffelen C.J., Van Koetsveld P.M., Lichtenauer-Kaligis E.G., Waaijers A.M., Uitterlinden P., *et al.* 17-beta-estradiol-dependent regulation of somatostatin receptor subtype expression in the 7315b prolactin secreting rat pituitary tumor *in vitro* and *in vivo*. *Endocrinology*, 1997 138(3): 1180-1189.
121. Froidevaux S., Hintermann E., Torok M., Macke H.R., Beglinger C. and Eberle A.N. Differential regulation of somatostatin receptor type 2 (sst_2) expression in AR4-2J tumor cells implanted into mice during octreotide treatment. *Cancer Res*, 1999 59(15): 3652-3657.
122. Viguerie N., Esteve J.P., Susini C., Logsdon C.D., Vaysse N. and Ribet A. Dexamethasone effects on somatostatin receptors in pancreatic acinar AR4-2J cells. *Biochem Biophys Res Commun*, 1987 147(3): 942-948.
123. Gunn S.H., Schwimer J.E., Cox M., Anthony C.T., O'Dorisio M.S. and Woltering E.A. *In vitro* modeling of the clinical interactions between octreotide and ^{111}In-pentetreotide: is there evidence of somatostatin receptor downregulation? *J Nucl Med*, 2006 47(2): 354-359.
124. Behe M., Püsken M., Henzel M., Gross M., Reitz I., Engenhart-Cabillic E., *et al.* Upregulation of gastrin and somatostatin receptor after irradiation. *Eur J Nucl Med Mol Imaging*, 2003 30: S218.
125. Behe M., Koller S., Püsken M., Gross M., Alfke H., Keil B., *et al.* Irradiation-induced upregulation of somatostatin and gastrin receptors *in vitro* and *in vivo*. *Eur J Nucl Med Mol Imaging*, 2004 31: S237-238.
126. Oddstig J., Bernhardt P., Nilsson O., Ahlman H. and Forssell-Aronsson E. Radiation-induced up-regulation of somatostatin receptor expression in small cell lung cancer *in vitro*. *Nucl Med Biol*, 2006 33(7): 841-846.
127. Capello A., Krenning E., Bernard B., Reubi J.C., Breeman W. and de Jong M. ^{111}In-labelled somatostatin analogues in a rat tumour model: somatostatin receptor status and effects of peptide receptor radionuclide therapy. *Eur J Nucl Med Mol Imaging*, 2005 32(11): 1288-1295.
128. Melis M., Forrer F., Capello A., Bijster M., Bernard H.F., Reubi J.-C., *et al.* Up-regulation of somatostatin receptor density on rat CA20948 tumours escaped from low dose [^{177}Lu-DOTA^0,Tyr^3] octreotate therapy. *Quarterly Journal of Nuclear Medicine and Molecular Imaging*, 2007 51.
129. Seth P. Vector-mediated cancer gene therapy: an overview. *Cancer Biol Ther*, 2005 4(5): 512-517.
130. Rogers B.E., McLean S.F., Kirkman R.L., Della Manna D., Bright S.J., Olsen C.C., *et al. In vivo* localization of [^{111}In]-DTPA-D-Phe^1-octreotide to human ovarian tumor xenografts induced to express the somatostatin receptor subtype 2 using an adenoviral vector. *Clin Cancer Res*, 1999 5(2): 383-393.
131. Zinn K.R., Chaudhuri T.R., Buchsbaum D.J., Mountz J.M. and Rogers B.E. Simultaneous evaluation of dual gene transfer to adherent cells by gamma-ray imaging. *Nucl Med Biol*, 2001 28(2): 135-144.
132. Hemminki A., Belousova N., Zinn K.R., Liu B., Wang M., Chaudhuri T.R., *et al.* An adenovirus with enhanced infectivity mediates molecular chemotherapy of ovarian cancer cells and allows imaging of gene expression. *Mol Ther*, 2001 4(3): 223-231.

133. Zinn K.R., Chaudhuri T.R., Krasnykh V.N., Buchsbaum D.J., Belousova N., Grizzle W.E., *et al.* Gamma camera dual imaging with a somatostatin receptor and thymidine kinase after gene transfer with a bicistronic adenovirus in mice. *Radiology*, 2002 223(2): 417-425.
134. Hemminki A., Zinn K.R., Liu B., Chaudhuri T.R., Desmond R.A., Rogers B.E., *et al. In vivo* molecular chemotherapy and noninvasive imaging with an infectivity-enhanced adenovirus. *J Natl Cancer Inst*, 2002 94(10): 741-749.
135. Rogers B.E., Zinn K.R., Lin C.Y., Chaudhuri T.R. and Buchsbaum D.J. Targeted radiotherapy with [^{90}Y]-SMT 487 in mice bearing human nonsmall cell lung tumor xenografts induced to express human somatostatin receptor subtype 2 with an adenoviral vector. *Cancer*, 2002 94(4 Suppl): 1298-1305.
136. Payne C.M., Bjore C.G., Jr. and Schultz D.A. Change in the frequency of apoptosis after low- and high-dose X-irradiation of human lymphocytes. *J Leukoc Biol*, 1992 52(4): 433-440.
137. Freeman S.M., Abboud C.N., Whartenby K.A., Packman C.H., Koeplin D.S., Moolten F.L., *et al.* The "bystander effect": tumor regression when a fraction of the tumor mass is genetically modified. *Cancer Res*, 1993 53(21): 5274-5283.
138. Buchsbaum D.J., Chaudhuri T.R., Yamamoto M. and Zinn K.R. Gene expression imaging with radiolabeled peptides. *Ann Nucl Med*, 2004 18(4): 275-283.
139. ter Horst M., Verwijnen S.M., Brouwer E., Hoeben R.C., de Jong M., de Leeuw B.H., *et al.* Locoregional delivery of adenoviral vectors. *J Nucl Med*, 2006 47(9): 1483-1489.
140. Gotthardt M., Librizzi D., Wolf D., Lalyko G., Behr T.M. and Behe M. Increased therapeutic efficacy through combination of Lu-177-DOTATOC and chemotheray in neuroendocrine tumours *in vivo*. *Eur J Nucl Med Mol Imaging*, 2006 33(suppl 2): S115.
141. Kong G., Lau E., Ramdave S. and Hicks R.J. High-dose In-111 octreotide therapy in combination with radiosensitizing 5-FU chemotherapy for treatment of SSR-expressing neuroendocrine tumors. *J Nucl Med*, 2005 46(suppl 2): 151P-152P.
142. Wild D., Wicki A. and Christofori G. Combination therapy with [(lys40(Ahx-[^{111}In-DTPA])]-Exendin-4 and VEGF-receptor tyrosine kinase inhibitor PTK in a glucagon-like-peptide-1 receptor-positive transgenic mouse tumor model. *J Nucl Med*, 2007 48, suppl 2: 83P.
143. Fueger B.J., Hamilton G., Raderer M., Pangerl T., Traub T., Angelberger P., *et al.* Effects of chemotherapeutic agents on expression of somatostatin receptors in pancreatic tumor cells. *J Nucl Med*, 2001 42(12): 1856-1862.
144. Schally A.V. and Nagy A. Cancer chemotherapy based on targeting of cytotoxic peptide conjugates to their receptors on tumors. *Eur J Endocrinol*, 1999 141(1): 1-14.
145. Nagy A. and Schally A.V. Targeting cytotoxic conjugates of somatostatin, luteinizing hormone-releasing hormone and bombesin to cancers expressing their receptors: a "smarter" chemotherapy. *Curr Pharm Des*, 2005 11(9): 1167-1180.
146. Hofland L.J., Capello A., Krenning E.P., de Jong M. and van Hagen M.P. Induction of apoptosis with hybrids of Arg-Gly-Asp molecules and peptides and antimitotic effects of hybrids of cytostatic drugs and peptides. *J Nucl Med*, 2005 46 Suppl 1: 191S-198S.
147. Keller G., Schally A.V., Nagy A., Baker B., Halmos G. and Engel J.B. Effective therapy of experimental human malignant melanomas with a targeted cytotoxic somatostatin analogue without induction of multi-drug resistance proteins. *Int J Oncol*, 2006 28(6): 1507-1513.
148. Engel J.B., Schally A.V., Halmos G., Baker B., Nagy A. and Keller G. Targeted therapy with a cytotoxic somatostatin analog, AN-238, inhibits growth of human experimental endometrial carcinomas expressing multidrug resistance protein MDR-1. *Cancer*, 2005 104(6): 1312-1321.
149. Buchholz S., Keller G., Schally A.V., Halmos G., Hohla F., Heinrich E., *et al.* Therapy of ovarian cancers with targeted cytotoxic analogs of bombesin, somatostatin, and luteinizing hormone-releasing hormone and their combinations. *Proc Natl Acad Sci U S A*, 2006 103(27): 10403-10407.

150. Kanashiro C.A., Schally A.V., Nagy A. and Halmos G. Inhibition of experimental U-118MG glioblastoma by targeted cytotoxic analogs of bombesin and somatostatin is associated with a suppression of angiogenic and antiapoptotic mechanisms. *Int J Oncol*, 2005 27(1): 169-174.
151. Kiaris H., Schally A.V., Nagy A., Sun B., Szepeshazi K. and Halmos G. Regression of U-87 MG human glioblastomas in nude mice after treatment with a cytotoxic somatostatin analog AN-238. *Clin Cancer Res*, 2000 6(2): 709-717.
152. Szereday Z., Schally A.V., Nagy A., Plonowski A., Bajo A.M., Halmos G., *et al.* Effective treatment of experimental U-87MG human glioblastoma in nude mice with a targeted cytotoxic bombesin analogue, AN-215. *Br J Cancer*, 2002 86(8): 1322-1327.
153. Moody T.W., Fuselier J., Coy D.H., Mantey S., Pradhan T., Nakagawa T., *et al.* Camptothecin-somatostatin conjugates inhibit the growth of small cell lung cancer cells. *Peptides*, 2005 26(9): 1560-1566.
154. Sun L.C., Luo J., Mackey L.V., Fuselier J.A. and Coy D.H. A conjugate of camptothecin and a somatostatin analog against prostate cancer cell invasion via a possible signaling pathway involving PI3K/Akt, $alpha_V beta_3$/$alpha_V beta_5$ and MMP-2/-9. *Cancer Lett*, 2007 246(1-2): 157-166.
155. Moody T.W., Sun L.C., Mantey S.A., Pradhan T., Mackey L.V., Gonzales N., *et al. In vitro* and *in vivo* antitumor effects of cytotoxic camptothecin-bombesin conjugates are mediated by specific interaction with cellular bombesin receptors. *J Pharmacol Exp Ther*, 2006 318(3): 1265-1272.
156. Sun L.C., Luo J., Mackey V.L., Fuselier J.A. and Coy D.H. Effects of camptothecin on tumor cell proliferation and angiogenesis when coupled to a bombesin analog used as a targeted delivery vector. *Anticancer Drugs*, 2007 18(3): 341-348.
157. Bernard B., Capello A., van Hagen M., Breeman W., Srinivasan A., Schmidt M., *et al.* Radiolabeled RGD-DTPA-Tyr^3-octreotate for receptor-targeted radionuclide therapy. *Cancer Biother Radiopharm*, 2004 19(2): 173-180.
158. Capello A., Krenning E.P., Bernard B.F., Breeman W.A., van Hagen M.P. and de Jong M. Increased cell death after therapy with an Arg-Gly-Asp-linked somatostatin analog. *J Nucl Med*, 2004 45(10): 1716-1720.
159. Capello A., Krenning E.P., Bernard B.F., Breeman W.A., Erion J.L. and de Jong M. Anticancer activity of targeted proapoptotic peptides. *J Nucl Med*, 2006 47(1): 122-129.
160. Buckley C.D., Pilling D., Henriquez N.V., Parsonage G., Threlfall K., Scheel-Toellner D., *et al.* RGD peptides induce apoptosis by direct caspase-3 activation. *Nature*, 1999 397(6719): 534-539.
161. Lambert B., Cybulla M., Weiner S.M., Van De Wiele C., Ham H., Dierckx R.A., *et al.* Renal toxicity after radionuclide therapy. *Radiat Res*, 2004 161(5): 607-611.
162. Kwekkeboom D.J., Mueller-Brand J., Paganelli G., Anthony L.B., Pauwels S., Kvols L.K., *et al.* Overview of results of peptide receptor radionuclide therapy with 3 radiolabeled somatostatin analogs. *J Nucl Med*, 2005 46 Suppl 1: 62S-66S.
163. Valkema R., Pauwels S.A., Kvols L.K., Kwekkeboom D.J., Jamar F., de Jong M., *et al.* Long-term follow-up of renal function after peptide receptor radiation therapy with ^{90}Y-$DOTA^0$,Tyr^3-octreotide and ^{177}Lu-$DOTA^0$,Tyr^3-octreotate. *J Nucl Med*, 2005 46 Suppl 1: 83S-91S.
164. Melis M., Krenning E.P., Bernard B.F., Barone R., Visser T.J. and de Jong M. Localisation and mechanism of renal retention of radiolabelled somatostatin analogues. *Eur J Nucl Med Mol Imaging*, 2005 32(10): 1136-1143.
165. De Jong M., Valkema R., Van Gameren A., Van Boven H., Bex A., Van De Weyer E.P., *et al.* Inhomogeneous Localization of Radioactivity in the Human Kidney After Injection of [^{111}In-$DTPA^0$]Octreotide. *J Nucl Med*, 2004 45(7): 1168-1171.
166. de Jong M., Barone R., Krenning E., Bernard B., Melis M., Visser T., *et al.* Megalin is essential for renal proximal tubule reabsorption of ^{111}In-DTPA-octreotide. *J Nucl Med*, 2005 46(10): 1696-1700.

167. Rolleman E.J., Kooij P.P., de Herder W.W., Valkema R., Krenning E.P. and de Jong M. Somatostatin receptor subtype 2-mediated uptake of radiolabelled somatostatin analogues in the human kidney. *Eur J Nucl Med Mol Imaging*, 2007.
168. Verwijnen S.M., Krenning E.P., Valkema R., Huijmans J.G. and de Jong M. Oral versus intravenous administration of lysine: equal effectiveness in reduction of renal uptake of [^{111}In-DTPA^{0}] octreotide. *J Nucl Med*, 2005 46(12): 2057-2060.
169. Bernard B.F., Krenning E.P., Breeman W.A., Rolleman E.J., Bakker W.H., Visser T.J., *et al.* D-lysine reduction of indium-111 octreotide and yttrium-90 octreotide renal uptake. *J Nucl Med*, 1997 38(12): 1929-1933.
170. van Eerd J.E., Vegt E., Wetzels J.F., Russel F.G., Masereeuw R., Corstens F.H., *et al.* Gelatin-based plasma expander effectively reduces renal uptake of ^{111}In-octreotide in mice and rats. *J Nucl Med*, 2006 47(3): 528-533.
171. Vegt E., Wetzels J.F., Russel F.G., Masereeuw R., Boerman O.C., van Eerd J.E., *et al.* Renal uptake of radiolabeled octreotide in human subjects is efficiently inhibited by succinylated gelatin. *J Nucl Med*, 2006 47(3): 432-436.
172. Rolleman E.J., Krenning E.P., Van Gameren A., Bernard B.F. and De Jong M. Uptake of [^{111}In-DTPA^{0}]octreotide in the rat kidney is inhibited by colchicine and not by fructose. *J Nucl Med*, 2004 45(4): 709-713.
173. Rolleman E.J., Forrer F., Bernard B., Bijster M., Vermeij M., Valkema R., *et al.* Amifostine protects rat kidneys during peptide receptor radionuclide therapy with [^{177}Lu-DOTA^{0},Tyr^{3}] octreotate. *Eur J Nucl Med Mol Imaging*, 2006.

2

Molecular imaging of adenoviral gene transfer

2.1

Molecular imaging and treatment of malignant gliomas following adenoviral transfer of the Herpes Simplex virus-thymidine kinase gene and the somatostatin receptor subtype 2 gene

S.M. Verwijnen, P.A.E. Sillevis Smitt, R.C. Hoeben, M.J.W.E Rabelink, L. Wiebe, D.T. Curiel, A. Hemminki, E.P. Krenning, M. de Jong.

Cancer Biotherapy and Radiopharmaceuticals, 2004; 19(1), 111-120.

Abstract

Patients suffering from malignant glioma have a very poor prognosis. New therapy approaches for gliomas are necessary; these tumors are attractive targets for gene therapy. Our research concentrated on evaluation of the use of the Herpes Simplex Virus-thymidine kinase (tk) enzyme and the somatostatin receptor subtype 2 (sst_2). [DOTA,Tyr^3]octreotate is an analog of somatostatin with high affinity for sst_2. It shows rapid internalization in sst_2-positive tumor cells *in vitro* and *in vivo*. For gene therapy, we used the adenoviral vector Ad5.tk.sst_2, which carries the tk gene and the sst_2 gene. The aim of our study was to compare uptake of the tk substrate 1-(2-fluoro-2-deoxy-β-D-ribofuranosyl)-5-[*I]iodouracil (FIRU) labeled with ^{125}I and the somatostatin analog [^{111}In-DOTA,Tyr^3]octreotate in several glioma cell lines after infection with Ad5.tk.sst_2. Uptake of ^{125}I-FIRU was measured in rat 9L-tk glioma cells without infection with Ad5.tk.sst_2. Results showed that the uptake of ^{125}I-FIRU was concentration and time dependent. We also used several rat and human glioma cell lines for infection with Ad5.tk.sst_2. Forty-eight hours after infection, uptake studies were performed using ^{125}IFIRU and [^{111}In-DOTA,Tyr^3]octreotate. In all cell lines, the uptake of ^{125}I-FIRU and [^{111}In-DOTA,Tyr^3]octreotate increased with increasing multiplicity of infection of virus and showed that the uptake of [^{111}In-DOTA,Tyr^3] octreotate was higher than that of ^{125}I-FIRU in all cell lines. We conclude that the sst_2 imaging and therapy modality is most promising for glioma gene therapy, either alone or in combination with HSV-tk suicide gene therapy. Therapy can be performed using combinations of [DOTA,Tyr^3]octreotate radiolabeled with ^{177}Lu or ^{90}Y, ^{131}I-FIRU and/or the prodrug ganciclovir.

Introduction

Malignant gliomas are the most common primary brain tumors in the Western world. The overall incidence of malignant gliomas is about 3 per 100,000 people per year [1]. Despite the advances in neurosurgery, radiation treatment and chemotherapy, the overall median survival remains less than 1 year and fewer than 5% of the patients survive 5 years or longer [2]. Initial treatment consists of surgery followed by radiotherapy, and sometimes additional chemotherapy. Eventually all malignant gliomas recur and at recurrence the median survival is 2–3 months [3-5]. The high rate of local recurrence within the region of the original tumor combined with the very low incidence of distant metastases warrants the further pursuit of novel locoregional treatment strategies such as gene therapy.

Gene therapy aims to deliver a therapeutic gene (or therapeutic genes) to cancer cells, either to directly kill those cells or to render them more sensitive to radiotherapy or chemotherapy [6-9]. Efficacy of gene therapy for brain tumors has been demonstrated in a variety of animal models using many different vector systems including retrovirus, adenovirus, adeno-associated virus, and herpes virus vectors [10-12]. Transduction of tumor cells with the herpes simplex virus thymidine kinase (HSV-tk) gene, which activates the nucleoside prodrug ganciclovir (GCV), has been one of the most effective approaches in treating experimental brain tumors [10,11,13]. The efficacy of this treatment is enhanced by the "bystander effect," whereby nontransduced tumor cells are also killed by the transfer of toxic metabolites through gap junctions [14], the induction of apoptosis [15], the killing of tumor endothelial cells [16], and the activation of a host immune response [17]. However, in human glioma trials, adenoviral gene therapy was safe, but so far the clinical efficacy was limited [18-20]. The efficacy of this therapy may be increased by enhancing the distribution of the vector throughout the tumor. Monitoring the magnitude, location and duration of transgene expression is therefore a crucial step in the development of gene therapy as an anti-cancer treatment modality. Noninvasive treatment of transgene expression levels has proven feasible following adenoviral transfer of the HSV-tk, sst_2 and several other genes, using radiolabeled tracers [9,21].

In our research, we focus on the replication-incompetent adenovirus serotype 5-derived vectors (Ad5). The wild type Ad5 genome has been characterized in detail and contains several regions with genes used for the viral life cycle. The E1 region contains the first genes expressed after infection and is essential for viral replication. The E3 region is involved in immune evasion and is dispensable for virus replication in cell culture. These two regions allow insertion of therapeutic and imaging genes. Ad5 vectors with an E1 deletion are replication incompetent, which means that the infected cell will not die as a result of the infection and the virus is capable of infecting a cell only once [22-25].

Advantages of replication-incompetent Ad5-derived vectors include their ability to infect both dividing and non-dividing cells, making them particularly suitable for *in vivo* gene transfer. Other advantages are the high titers that can be achieved and the high levels of transgene expression that can be obtained. In addition, the virus does not integrate into the host genome as a part of its life cycle, thus reducing the risk of mutations in the host genome. A disadvantage is the strong immune response against the Ad5 vector that limits the duration of gene expression. However, gene therapy for brain tumors using the Ad5 as vector was demonstrated efficient in several animal models [26,27].

The HSV-tk gene codes for the enzyme thymidine kinase (tk), which modifies the nontoxic prodrug GCV into a toxic molecule by phosphorylation, leading to cell death in cells expressing this gene. GCV is a specific anti-herpic drug and kills specifically herpes-virus infected cells. Normal cells are insensitive, since mammalian tk cannot phosphorylate GCV into the toxic form. Once phosphorylated, GCV is trapped in the cell. To be able to image the expression of HSV-tk, several nucleoside analogs were developed which are phosphorylated in the same way as GCV [28,29]. One of these analogs is 1-(2-fluoro-2-deoxy-β-D-ribofuranosyl)-5-[*I]iodouracil (FIRU), which can be labeled with ^{123}I and ^{131}I for imaging with a gamma camera or labeled with ^{124}I for visualization with positron emission tomography (PET) [29].

Radiolabeled somatostatin analogs, such as octreotide and octreotate, bind with high affinity to this receptor, followed by internalization into the cell, which expresses the somatostatin subtype 2 receptor (sst_2) [30-33]. When labeled with ^{111}In, these analogs can be detected with a gamma camera and sst^2-positive tumors can be visualized. This technique of peptide receptor scintigraphy (PRS) is widely used in nuclear medicine to visualize tumors expressing sst_2, such as neuroendocrine tumors. Radiolabeled with ^{177}Lu and ^{90}Y, [Tyr^3]octreotate (conjugated with the chelator DOTA) is also used for peptide receptor radionuclide therapy (PRRT) of neuroendocrine tumors [30,33,34]. [DOTA,Tyr^3]octreotate, used in these experiments, has a high affinity for the sst_2 receptor and it shows a rapid internalization in sst_2-positive tumors *in vitro* as well as *in vivo*. A new approach to gene therapy for gliomas is to combine the HSV-tk/GCV system with the sst_2/[DOTA,Tyr^3]octreotate system. A vector that contains both HSV-tk and sst_2 transgenes driven by the same cytomegalovirus (CMV) promoter was developed: the Ad5.tk.sst_2 [35]. When gene therapy is performed, imaging of gene transfer is possible using radiolabeled octreotate or FIRU. This would enable us to monitor both the efficiency of the transduction of the viral genes and the location, magnitude, and duration of gene expression. Also, therapy can then be performed using [DOTA,Tyr^3]octreotate labeled with ^{177}Lu or ^{90}Y, using FIRU labeled with ^{131}I and using GCV, or combinations of these.

The aim of our current experiments was to compare internalization and uptake of radiolabeled [DOTA,Tyr^3]octreotate and FIRU after infection with increasing amounts of Ad5.tk.sst$_2$. For these experiments, we used two rat (9L and 9L-tk) and four human glioma cell lines (U251, U87MG, U118, T98G) and the rat pancreatic tumor cell line CA20948, which expresses a high density of sst$_2$ on the cell membranes, as a positive control. First, we performed studies to characterize FIRU uptake and to establish the native sst$_2$ expression in the glioma cell lines. We then performed experiments comparing [^{111}In-DOTA,Tyr^3]octreotate and ^{125}I-FIRU uptake after infection with Ad5.tk.sst$_2$ in these rat and human glioma cell lines.

Materials and methods

Cell culture

The rat pancreatic CA20948 tumor cells were grown in Dulbecco's modified Eagle's medium

(DMEM, Gibco, Life Technologies, Breda, The Netherlands) supplemented with 10% heat-inactivated fetal bovine serum (FBS), 1% of glutamate, 2% penicillin/streptomycin (Gibco), 0.2% sodiumpyruvate and 0.1% fungizone. The human anaplastic thyroid cancer cells ARO were grown in DMEM-F12 medium supplemented with 10% FBS, 1% of glutamate, 2% penicillin/streptomycin, 0.2% sodiumpyruvate and 0.1% fungizone.

The 9L rat gliosarcoma brain tumor cells (a gift of Dr. K.M. Hebeda, Department of Experimental Neurosurgery, Free University Hospital, Amsterdam, The Netherlands), the human glioma cell lines U87MG (glioblastoma/astrocytoma), T98G (glioblastoma multiforme), U251 (glioblastoma), CCF-SSTG1 (astrocytoma), and U118 (glioblastoma/astrocytoma) (all obtained from ATCC) were grown in RPMI medium (RPMI, Gibco, The Netherlands) supplemented with 10% FBS and 2% penicillin/streptomycin (Gibco).

The 9L-tk rat gliosarcoma brain tumor cells, stably transfected with the HSV-tk gene [29], were grown in RPMI medium (Gibco, The Netherlands) supplemented with 10% heat-inactivated fetal bovine serum (FBS), 2% penicillin/streptomycin (Gibco) and 0.25 mg/ml geneticin (Gibco).

Medium was changed twice or three times a week. Cells were cultured at 37°C in a 5% CO_2 atmosphere.

Radiolabeled peptides and nucleosides

[DOTA,Tyr^3]octreotate was labeled with ^{111}In and ^{125}I according to the protocols described earlier [31,36]. The mean radiochemical purity was 95%. The mean specific

activity of [^{111}In-DOTA,Tyr^3]octreotate was 143 MBq/nmol. The mean specific activity of [DOTA-^{125}I-Tyr^3]octreotate was 0.6 MBq/mmol.

FIRU was labeled with ^{125}I according to Wiebe et al. [28]. The precursor compound of FIRU, 1-(2-fluoro-2-deoxy-β-D-ribofuranosyl)-5-tributylstannyl uracil (FTBSRU, 100 mg) was dissolved in 10 ml ethanol/acetic acid (v/v: 50/50), vortexed and centrifuged. ICl was dissolved in ethanol/acetic acid at a concentration of 1 mg/ml; 100 ml was dissolved in 900 ml ethanol/acetic acid. 30 ml of this solution was added to 11 ml ^{125}I (± 42 MBq). Then, 5 ml of the dissolved precursor was added and the mixture was incubated at room temperature for 10 minutes. A Sep-Pak column was activated with 5 ml 2-propanol and rinsed with 5 ml H_2O. The labeling mixture was pushed through the column. Free iodine was first eluted in 15 ml of H_2O, followed by elution of ^{125}I-FIRU in ethanol/H_2O (v/v: 50/50). The FTBSRU precursor was eluted in 99% ethanol. The mean labeling yield was ± 2 MBq/nmol.

Production of the viral vector Ad5.tk.sst$_2$

The Ad5.tk.sst$_2$ virus was constructed with an E1 deletion, containing the human somatostatin receptor subtype-2 (sst$_2$) and the herpes simplex virus thymidine kinase (HSV-tk) [35]. Both genes have their own immediate early CMV promotor and poly(A). Large scale amplification of Ad5.tk.sst$_2$ was carried out on PerC6 cells as previously described [37] and the virus was titered by plaque assay on 911 cells, yielding a mean of 5.2x10^9 plaque forming units/ml (PFU/ml).

^{125}I-FIRU uptake

The ^{125}I-FIRU uptake in 9L-tk cells was measured after incubation at 37°C with increasing amounts of the radiolabeled nucleoside in 250 ml incubation medium at different time points. Incubation medium contained RPMI 1640 medium supplemented with 20 mM Hepes and 1% bovine serum albumine. After the incubation period the cells were washed twice with cold phosphate buffered saline (PBS) and lysed with 0.1 M NaOH. These radioactive fractions were measured in an LKB-1282-Compugammasystem (Perkin Elmer, Oosterhout, The Netherlands). The amount of protein in these fractions was measured using a commercially available kit (Biorad, Veenendaal, The Netherlands). Data were expressed as percentage of the total dose per mg protein (mean ± SEM).

Internalization of radiolabeled [DOTA,Tyr^3]octreotate before infection with Ad5.tk.sst$_2$

In this experiment, we used several tumor cell lines: the rat pancreatic tumor cell line CA20948 (sst$_2$-positive), the human anaplastic thyroid cancer cell line ARO (sst$_2$-negative), the rat gliosarcoma cell lines 9L and 9L-tk and the human glioblastoma cell lines U251, U118, U87MG and T98G. Binding of ^{125}I labeled [DOTA,Tyr^3]octreotate to

its receptor on the cell membranes of these cells and subsequent internalization was performed as earlier described [30]. In short, cells were transferred in 6-wells culture plates at a concentration of 10^6 cells/well. After 24 hours, the cells were washed twice with PBS of 37°C. Then the cells were incubated in triplicate for 1 hour with 1 ml incubation medium containing 40 kBq ($5x10^{-10}$ M) of radiolabeled peptide at 37°C. To determine whether the internalization of the peptide was receptor-specific, cells were also incubated in triplicate with the same medium supplemented with 10^{-6} M unlabeled octreotide. After the incubation period, cells were washed with PBS (4°C) and incubated for 10 minutes with 20 mM sodium acetate (pH 5.0) to remove non-internalized radioactivity. Then the cells were lysed with 0.1 M sodium hydroxide (internalized fraction). Radioactivity was measured in an LKB-1282-Compugammasystem. The amount of protein was measured using a commercially available kit (Biorad, Veenendaal, The Netherlands). Data were expressed as percentage of the total dose per mg protein (mean ± standard error of the mean).

Uptake of [^{111}In-DOTA,Tyr^3]octreotate and ^{125}I-FIRU after infection with Ad5.tk.sst$_2$

Cells (U251, U118, U87MG, T98G, 9L, and 9Ltk) were transferred into 24-well culture plates at a concentration of 10^5 cells/well. After 24 hours, the cells were infected with Ad5.tk.sst$_2$ at multiplicity of infection (moi) 0, 1, 10, or 100. Infection was allowed during two hours using normal medium with Ad5.tk.sst$_2$ in different concentrations. After the 2-hour incubation period, the medium was refreshed and cells were left in the 37°C incubator for 48 hours to allow the viral genome to be transcribed in the cells.

After 48 hours, uptake and internalization experiments as described above were performed. The cells were incubated with 250 ml internalization medium containing $5x10^{-10}$ M [^{111}In-DOTA,Tyr^3]octreotate (40 kBq/well), $5x10^{-10}$ M [^{111}In-DOTA,Tyr^3] octreotate plus 10^{-6} M octreotide (40 kBq/well), or 10^{-9} M ^{125}I-FIRU (0.5 kBq/well). After an incubation period of 1 hour at 37°C, cells that were incubated with [^{111}In-DOTA,Tyr^3]octreotate, were harvested as described above, and counted in the LKB-1282-Compugammasystem. Cells incubated with ^{125}I-FIRU were lysed after incubation and also counted in the LKB-1282-Compugammasystem.

Results

Characteristics of ^{125}I-FIRU uptake in 9L-tk cells

In figure 1A the uptake of radiolabeled FIRU is presented as %Dose/mg protein and plotted against the incubation time in minutes. The concentration used was $3.8x10^{-10}$ M ^{125}I-FIRU. The results show that the uptake of radiolabeled FIRU *in vitro* in 9L-tk cells is time-dependent with an optimum after 2–3 hours of incubation.

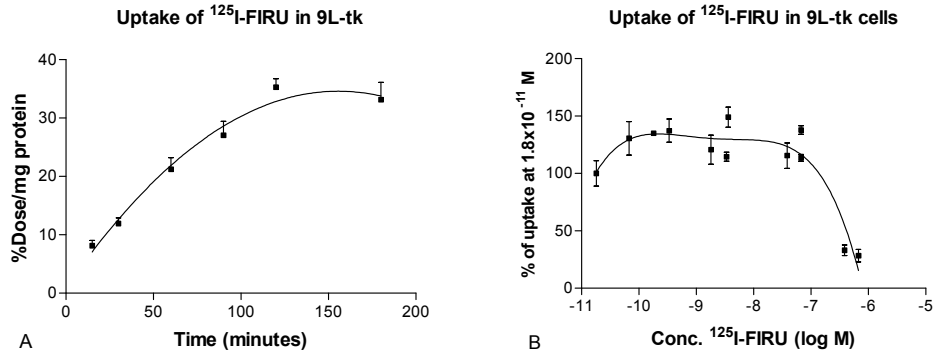

Figure 1: (A) Uptake of ^{125}I-FIRU in 9L-tk cells after different incubation times at high specific activity (3.8 x10^{-10} M ^{125}I-FIRU). The uptake is expressed as mean % dose/mg protein ± standard error of the mean of four replicas. (B) Uptake of ^{125}I-FIRU in 9L-tk cells after increasing concentrations of ^{125}I-FIRU at an incubation time of 1 hour. The uptake of the lowest concentration (in % dose/mg protein) was set on 100%. (n = 4)

In figure 1B the uptake of ^{125}I-FIRU is normalized as % of uptake obtained with the lowest ^{125}I-FIRU concentration (1.81x10^{-11} M) and plotted against the concentration ^{125}I-FIRU. The uptake of FIRU is decreased at a concentration of 10^{-7} M and higher. The optimal concentration used *in vitro* is between 10^{-10} and 10^{-8} M, the uptake decreases rapidly at a concentration exceeding 10^{-7} M.

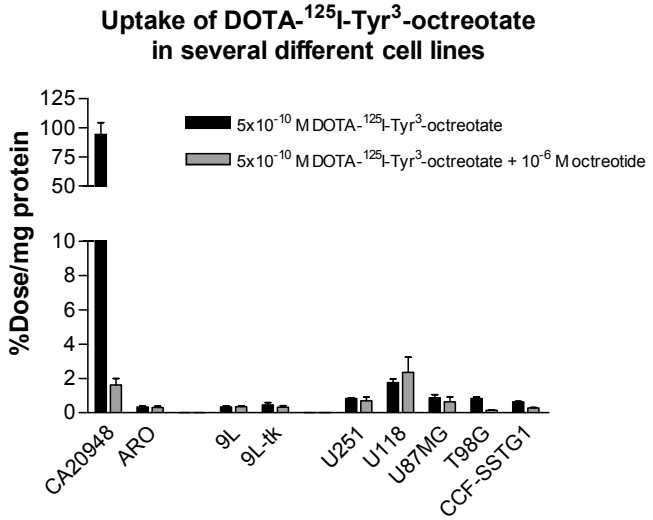

Figure 2: Uptake of [DOTA-^{125}I-Tyr^3]octreotate in different non-glioma and glioma cell lines after 1 hour of incubation. Cells were incubated with 1 ml of incubation medium containing 40 kBq/ml. The rat pancreatic tumor cell line CA20948 was used as a positive control and the human thyroid cancer cell line ARO was used as a negative control. Results are presented as mean % dose/mg protein ± standard deviation of three replicas.

Internalization of radiolabeled [DOTA,Tyr³]octreotate before infection with Ad5.tk.sst₂

In figure 2, the uptake of radiolabeled [DOTA,Tyr³]octreotate following incubation in different cell lines is shown. The different cell lines were incubated for 1 hour with [DOTA-^{125}I-Tyr³]octreotate or with [DOTA-^{125}I-Tyr³]octreotate plus an excess

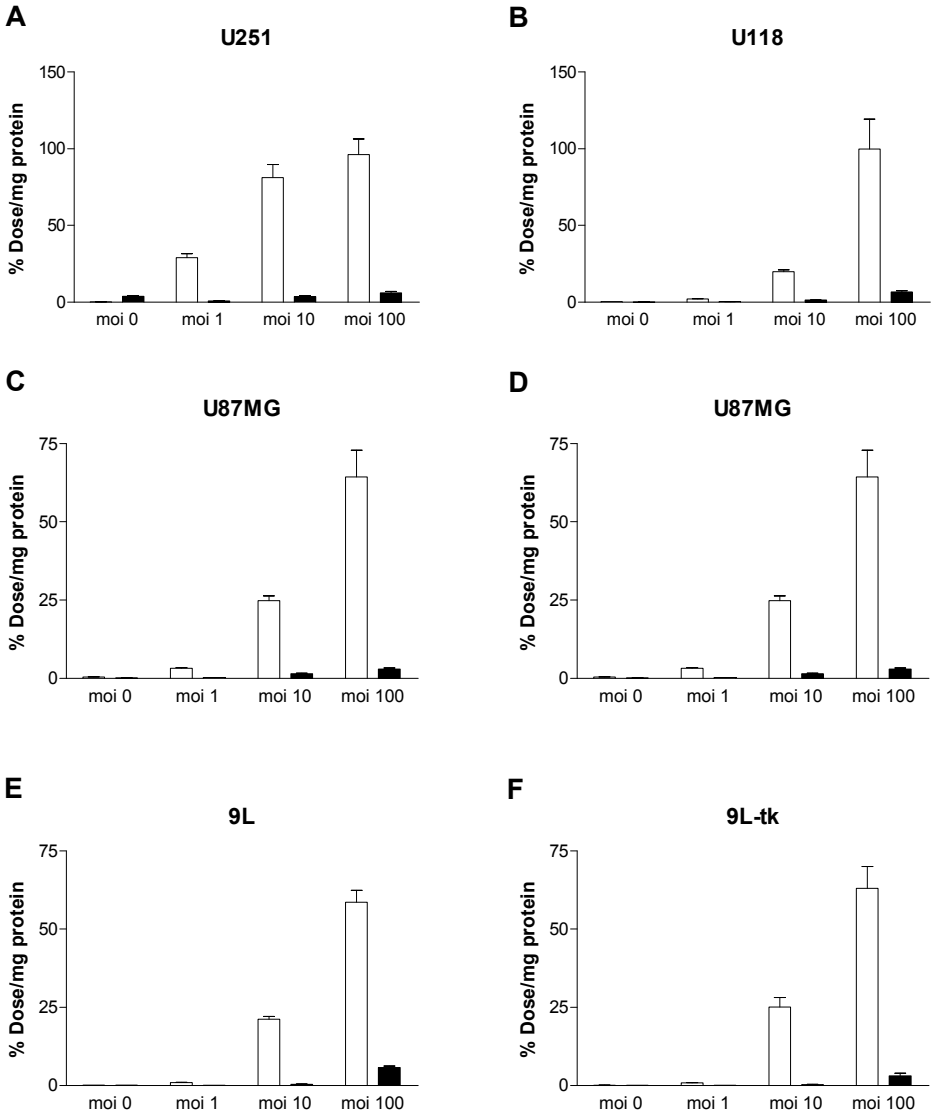

Figure 3: Uptake of [^{111}In-DOTA,Tyr³]octreotate in six glioma cell lines. The data are presented as mean % dose/mg protein ± standard error of the mean of $5x10^{-10}$ M [^{111}In-DOTA,Tyr³]octreotate (white bars) and $5x10^{-10}$ M [^{111}In-DOTA,Tyr³]octreotate + 10^{-6} M octreotide (black bars) of four replicas. Graphs A to D represent human glioma cell lines, whereas graphs E and F represent rat glioma cell lines. Cells were incubated with 250 ml of one of the solutions, each containing 40 kBq/250 ml.

of unlabeled octreotide. Native expression levels of the sst_2 gene are low in the rat and human glioma cell lines, compared to the positive control, the rat pancreatic CA20948 cell line. This was in accordance with Q-PCR data (results not shown).

Uptake of [^{111}In-DOTA,Tyr^3]octreotate and ^{125}I-FIRU after infection with Ad5.tk.sst_2

An uptake experiment was performed to measure the uptake of [^{111}In-DOTA,Tyr^3] octreotate and ^{125}I-FIRU after infection with Ad5.tk.sst_2 with increasing moi's. In figure 3, the results of the uptake study of [^{111}In-DOTA,Tyr^3]octreotate in six glioma cell lines are presented. The uptake of this compound at moi 0 of Ad5.tk.sst_2 in all cell lines was very low, confirming the results shown in figure 2. However, at moi 1, 10, and 100 the uptake increased in all cell lines up to 50% Dose/mg protein or more with increasing dose of the vector. Only in the T98G cell line, the uptake of [^{111}In-DOTA,Tyr^3]octreotate following infection at moi 100 was below 50% Dose/mg protein. The uptake of labeled octreotate was reduced in the presence of an excess of unlabeled octreotide, indicating receptor-specific uptake. Figure 4 presents the data of ^{125}I-FIRU uptake in the same six glioma cell lines. These results show that the uptake of ^{125}I-FIRU increased with increasing moi's as well. In the 9L-tk cell line the uptake of ^{125}I-FIRU did not increase with higher moi's. As can be seen in figures 3 and 4, the uptake of [^{111}In-DOTA,Tyr^3]octreotate is higher than the uptake of ^{125}I-FIRU in all these cell lines.

Discussion

We present here an adenovirus for gene therapy containing not only the tk gene but also the sst_2 gene [35]. The sst_2 receptor is widely used for scintigraphy and therapy in nuclear medicine nowadays. Analogs of somatostatin, such as octreotate, are radiolabeled and after i.v. injection internalize via the sst_2 receptor in cells expressing this receptor. Sst_2-positive neuroendocrine tumors are very well visualized by this peptide receptor scintigraphy (PRS) technique and also peptide receptor radionuclide therapy (PRRT) is most successful in the clinic and in pre-clinical research [30-34,38].

The application of these two genes enables us to image *in vivo* the expression of the desired genes, by using radiolabeled octreotate or FIRU. Moreover, therapy can be performed using octreotate labeled with ^{177}Lu or ^{90}Y, with FIRU labeled with ^{131}I, with GCV, or combinations of these compounds to accomplish better therapy results and less radiotoxicity to non-target tissues. Other authors have shown that GCV, and also another nucleoside prodrug acyclovir (ACV), increased the radiosensitivity of

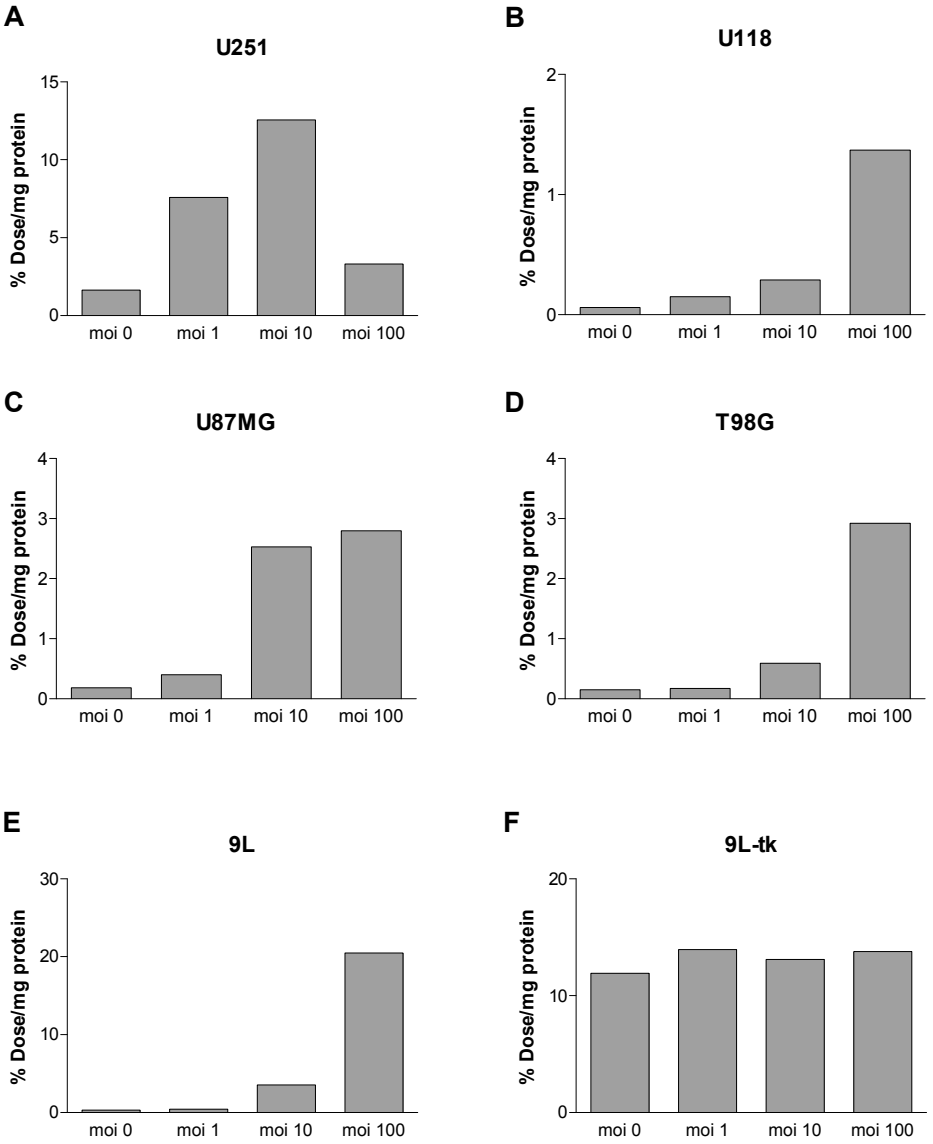

Figure 4: Uptake of ^{125}I-FIRU in six glioma cell lines. Cells were incubated with 250 ml incubation medium containing 0.5 kBq/250 ml (10^{-9} M ^{125}I-FIRU). Graphs A to D present data for human glioma cell lines, whereas graphs E and F present data from rat glioma cell lines. The data are presented as mean % dose/mg protein ± standard error of the mean SEM of four replicas.

several tumor cell lines [7,8,39]. The use of GCV in combination with radiolabeled octreotate and FIRU could therefore enhance the tumoricidal effect.

[Tyr^3]octreotate was characterized earlier and we found that it has very high affinity for the sst_2 [30,40] and in biodistribution studies the uptake of this compound in sst_2-positive tumor models was high compared to other sst_2 binding analogs. Here

we performed uptake studies to characterize FIRU uptake *in vitro*. The results of these experiments showed that the uptake of ^{125}I-FIRU is time-dependent and, at concentrations of 10^{-7} M and higher, the uptake decreases. Nanda et al. found an optimum of ^{123}I-FIRU uptake in 9L-tk cells between 2 and 4 hours incubation [29]. We found a plateau after 2–3 hours incubation with ^{125}I-FIRU, which is in accordance with these earlier findings.

We then performed an internalization and uptake experiment to establish the amount of octreotate internalized in non-infected glioma cell lines. Our results show a very low uptake of [DOTA-^{125}I-Tyr^3]octreotate. Also the uptake could not be blocked in most rat and glioma cell lines, in accordance with several reports that have shown sst on astrocytomas and oligodendrogliomas, but not on poorly differentiated glioblastomas [41-43]. Other studies showed sst_2 expression on low-grade gliomas [44], on medullablastomas [42,45] and on cultured astrocytomas and gliomas [46]. Dutour et al. found sst_2 expression on meningiomas and gliomas using RT-PCR [47]. However, Reubi et al. studied sst_2 expression in human glioma tissue using autoradiography [41]. They found low expression in most of the differentiated glia-derived tumors (astrocytomas and oligodendrogliomas), while the more malignant glioblastomas were usually free of sst_2. Furthermore, Cevera et al. reported that in gliomas, sst expression is restricted to endothelial cells on proliferating vessels, including parenchyma and reactive microglia [42]. These findings have been confirmed by sst receptor scintigraphy in brain tumor patients demonstrating no or low uptake of labeled somatostatin analogs in high-grade gliomas [48], in agreement with our findings. Therefore, gene therapy for expression of sst_2 in malignant gliomas is a requisite when we want to perform PRS and PRRT with radiolabeled sst analogs.

Finally we performed uptake experiments after infection with Ad5.tk.sst_2 of the glioma cell lines comparing radiolabeled [DOTA,Tyr^3]octreotate and FIRU as radiotracers for the expression of the sst^2 and tk enzyme, respectively. We found a huge increase in uptake of the sst_2 analog after infection with moi 10 and 100 of Ad5.tk.sst_2 compared with moi 0 in all cell lines. [^{111}In-DOTA,Tyr^3]octreotate uptake could be blocked by an excess of unlabeled octreotide in all cell lines, indicating receptor specific uptake.

The uptake of ^{125}I-FIRU was much lower in all cell lines compared to the uptake of [^{111}In-DOTA,Tyr^3]octreotate . The highest uptake of FIRU was found in U251 and 9L. In the U251 cell line, we found a lower uptake of FIRU at moi 100 than at moi 1 and 10. This was unexpected, since the uptake of [^{111}In-DOTA,Tyr^3]octreotate in that same cell line at moi 100 is not decreased. This could be due to toxicity of the vector or toxicity of tk at higher concentrations and this needs further examination. Except for the U251 and 9Ltk, all other cells lines had a higher uptake of ^{125}I-FIRU at moi 10 and 100 compared to moi 0. The results in 9L-tk cells showed that the

uptake of ^{125}I-FIRU did not further increase after Ad5.tk.sst$_2$ incubation. This might be explained by the fact that the stably transfected cell line already expresses a high amount of HSV-tk.

Zinn et. al. showed in earlier publications that imaging with sst$_2$ analogs was successful in a variety of disease models, with results equivalent or superior to tk imaging *in vivo* [6,49,50]. Imaging was performed using the tk substrate 2'-deoxy-2'-fluoro-β-D-arabinofuranosyl-5[*I]-iodouracil (^{131}I-FIAU) and the sst analog ^{99m}Tc-P2045.

We conclude that the uptake of [DOTA-^{125}I-Tyr^3]octreotate, which specifically binds to the human sst^2 receptor, is very low in the tested native rat and human glioma cell lines compared to our positive control CA20948. However, after infection with Ad5.tk.sst$_2$, the uptake of both [^{111}In-DOTA,Tyr^3]octreotate and ^{125}I-FIRU is increased and [^{111}In-DOTA,Tyr^3]octreotate uptake is higher than the uptake of ^{125}I-FIRU in the glioma cells. These results indicate that [^{111}In-DOTA,Tyr^3]octreotate and to a lesser extent I-123 or I-131 labeled FIRU is promising for imaging the magnitude, duration and location of transgene expression in patients. Furthermore, for therapy the prodrug GCV can be used, as well as ^{177}Lu- or ^{90}Y-labeled [DOTA,Tyr^3]octreotate or ^{131}I-FIRU or combinations of these.

References

1. Visser O. and Coebergh J.W.W. Incidence of cancer in The Netherlands. *Utrecht: Vereniging van Integrale Kankercentra* 1998.
2. Surawicz T.S., Davis F., Freels S., Laws E.R., Jr. and Menck H.R. Brain tumor survival: results from the National Cancer Data Base. *J Neurooncol* 1998; 40(2): 151-160.
3. Salcman M. *Glioblastoma and malignant astrocytoma.* Brain Tumors, ed. Kaye A.H., Laws E.R. Vol. 449. 1995, New York: Churchill Livingstone.
4. Yung W.K., Prados M.D., Yaya-Tur R., Rosenfeld S.S., Brada M., Friedman H.S., *et al.* Multicenter phase II trial of temozolomide in patients with anaplastic astrocytoma or anaplastic oligoastrocytoma at first relapse. Temodal Brain Tumor Group. *J Clin Oncol* 1999; 17(9): 2762-2771.
5. Friedman H.S., Petros W.P., Friedman A.H., Schaaf L.J., Kerby T., Lawyer J., *et al.* Irinotecan therapy in adults with recurrent or progressive malignant glioma. *J Clin Oncol* 1999; 17(5): 1516-1525.
6. Rogers B.E., Zinn K.R. and Buchsbaum D.J. Gene transfer strategies for improving radiolabeled peptide imaging and therapy. *Q J Nucl Med* 2000; 44(3): 208-223.
7. Valerie K., Brust D., Farnsworth J., Amir C., Taher M.M., Hershey C., *et al.* Improved radiosensitization of rat glioma cells with adenovirus-expressed mutant herpes simplex virus-thymidine kinase in combination with acyclovir. *Cancer Gene Ther* 2000; 7(6): 879-884.
8. Rogulski K.R., Kim J.H., Kim S.H. and Freytag S.O. Glioma cells transduced with an Escherichia coli CD/HSV-1 TK fusion gene exhibit enhanced metabolic suicide and radiosensitivity. *Hum Gene Ther* 1997; 8(1): 73-85.
9. Hemminki A., Zinn K.R., Liu B., Chaudhuri T.R., Desmond R.A., Rogers B.E., *et al.* In vivo molecular chemotherapy and noninvasive imaging with an infectivity-enhanced adenovirus. *J Natl Cancer Inst* 2002; 94(10): 741-749.
10. Culver K.W., Ram Z., Wallbridge S., Ishii H., Oldfield E.H. and Blaese R.M. In vivo gene transfer with retroviral vector-producer cells for treatment of experimental brain tumors. *Science* 1992; 256(5063): 1550-1552.
11. Vincent A.J., Vogels R., Someren G.V., Esandi M.C., Noteboom J.L., Avezaat C.J., *et al.* Herpes simplex virus thymidine kinase gene therapy for rat malignant brain tumors. *Hum Gene Ther* 1996; 7(2): 197-205.
12. Kramm C.M., Chase M., Herrlinger U., Jacobs A., Pechan P.A., Rainov N.G., *et al.* Therapeutic efficiency and safety of a second-generation replication-conditional HSV1 vector for brain tumor gene therapy. *Hum Gene Ther* 1997; 8(17): 2057-2068.
13. Chen S.H., Shine H.D., Goodman J.C., Grossman R.G. and Woo S.L. Gene therapy for brain tumors: regression of experimental gliomas by adenovirus-mediated gene transfer in vivo. *Proc Natl Acad Sci U S A* 1994; 91(8): 3054-3057.
14. Touraine R.L., Ishii-Morita H., Ramsey W.J. and Blaese R.M. The bystander effect in the HSVtk/ganciclovir system and its relationship to gap junctional communication. *Gene Ther* 1998; 5(12): 1705-1711.
15. Hamel W., Magnelli L., Chiarugi V.P. and Israel M.A. Herpes simplex virus thymidine kinase/ganciclovir-mediated apoptotic death of bystander cells. *Cancer Res* 1996; 56(12): 2697-2702.
16. Ram Z., Walbridge S., Shawker T., Culver K.W., Blaese R.M. and Oldfield E.H. The effect of thymidine kinase transduction and ganciclovir therapy on tumor vasculature and growth of 9L gliomas in rats. *J Neurosurg* 1994; 81(2): 256-260.
17. Vile R.G., Castleden S., Marshall J., Camplejohn R., Upton C. and Chong H. Generation of an anti-tumour immune response in a non-immunogenic tumour: HSVtk killing in vivo stimulates a mononuclear cell infiltrate and a Th1-like profile of intratumoural cytokine expression. *Int J Cancer* 1997; 71(2): 267-274.

18. Smitt P.S., Driesse M., Wolbers J., Kros M. and Avezaat C. Treatment of relapsed malignant glioma with an adenoviral vector containing the herpes simplex thymidine kinase gene followed by ganciclovir. *Mol Ther* 2003; 7(6): 851-858.
19. Trask T.W., Trask R.P., Aguilar-Cordova E., Shine H.D., Wyde P.R., Goodman J.C., *et al*. Phase I study of adenoviral delivery of the HSV-tk gene and ganciclovir administration in patients with current malignant brain tumors. *Mol Ther* 2000; 1(2): 195-203.
20. Sandmair A.M., Loimas S., Puranen P., Immonen A., Kossila M., Puranen M., *et al*. Thymidine kinase gene therapy for human malignant glioma, using replication-deficient retroviruses or adenoviruses. *Hum Gene Ther* 2000; 11(16): 2197-2205.
21. Chaudhuri T.R., Rogers B.E., Buchsbaum D.J., Mountz J.M. and Zinn K.R. A noninvasive reporter system to image adenoviral-mediated gene transfer to ovarian cancer xenografts. *Gynecol Oncol* 2001; 83(2): 432-438.
22. Alemany R., Gomez-Manzano C., Balague C., Yung W.K., Curiel D.T., Kyritsis A.P., *et al*. Gene therapy for gliomas: molecular targets, adenoviral vectors, and oncolytic adenoviruses. *Exp Cell Res* 1999; 252(1): 1-12.
23. Kay M.A., Liu D. and Hoogerbrugge P.M. Gene therapy. *Proc Natl Acad Sci U S A* 1997; 94(24): 12744-12746.
24. Buchsbaum D.J., Rogers B.E., Khazaeli M.B., Mayo M.S., Milenic D.E., Kashmiri S.V., *et al*. Targeting strategies for cancer radiotherapy. *Clin Cancer Res* 1999; 5(10 Suppl): 3048s-3055s.
25. Russell W.C. Update on adenovirus and its vectors. *J Gen Virol* 2000; 81(Pt 11): 2573-2604.
26. Wiewrodt R., Amin K., Kiefer M., Jovanovic V.P., Kapoor V., Force S., *et al*. Adenovirus-mediated gene transfer of enhanced Herpes simplex virus thymidine kinase mutants improves prodrug-mediated tumor cell killing. *Cancer Gene Ther* 2003; 10(5): 353-364.
27. Badie B., Hunt K., Economou J.S. and Black K.L. Stereotactic delivery of a recombinant adenovirus into a C6 glioma cell line in a rat brain tumor model. *Neurosurgery* 1994; 35(5): 910-915; discussion 915-916.
28. Wiebe L.I., Knaus E.E. and Morin K.W. Radiolabelled pyrimidine nucleosides to monitor the expression of HSV-1 thymidine kinase in gene therapy. *Nucleosides Nucleotides* 1999; 18(4-5): 1065-1066.
29. Nanda D., de Jong M., Vogels R., Havenga M., Driesse M., Bakker W., *et al*. Imaging expression of adenoviral HSV1-tk suicide gene transfer using the nucleoside analogue FIRU. *Eur J Nucl Med Mol Imaging* 2002; 29(7): 939-947.
30. de Jong M., Breeman W.A., Bakker W.H., Kooij P.P., Bernard B.F., Hofland L.J., *et al*. Comparison of ^{111}In-labeled somatostatin analogues for tumor scintigraphy and radionuclide therapy. *Cancer Res* 1998; 58(3): 437-441.
31. de Jong M., Breeman W.A., Bernard B.F., Bakker W.H., Schaar M., van Gameren A., *et al*. [^{177}Lu-DOTA^{0},Tyr^{3}] octreotate for somatostatin receptor-targeted radionuclide therapy. *Int J Cancer* 2001; 92(5): 628-633.
32. De Jong M., Valkema R., Jamar F., Kvols L.K., Kwekkeboom D.J., Breeman W.A., *et al*. Somatostatin receptor-targeted radionuclide therapy of tumors: preclinical and clinical findings. *Semin Nucl Med* 2002; 32(2): 133-140.
33. Kwekkeboom D.J., Bakker W.H., Kooij P.P., Konijnenberg M.W., Srinivasan A., Erion J.L., *et al*. [^{177}Lu-DOTA^{0},Tyr^{3}]octreotate: comparison with [^{111}In-DTPA^{0}]octreotide in patients. *Eur J Nucl Med* 2001; 28(9): 1319-1325.
34. de Jong M., Kwekkeboom D., Valkema R. and Krenning E.P. Radiolabelled peptides for tumour therapy: current status and future directions. Plenary lecture at the EANM 2002. *Eur J Nucl Med Mol Imaging* 2003; 30(3): 463-469.
35. Hemminki A., Belousova N., Zinn K.R., Liu B., Wang M., Chaudhuri T.R., *et al*. An adenovirus with enhanced infectivity mediates molecular chemotherapy of ovarian cancer cells and allows imaging of gene expression. *Mol Ther* 2001; 4(3): 223-231.

36. Bakker W.H., Krenning E.P., Breeman W.A., Kooij P.P., Reubi J.C., Koper J.W., *et al. In vivo* use of a radioiodinated somatostatin analogue: dynamics, metabolism, and binding to somatostatin receptor-positive tumors in man. *J Nucl Med* 1991; 32(6): 1184-1189.
37. Fallaux F.J., Bout A., van der Velde I., van den Wollenberg D.J., Hehir K.M., Keegan J., *et al.* New helper cells and matched early region 1-deleted adenovirus vectors prevent generation of replication-competent adenoviruses. *Hum Gene Ther* 1998; 9(13): 1909-1917.
38. Lewis J.S., Lewis M.R., Cutler P.D., Srinivasan A., Schmidt M.A., Schwarz S.W., *et al.* Radiotherapy and dosimetry of ^{64}Cu-TETA-Tyr^{3}-octreotate in a somatostatin receptor-positive, tumor-bearing rat model. *Clin Cancer Res* 1999; 5(11): 3608-3616.
39. Rosenberg E., Hawkins W., Holmes M., Amir C., Schmidt-Ullrich R.K., Lin P.S., *et al.* Radiosensitization of human glioma cells *in vitro* and *in vivo* with acyclovir and mutant HSV-TK75 expressed from adenovirus. *Int J Radiat Oncol Biol Phys* 2002; 52(3): 831-836.
40. Reubi J.C., Schar J.C., Waser B., Wenger S., Heppeler A., Schmitt J.S., *et al.* Affinity profiles for human somatostatin receptor subtypes SST1-SST5 of somatostatin radiotracers selected for scintigraphic and radiotherapeutic use. *Eur J Nucl Med* 2000; 27(3): 273-282.
41. Reubi J.C., Cortes R., Maurer R., Probst A. and Palacios J.M. Distribution of somatostatin receptors in the human brain: an autoradiographic study. *Neuroscience* 1986; 18(2): 329-346.
42. Cervera P., Videau C., Viollet C., Petrucci C., Lacombe J., Winsky-Sommerer R., *et al.* Comparison of somatostatin receptor expression in human gliomas and medulloblastomas. *J Neuroendocrinol* 2002; 14(6): 458-471.
43. Lamszus K., Meyerhof W. and Westphal M. Somatostatin and somatostatin receptors in the diagnosis and treatment of gliomas. *J Neurooncol* 1997; 35(3): 353-364.
44. Schumacher T., Hofer S., Eichhorn K., Wasner M., Zimmerer S., Freitag P., *et al.* Local injection of the ^{90}Y-labelled peptidic vector DOTATOC to control gliomas of WHO grades II and III: an extended pilot study. *Eur J Nucl Med Mol Imaging* 2002; 29(4): 486-493.
45. Guyotat J., Champier J., Pierre G.S., Jouvet A., Bret P., Brisson C., *et al.* Differential expression of somatostatin receptors in medulloblastoma. *J Neurooncol* 2001; 51(2): 93-103.
46. Feindt J., Becker I., Blomer U., Hugo H.H., Mehdorn H.M., Krisch B., *et al.* Expression of somatostatin receptor subtypes in cultured astrocytes and gliomas. *J Neurochem* 1995; 65(5): 1997-2005.
47. Dutour A., Kumar U., Panetta R., Ouafik L., Fina F., Sasi R., *et al.* Expression of somatostatin receptor subtypes in human brain tumors. *Int J Cancer* 1998; 76(5): 620-627.
48. Maini C.L., Sciuto R., Tofani A., Ferraironi A., Carapella C.M., Occhipinti E., *et al.* Somatostatin receptor imaging in CNS tumours using ^{111}In-octreotide. *Nucl Med Commun* 1995; 16(9): 756-766.
49. Zinn K.R., Chaudhuri T.R., Buchsbaum D.J., Mountz J.M. and Rogers B.E. Simultaneous evaluation of dual gene transfer to adherent cells by gamma-ray imaging. *Nucl Med Biol* 2001; 28(2): 135-144.
50. Zinn K.R., Chaudhuri T.R., Buchsbaum D.J., Mountz J.M. and Rogers B.E. Detection and measurement of *in vitro* gene transfer by gamma camera imaging. *Gene Ther* 2001; 8(4): 291-299.

2.2 Molecular imaging following adenoviral gene transfer visualizes sst_2 and HSV1-tk expression

S.M. Verwijnen, M. ter Horst, P.A.E. Sillevis Smitt, R.C. Hoeben, F. Forrer, C. Müller, W.A.P. Breeman, E.P. Krenning, M. de Jong

Submitted

Abstract

Purpose: Gene therapy is an interesting approach to improve cancer treatment. Single photon emission computed tomography (SPECT) allows imaging of reporter gene expression non-invasively over time following gene transfer. The aim of this study was to use a novel integrated animal SPECT/CT to image and quantify human somatostatin receptor subtype 2 (sst_2) and to monitor Herpes Simplex Virus thymidine kinase (HSV-tk) expression following Ad5.tk.sst_2 gene transfer into tumor-bearing mice.

Methods: U87MG tumor-bearing mice were infected with Ad5.tk.sst_2 by intra-tumoral injection. Three days thereafter mice were injected with either [^{99m}Tc-N_4^{0-1},Asp^0,Tyr^3] octreotate or 1-(2'-deoxy-2'-fluoro-1'-β-D-ribofuranosyl)-5-[^{123}I]iodo-uracil to target sst_2 and HSV-tk, respectively and SPECT images were acquired. At several time points (3-7 days) post infection, sst_2 expression was imaged and quantified using SPECT/CT. Three days post infection, mice were euthanized for biodistribution studies and tumors were cryosectioned for *ex vivo* and *in vitro* autoradiography and immunohistochemistry to visualize the distribution pattern of sst_2 or HSV-tk expression.

Results: Using SPECT/CT, we could non-invasively image sst_2 and HSV-tk expression after Ad5.tk.sst_2 gene therapy. Up to a week after infection, sst_2 expression could be imaged and quantified. Autoradiography and immunohistochemistry showed non-homogeneous expression patterns of sst_2 and HSV-tk in infected tumors, probably visualizing the needle tracts of the viral injection.

Conclusions: This study demonstrates that sst_2 and HSV-tk genes can be used to image the location and duration of gene expression after intra-tumoral Ad5.tk.sst_2 gene transfer using SPECT/CT imaging. SPECT/CT is a useful tool for monitoring and quantification of receptor expression in vector-based gene transfer.

Introduction

Over the last years, the interest for and research in non-invasive imaging of small animals has grown extensively [1]. These imaging techniques include positron emission tomography (PET), single-photon emission computed tomography (SPECT), computed tomography (CT), magnetic resonance imaging and optical imaging. PET and SPECT enable visualization of e.g. biological processes in living animals. In the last decade, dedicated small animal imaging equipment with high resolution and high sensitivity has been developed [2-5]. These systems enable accurate quantification of radioactivity in particular organs, such as rat kidneys [6]. In the field of gene therapy, SPECT and PET imaging are helpful techniques to determine the location, duration and level of expression of the desired transgene [7], in preclinical as well as in clinical studies.

A good tumor candidate for gene therapy is glioblastoma multiforme (GBM). Patients suffering from GBM have a median survival rate of less than one year [8], showing the extreme aggressiveness of this tumor. The current standard treatment for GBM patients includes surgery, radiotherapy and chemotherapy. However, it is evident that these treatment modalities are not sufficiently effective, since the prognosis of these patients remains poor. Gene therapy is anticipated to be an attractive treatment option for GBM patients because of the localization of the tumor in the skull and the fact that distant metastases are uncommon. Clinical gene therapy trials for GBM have proven to be safe for patients and the environment, although the tumoricidal effects in these trials have been limited [9]. The lack of quantitative information on vector-mediated gene expression or functional protein activity was one of the weak points in these trials. Therefore, non-invasive imaging of transgene expression following treatment is of high interest.

In the present preclinical study, we investigated whether high-resolution animal SPECT/CT imaging would be suitable for monitoring transgene expression of human GBM tumors in mice. We used the Ad5.tk.sst_2 adenoviral vector [7, 10, 11], that carries two reporter genes encoding Herpes Simplex Virus type 1 thymidine kinase (HSV-tk) enzyme and human somatostatin receptor subtype 2 (sst_2). The HSV-tk gene is widely used in suicide gene therapy studies [12, 13]. Expression of HSV-tk in the target tissue leads to the production of the enzyme thymidine kinase (tk), which phosphorylates, for example, the prodrug ganciclovir (GCV). Phosphorylated forms of GCV are incorporated into the cellular DNA, followed by inhibition of DNA synthesis and thus leading to tumor cell death [14]. Monitoring of HSV-tk gene expression can be achieved using various radiolabeled nucleoside analogs, including ^{123}I or ^{124}I labeled 1-(2'-deoxy-2'-fluoro-1'-β-D-arabinofuranosyl)-5-iodo-uracil (FIAU) [15, 16], 1-(2'-deoxy-2'-fluoro-1'-β-D-arabinofurasyl)-5-methyl-uracil (FMAU)

[17], (E)-5-(2-iodovinyl)-2'-fluoro-2'-deoxyuridine (IVFRU) [18], 1-(2'-deoxy-2'-fluoro-1'-β-D-ribofuranosyl)-5-iodo-uracil (FIRU) [19] or ^{18}F-labeled 9-(4-fluoro-3-hydroxy-methyl-butyl)guanine (FHBG) [20]. These compounds are specifically phosphorylated by HSV-tk in the same way as GCV and consequently trapped in the cell interior.

The second transgene in the Ad5.tk.sst$_2$ vector is the sst$_2$-encoding gene. Since the discovery of the frequent overexpression of somatostatin receptors (sst) on diverse tumor types, radiolabeled somatostatin analogs that bind to sst on tumors have been developed for imaging and therapeutic application. Examples of sst targeting peptides currently being used in the clinic include [DTPA]octreotide [21], [DOTA,Tyr^3] octreotide[22], DOTA-lanreotide [23] and [DOTA^0,Tyr^3]octreotate [24]. Sst imaging and therapy are mostly being performed in patients with neuroendocrine tumors, because of the high expression level of receptors on these tumors. Other sst-positive tumors can be visualized and treated as well, provided that the accumulation of the radiolabeled sst analog in the tumor is high enough [25]. The above mentioned peptides can be used for peptide receptor radionuclide therapy (PRRT) when they are labeled with therapeutic radionuclides that emit β-particles such as ^{177}Lu or ^{90}Y, that have a higher energy and a longer particle range compared to γ-emitters used for imaging.

Previously we reported on the high expression of both sst$_2$ and HSV-tk after viral infection of human glioma cell lines *in vitro* [7]. In the present study we aimed to non-invasively image gene expression, i.e. both sst$_2$ and HSV-tk, using [^{99m}Tc-N$_4^{0-1}$,Asp^0,Tyr^3]octreotate ([^{99m}Tc]Demotate 2) [26] and [^{123}I]FIRU [19], respectively, *in vivo*. We used human U87MG glioma tumor cells in this study that originally express neither sst$_2$ nor HSV-tk. Following intra-tumoral viral infection of U87MG tumor-bearing mice, we performed *in vivo* imaging, quantification and longitudinal expression studies using a novel animal SPECT/CT platform with high resolution and sensitivity and *in vitro* and *ex vivo* autoradiography. In addition, we determined the pattern of gene expression in order to investigate whether or not both genes were expressed simultaneously after viral infection.

Materials and methods

Cell culture

The U87MG human glioblastoma/astrocytoma tumor cell line was purchased from the American Type Culture Collection (Manassas, Virginia). The CA20948 rat pancreatic tumor cell line was originally induced by azaserine [27, 28]. The 9L and 9L-tk rat gliosarcoma tumor cell lines were kindly provided by Dr. K.M. Hebeda (Dept. of Experimental Neurosurgery, Free University Hospital Amsterdam, The

Netherlands). 9L-tk was stably transfected with the HSV-tk gene under G418 selection [29]. CA20948 and 9L-tk tumor cells were used as positive controls for sst_2 and HSV-tk gene expression, respectively, while 9L was used as a negative control for HSV-tk gene expression.

CA20948 cells were cultured in Dulbecco's modified Eagle's medium (DMEM, Gibco, Breda, The Netherlands) supplemented with 2 mM glutamate (Gibco), 1 mM sodium pyruvate (Gibco) and 0.1 mg/l fungizone (Gibco). 9L and 9L-tk were both grown in DMEM, the latter supplemented with 0.25 mg/ml G418 (Gibco). U87MG were grown in modified Eagle's medium (MEM, Gibco) supplemented with 0.1 mM non-essential amino acids (Gibco), 2 mM L-glutamine (Gibco) and 1 mM sodium pyruvate. All media were also supplemented with 10% heat-inactivated fetal bovine serum (Gibco) and 50 IU/ml penicillin/streptomycin (Gibco). All cells were cultured in a humidified atmosphere at 37ºC containing 5% CO_2.

Radiolabeling with ^{99m}Tc

Demotate 2 stock solution (a kind gift from Dr. Nock and Dr. Maina, Demokritos, Athens, Greece) was prepared by dissolving 300 nmol lyophilized material in 300 µl milliQ and stored in small aliquots at –20°C. The labeling was slightly modified as described earlier [26]. In short, saline solution containing [^{99m}Tc]Na-TcO^{4-} (2.5-4 GBq ^{99m}Tc/ml) was eluted from a commercial ^{99}Mo/^{99m}Tc generator (Ultratechnekow, Tyco Healthcare, Petten, The Netherlands). Two µl of the stock solution was mixed with 50 µl 0.5 mol/l Na_2HPO_4 (pH 11.5–12), 5 µl 0.1 mol/l trisodiumcitrate solution, 420 µl eluate (range 900–1500 MBq $^{99m}TcO^{4-}$) and 10 µL of freshly prepared $SnCl_2$ solution (2 mg/ml $SnCl_2$/ethanol, Sigma, Zwijndrecht, The Netherlands). After a 15 minute (min) incubation at room temperature (RT), the pH was adjusted to 7-8 by addition of 10 µl 1 mol/l HCl, and finally 50 µl ethanol was added.

Radiolabeling with ^{111}In

$^{111}InCl_3$ was purchased from Mallinckrodt Medical (Petten, The Netherlands). [$DOTA^0$,Tyr^3]octreotate was labeled with ^{111}In as previously reported [30]. In order to prevent oxidation and radiolysis quenchers such as ascorbate (Bufa BV, Uitgeest, The Netherlands), ethanol and gentisic acid (Tyco Health Care, Petten, The Netherlands) were added prior to radiolabeling [31]. After cooling the samples, 10 µl 4 mM DTPA was added.

Commercially available [$DTPA^0$]octreotide (OctreoScan) kits were obtained from Mallinckrodt Medical/Tyco Health Care and radiolabeled as previously described [7]. The radiochemical purity was tested using instant thin layer chromatography and was determined to be >95%.

HPLC

Chromatographic analysis of [^{99m}Tc]Demotate 2 and [^{111}In-DOTA^{0},Tyr^{3}]octreotate was performed on a Waters Breeze HPLC system (Waters, Etten-Leur, The Netherlands) based on a 1525 binary HPLC pump also connected to a Unispec MCA γ-detector (Canberra, Zellik, Belgium). A Symmetry C_{18} 4.6 • 250 mm 5 µm HPLC column (Waters) was used as stationary phase, whereas the eluent system consisted of 0.1% TFA in H_2O (solvent A) and methanol (solvent B) applying the following gradient protocol: 0-2 min 100% A (flow rate 1 ml/min), 2-3 min 55% B, 3-30 min 65% B (flow rate 0.5 ml/min), 30-38 min 100% B (flow rate 1 ml/min), 38-40 min 100% B (flow rate 1 ml/min), 40-46 min 100% A (flow rate 1 ml/min).

Radiolabeling with ^{123}I

^{123}I-NaI was purchased from Cygne (Eindhoven, The Netherlands). FIRU was labeled with ^{123}I as previously published [18]. After the labeling procedure, ethanol in the solution was vaporized by air flow for ten minutes.

Amplification of the viral vector Ad5.tk.sst$_2$

The Ad5.tk.sst$_2$ is a replication incompetent adenoviral vector that contains the sst$_2$ and the HSV1-tk genes [10]. A separate early CMV promoter regulates both genes. Large scale amplification of Ad5.tk.sst$_2$ was carried out on PER.C6 cells as previously described [32] and the virus was titrated by plaque assay on 911 cells, yielding a mean of 3 x 10^{10} plaque forming units/ml (PFU/ml).

Tumor-bearing animals

The animal experimental protocol was approved by the Institutional Animal Care and Use Committee, and was in compliance with the Guide for the Care and Use of Laboratory Animals. Four to six week-old male NMRI nude/nude mice were purchased from Charles River Laboratories (Sulzfeld, Germany). One week after arrival, the animals were inoculated subcutaneously with CA20948, 9L, 9L-tk or U87MG tumor cells on the left and right flank or on the shoulder, under isoflurane/oxygen anaesthesia (Pharmachemie, Haarlem, The Netherlands). Suspensions of about 10^7 cells in 200 µl Hanks' Balanced Salt Solution (HBSS, Gibco) was prepared.

In vivo viral infection

Three days prior to the *in vivo* experiments, the mice were anaesthetized with inhalation anaesthesia (isoflurane/oxygen, Pharmachemie) and the U87MG tumors (with a volume of 150-300 mm^3) were injected in 4-5 different directions with 50 µl viral solution, containing 1.5x10^9 PFU Ad5.tk.sst$_2$. CA20948, 9L, 9L-tk and additional U87MG tumors were simultaneously injected with saline.

Tracer injection

On the day of the SPECT/CT scan, the animals (n=3 per group) were injected into the penis vein with 200 µl of radiolabeled tracer (either 100 MBq/1 µg [^{99m}Tc] Demotate 2 or 40 MBq/0.6 µg [^{123}I]FIRU) under inhalation anaesthesia. Due to the non-homogeneous expression, we expected a suboptimal SPECT image and decided to inject a high amount of radioactivity in order to visualize the expression of these genes. Biodistribution studies were performed on animals injected with 10 MBq/0.5µg [^{99m}Tc]Demotate 2 and 3 MBq/0.1 µg [^{123}I]FIRU. Both biodistribution studies and SPECT/CT scans were performed at 4 hours post injection (p.i.) of the tracer.

SPECT and CT imaging studies

SPECT and CT imaging were performed with a four-headed multiplexing multi-pinhole NanoSPECT/CT camera (Bioscan Inc., Washington D.C., USA). SPECT was acquired as described previously [6]. Briefly, animals were anaesthetized with a mixture of ketalin and xylazine and were imaged with mouse apertures that comprise a total of 36 1.4-mm-diameter pinholes. The energy-peak of the camera was set at 140 keV for ^{99m}Tc and 159 keV for ^{123}I. An acquisition time of 40 seconds/projection was chosen, resulting in an total acquisition time of 20 min per animal, imaging the whole body. CT scans were performed with the integrated CT-scanner. The tube voltage was set at 45 kVp. An exposure time of 1 second/projection was chosen, imaging with 180 projections/rotation, lasting 6 min for a whole body CT. The SPECT acquisitions were reconstructed iteratively with the HiSPECT software (Bioscan Inc.) and quantification was performed using the MIPtool program (Mediso Ltd., Budapest, Hungary).

Longitudinal study

In an additional study we examined sst_2 expression in Ad5.tk.sst_2 infected U87MG tumors over time. Three animals bearing two U87MG tumors were injected with $2x10^9$ PFU Ad5.tk.sst_2 in one tumors and with saline in the other. Three days after infection, a SPECT/CT scan was made 4 hours after injection of 100 MBq/1 µg [^{99m}Tc] Demotate 2. At days 4 and 6, the animals were injected with 50 MBq/0.5 µg and 100 MBq/1 µg [^{111}In-DTPA^0]octreotide, respectively, and scanned at 4 hours post tracer injection. Quantification of the scans was performed as described above.

Biodistribution and ex vivo autoradiography

Four hours p.i. of the radiolabeled tracer, the animals were sacrificed and blood, tissue samples and tumors were collected and counted in a gamma counter (LKB-1282-Compugammasystem, Perkin Elmer, Groningen, The Netherlands). The tumors were frozen immediately after counting, embedded in TissueTek (Sakura, Zoeterwoude,

The Netherlands) and processed for cryosectioning. Ten µm tissue sections were mounted on SuperFrostPlus glass slides (Menzel, Braunschweig, Germany) and exposed overnight to phosphor imaging screens (Perkin Elmer, Boston, USA) in X-ray cassettes (Kodak, Vianen, The Netherlands) for *ex vivo* autoradiography. Three adjacent sections were stored at -20°C and used only after radioactive decay for *in vitro* autoradiography and immunohistochemistry (see below). The exposed phosphor screens were analyzed using a Cyclone phosphor imager and a computer-assisted OptiQuant image processing system (version 03.00, Perkin Elmer).

In vitro autoradiography

In vitro autoradiography was performed as previously described [33] in order to investigate viral gene expression in the infected U87MG tumors. CA20948 and 9L-tk tumors were used as a positive control for sst_2 and HSV-tk gene expression, respectively. Sections of Ad5.tk.sst_2-infected and saline injected U87MG tumors, CA20948, 9L-tk tumors and rat brain (that also served as a positive control for sst_2-specific binding) were incubated 10^{-10} M [^{111}In-DOTA^0-Tyr^3]octreotate. Blocking experiments were performed with adjacent sections by incubation with 10^{-10} M [^{111}In-DOTA^0,Tyr^3] octreotate with 10^{-6} M octreotide (Novartis, Basel, Switzerland) in the same buffer. After incubation the sections were washed, dried and exposed to phosphor screens overnight. The screens were analyzed as explained above.

Immunohistochemistry

Immunohistochemistry was performed as previously reported [34]. The primary antibody Rabbit-anti-HSV-thymidine kinase (with the courtesy of Dr. W. Summers, Yale University, New Haven, Connecticut) was used in a dilution of 2% and incubated for one hour at RT. After washing, horseradish peroxidase-conjugated secondary antibody swine-anti-rabbit-Ig (DAKOcytomation, Glostrup, Denmark) was incubated in optimal dilution (4%) for 1 hour at RT. Visualization of the specific signal was achieved with H_2O_2 activated diaminobenzidine (DAB) substrate (DAKOcytomation). Nuclei were counterstained using haematoxylin (Fluka Chemika, Buchs, Switzerland).

Statistical analysis

Data are expressed as mean ± SEM. Results were statistically analyzed using two-way ANOVA. Differences were considered statistically significant when P was <0.05. When this was the case, a Bonferroni post-test was performed to compare all groups. All statistical analysis was performed with GraphPad Prism 4.0 program.

Results

Labeling of [^{99m}Tc]Demotate 2, [^{111}In-DOTA^0,Tyr^3]octreotate and [^{123}I]FIRU

Labeling of [^{99m}Tc]Demotate 2 could be performed up to a specific activity (SA) of 250 MBq ^{99m}Tc per nmol [^{99m}Tc]Demotate 2 and a radiochemical purity (RCP) of >80% (range 80-87%, n=6), with no significant reduction of ^{99m}Tc-incorporation or reduction in RCP (HPLC results are not shown). Increase in amount or multiple additions of $SnCl_2$ or prolongation of the reaction time did not result in an increase of ^{99m}Tc-incorporation or RCP.

The incorporation of ^{111}In was >95%. The mean SA of [^{111}In-DOTA^0,Tyr^3]octreotate was 144 MBq/nmol and the mean SA of [^{111}In-DTPA^0]octreotide was 139 MBq/nmol.

The mean labeling yield of [^{123}I]FIRU was 38% (0.89 MBq/nmol). No purification steps were necessary, due to high radiochemical purity of >97% [35].

Animal SPECT/CT imaging studies

Figure 1 shows two examples of SPECT/CT images of animals injected with [^{99m}Tc] Demotate 2. Visually, the saline-injected U87MG tumor showed no [^{99m}Tc]Demotate 2 uptake, while accumulation of the radiopharmaceutical was found in Ad5.tk.sst$_2$-infected U87MG tumors. The quantification results showed 200 times more radioactivity in the Ad5.tk.sst$_2$ infected tumor than in the saline injected tumor. Furthermore, the radiolabeled tracer was not homogeneously distributed throughout the Ad5.tk.sst$_2$-infected tumor probably because the virus did not spread within the tumor tissue. The CA20948 sst$_2$-positive tumor, used as a positive control, showed a higher and more homogeneous uptake compared to the viral infected tumor. In addition, these SPECT/CT images showed accumulation of radioactivity in the thyroid, bowel, liver, kidneys and bladder.

Uptake of [^{123}I]FIRU was found in Ad5.tk.sst$_2$-infected tumors, as shown in figure 2. No CT acquisition was made of these animals. 9L-tk tumors, serving as a positive control for HSV-tk expression, showed high radioactivity while the radioactivity in saline injected U87MG and 9L tumors, that do not express viral tk, was not above background. Thyroid, bladder and to a lesser extent liver also showed some accumulation of radioactivity in these animals.

Longitudinal study

The results of longitudinal imaging of Ad5.tk.sst$_2$-induced sst$_2$ expression in U87MG tumors are shown in figure 3. The images are depicted with the same settings of the color scale and show that the tumoral radioactivity after injection of sst$_2$ analogs decreased over time. Quantification of these images showed that, even though

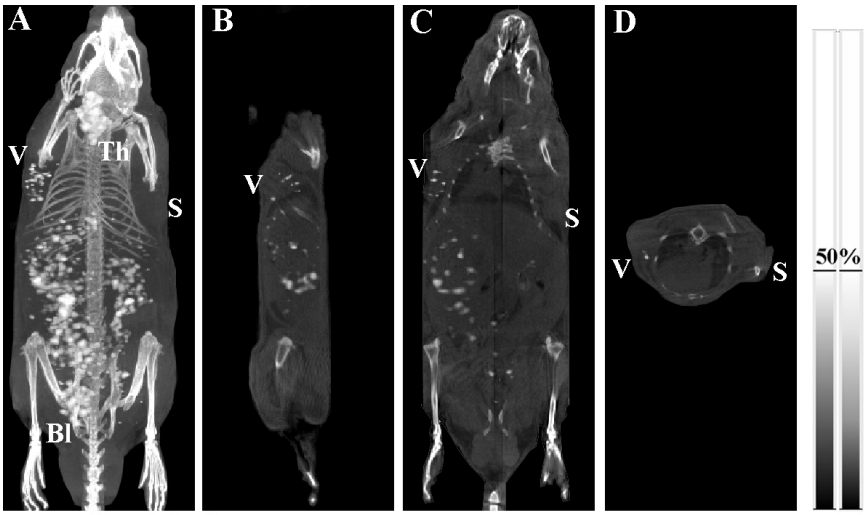

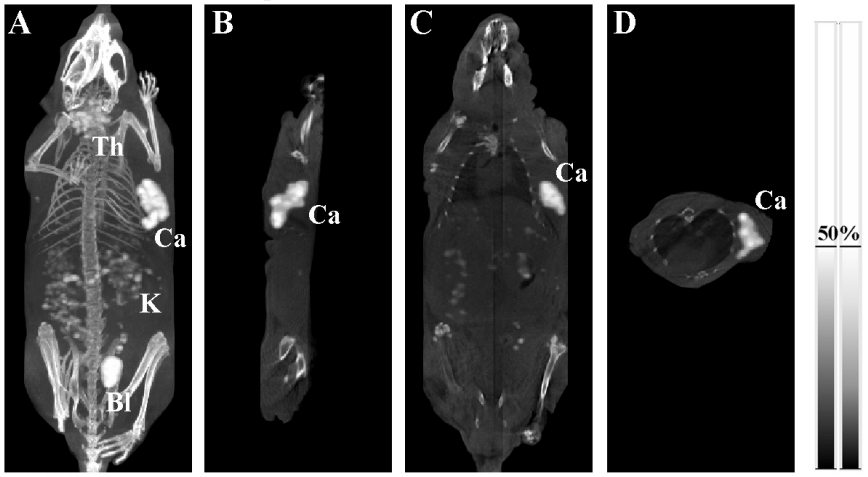

	U87MG + Ad5.tk.sst_2	U87MG + saline	CA20948
^{99m}Tc activity (kBq)	0.0275	0.0002	0.1295
measured volume (mm^3)	104	137	158
Uptake (kBq/mm^3)	0.2637	0.00113	0.8189

Figure 1: Animal SPECT/CT scans. The upper panel shows a mouse bearing one Ad5.tk.sst_2 infected U87MG tumor and one saline-injected U87MG tumor. The lower panel shows a sst_2-positive CA20948 tumour-bearing mouse. Both where scanned 4 hours p.i. of 100 MBq (1 µg) [^{99m}Tc]Demotate 2. Maximum intensity projection images (A), sagittal (B), coronal (C) and transversal (D) slices are shown at the height of the tumor. Images are representative examples of n=3 animals per group. Grey scale = CT image, Color scale = SPECT image, slice thickness=0.30 mm. (Th=thyroid, Bl=bladder, K=kidney, V=viral-infected U87MG tumor, S=saline-injected U87MG tumor, Ca=CA20948 tumor). The table shows quantification results of these images.

For color figure see page 237.

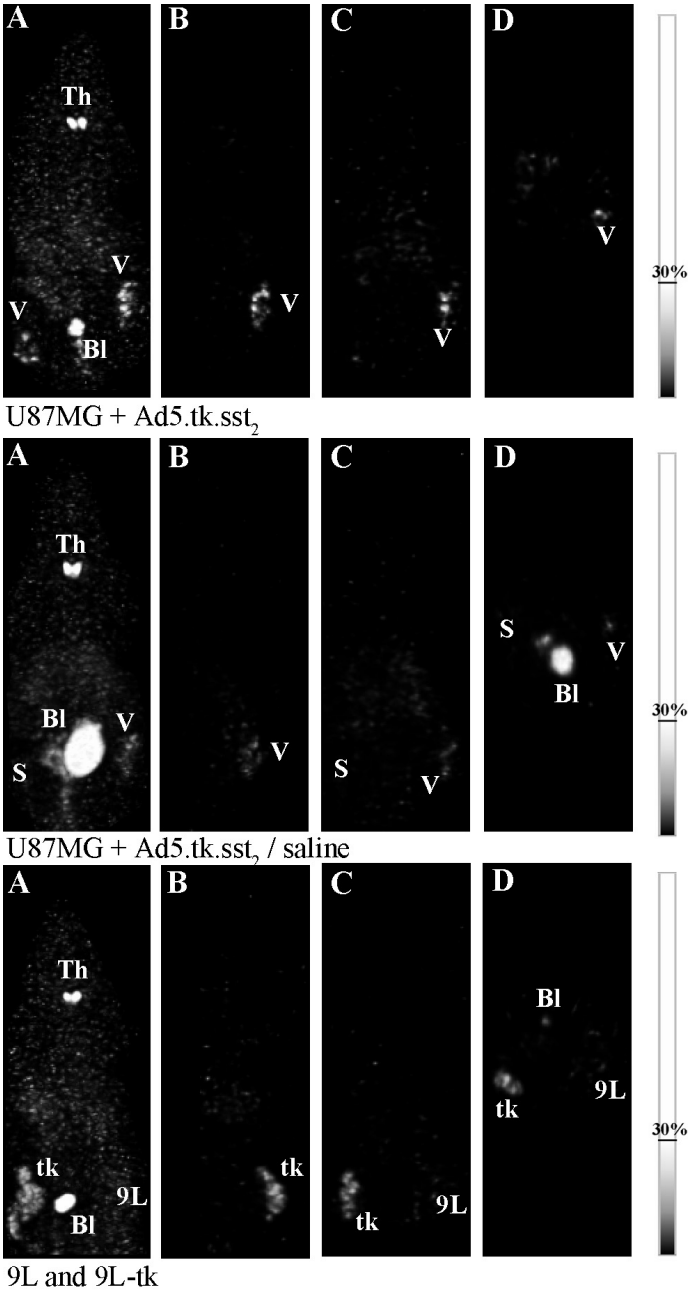

Figure 2: Animal SPECT scans of Ad5.tk.sst$_2$ infected or saline injected U87MG and 9L-tk/9L tumor bearing mice injected with 40 MBq/0.6 µg [^{123}I]FIRU, 4 hours p.i. of the radiolabelled tracer. Whole body images (A), coronal (B), sagittal (C) and transversal (D) slices are shown at the height of the tumor, slice thickness=0.30 mm. Images are examples of n=3 animals per group. (Th=thyroid, Bl=bladder, V=viral-infected U87MG tumor, S=saline injected U87MG tumor, tk=9L-tk tumor, 9L=9L tumor)
For color figure see page 238.

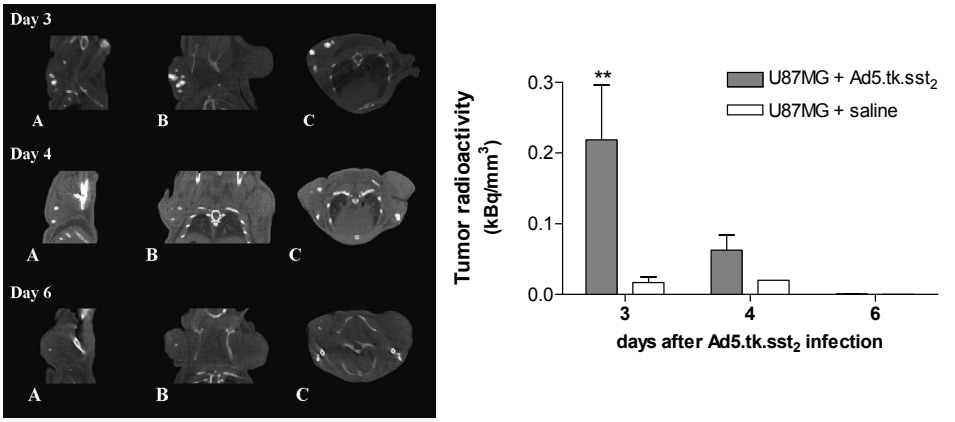

Figure 3: Longitudinal study in a mouse bearing one Ad5.tk.sst_2 infected and one saline injected U87MG tumor. On day 3, 4 and 6 after infection the mouse was injected with either 100 MBq/1 µg [^{99m}Tc]Demotate 2 (on day 3) or [^{111}In-DTPA^0]octreotide (on days 4 and 6); SPECT and CT images were made. SPECT images are shown at the height of the tumor, slice thickness=0.30 mm. The graph shows the quantification results of at least n=2 animals. (sagittal (A), coronal (B) and transversal (C) slices are shown). Data is expressed as mean ± SEM kBq/mm^3. ** P<0.01.
For color figure see page 239.

tracer radioactivity decreased, it remained detectable until at least seven days after infection. All SPECT images showed higher radioactivity accumulation in the virally infected tumors than in the saline injected tumors.

Biodistribution

The results of the biodistribution study are summarized in figure 4. The mean of four ([^{99m}Tc]Demotate 2) or two ([^{123}I]FIRU) independent experiments was calculated, resulting in at least 5 animals per tracer group. The organ distribution (figure 4A) shows a significant higher uptake of [^{99m}Tc]Demotate 2 in liver of viral infected animals than in the saline treated animals. In Ad5.tk.sst_2-infected U87MG tumors, we found almost 2% ID/g tumor in animals injected with [^{99m}Tc]Demotate 2 at 4 hr p.i., while the saline-injected U87MG tumors showed only 0.1% uptake at this time point (figure 4B). These findings indicate that the uptake of [^{99m}Tc]Demotate 2 in Ad5.tk.sst_2-infected U87MG tumors was mediated via sst_2 expressed on Ad5.tk.sst_2-infected tumor cells.

The biodistribution of [^{123}I]FIRU, however, showed no specific differences between infected and non-infected animals (figure 4C). Especially, we could not find a significantly higher uptake in Ad5.tk.sst_2 infected tumors compared to that in the saline-injected controls (Figure 4D). The uptake of [^{123}I]FIRU in HSV-tk-expressing cells was comparable to that of [^{99m}Tc]Demotate 2 in sst_2-expressing tumors (1.625 vs 1.744 %IA/g tissue, respectively).

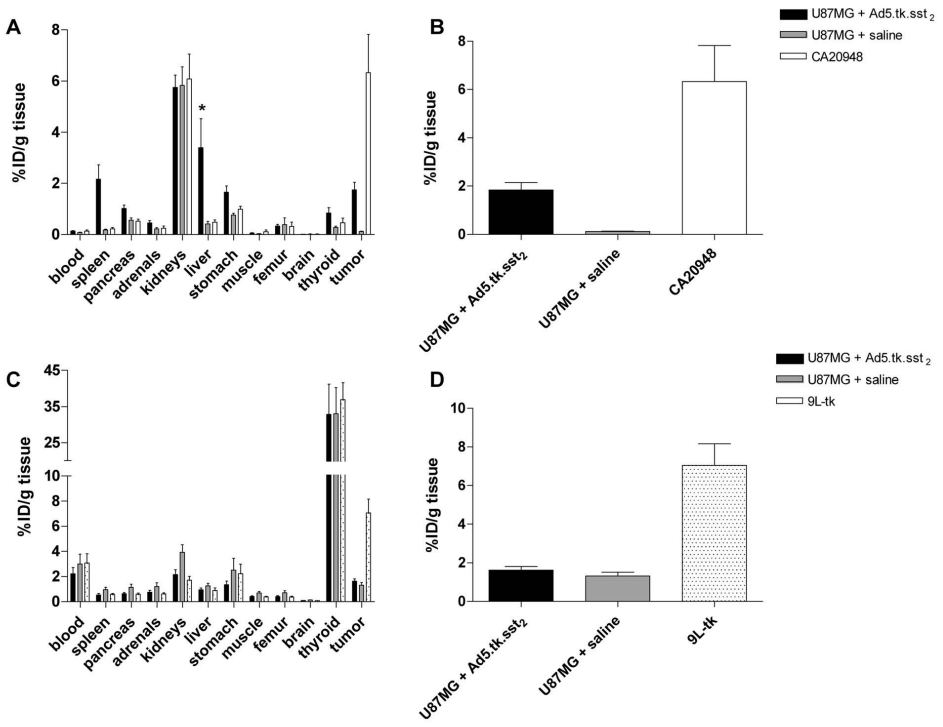

Figure 4: (A) Biodistribution of [^{99m}Tc]Demotate 2 at 4 hours p.i. (B) Tumour uptake in Ad5.tk.sst$_2$ (n=35) and saline injected U87MG (n=12) bearing mice 4 hours after i.v. injection of 10 MBq/0.5 µg [^{99m}Tc]Demotate 2. CA20948 tumor was used as a sst$_2$-positive control (n=14). (C) Biodistribution of [^{123}I]FIRU at 4 hours p.i. (D) Tumour uptake in Ad5.tk.sst$_2$ (n=10) and saline injected U87MG (n=14) bearing mice 4 hours after i.v. injection of 3 MBq/0.1 µg [^{123}I]FIRU. 9L-tk tumor was used as a HSV-tk-positive control (n=10). U87MG tumors were infected 72 hours prior to the biodistribution with 1.5 x 10^9 PFU Ad5.tk.sst$_2$. All data are expressed as mean + SEM %IA/g tissue. Figure A and C show results of at least n=5. * P<0.05.

Ex vivo and in vitro autoradiography

Figure 5 shows examples of *ex vivo* autoradiographs of frozen tumor sections at 4 hours after injection of [^{99m}Tc]Demotate 2 (A) or [^{123}I]FIRU (B). We found that the radioactivity distribution of both tracers was not homogeneous in Ad5.tk.sst$_2$-infected tumors, probably because the virus did not distribute evenly in the tumor. High and more homogeneous tracer radioactivity was found in the CA20948 and 9L-tk tumors, the sst$_2$- and HSV-tk-positive controls, respectively. We did not find an increased uptake in saline-injected U87MG tumors after injection of both tracers, indicating that the uptake of the tracers in the Ad5.tk.sst$_2$-infected tumors was mediated by the expression of the targeted proteins.

Figure 5 also shows the *in vitro* autoradiographies of sections adjacent to those used for *ex vivo* autoradiography. These data shows sst$_2$-mediated binding in these tissues, resembling the pattern of sst$_2$ and HSV-tk expression in the *ex vivo*

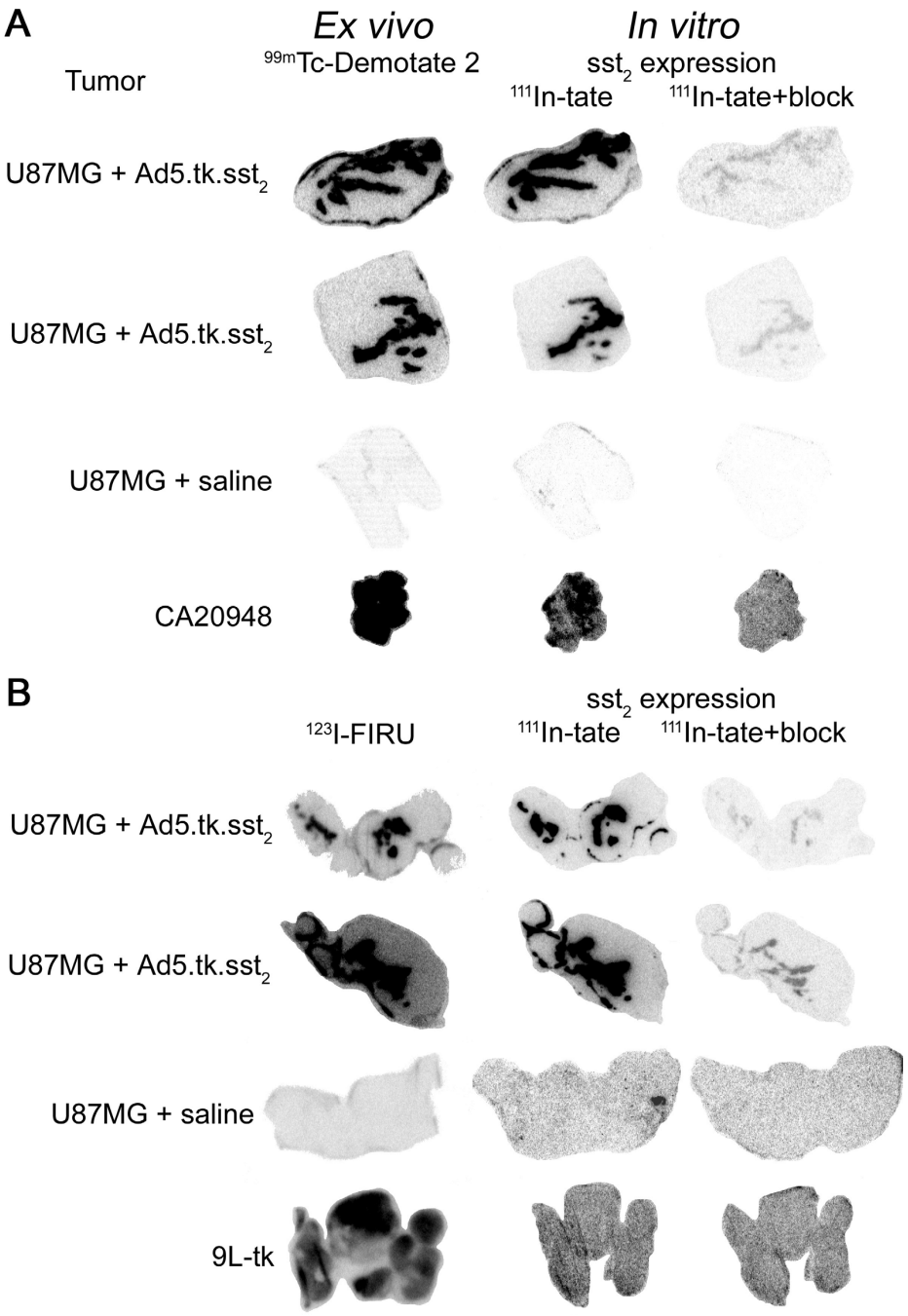

Figure 5: *Ex vivo* autoradiography images showing the intra-tumoral distribution of [^{99m}Tc]Demotate 2 (A) and [^{123}I]FIRU (B) as well as *in vitro* autoradiography images showing [^{111}In-DOTA^{0},Tyr^{3}]octreotate binding in the adjacent tumor sections. Two representative Ad5.tk.sst$_2$ infected U87MG tumors, CA20948, 9L-tk and saline injected U87MG tumors are shown for each radiolabelled tracer.

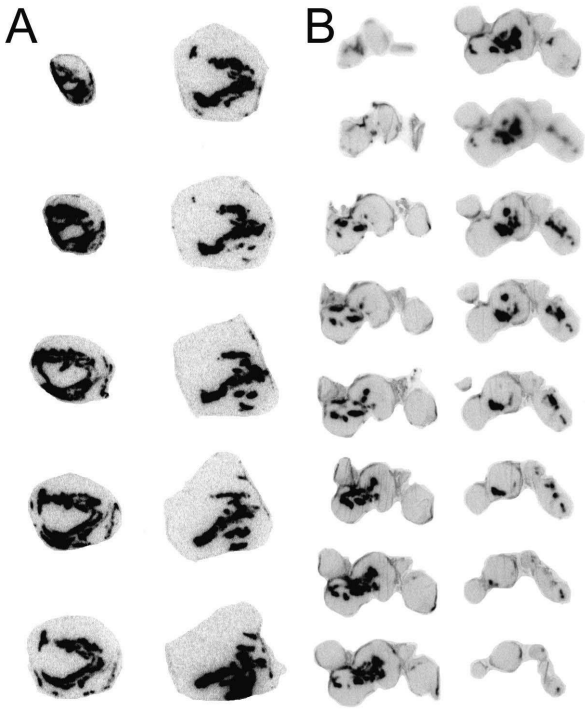

Figure 6: *Ex vivo* autoradiography of different sections taken throughout two Ad5.tk.sst_2 infected U87MG tumors. Tumor sections show radioactivity of [^{99m}Tc]Demotate 2 (A) and [^{123}I]FIRU (B). The distance between each section is 250 µm.

autoradiography. In addition, the binding of [^{111}In-DOTA^0,Tyr^3]octreotate could be blocked in all Ad5.tk.sst_2-infected tumor sections and in that of the sst_2-positive controls: rat brain tissues (data not shown) and CA20948. No receptor binding of [^{111}In-DOTA^0,Tyr^3]octreotate was seen in the non-infected U87MG tumors and the HSV-tk-positive control, which do not express sst_2 on their cell membranes.

Two series of tumor sections from different tumor levels revealing the pattern of both [^{99m}Tc]Demotate 2 and [^{123}I]FIRU radioactivity using *ex vivo* autoradiography are depicted in figure 6. Again, it could be shown that sst_2 and HSV-tk genes were not homogeneously expressed following Ad5.tk.sst_2 infection. We found a striped pattern, probably representing the needle tracks of the viral injection.

Immunohistochemistry

Figure 7 shows *ex vivo* and *in vitro* autoradiographs and HSV-tk-immunohistochemistry sections of an Ad5.tk.sst_2-infected U87MG tumor at increasing magnification. Only U87MG tissue that was infected with Ad5.tk.sst_2 showed both HSV-tk and sst_2 expression as can be seen from the matching autoradiography and the immunohistochemistry results.

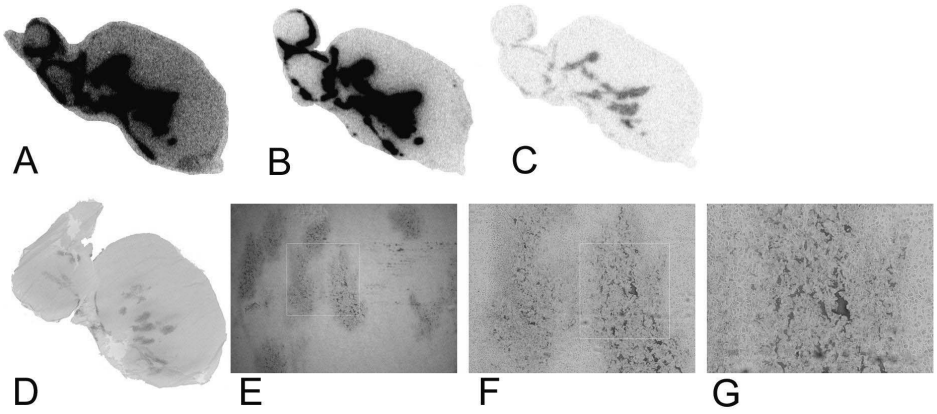

Figure 7: *Ex vivo* autoradiography 4 hours after injection of 3 MBq of [^{123}I]FIRU (A), *in vitro* autoradiography using 10^{-10} M [^{111}In-DOTA^0,Tyr^3]octreotate (B), or [^{111}In-DOTA^0,Tyr^3]octreotate plus an excess of octreotide (C) and immunohistochemistry (D-G) staining using rabbit-anti-HSV-tk primary antibody, at different magnifications; D: section overview (no magnification), E: 40x, F: 100x, G: 200x.
For color figure see page 240.

Discussion

One of the challenges of gene therapy in clinical studies is the current lack of quantitative information about the expression of the genes of interest and their products, such as enzymes or receptors, after vector administration to the tumor cells [9]. In this study, we used a novel animal SPECT/CT imaging system and we showed that during pre-clinical studies this can be a most useful tool for non-invasive imaging of reporter genes, such as sst_2 and HSV-tk, expressed after Ad5.tk.sst_2 infection *in vivo*. We were also able to quantify the radioactivity in the tumors using the imaging data, which was previously shown for rat kidneys [6] and is now shown feasible for tumors as well.

We used a subcutaneous human glioma tumor model in nude mice that was injected with a non-replicating Ad5.tk.sst_2 viral vector, followed by intravenous injection three days later of radiolabeled tracers to show transgene expression. The results of *in vivo* SPECT imaging using [^{99m}Tc]Demotate 2 and [^{123}I]FIRU for sst_2 and HSV-tk expression, respectively, showed a non-homogeneous uptake of both tracers in the Ad5.tk.sst_2-infected tumors. The striped and spotted pattern of the radioactivity of these tracers revealing sst_2 and HSV-tk expression can be explained by the fact that the viral vector was injected directly into the tumor and that we used a non-replicating viral vector. This heterogeneous gene expression was also shown by Buchsbaum et al. in an A-427 tumor infected with an adenoviral vector carrying the sst_2 gene and after injection of ^{99m}Tc-P2045 [36]. In an earlier study we investigated the viral spread in solid tumor tissue and compared single and multiple injections

with convection enhanced delivery (CED), i.e. slow infusion of the virus [37]. Using all delivery modalities, spread of the viral vector was low in glioma tumor tissues, although multiple injections resulted in enhanced distribution when compared to CED or single injection.

The results of our longitudinal study indicate that sst_2 expression decreased over time in Ad5.tk.sst_2 infected tumors. Hemminki and co-workers were able to detect sst_2 expression for at least 15 days after RGDTKSSTR infection in Hey ovarian cancer cells *in vivo* using a gamma camera [38]. This is longer than in our study, which can be explained by the fact that the Hey tumors were infected twice during these 15 days. We also expect that the use of a replicating viral vector will increase the long-term gene expression in our study. Nevertheless, similar to our findings, Hemminki et al. found that sst_2 expression decreased over time, measured with region of interest analysis.

Biodistribution results showed an increased [^{99m}Tc]Demotate 2 radioactivity in the livers of viral infected U87MG-bearing animals compared to the saline injected animals. This phenomenon was observed in less than half of the animals in this group. It is conceivable that in these animals a blood vessel had been punctured during intra-tumoral infection with subsequent infection of the liver by the viral particles. This, however, has no impact on the amount of radioactivity in the Ad5.tk.sst_2 infected tumors (data not shown). In addition, the biodistribution results also show that there is hardly any difference in uptake of radioactivity between infected and non-infected U87MG tumors after injection with [^{123}I]FIRU, while SPECT images do show such differences. Unfortunately, at this stage we cannot explain the discrepancy between these results. One possible explanation could be that we injected a higher amount radiolabeled FIRU mass in the SPECT studies compared to that in the biodistribution studies, because of the higher radioactivity levels needed for SPECT studies. We plan to investigate this phenomenon in more detail in future experiments.

The non-homogeneous expression of reporter genes in the viral infected tumors which was found with SPECT imaging, was confirmed by the *ex vivo* and *in vitro* autoradiographs of Ad5.tk.sst_2-infected U87MG tumor sections. This can be one of the explanations of the lower levels of therapeutic efficacy in clinical gene therapy trials [9]. To increase the effectiveness of viral based gene therapy, the need for a more homogeneous transgene expression is evident. Several methods to increase intra-tumoral spread of adenoviruses have been published, including pre-treatment with protease [39] and elastase [40] and the use of relaxin-expressing adenoviruses [41]. Results from these studies show that connective tissue and the extracellular matrix play a role in reducing the viral spread in tumors.

Ex vivo autoradiography also showed that the pattern of both [^{99m}Tc]Demotate 2 and [^{123}I]FIRU uptake corresponded with sst_2 expression according to the adjacent *in vitro* autoradiographs. *In vitro* autoradiography studies were performed with three purposes: 1) to show that uptake of [^{99m}Tc]Demotate 2 was receptor-specific using a blockade with an excess of unlabeled peptide, 2) to show that the binding pattern of both tracers in these tumor sections was similar and resembled the expression of sst_2 in these tissues because of viral gene expression and not because of inflammation and 3) to show that both sst_2 and HSV-tk were simultaneously expressed in infected tumor tissue. Immunohistochemistry confirmed that the pattern of HSV-tk expression was similar with the pattern of sst_2 expression, indicating that both genes were expressed simultaneously after infection with Ad5.tk.sst_2. We therefore consider that sst_2 expression in these tissues is probably not due to inflammation in the tumor after the viral infection, but due to the viral gene transfer.

In our studies, we found that both genes can be used to visualize the location of gene expression following Ad5.tk.sst_2 gene transfer. Sst_2 imaging can be used when the sst_2 expression in the surrounding tissue is low, while in tissues with high sst_2-expression imaging with HSV-tk substrates will be preferable. It is published that normal human brain tissue shows expression of sst [42] and we therefore recommend that post-infection imaging in GBM tissue would be performed using HSV-tk gene expression. We were able to show that FIRU radiolabeled with ^{123}I is suitable for SPECT imaging. In addition, other nucleosides, such as FHBG or FIAU, can be used for visualization of HSV-tk expression in sst_2-rich areas. While FIAU is not known for crossing the blood-brain-barrier (BBB) [43], this nucleoside can still be used for HSV-tk expression imaging studies when the BBB is disrupted, which is often the case in GBM patients. Depending on the radionuclide, these nucleosides can be used for PET [16] as well as SPECT imaging [44], with high uptake in HSV-tk expressing tissue. Provided that sst_2 expression in the tissue surrounding the tumor is low, radiolabeled somatostatin analogs are our preferred choice for *in vivo* imaging. They have the advantage of high and specific membrane binding and uptake in sst_2-expressing tissue [45], the radiolabeling can be performed routinely at high specific activity [30].

The use of this dual transgene expressing viral vector offers the possibility to apply a combination with both sst_2 radionuclide therapy and HSV-tk/GCV suicide therapy, which is expected to have a higher tumoricidal effect than each of the therapeutic methods alone. Boucher et al. combined GCV treatment with 5-fluorocytosine (5-FC) administration in a double suicide gene therapy modality [46]. They found that the sequential incubation of DU145 human prostate cancer cells with 5-FC and GCV increased cytotoxicity *in vitro*. We plan to perform a combination therapy in U87MG infected tumors *in vivo* with peritoneally injected GCV and systemically injected

^{177}Lu or ^{90}Y labeled [DOTA^{0},Tyr^{3}]octreotate to show improved therapeutic effect when these compounds are used together. In our case, it might be more interesting to use an ^{90}Y-labeled compound in a therapy study, since ^{90}Y emits β-particles with higher energy (2.3 MeV) and longer path length (12 mm) compared to ^{177}Lu (0.49 MeV and 2 mm, respectively). Taken into account the non-homogeneous expression of sst_2 in Ad5.tk.sst_2 infected tumors, it can be expected that more damage to the tumor cells would be induced using ^{90}Y.

Zinn et al. showed simultaneous imaging of both sst_2 and HSV-tk expression in transfected A-427 human non-small cell lung cancer cells using gamma camera imaging [11]. They concluded that this double transgene approach in gene transfer allows dual isotope detection with a gamma camera to show simultaneous *in vivo* monitoring of the expression of more than one transgene. They also found that sst_2 expression imaging *in vivo* using ^{99m}Tc-P2045 showed excellent sensitivity and linearity related to the dose of the adenovirus, which was in contrast with the HSV-tk expression, which was not reliably detected using ^{131}I-FIAU. They state that the HSV-tk system may have inherent problems for *in vivo* imaging due to the difference in delivery to the HSV-tk-expressing cells, compared to sst_2 (diffusion instead of receptor binding and internalization), making the latter more interesting at least for imaging. Our biodistribution results showed that ^{123}I-FIRU in viral-infected tumor tissue was not significantly increased compared to non-infected tissue, indicating that ^{123}I-FIRU is not exclusively taken up in cells that are expressing the HSV-tk gene. These results differ from the results reported by Nanda et al. who found a slightly higher uptake in IG.AdApt.TK infected tumors at 4 hours p.i. [19]. This discrepancy might be caused by a different time period after viral infection (2 days reported by Nanda et al. compared to 3 days in our study). However, we believe that, although the mechanism of delivery is different compared to sst_2 binding and internalization, imaging of HSV-tk expression using ^{123}I-FIRU is feasible *in vivo*.

This study is one of the first in using animal SPECT/CT imaging for the detection and quantification of viral gene expression after Ad5.tk.sst_2 gene transfer in human glioma tumor-bearing mice. We performed viral infections intra-tumorally in U87MG tumors that did not express HSV-tk or sst_2 prior to the introduction of the viruses representing the patient situation. We conclude that intra-tumoral *in vivo* infection using Ad5.tk.sst_2 resulted in the simultaneous and non-homogenous expression of both HSV-tk and sst_2 and that these reporter genes can be used for imaging viral gene expression using radiolabeled HSV-tk and sst_2 substrates. Infected tumors showed only limited long-term expression of transgenes *in vivo*. Non-invasive imaging techniques, such as SPECT/CT, can be applied for monitoring and quantification of gene expression following vector-based gene transfer and subsequent treatment of cancer.

References

1. Massoud T.F. and Gambhir S.S. Molecular imaging in living subjects: seeing fundamental biological processes in a new light. *Genes Dev*, 2003 17(5): 545-580.
2. Beekman F.J., van der Have F., Vastenhouw B., van der Linden A.J., van Rijk P.P., Burbach J.P., *et al.* U-SPECT-I: a novel system for submillimeter-resolution tomography with radiolabeled molecules in mice. *J Nucl Med*, 2005 46(7): 1194-1200.
3. Schramm N.U., Ebel G., Engeland U., Schurrat T., Behe M. and Behr T.M. High-resolution SPECT using multipinhole collimation. *IEEE Trans Nucl Sci*, 2003 50(3): 315-320.
4. Chatziioannou A., Tai Y.C., Doshi N. and Cherry S.R. Detector development for microPET II: a 1 microl resolution PET scanner for small animal imaging. *Phys Med Biol*, 2001 46(11): 2899-2910.
5. Ritman E.L. Molecular imaging in small animals--roles for micro-CT. *J Cell Biochem Suppl*, 2002 39: 116-124.
6. Forrer F., Valkema R., Bernard B., Schramm N.U., Hoppin J.W., Rolleman E., *et al. In vivo* radionuclide uptake quantification using a multi-pinhole SPECT system to predict renal function in small animals. *Eur J Nucl Med Mol Imaging*, 2006 33(10): 1214-1217.
7. Verwijnen S.M., Sillevis Smitt P.A., Hoeben R.C., Rabelink M.J., Wiebe L., Curiel D.T., *et al.* Molecular imaging and treatment of malignant gliomas following adenoviral transfer of the herpes simplex virus-thymidine kinase gene and the somatostatin receptor subtype 2 gene. *Cancer Biother Radiopharm*, 2004 19(1): 111-120.
8. Surawicz T.S., Davis F., Freels S., Laws E.R., Jr. and Menck H.R. Brain tumor survival: results from the National Cancer Data Base. *J Neurooncol*, 1998 40(2): 151-160.
9. Rainov N.G. and Ren H. Gene therapy for human malignant brain tumors. *Cancer J*, 2003 9(3): 180-188.
10. Hemminki A., Belousova N., Zinn K.R., Liu B., Wang M., Chaudhuri T.R., *et al.* An adenovirus with enhanced infectivity mediates molecular chemotherapy of ovarian cancer cells and allows imaging of gene expression. *Mol Ther*, 2001 4(3): 223-231.
11. Zinn K.R., Chaudhuri T.R., Krasnykh V.N., Buchsbaum D.J., Belousova N., Grizzle W.E., *et al.* Gamma camera dual imaging with a somatostatin receptor and thymidine kinase after gene transfer with a bicistronic adenovirus in mice. *Radiology*, 2002 223(2): 417-425.
12. Rainov N.G. A phase III clinical evaluation of herpes simplex virus type 1 thymidine kinase and ganciclovir gene therapy as an adjuvant to surgical resection and radiation in adults with previously untreated glioblastoma multiforme. *Hum Gene Ther*, 2000 11(17): 2389-2401.
13. Trask T.W., Trask R.P., Aguilar-Cordova E., Shine H.D., Wyde P.R., Goodman J.C., *et al.* Phase I study of adenoviral delivery of the HSV-tk gene and ganciclovir administration in patients with current malignant brain tumors. *Mol Ther*, 2000 1(2): 195-203.
14. Moolten F.L. Drug sensitivity ("suicide") genes for selective cancer chemotherapy. *Cancer Gene Ther*, 1994 1(4): 279-287.
15. Tjuvajev J.G., Chen S.H., Joshi A., Joshi R., Guo Z.S., Balatoni J., *et al.* Imaging adenoviral-mediated herpes virus thymidine kinase gene transfer and expression *in vivo*. *Cancer Res*, 1999 59(20): 5186-5193.
16. Jacobs A., Voges J., Reszka R., Lercher M., Gossmann A., Kracht L., *et al.* Positron-emission tomography of vector-mediated gene expression in gene therapy for gliomas. *Lancet*, 2001 358(9283): 727-729.
17. de Vries E.F., van Waarde A., Harmsen M.C., Mulder N.H., Vaalburg W. and Hospers G.A. [^{11}C] FMAU and [^{18}F]FHPG as PET tracers for herpes simplex virus thymidine kinase enzyme activity and human cytomegalovirus infections. *Nucl Med Biol*, 2000 27(2): 113-119.

18. Wiebe L.I., Knaus E.E. and Morin K.W. Radiolabelled pyrimidine nucleosides to monitor the expression of HSV-1 thymidine kinase in gene therapy. *Nucleosides Nucleotides*, 1999 18(4-5): 1065-1066.
19. Nanda D., de Jong M., Vogels R., Havenga M., Driesse M., Bakker W., *et al.* Imaging expression of adenoviral HSV1-tk suicide gene transfer using the nucleoside analogue FIRU. *Eur J Nucl Med Mol Imaging*, 2002 29(7): 939-947.
20. Green L.A., Nguyen K., Berenji B., Iyer M., Bauer E., Barrio J.R., *et al.* A tracer kinetic model for ^{18}F-FHBG for quantitating herpes simplex virus type 1 thymidine kinase reporter gene expression in living animals using PET. *J Nucl Med*, 2004 45(9): 1560-1570.
21. de Jong M., Breeman W.A., Bakker W.H., Kooij P.P., Bernard B.F., Hofland L.J., *et al.* Comparison of ^{111}In-labeled somatostatin analogues for tumor scintigraphy and radionuclide therapy. *Cancer Res*, 1998 58(3): 437-441.
22. Kwekkeboom D.J., Kooij P.P., Bakker W.H., Macke H.R. and Krenning E.P. Comparison of ^{111}In-DOTA-Tyr^3-octreotide and ^{111}In-DTPA-octreotide in the same patients: biodistribution, kinetics, organ and tumor uptake. *J Nucl Med*, 1999 40(5): 762-767.
23. Virgolini I., Britton K., Buscombe J., Moncayo R., Paganelli G. and Riva P. In- and Y-DOTA-lanreotide: results and implications of the MAURITIUS trial. *Semin Nucl Med*, 2002 32(2): 148-155.
24. Kwekkeboom D.J., Bakker W.H., Kooij P.P., Konijnenberg M.W., Srinivasan A., Erion J.L., *et al.* [^{177}Lu-DOTA^0,Tyr^3]octreotate: comparison with [^{111}In-DTPA^0]octreotide in patients. *Eur J Nucl Med*, 2001 28(9): 1319-1325.
25. Teunissen J.J., Kwekkeboom D.J. and Krenning E.P. Staging and treatment of differentiated thyroid carcinoma with radiolabeled somatostatin analogs. *Trends Endocrinol Metab*, 2006 17(1): 19-25.
26. Maina T., Nock B., Nikolopoulou A., Sotiriou P., Loudos G., Maintas D., *et al.* [^{99m}Tc]Demotate, a new ^{99m}Tc-based [Tyr^3]octreotate analogue for the detection of somatostatin receptor-positive tumours: synthesis and preclinical results. *Eur J Nucl Med Mol Imaging*, 2002 29(6): 742-753.
27. Longnecker D.S., Lilja H.S., French J., Kuhlmann E. and Noll W. Transplantation of azaserine-induced carcinomas of pancreas in rats. *Cancer Lett*, 1979 7(4): 197-202.
28. Bernard B.F., Krenning E., Breeman W.A., Visser T.J., Bakker W.H., Srinivasan A., *et al.* Use of the rat pancreatic CA20948 cell line for the comparison of radiolabelled peptides for receptor-targeted scintigraphy and radionuclide therapy. *Nucl Med Commun*, 2000 21(11): 1079-1085.
29. Vincent A.J., Vogels R., Someren G.V., Esandi M.C., Noteboom J.L., Avezaat C.J., *et al.* Herpes simplex virus thymidine kinase gene therapy for rat malignant brain tumors. *Hum Gene Ther*, 1996 7(2): 197-205.
30. Breeman W.P., Van Der Wansem K., Bernard B.F., Van Gameren A., Erion J.L., Visser T.J., *et al.* The addition of DTPA to [^{177}Lu-DOTA^0,Tyr^3]octreotate prior to administration reduces rat skeleton uptake of radioactivity. *Eur J Nucl Med Mol Imaging*, 2003 30(2): 312-315.
31. Breeman W.A.P., deBlois E.H. and Krenning E.P. Effects of quenchers on the radiochemical purity of ^{111}In-labeled peptides. *J Nucl Med*, 2007 48, suppl 2: 73P.
32. Fallaux F.J., Bout A., van der Velde I., van den Wollenberg D.J., Hehir K.M., Keegan J., *et al.* New helper cells and matched early region 1-deleted adenovirus vectors prevent generation of replication-competent adenoviruses. *Hum Gene Ther*, 1998 9(13): 1909-1917.
33. de Visser M., van Weerden W.M., de Ridder C.M., Reneman S., Melis M., Krenning E.P., *et al.* Androgen-dependent expression of the gastrin-releasing Peptide receptor in human prostate tumor xenografts. *J Nucl Med*, 2007 48(1): 88-93.
34. Melis M., Krenning E.P., Bernard B.F., Barone R., Visser T.J. and de Jong M. Localisation and mechanism of renal retention of radiolabelled somatostatin analogues. *Eur J Nucl Med Mol Imaging*, 2005 32(10): 1136-1143.

35. Ter Horst M., Nanda D., Morin K., Bakker W.H., de Jong L.C., Verwijnen S.M., *et al.* [^{123}I]FIRU, a tracer for the 'molecular imaging' of HSV1-tk suicide gene transfer. *in press*, 2007.
36. Buchsbaum D.J. Imaging and therapy of tumors induced to express somatostatin receptor by gene transfer using radiolabeled peptides and single chain antibody constructs. *Semin Nucl Med*, 2004 34(1): 32-46.
37. ter Horst M., Verwijnen S.M., Brouwer E., Hoeben R.C., de Jong M., de Leeuw B.H., *et al.* Locoregional delivery of adenoviral vectors. *J Nucl Med*, 2006 47(9): 1483-1489.
38. Hemminki A., Zinn K.R., Liu B., Chaudhuri T.R., Desmond R.A., Rogers B.E., *et al. In vivo* molecular chemotherapy and noninvasive imaging with an infectivity-enhanced adenovirus. *J Natl Cancer Inst*, 2002 94(10): 741-749.
39. Kuriyama N., Kuriyama H., Julin C.M., Lamborn K.R. and Israel M.A. Protease pretreatment increases the efficacy of adenovirus-mediated gene therapy for the treatment of an experimental glioblastoma model. *Cancer Res*, 2001 61(5): 1805-1809.
40. Maillard L., Ziol M., Tahlil O., Le Feuvre C., Feldman L.J., Branellec D., *et al.* Pre-treatment with elastase improves the efficiency of percutaneous adenovirus-mediated gene transfer to the arterial media. *Gene Ther*, 1998 5(8): 1023-1030.
41. Kim J.H., Lee Y.S., Kim H., Huang J.H., Yoon A.R. and Yun C.O. Relaxin expression from tumor-targeting adenoviruses and its intratumoral spread, apoptosis induction, and efficacy. *J Natl Cancer Inst*, 2006 98(20): 1482-1493.
42. Reubi J.C., Cortes R., Maurer R., Probst A. and Palacios J.M. Distribution of somatostatin receptors in the human brain: an autoradiographic study. *Neuroscience*, 1986 18(2): 329-346.
43. Jacobs A., Braunlich I., Graf R., Lercher M., Sakaki T., Voges J., *et al.* Quantitative kinetics of [^{124}I]FIAU in cat and man. *J Nucl Med*, 2001 42(3): 467-475.
44. Choi S.R., Zhuang Z.P., Chacko A.M., Acton P.D., Tjuvajev-Gelovani J., Doubrovin M., *et al.* SPECT imaging of herpes simplex virus type1 thymidine kinase gene expression by [^{123}I] FIAU(1). *Acad Radiol*, 2005 12(7): 798-805.
45. De Jong M., Valkema R., Jamar F., Kvols L.K., Kwekkeboom D.J., Breeman W.A., *et al.* Somatostatin receptor-targeted radionuclide therapy of tumors: preclinical and clinical findings. *Semin Nucl Med*, 2002 32(2): 133-140.
46. Boucher P.D., Im M.M., Freytag S.O. and Shewach D.S. A novel mechanism of synergistic cytotoxicity with 5-fluorocytosine and ganciclovir in double suicide gene therapy. *Cancer Res*, 2006 66(6): 3230-3237.

2.3 Locoregional delivery of adenoviral vectors

M. ter Horst, S.M. Verwijnen, E. Brouwer, R.C. Hoeben, M. de Jong, B. de Leeuw, P.A.E. Sillevis Smitt

Journal of Nuclear Medicine 2006; 47:1483–1489

Alavi-Mandell award 2006

Abstract

The overall median survival of patients with a malignant glioma is <1 y. Because malignant gliomas rarely metastasize outside the skull, locoregional treatment strategies, such as gene therapy, are under investigation. Recently, convection-enhanced delivery (CED) has been presented as a method to improve delivery of large molecules. The goal of this study was to evaluate whether CED improves intratumoral delivery of adenoviral vectors and compare it with single injection (SI) and multiple injection (4x, MI).

Methods: A replication-deficient adenoviral vector encoding the herpes simplex virus thymidine kinase (HSV-tk) and the human somatostatin receptor subtype 2 (sst_2) was administered into nude mice bearing subcutaneous U87 xenografts. Tumors were injected with $1.5x10^9$ plaque-forming units of Ad5.tk.sst_2 by CED, SI, or MI. Three days later, [^{99m}Tc-N_4^{0-1},Asp^0,Tyr^3]octreotate (^{99m}Tc-Demotate 2) was injected intravenously to monitor the virus-induced sst_2 expression. γ-Camera imaging was performed for *in vivo* imaging, and the tumor uptake of ^{99m}Tc-Demotate 2 was determined by γ-counter. Furthermore, the tumor was sectioned and *ex vivo* autoradiography was performed. After decay of radioactivity, adjacent sections were submitted to *in vitro* autoradiography with [DOTA-^{125}I-Tyr^3]octreotate, which was used to calculate the transduced areas.

Results: Transfected xenograft tissues showed high sst_2 expression and were clearly visualized with a γ-camera. Accumulation of radioactivity was 2-fold higher in the tumors that were injected with MI compared with CED and SI ($P = 0.01$). CED and SI resulted in equal uptake of radioactivity in the tumors. The measured areas of transduction in *ex vivo* and *in vitro* autoradiographs showed a high concordance (r^2 5 0.89, $P < 0.0001$). The maximum area of transfection was significantly larger after MI than after CED ($P < 0.05$) or SI ($P = 0.05$). Also, the measured volume of distribution was twice as high after administration of Ad5.tk.sst_2 by MI (56.6 mm^3) compared with SI (25.3 mm^3) or CED(26.4mm^3).

Conclusion: CED does not increase adenoviral vector distribution in a glioma xenograft model compared with SI. Therefore, in the clinic MI is probably the most effective delivery method for the large adenoviral particle (70 nm) in malignant gliomas.

Introduction

The overall prognosis of patients with malignant gliomas is dismal, with a median survival of <1 y [1]. Despite progress in neurosurgery, chemotherapy, and radiotherapy, the survival of these patients has not changed during the last several decades. Because of the poor prognosis of malignant gliomas, new treatment modalities are being developed. As malignant gliomas rarely metastasize outside the skull, some modalities focus on locoregional treatment strategies. Examples include local application of wafers impregnated with cytotoxic drugs, local application of targeted toxins, and intratumoral injection of viral vectors for gene therapy or virotherapy [2-4].

Adenoviral vectors are among the most promising gene delivery vehicles currently available for glioma therapy, because they can be produced in large quantities in high titer batches and because relatively large segments of foreign DNA carrying therapeutic genes can be incorporated. Recently, a small randomized study clearly demonstrated the efficacy of an adenovirus serotype 5 (Ad5) carrying the herpes simplex virus thymidine kinase gene (HSV1-tk) in combination with ganciclovir in malignant glioma [5]. Ad5-tk treatment significantly increased the mean survival from 39 to 71 wk ($P < 0.01$), indicating some efficacy of the treatment.

In spite of these promising results, 2 major hurdles have been identified that limit the efficacy of Ad5-based gene therapy in malignant gliomas. First, the coxsackie adenovirus receptor (CAR) is poorly expressed on primary glioma cells, resulting in low transduction efficiency compared with established cell lines [6]. Various strategies have been developed to successfully retarget adenoviral vectors to other receptors that are expressed at higher levels on malignant glioma cells, such as integrins or CD46 [7, 8]. Another major obstacle is the limited tissue penetration of the virus after injection into glioma tissue. A carefully conducted clinical study demonstrated that the distribution of the vector into brain tissue is limited to an average 5 mm from the needle tract [9]. One approach to improve tissue penetration is the development of conditionally replicative adenoviruses (CRAds) [10, 11]. The release of CRAd progeny by infected tumor cells provides a potential to amplify the oncolytic effect by lateral spread through solid tumors.

Another way to improve tissue penetration of the virus is the exploration of new delivery methods. Recently, convection-enhanced delivery (CED) was developed as a means to improve delivery of macromolecules throughout the brain [12-14]. CED is based on continuous infusion of drugs via intracranial catheters, enabling convective distribution of high drug concentrations over large volumes of the target tissue [15]. CED has been successfully applied in clinical glioma trials to administer large molecules, including immunotoxins [4, 16]. CED has also been used to deliver viral vectors, including adenovirus, to the brain. In experimental models, delivery of viral vectors by CED resulted in improved transduction of the brain [17-21].

In clinical gene therapy trials, the adenoviral vectors were administered into the gliomas by either a single injection (SI), through a catheter, or by multiple wound bed injection after reresection [2, 5, 9]. The goal of this study was to evaluate whether CED improves intratumoral delivery of an adenoviral vector in a mouse xenograft glioma model. We compared the volume of tumor that was transduced by the adenoviral vector after CED with the volumes obtained by SI and multiple injection (4·, MI) of the same amount of virus.

To monitor the distribution of the adenoviral vector, we used the human somatostatin receptor subtype 2 (sst_2) gene in combination with the radiolabeled tracer [^{99m}Tc-N_4^{0-1},Asp^0,Tyr^3]Octreotate (^{99m}Tc-Demotate 2), which has high selectivity and high affinity for the sst_2 receptor [22]. We found that radioactive uptake and volume of distribution after CED were comparable to SI. After MI, the transduced tumor volume and the maximum area of transduction were 2- to 3-fold increased compared with both SI and CED.

Materials and methods

Cell culture

The U87MG human glioblastoma multiforme (GBM) cell line was obtained from the American Type Culture Collection; the U251 human GBM cell line was from P. Körnblith (National Institutes of Health, Bethesda, MD), and the rat pancreatic tumor cell line CA20948 was available at our institution [23]. U87MG cells were cultured in minimum essential medium (MEM) Invitrogen) with 0.1 mmol/. nonessential amino acids, 2 mmol/l L-glutamine, 1 mmol/l sodium pyruvate, 1,500 mg/l sodiumbicarbonate, 10% heat-inactivated (30 min, 56°C) fetal bovine serum (FBS) (Invitrogen), 100 IU/ml penicillin, and 100 mg/ml streptomycin (Invitrogen). U251 was cultured in Dulbecco's modified Eagle medium (DMEM) (Invitrogen) containing 4,500 mg/l glucose, 580 mg/l L-glutamine, and 110 mg/l pyruvate with 10% FBS (Invitrogen), 100 IU/ml penicillin, and 100 mg/ml streptomycin (Invitrogen). CA20948 was cultured in DMEM as described with 0.1 mg/l fungizone supplemented. Medium was changed twice a week. Cells were cultured at 37°C in a 5% CO_2 atmosphere.

Adenoviral vectors Ad5.tk.sst$_2$ and Ad5.CMV.nLacZ

Construction of Ad5.tk.sstr and Ad5.CMV.nLacZ has been described earlier [24, 25]. Briefly, Ad5.tk.sstr is a replication incompetent adenoviral vector that contains the sst_2 and the herpes simplex virus thymidine kinase (tk) genes in the deleted E1 region. Both genes are regulated by separate immediate early cytomegalovirus (CMV) promoters. The E1-deleted Ad5.CMV.nLacZ vector contains the β-galactosidase (nLacZ)

driven by a CMV promoter. Both vectors were propagated to high titers on PER.C6 cells, CsCl gradient purified, dialyzed, and stored at –80°C in sucrose buffer (140 mmol/l NaCl, 5 mmol/l Na_2HPO_4, 1.5 mmol/l KH_2PO_4, 20 mmol/l $MgCl_2$, and 5% sucrose). All batches were screened for replication-competent adenovirus (RCA) [26] and met the criterion of <1 plaque-forming unit (PFU) of wtE1A promoter containing virus per 10^7 PFU. Titrations were performed on 911 cells and are presented as PFU/ml [27]. The titers ranged from $6x10^{10}$ to $3x10^{11}$ PFU/ml.

Radiolabeling of peptides

^{99m}Tc-Demotate 2 was provided by Dr. Theodosia Maina (Institute of Radioisotopes, Athens, Greece) and prepared as described earlier [22]. Briefly, 20 mg Demotate 2 (1023 mol/l), in 50 ml 0.5 mol/l phosphate buffer (pH 10.5), and 5 ml 0.1 mol/l Na_3-citrate and 410 µl $^{99m}TcO_4$ (Ultratechnekow generator; Mallinckrodt Medical) were mixed, and the reaction was started by the addition of 20 mg $SnCl_2$ (2 mg $SnCl_2$ per ml ethanol, freshly made) at room temperature. After 15 min, another 20 mg $SnCl_2$ in ethanol were added and mixed. After 30 min, 8 ml of mol/l HCl and 50 ml ethanol were added and the solution was sterilized by filtration through a Millex 0.22-µm GV filter (Millipore). The radiochemical purity was tested by high-performance liquid chromatography and was >90%. The mean specific activity of ^{99m}Tc-Demotate 2 was 40–200 MBq/mg.

[DOTA,Tyr^3]octreotate was labeled with ^{125}I as described earlier [28]. The mean radiochemical purity was >90%. The mean specific activity of [DOTA-^{125}I-Tyr^3]octreotate was 0.2 MBq/mmol. Octreotide was supplied by Novartis. All chemicals used were purchased from Aldrich.

Adenoviral stability

During CED, the adenoviral vector is exposed to room temperature for up to 3 h and to transport through Teflon (DuPont) tubing. To examine the effect of room temperature on adenoviral stability, we sampled aliquots of Ad5.CMV.nLacZ placed on the bench at room temperature every 30 min. To study the effect of passage through tubing, Ad5.CMV.nLacZ from the same batch was pushed (1 ml/min) through the same tubing used for CED experiments over a 3-h period and aliquots were sampled every 30 min. Infectivity of the aliquots was examined by infecting U251 cells and measuring b-galactosidase activity. U251 cells were plated into 24-well plates at a density of $2x10^5$ cells per well in 1 ml DMEM containing 10% FBS and incubated overnight at 37°C. After changing the medium, the aliquots containing Ad5.CMV.nLacZ were added in triplicate at a concentration of 100 PFU per cell. The medium was changed 2 h after starting the infection. After 48 h of incubation at 37°C the medium was removed, the cells were washed with phosphate-buffered saline (PBS),

and assayed for β-galactosidase activity by the Galacto-Light Plus system (Applied Biosystems) using a Packard Top Count NXT luminometer (PerkinElmer Life Sciences). The same experiments were repeated after the addition of bovine serum albumin (BSA) (New England Biolabs) at a concentration of 0.1 mg/ml.

Animal experiments

All experimental protocols were approved by the Institutional Animal Care and Use Committee, in compliance with the Guide for the Care and Use of Laboratory Animals. Male NMRI nu/nu mice (Charles River, Les Oncins, France), 5-6 wk of age were purchased. Mice were maintained at 3 or 4 per cage and allowed access to food and water ad libitum. After one week, $1x10^7$ U87MG or CA20948 cells were inoculated subcutaneously into both flanks in 250 µl of HBSS (Invitrogen). The tumor growth was assessed 3 times a week by measuring bidimensional diameters with calipers. The tumor volume was determined by using the simplified formula of a rotational ellipse (length x $width^2$ x 0.5) [29]. Anesthesia was induced with isoflurane in oxygen and nitrous oxygen. Body temperature was maintained at 37°C using a heat pad. When the tumors reached a volume of approximately 250 mm^3, animals were injected with a total dose of $1.5x10^9$ PFU of Ad5.tk.sst_2 or PBS into the tumor. We compared 3 delivery strategies: SI, (4x MI) and CED. In SI experiments, the total viral dose was administered in 22 µl with 1 injection. In the MI experiments, the total viral dose was diluted in 50 µl and was administered by 4 separate injections into 4 different tumor quadrants. In CED, the viral dose was diluted in 180 µl and was infused at 1µl/min for 180 min. The continuous infusion was performed with a constant flow pump (Harvard Apparatus). A 27-gauge hypodermic needle was connected to an air tight 250-µl Hamilton syringe with 30 cm of Teflon tubing. For SI and MI, we used a 50 µl Hamilton syringe fitted with a 27-gauge needle. As a positive control we used mice bearing sst_2-positive rat pancreatic CA20948 xenografts. Seventy-two hours after administration of the vector, 0.5 µg ^{99m}Tc-Demotate 2 was injected into the dorsal vein of the penis in a total volume of 200 µl. γ-Camera images were acquired for 10 min, 3.5 hr after ^{99m}Tc-Demotate 2 injection, using a Rota II γ -camera system (Siemens) equipped with a low energy collimator. The animals were sacrificed 4 hr after ^{99m}Tc-Demotate 2 injection. The tumors were taken out and weighed. After determining the radioactivity in an LKB-1282-Compugammasystem (Perkin Elmer) γ-counter, the tumors were frozen in Tissue-Tek (Sakura). For each adenovirus injected tumor the total background activity was calculated on the basis of the means of the PBS-injected U87MG tumors (percentage injected-dose per gram of tissue[%ID/g]). After subtracting the background activity, the adenoviral vector-induced radioactivity was expressed as percentage of injected dose (%ID) per tumor.

Autoradiography

The presence of radioactivity in tissue sections was detected by *ex vivo* and *in vitro* autoradiography. Tumors were embedded in TissueTek and processed for cryosectioning. Tissue sections (10 µm) were obtained at 0.3-mm intervals throughout the tumor and mounted on SuperFrost Plus slides (Menzel). For *ex vivo* autoradiography, sections were exposed to phosphor screens (Packard Instruments) for 2 days. The screens were analyzed using a Cyclone Phosphor Imager (Packard Instruments) and a computer-assisted OptiQuant 03.00 image-processing system (Packard Instruments). *In vitro* autoradiography was performed on the tumor sections after decay of ^{99m}Tc-Demotate 2. Tissue sections (10 µm) were mounted on glass slides and stored at –20°C for at least 1 day to improve adhesion of the tissue to the slide. The sections were pre-incubated for 10 min at 4°C, using buffer A, containing 167 mmol/l Tris-HCl (pH 7.7), 5 mmol/l $MgCl_2$, and 0.25% BSA. The sections were then incubated for 60 min in the same buffer, in the presence of 10^{-10} mol/l [DOTA-^{125}I-Tyr^3]octreotate (DOTA is 1,4,7,10-tetraazacyclododecane-N,N9,N$,N%-tetraacetic acid), 1%

BSA, and 40 mg/ml Bacitracin (Sigma-Aldrich). The sections were then washed twice for 5 min in buffer A and once in buffer A without BSA. After a short wash with distilled water, the sections were dried and exposed to phosphor image screens for 1 day. Nonspecific binding was determined in an adjacent section in the presence of 10^{-6} mol/l octreotide. Sections of rat brain and CA20948 tumor served as positive controls.

Volume of adenoviral vector distribution

We used the *in vitro* autoradiography slides to calculate the volume of tumor transduced by the adenoviral vector. On the sections, we defined the boundaries of radioactivity by setting a threshold of 5 times background activity. We then used Scion Image software (Scion) to calculate the area of radioactivity. Then, we plotted the areas of all adjacent slides and determined the area under the curve expressing the volume of distribution using GraphPad Prism version 4.0 software (GraphPad Software, Inc.).

Statistical analysis

Data were analyzed using GraphPad Prism software. All tests (t test, ANOVA) were 2-sided and $P<0.05$ was considered statistically significant.

Results

Adenoviral stability during CED

Delivery by CED exposes the adenoviral vector to 3 h of room temperature and to passage through the tubing. To determine the effect of these factors on adenoviral stability, we simulated a 3-h CED experiment on the bench top. After exposure to 3 h of room temperature, the infectivity of the vector dropped from $2.3x10^6$ relative light units (RLU) to $1.3x10^6$ RLU without passage through the tubing and to $1.4x10^6$ RLU after additional exposure to the tubing (Fig. 1). The decline of infectivity over time was significant in both instances ($P< 0.01$) but was primarily due to a drop in the first 30 min. Clearly, passage through the tubing did not negatively affect the infectivity of the vector. We then examined the effect of addition of BSA on stability. After 3 h on the bench top at room temperature, the infectivity remained stable at $2.0x10^6$ RLU. After a 3-h exposure followed by passage through the tubing, the infectivity of the vector dropped from $2.0x10^6$ to $1.5x10^6$ RLU ($P = 0.09$). Because addition of BSA did not significantly increase vector stability during simulation of CED on the bench top, *in vivo* experiments were performed without BSA.

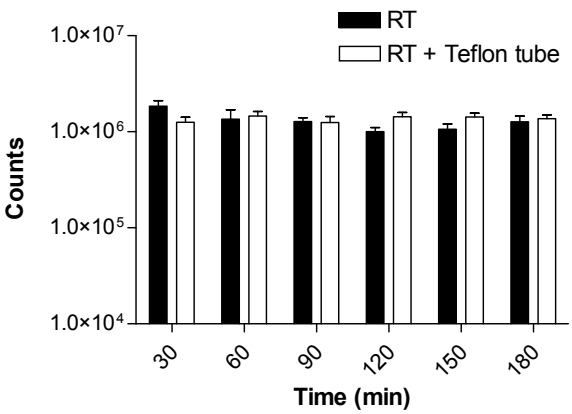

Figure 1: Adenoviral vector stability at room temperature after passage through Teflon tubing. Aliquots of Ad5.CMV.nLacZ, stored at room temperature (RT), were sampled every 30 min over a 3-h period. In parallel, aliquots from the same batch were collected after transport through Teflon tubing (1 ml/min). U251 cells were incubated with aliquots (100 PFU/cell), and β-galactosidase activity was measured 2 days later. β-Galactosidase activity decreased over time but was not affected by transport through tubing. Error bars represent SD.

γ-Camera images after CED, SI and MI of Ad5.tk.sst$_2$

Animals carrying established bilateral subcutaneous U87MG tumors were injected with $1.5x10^9$ PFU of Ad5.tk.sst$_2$ or PBS. Three different delivery strategies were used: SI, (4x MI), and CED. Three days after the injection of the viral vector, the radioactive

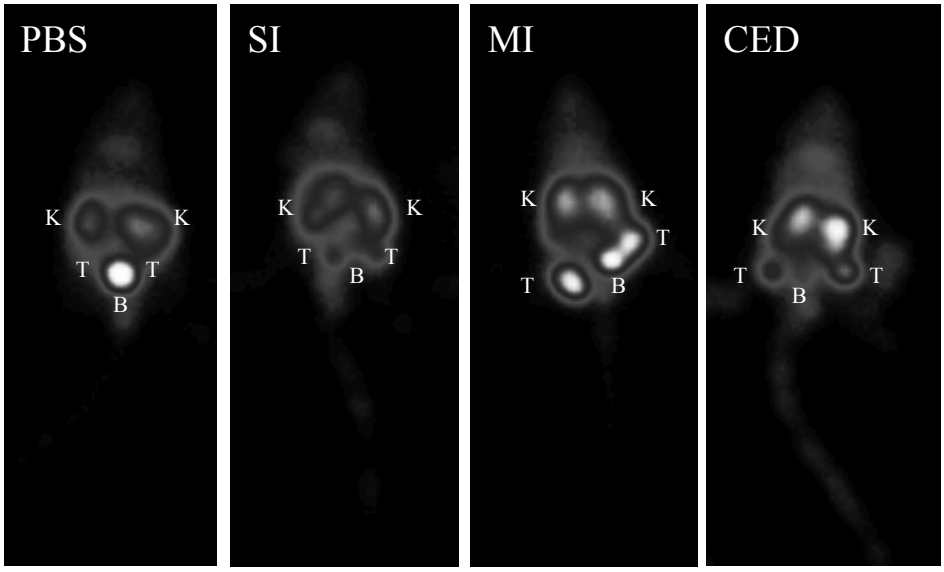

Figure 2: γ-Camera images of NMRI nu/nu mice. Mice bearing U87MG xenografts 3.5 h after intravenous administration of 0.5 µg ^{99m}Tc-Demotate 2 (100 MBq). Three days before imaging, tumors had been injected with PBS (left) or 1.5x10^9 PFU of Ad5.tk.sst$_2$ administered with CED, SI, or MI (4x, MI). Both tumors in each animal received the same treatment. Images are representative and demonstrate that MI results in better tracer uptake than CED and SI. B = bladder; K = kidney; T = tumor.
For color figure see page 241.

tracer ^{99m}Tc-Demotate 2 was injected intravenously and the animals were imaged. All Ad5.tk.sst$_2$–injected tumors were readily visualized with radioactive ^{99m}Tc-Demotate 2 with a γ-camera (Fig. 2). In addition, a stronger signal was visible in tumors injected with MI than that in tumors treated with SI or CED. These findings indicate the feasibility of *in vivo* imaging using the Ad5.tk.sst$_2$/^{99m}Tc-Demotate 2 system.

Radioactivity accumulation in the tumor

After imaging, the animals were sacrificed and the radioactivity in the tumors was measured (Table 1). The accumulation of radioactivity (%ID) was significantly higher in the tumors that were injected with MI compared with CED and SI (P = 0.01),

Table 1: Virus-induced tumor uptake of ^{99m}Tc-Demotate 2 in xenograft-bearing mice after Ad5.tk.sst$_2$ administration by CED, SI, or MI. Three days after infection, each mouse was injected intravenously with 0.5 µg ^{99m}Tc-Demotate 2 (20–100 MBq) and euthanized 4 h later (14 or 15 tumors per group). Uptake is expressed as %ID of infected tumor tissue. Accumulation of radioactivity was significantly higher in tumors that were injected with MI compared with CED and SI (ANOVA, P < 0.05).

Injection	%ID	SEM
CED	0.34	0.08
SI	0.37	0.08
MI	0.82	0.17

confirming the γ-camera results. CED and SI resulted in equal uptake of radioactivity in the tumors.

Autoradiography and quantification of vector distribution

After sectioning, U87MG xenografts were submitted to autoradiography (Fig. 3). *Ex vivo* autoradiographs visualized transduced areas of the tumors (Figs. 3A and 3E). The representative autoradiographs clearly showed a larger area of radioactivity in the section of the tumor treated with MI (Fig. 3E) than that treated with SI (Fig. 3A). After decay of ^{99m}Tc-Demotate 2, *in vitro* autoradiographic studies were performed with [DOTA-^{125}I-Tyr^3]octreotate and showed areas of transduction similar to the *ex vivo* autoradiographs (Figs. 3B and 3F). Adding excess unlabeled octreotide completely blocked uptake of radioactivity, indicating the specificity of the observed binding of [DOTA-^{125}I-Tyr^3]octreotate to the transduced sst_2 receptor (Figs. 3C and 3G). The area of transduction was calculated for each section using Scion Image software. The area of transduction calculated on the *in vitro* autoradiographs correlated significantly with the area calculated on the *ex vivo* autoradiograph

of the same section ($r^2 = 0.89$, $P < 0.0001$). Because the *in vitro* autoradiographs can be obtained from a large number of sections at the same time, we used this method to determine the maximum area and volume of transduction for all tumors.

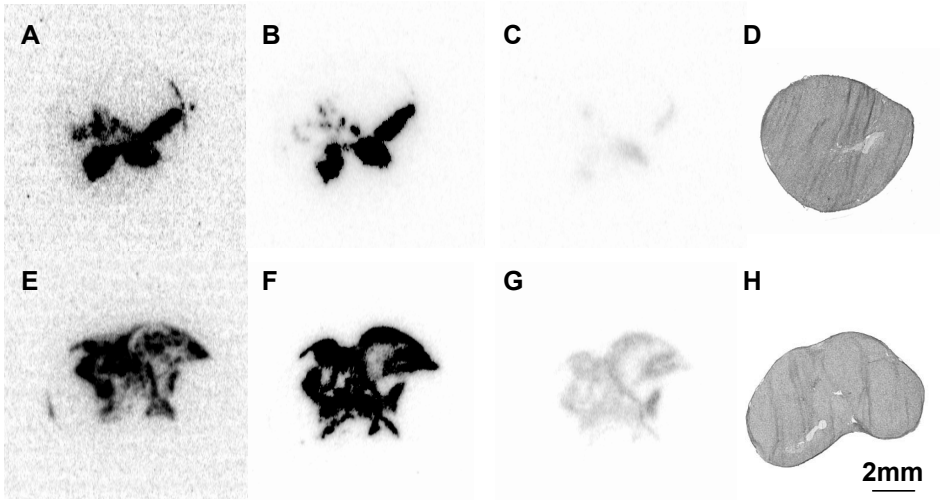

Figure 3: Autoradiographs of Ad5.tk.sst_2–injected U87MG xenografts by single injection (A–D) or by multiple injection (E–H). *Ex vivo* autoradiographs were performed 4 h after injection of ^{99m}Tc-Demotate 2 (A and E). *In vitro* autoradiographs were performed on adjacent slides with [DOTA-^{125}I-Tyr^3]octreotate (B and F). Binding was displaced by excess unlabeled octreotide (C and G). Adjacent tumor sections were visualized with hematoxylin–eosin staining (D and H). Representative sections demonstrate that the area of viral distribution is larger in sections from tumors injected with MI compared with SI.
For color figure see page 242.

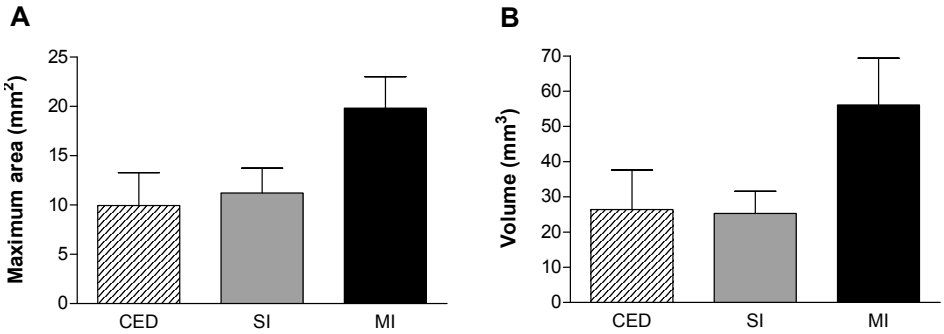

Figure 4: Quantification of vector distribution. Area of vector distribution was calculated using serial *in vitro* autoradiography sections incubated with [DOTA-^{125}I-Tyr^3]octreotate. (A) In each tumor, the section with the largest area was selected. Maximum area of vector distribution depends significantly on method of vector delivery (MI vs. CED, $P < 0.05$; MI vs. SI, $P = 0.05$; CED vs. SI, $P = 0.8$). (B) To calculate volume of vector distribution, all radioactive areas of consecutive sections were plotted and the area under the curve was calculated. Data are mean ± SEM, 8 tumors in each group.

First, we determined for each tumor the maximum area of transduction on a single section for each delivery method (Fig. 4A). The maximum area of transduction was significantly larger after MI than after CED ($P < 0.05$) or SI ($P = 0.05$). Then, we plotted the areas of all adjacent slides and calculated the area under the curve representing the volume of distribution. Figure 4B presents the volumes of distribution obtained with the 3 different delivery techniques. The volume of distribution was twice as high after administration of Ad5.tk.sst$_2$ by MI (56.6 mm^3) compared with SI (25.3 mm^3) or CED (26.4 mm^3).

Discussion

The local pattern of recurrence and absence of metastasis outside the central nervous system make malignant gliomas suitable candidates for locoregional treatment strategies, including gene therapy. CED was recently developed to increase the volume of distribution of large molecules through the brain [12-14, 21]. In this study, we applied CED in an attempt to improve the local delivery of adenoviral vectors. We compared CED with SI and (4x MI) of a replication-deficient adenoviral vector in a subcutaneous mouse xenograft tumor model. To monitor the distribution of the virus, we inserted the gene encoding the human sst$_2$. Expression of sst$_2$ was visualized *in vivo* by intravenous injection of ^{99m}Tc-Demotate 2 followed by γ-camera imaging, and the accumulation of radioactivity was quantified with a γ-counter. The volume and maximum area of transduction of the tumor were taken as a measure of *in vivo* vector distribution and was measured using *in vitro* autoradiography. Before comparing CED with MI and SI, we investigated the adenoviral stability and recovery

from the CED infusion device. Sanftner et al. [21] found up to 90% absorption of an adeno-associated virus, determined by quantitative polymerase chain reaction, to the device depending on the tubing used. These authors observed excellent vector recovery when using fused silica and silicon tubing. In our adenoviral test setting, the Teflon tubing did not affect adenoviral infectivity, indicating good vector recovery. However, exposure of the vector for 3 h at room temperature resulted in a 43% decline of infectivity. The decline in infectivity by exposure to room temperature was most prominent in the first 30 min and was not prevented by addition of BSA.

Direct comparison of CED with SI and MI demonstrated that both accumulation of radioactivity and the largest area of transduction on a single section were significantly larger after MI than after CED or SI. Also, the volume of transduction was increased 2-fold. However, CED did not increase the maximum area or the volume of tumor transduction compared with SI. Lack of distribution enhancement by CED compared with SI could be attributed to the flow, time, and volume settings of CED; the size of the adenoviral particle; or the interaction between the adenovirus and the tissue.

For optimal CED of drugs, several relevant variables have been identified, including catheter size, flow rate, molecular weight of the drug, and tissue characteristics [30, 31]. Backflow of the infused drugs is dependent on catheter size and flow rate [30], which should not exceed 1 µl/min [19]. We used the recommended maximum flow rate and did not observe backflow. Furthermore, increased molecular weight and particle size decrease delivery [12, 14, 32, 33]. Betz et al. [18] applied CED to deliver a replication-defective adenoviral vector (70–100 nm) [34] to rat brain and studied various infusion parameters. Variations in flow rate, concentration, and infectious titer resulted in a volume of adenoviral transduction ranging from 4 to 27 mm^3 for 0.3–9x10^9 virus particles. MacKay et al. [32] performed CED experiments using different-sized liposomes (40–200 nm in diameter) and reported a reduction in brain penetration with increase in size. Kroll et al. [35] reported that increasing the dose of monocrystalline iron oxide nanocompounds (viral-sized agent) rather than convection might result in the best volume of transduction. On the other hand, Brust et al. [19] showed that infusion of 1 ml/min over a longer period of time (2.5 h) is more effective than infusion of smaller volumes with the same dose of adenovirus. Although we used the same infusion rate and a volume of 180 ml, we found comparable levels of radioactive accumulation between SI and CED, indicating that in our setting the increase of injected volume did not result in an improved volume of distribution.

We used the sst_2 marker gene to visualize adenoviral vector distribution *in vivo* and *ex vivo*. Recently, Maina et al. [22, 36] described new somatostatin analogs, ^{99m}Tc-Demotate 1 and ^{99m}Tc-Demotate 2, for the visualization of the somatostatin receptor in endocrine tumors. At present, [^{111}In-DTPA^0]octreotide (DTPA =

diethylenetriaminepentaacetic acid) (^{111}In-OctreoScan; Mallinckrodt) is the standard substrate for diagnostic imaging and staging of sst_2-expressing tumors. However, somatostatin analogs based on ^{99m}Tc are promising alternatives because of optimal nuclear characteristics, low cost, and easy availability via commercial ^{99}Mo/^{99m}Tc generators [22]. In this study, we found high ^{99m}Tc-Demotate 2 uptake in infected U87MG xenografts by *in vivo* γ-camera imaging and *ex vivo* autoradiography. The high, significant correlation between the *ex vivo* and *in vitro* autoradiographs indicates that the intravenously injected ^{99m}Tc-Demotate 2 efficiently permeates the entire tumor.

Our results showed no significant difference in adenoviral vector distribution between CED and SI but, conversely, showed an increase in radioactive uptake and volume of distribution in MI. For that reason, in the clinic, MI is probably the most effective delivery method for the large adenoviral particle (70 nm) in malignant gliomas. Several clinical studies have demonstrated that administration of adenoviral vectors through multiple injections into the brain is probably safe, although silent hemorrhages and transient neurologic deficits have been described [2, 9]. Our study shows that even small experimental tumors are not entirely transduced after MI. Additional strategies such as radionuclide therapy with, for example, ^{177}Lu- and ^{90}Y-labeled somatostatin analogs [37] or the HSV-tk/ganciclovir "bystander effect" [38, 39] or using (conditional) adenoviral replication [10, 11] will be required to obtain eradication of experimental tumors or clinically relevant tumor responses.

Conclusion

Our study showed that CED did not increase adenoviral vector distribution in a glioma xenograft model compared with SI. Therefore, in the clinic, MI is probably the most effective method to deliver the large adenoviral particle into (brain) tumors. Furthermore, ^{99m}Tc-Demotate 2 seems a good candidate to image and quantify the distribution and expression level of the sst_2 marker.

Acknowledgements

We thank Mark Rodijk, Monique de Visser, Marleen Melis, and Wout Breeman for technical support. We also thank Theodosia Maina (Institute of Radioisotopes, Athens, Greece) for providing Demotate 2. Support was provided by the Dutch Cancer Society, Koningin Wilhelmina Fonds (grant DDHK 2001-2459), and an Erasmus Medical Center translational research grant.

References

1. Behin A., Hoang-Xuan K., Carpentier A.F. and Delattre J.Y. Primary brain tumours in adults. *Lancet*, 2003 361(9354): 323-331.
2. Smitt P.S., Driesse M., Wolbers J., Kros M. and Avezaat C. Treatment of relapsed malignant glioma with an adenoviral vector containing the herpes simplex thymidine kinase gene followed by ganciclovir. *Mol Ther*, 2003 7(6): 851-858.
3. Westphal M., Hilt D.C., Bortey E., Delavault P., Olivares R., Warnke P.C., *et al.* A phase 3 trial of local chemotherapy with biodegradable carmustine (BCNU) wafers (Gliadel wafers) in patients with primary malignant glioma. *Neuro Oncol*, 2003 5(2): 79-88.
4. Laske D.W., Youle R.J. and Oldfield E.H. Tumor regression with regional distribution of the targeted toxin TF-CRM107 in patients with malignant brain tumors. *Nat Med*, 1997 3(12): 1362-1368.
5. Immonen A., Vapalahti M., Tyynela K., Hurskainen H., Sandmair A., Vanninen R., *et al.* AdvHSV-tk gene therapy with intravenous ganciclovir improves survival in human malignant glioma: a randomised, controlled study. *Mol Ther*, 2004 10(5): 967-972.
6. Miller C.R., Buchsbaum D.J., Reynolds P.N., Douglas J.T., Gillespie G.Y., Mayo M.S., *et al.* Differential susceptibility of primary and established human glioma cells to adenovirus infection: targeting via the epidermal growth factor receptor achieves fiber receptor-independent gene transfer. *Cancer Res*, 1998 58(24): 5738-5748.
7. Fueyo J., Alemany R., Gomez-Manzano C., Fuller G.N., Khan A., Conrad C.A., *et al.* Preclinical characterization of the antiglioma activity of a tropism-enhanced adenovirus targeted to the retinoblastoma pathway. *J Natl Cancer Inst*, 2003 95(9): 652-660.
8. Brouwer E., Ophorst O., Havenga M., de Leeuw H.C.G.M., Hoeben R.C. and Sillevis Smitt P.A.E. Improved adenoviral vectors for gene therapy of malignant glioma. Presented at: 95th Annual Meeting of the American Association for Cancer Research; March 27-31, 2004; Orlando, Fl.
9. Lang F.F., Bruner J.M., Fuller G.N., Aldape K., Prados M.D., Chang S., *et al.* Phase I trial of adenovirus-mediated p53 gene therapy for recurrent glioma: biological and clinical results. *J Clin Oncol*, 2003 21(13): 2508-2518.
10. Kirn D.H. and McCormick F. Replicating viruses as selective cancer therapeutics. *Mol Med Today*, 1996 2(12): 519-527.
11. Russell S.J. Replicating vectors for cancer therapy: a question of strategy. *Semin Cancer Biol*, 1994 5(6): 437-443.
12. Bobo R.H., Laske D.W., Akbasak A., Morrison P.F., Dedrick R.L. and Oldfield E.H. Convection-enhanced delivery of macromolecules in the brain. *Proc Natl Acad Sci U S A*, 1994 91(6): 2076-2080.
13. Vogelbaum M.A. Convection enhanced delivery for the treatment of malignant gliomas: symposium review. *J Neurooncol*, 2005 73(1): 57-69.
14. Lieberman D.M., Laske D.W., Morrison P.F., Bankiewicz K.S. and Oldfield E.H. Convection-enhanced distribution of large molecules in gray matter during interstitial drug infusion. *J Neurosurg*, 1995 82(6): 1021-1029.
15. Mardor Y., Rahav O., Zauberman Y., Lidar Z., Ocherashvilli A., Daniels D., *et al.* Convection-enhanced drug delivery: increased efficacy and magnetic resonance image monitoring. *Cancer Res*, 2005 65(15): 6858-6863.
16. Husain S.R. and Puri R.K. Interleukin-13 receptor-directed cytotoxin for malignant glioma therapy: from bench to bedside. *J Neurooncol*, 2003 65(1): 37-48.
17. Bankiewicz K.S., Eberling J.L., Kohutnicka M., Jagust W., Pivirotto P., Bringas J., *et al.* Convection-enhanced delivery of AAV vector in parkinsonian monkeys; in vivo detection of gene expression and restoration of dopaminergic function using pro-drug approach. *Exp Neurol*, 2000 164(1): 2-14.

18. Betz A.L., Shakui P. and Davidson B.L. Gene transfer to rodent brain with recombinant adenoviral vectors: effects of infusion parameters, infectious titer, and virus concentration on transduction volume. *Exp Neurol*, 1998 150(1): 136-142.
19. Brust D., Feden J., Farnsworth J., Amir C., Broaddus W.C. and Valerie K. Radiosensitization of rat glioma with bromodeoxycytidine and adenovirus expressing herpes simplex virus-thymidine kinase delivered by slow, rate-controlled positive pressure infusion. *Cancer Gene Ther*, 2000 7(5): 778-788.
20. Nguyen T.T., Pannu Y.S., Sung C., Dedrick R.L., Walbridge S., Brechbiel M.W., *et al.* Convective distribution of macromolecules in the primate brain demonstrated using computerized tomography and magnetic resonance imaging. *J Neurosurg*, 2003 98(3): 584-590.
21. Sanftner L.M., Sommer J.M., Suzuki B.M., Smith P.H., Vijay S., Vargas J.A., *et al.* AAV2-mediated gene delivery to monkey putamen: evaluation of an infusion device and delivery parameters. *Exp Neurol*, 2005 194(2): 476-483.
22. Maina T., Nock B.A., Cordopatis P., Bernard B.F., Breeman W.A., van Gameren A., *et al.* [^{99m}Tc] Demotate 2 in the detection of sst_2-positive tumours: a preclinical comparison with [^{111}In] DOTA-tate. *Eur J Nucl Med Mol Imaging*, 2006 33(7): 831-840.
23. Reubi J.C., Horisberger U., Essed C.E., Jeekel J., Klijn J.G. and Lamberts S.W. Absence of somatostatin receptors in human exocrine pancreatic adenocarcinomas. *Gastroenterology*, 1988 95(3): 760-763.
24. Hemminki A., Belousova N., Zinn K.R., Liu B., Wang M., Chaudhuri T.R., *et al.* An adenovirus with enhanced infectivity mediates molecular chemotherapy of ovarian cancer cells and allows imaging of gene expression. *Mol Ther*, 2001 4(3): 223-231.
25. Michou A.I., Santoro L., Christ M., Julliard V., Pavirani A. and Mehtali M. Adenovirus-mediated gene transfer: influence of transgene, mouse strain and type of immune response on persistence of transgene expression. *Gene Ther*, 1997 4(5): 473-482.
26. Pietersen A.M., van der Eb M.M., Rademaker H.J., van den Wollenberg D.J., Rabelink M.J., Kuppen P.J., *et al.* Specific tumor-cell killing with adenovirus vectors containing the apoptin gene. *Gene Ther*, 1999 6(5): 882-892.
27. Fallaux F.J., Bout A., van der Velde I., van den Wollenberg D.J., Hehir K.M., Keegan J., *et al.* New helper cells and matched early region 1-deleted adenovirus vectors prevent generation of replication-competent adenoviruses. *Hum Gene Ther*, 1998 9(13): 1909-1917.
28. Bakker W.H., Krenning E.P., Breeman W.A., Kooij P.P., Reubi J.C., Koper J.W., *et al. In vivo* use of a radioiodinated somatostatin analogue: dynamics, metabolism, and binding to somatostatin receptor-positive tumors in man. *J Nucl Med*, 1991 32(6): 1184-1189.
29. Dethlefsen L.A., Prewitt J.M. and Mendelsohn M.L. Analysis of tumor growth curves. *J Natl Cancer Inst*, 1968 40(2): 389-405.
30. Chen M.Y., Lonser R.R., Morrison P.F., Governale L.S. and Oldfield E.H. Variables affecting convection-enhanced delivery to the striatum: a systematic examination of rate of infusion, cannula size, infusate concentration, and tissue-cannula sealing time. *J Neurosurg*, 1999 90(2): 315-320.
31. Chen Z.J., Broaddus W.C., Viswanathan R.R., Raghavan R. and Gillies G.T. Intraparenchymal drug delivery via positive-pressure infusion: experimental and modeling studies of poroelasticity in brain phantom gels. *IEEE Trans Biomed Eng*, 2002 49(2): 85-96.
32. MacKay J.A., Deen D.F. and Szoka F.C., Jr. Distribution in brain of liposomes after convection enhanced delivery; modulation by particle charge, particle diameter, and presence of steric coating. *Brain Res*, 2005 1035(2): 139-153.
33. Mamot C., Nguyen J.B., Pourdehnad M., Hadaczek P., Saito R., Bringas J.R., *et al.* Extensive distribution of liposomes in rodent brains and brain tumors following convection-enhanced delivery. *J Neurooncol*, 2004 68(1): 1-9.

34. Fields B.N., Knipe D.M. and Howley P.M., *Virology*. 1996, Philadelphia, PA: Lippincott Williams & Wilkins. 2113-2171.
35. Kroll R.A., Pagel M.A., Muldoon L.L., Roman-Goldstein S. and Neuwelt E.A. Increasing volume of distribution to the brain with interstitial infusion: dose, rather than convection, might be the most important factor. *Neurosurgery*, 1996 38(4): 746-752; discussion 752-744.
36. Maina T., Nock B., Nikolopoulou A., Sotiriou P., Loudos G., Maintas D., *et al.* [^{99m}Tc]Demotate, a new ^{99m}Tc-based [Tyr^3]octreotate analogue for the detection of somatostatin receptor-positive tumours: synthesis and preclinical results. *Eur J Nucl Med Mol Imaging*, 2002 29(6): 742-753.
37. de Jong M., Kwekkeboom D., Valkema R. and Krenning E.P. Radiolabelled peptides for tumour therapy: current status and future directions. Plenary lecture at the EANM 2002. *Eur J Nucl Med Mol Imaging*, 2003 30(3): 463-469.
38. Rubsam L.Z., Boucher P.D., Murphy P.J., KuKuruga M. and Shewach D.S. Cytotoxicity and accumulation of ganciclovir triphosphate in bystander cells cocultured with herpes simplex virus type 1 thymidine kinase-expressing human glioblastoma cells. *Cancer Res*, 1999 59(3): 669-675.
39. Vincent A.J., Esandi M.C., Avezaat C.J., Vecht C.J., Sillevis Smitt P., van Bekkum D.W., *et al.* Preclinical testing of recombinant adenoviral herpes simplex virus-thymidine kinase gene therapy for central nervous system malignancies. *Neurosurgery*, 1997 41(2): 442-451; discussion 451-442.

2.4 Directly radiolabeled adenoviruses show viral distribution *in vivo* following intra-tumoral injection

S.M. Verwijnen, P.A.E. Sillevis Smitt, H. Knight, M. Konijnenberg, R.C. Hoeben, B. de Leeuw, W.A.P. Breeman, E. de Blois, E.P. Krenning, M. de Jong

Submitted

Abstract

Virus-based gene therapy is a promising treatment modality for cancer patients. Here we describe a technique for visualizing distribution of vector particles that can be used in parallel with non-invasive visualization of viral gene expression. We radiolabeled adenoviruses with ^{99m}Tc for single photon emission computed tomography (SPECT) imaging purposes. The ^{99m}Tc-tricarbonyl labeling technology was used for radiolabeling of adenovirus type 5 particles carrying the thymidine kinase and somatostatin receptor subtype 2 genes as reporters. Human (U87MG, U251) and rat (9L) glioma cells were infected *in vitro* with either unlabeled, radiolabeled, or sham labeled viruses and the biological activity was assayed. After radiolabeling, the viral particles were still infectious and reporter gene expression could still be measured. Intratumoral administration of radiolabeled viruses in 9L-bearing rats and in U87MG-bearing nude mice showed most of the radioactivity in the tumor at 4 hours post injection. Three days after infection of U87MG tumors, sst_2 gene expression could also be imaged. These data show that radiolabeling and visualization of adenoviruses directly after injection is feasible. This technology should be widely applicable in human gene therapy trials involving viral-vector mediated gene transfer into solid tumors.

Introduction

While clinical gene therapy trials in glioma patients have not yet provided the expected therapeutic break-through, they have identified limitations of this strategy [1-5]. The results of these trials have emphasized that the delivery of vectors and prodrugs to the tumor cells plus the spatial distribution of the vectors need to be improved. Additionally, it is important to be able to non-invasively assess the transduction rates *in vivo*, since this might be a prediction for treatment outcome [6, 7]. Molecular imaging techniques are therefore valuable for improving gene therapy trials and thereby the therapeutic effect in patients. Positron emission tomography (PET) and single photon emission computed tomography (SPECT) are useful techniques to non-invasively visualize expression of viral genes [8-10]. Many studies have shown that transgene expression imaging and quantification in living animals is possible [9, 11] and that invasive procedures in patients can be avoided when applying these techniques.

Imaging and quantification of gene expression is an indirect way to observe the vector spread *in vivo* after infection. Viral gene expression takes several hours to days and imaging can therefore not be performed directly after viral administration [12, 13]. Monitoring of the vector distribution immediately after administration in patients would give direct information about the vector distribution; this is only possible when vector particles are radiolabeled.

Only a few studies reported radiolabeling (parts of) viral vectors to investigate vector distribution *in vivo*. Zinn et al. developed a ^{99m}Tc-labeled adenoviral knob (^{99m}Tc-Ad5K) and followed its distribution after intravenous injection in mice [14]. They found that ^{99m}Tc-Ad5K rapidly localizes mainly to the liver, with also specific binding to the heart, kidneys and lungs. Subbarayan and co-workers radiolabeled complete adenoviral particles with ^{99m}Tc and reported that intravenous injection of these particles resulted in a high accumulation in the liver [15]. Intratumoral and intramuscular injection of the radiolabeled viruses yielded radioactivity at the injection site, up to 24 hours post injection. In 1998 and 2000, Schellingerhout et al. reported a method to radiolabel Herpes Simplex Virus (HSV) particles with ^{111}In-oxine [16, 17]. They found that the labeling procedure did not significantly reduce the infectivity of the viral particle. In addition, imaging after intravenous injection of the radiolabeled HSV particles showed a fast accumulation in the liver [16]. After injection in an intracerebral rat glioma tumor model, they found that 71% of the virus remained at the site of injection up to 24 hours post injection [17].

In this study we aimed to directly radiolabel the adenoviral vector Ad5.tk.sst$_2$ using ^{99m}Tc and Isolink, a carbonyl radiolabeling agent. Ad5.tk.sst$_2$, an adenovirus type 5 derived vector carrying the somatostatin receptor subtype 2 (sst$_2$) and herpes

simplex virus thymidine kinase (HSV-tk) genes as reporters for SPECT imaging purposes, was previously used for gene expression imaging studies in mice bearing lung [18], ovarian [19]. The aim of this study was three-fold: first we wanted to provide proof of concept of radiolabeling adenoviral particles using Isolink. Secondly, we compared the infectivity and gene expression of ^{99m}Tc-Ad5.tk.sst$_2$ with unlabeled Ad5.tk.sst$_2$ in rat and human glioblastoma tumor cells (9L, U251 and U87MG) *in vitro*. Finally, we imaged and quantified viral distribution and gene expression of unlabeled and radiolabeled Ad5.tk.sst$_2$ *in vivo* after intra-tumoral injection. Imaging was performed in 9L rat glioma bearing rats using a planar gamma camera and in U87MG human glioma bearing nude mice using an animal SPECT/CT system. Gene expression imaging three days after injection of the radiolabeled virus was performed in the same U87MG bearing mice.

Materials and methods

Cell culture

Unless stated otherwise, all cell lines were cultured in DMEM (Gibco Life Technologies, Breda, The Netherlands) with 10% heat-inactivated fetal bovine serum (Gibco Life Technologies). The adenovirus type 5 E1-transformed embryonal retina cell line 911 was cultured in medium with extra glucose (3 g/l). The glioma cell lines U251 (human origin, with the courtesy of P. Körnblith, NIH), U87MG (cultured in MEM, human origin, American Type Tissue Collection, Manassas, Virginia) and 9L (rat origin, with the courtesy of Dr. K.M. Hebeda, Free University Hospital Amsterdam, The Netherlands) were cultured in a humidified atmosphere at 37ºC containing 5% CO_2.

Amplification of the Viral Vector Ad5.tk.sst$_2$

The Ad5.tk.sst$_2$ is a replication incompetent adenoviral vector that contains the sst$_2$ and the HSV1-tk genes [19]. A separate early CMV promoter regulates both genes. Large scale amplification of Ad5.tk.sst$_2$ was carried out on PER.C6 cells as previously described [20] and the virus was titrated by plaque assay on 911 cells, yielding a mean of 3 x 10^{10} plaque forming units/ml (PFU/ml).

^{99m}Tc-Ad5.tk.sst$_2$ Preparation

[Na^{99m}TcO$_4$] was eluted from a ^{99}Mo/^{99m}Tc generator (Mallinckrodt Medical B.V., Petten, The Netherlands) using a 0.9% saline solution. The precursor [^{99m}Tc(CO)$_3$(OH$_2$)$_3$]$^+$ was prepared using the Isolink™ kit provided by Mallinckrodt Medical B.V. (Petten, The Netherlands). We used an excess of [^{99m}Tc(CO)$_3$(OH$_2$)$_3$]$^+$ over PFU Ad5.tk.sst$_2$, in order to radiolabel all the viruses in the solution. On average, 4x10^9 plaque forming units (PFU)

Ad5.tk.sst$_2$ adenoviruses were radiolabeled by adding an excess of $[^{99m}Tc(CO)_3(OH_2)_3]^+$ (about 900 MBq). This mixture was incubated one hour at 37°C. After incubation, the radiolabeled adenoviruses were separated from the free ^{99m}Tc molecules by either PD10 column separation (Amersham Biosciences B.V., Uppsala, Sweden) or a Microcon Centrifugal Filter Device (Millipore, Amsterdam, The Netherlands) with a molecular weight limit of 30,000 Daltons. Using PD10 separation, fractions of 500 µl saline + 0.1% human serum albumin were collected. Using Microcon purification, 500 µl of reaction volume was added to the filter and centrifuged for 10 minutes at 10,000 rpm. Thereafter, the retentate was transferred into a new vial and centrifuged for 3 minutes at 3,000 rpm. All samples were measured in a CRC®-10R dose calibrator (Capintec, Veenstra Instruments, Holland) to calculate the labeling efficiency.

Sham labeling was performed by adding a similar volume of that was used for the ^{99m}Tc-labeling, of saline to the solution with viral particles. This was also incubated for one hour at 37°C. After the incubation period, this mixture was also centrifuged using the Microcon filter.

Dose calculations

Initial labeling of the viral particles was performed with a mean activity of 900 MBq ^{99m}Tc in a volume of about 1 ml. The absorbed dose in this situation can be derived from the small spheres dosimetry model [21]. The dose per cumulated activity for ^{99m}Tc is 9.68 mGy/MBq*h. The cumulated activity is expressed by: $A(1-e^{-\lambda t})/\lambda$, with A the activity, λ the physical half-life of ^{99m}Tc and t the time period needed for the labeling. For the labeling period the dose to the viruses is given by the product of the cumulated activity $\tilde{A}$ and AS: $\tilde{A}$ x S. After purification with the Microcon method, a mean volume of 72.5 µl was left containing a mean activity of 80 MBq ^{99m}Tc. This volume is at the verge of where macrodosimetry still can be considered valid [22]. Adenoviral particles have an average diameter of 75 nm [23]. For a virus specific S-factor all electron energies emitted by ^{99m}Tc with a CSDA range below the virus diameter are summed and weighted with their emission abundance. The Auger electron spectra for ^{99m}Tc from Howell et al. was used [24]. The dose conversion is shown in table 1. Inside the 75 nm sphere the S-value is 292 Gy/Bq*sec. The dose rate per virus particle is obtained by multiplying this S-value with the mean activity per particle.

Radiolabeled Peptides

$^{111}InCl_3$ was purchased from Mallinckrodt Medical (Petten, The Netherlands). Commercially available OctreoScan kits were obtained from Mallinckrodt Medical/Tyco Health Care and radiolabeled as previously described [25]. The radiochemical purity was tested using ITLC and was determined to be >95%.

Table 1: Energy spectrum and dose conversion factors for electron spectrum from ^{99m}Tc with a range in water below 75 nm [24]. CK: Coster Kronig electrons, LMN: electron shell. Total energy released per decay by electrons with a range < 75 nm is 402 eV = 45% of total Auger and CK energy released per decay.

^{99m}Tc electrons	Energy (MeV)	Yield/decay (electrons/Bq·s)	Energy/decay (Gy·g/Bq·sec)	Range (nm)
CK LLX	4.29e-05	0.0193	1.33e-16	2.83
CK MMX	1.16e-04	0.747	1.39e-14	5.98
Auger MXY	2.26e-04	1.10	3.98e-14	10.5
CK NNX	3.34e-05	1.98	1.06e-14	2.05
Total		3.85	6.44e-14	

SDS-PAGE

^{99m}Tc-labeled viruses were either boiled for ten minutes or kept at room temperature. Thereafter, the samples were mixed 1:1 with sample buffer and separated on a 10% acrylamide gel using SDS-PAGE. Gels were transferred onto Hybond-C-super membrane (Amersham Biosciences, Berks, United Kingdom). Part of the membrane was stained with an anti-hexon antibody, while the other part was blocked in sterile low-fat milk and exposed to phosphor imaging screens (Perkin Elmer, Boston, USA) in X-ray cassettes (Kodak, Vianen, The Netherlands) for 18 hours. The exposed phosphor screens were analyzed using a Cyclone phosphor imager and a computer-assisted OptiQuant image processing system (version 03.00, Perkin Elmer).

In Vitro Internalization and Expression Studies

In vitro internalization of ^{99m}Tc-Ad5.tk.sst$_2$ was studied in U87MG, U251 and 9L cells. Cells (10^5 cells/well) were transferred to 24-wells plates one day prior to the experiments. Following radiolabeling, the cells were incubated for 1, 2, 4, 24 and/or 48 hours with ^{99m}Tc-Ad5.tk.sst$_2$ and at increasing multiplicity of infection (moi). After the incubation, the cells were washed with ice-cold PBS and shortly incubated with 0.5 ml of 1 M sodium hydroxide in order to lyse the cells. The radioactivity of these fractions was counted in an LKB-1282-Compugamma system (Perkin Elmer, Groningen, the Netherlands). As a control study, we also measured ^{99m}Tc in uninfected (denoted as mock infected) cells. Additionally, U251 and 9L cells were also incubated with ^{99m}Tc-Isolink.

Internalization and uptake studies [26] were performed in U87MG cells that were infected three days before the experiment. Viral infection was allowed during two hours, with increasing moi's of either unlabeled, radiolabeled or sham labeled Ad5.tk.sst$_2$. One hour internalization was allowed using the sst analog [^{111}In-DTPA^0] octreotide. Again, the cell fractions were collected and counted in the LKB-1282-Compugamma system.

Gamma Camera Imaging

All animal experiments were approved by the Institutional Animal Care and Use Committee, and were in compliance with the Guide for the Care and Use of Laboratory Animals. Male Lewis rats were implanted on both flanks with a 0.5 ml Hanks Buffered Salt Solution (HBBS) containing an average of $2x10^6$ 9L cells. After 14 days, each tumor was injected with 9 MBq ^{99m}Tc-labeled Ad5.tk.sst$_2$ (a total of 10^8 PFU) in 50µl. Four hours after injection of the radiolabeled adenovirus, static scans were made of three rats during 10 minutes using a one-headed gamma-camera (Siemens, Erlangen, Germany). Immediately after imaging, the rats were sacrificed and a biodistribution study was performed; tumors and tissues were collected and counted in a LKB-1282-Compugammasystem (Perkin Elmer, Groningen, The Netherlands).

SPECT/CT Imaging

One week after arrival, male NMRI nude/nude mice (Charles River Laboratories, Sulzfeld, Germany) were inoculated subcutaneously with 0.2 ml HBBS solution containing an average of 10^7 U87MG cells on both shoulders. At a volume of 150-300 mm^3, each U87MG tumor was injected with $2x10^9$ PFU in 50 µL of either Ad5.tk.sst$_2$ or ^{99m}Tc-Ad5.tk.sst$_2$, the latter containing approximately 18 MBq of ^{99m}Tc. Four hours after injection of the radiolabeled virus, the animals were scanned with the NanoSPECT/CT camera (Bioscan Inc., Washington D.C., USA) as described earlier [27]. Briefly, animals were imaged using mouse pinhole apertures that comprise a total of 36 1.4-mm-diameter pinholes. The energy-peak of the camera was set at 140 keV for ^{99m}Tc. An acquisition time of 30 seconds per projection was chosen, resulting in a total acquisition time of 12 minutes per animal, imaging the whole body. CT scans were performed using the integrated CT-scanner. The tube voltage was set at 45 kVp and an exposure time of 1000 ms per projection was chosen, imaging with 180 projections per rotation, with a total acquisition time of 6 minutes.

Three days after virus administration, the mice were injected with 200 MBq/200 µl [^{111}In-DTPA^0]octreotide into the penis vein and again scanned with the NanoSPECT/CT camera, 4 hours post injection. Now, the energy peak of the camera was set at 171 keV and 245 keV for ^{111}In; CT acquisition was performed as described above. Immediately after scanning a biodistribution study was performed as described above.

The SPECT acquisitions were reconstructed iteratively with the HiSPECT software (Bioscan Inc.) as described before [28] and quantification was performed using the MIPtool program (Mediso Ltd., Budapest, Hungary).

Statistical Analysis

Data are expressed as mean ± SEM. Results were statistically analyzed using one-way ANOVA. Differences were considered statistically significant when P was <0.05, in which case a Dunnet's Multiple Comparison test was performed to compare for post-hoc analysis. All statistical analyses were performed with GraphPad Prism 4.0 program.

Results

^{99m}Tc-Ad5.tk.sst$_2$ Preparation

The mean labeling yield was 21 MBq/10^9 plaque forming units (PFU). For all experiments, the labeling efficiency was calculated (see table 2), with a mean of 22%. Concerning the labeling efficiency, we found no statistical difference between the two purification methods: PD10 column or Microcon. However, the Microcon method was more user-friendly, less time-consuming and yielded smaller volumes, which is more convenient for *in vivo* use. Therefore, this method had our preference for further experiments.

Table 2: Labeling efficiencies of ^{99m}Tc-Ad5.tk.sst$_2$ using two different purification methods following radiolabeling.

	Mean Lab. Eff. (%)	SD	n =	Highest Lab. Eff.	Lowest Lab. Eff.
All experiments	21.9	9.2	17	41.3	8.2
PD10 column	21.1	9.5	8	41.3	12.6
Microcon	22.7	9.5	9	35.3	8.2

Dose Calculations

The cumulated activity during the 1 hour incubation time with 900 MBq is: 850 MBq*h. We calculated that during this incubation period of Ad5.tk.sst$_2$ with the ^{99m}Tc-tricarbonyl compound, the radiation dose to the viral particles was about 8 Gy. After the purification procedure, each PFU had a calculated activity of 0.02 Bq, which resulted in a dose rate of 5.8 Gy/sec per PFU.

SDS-PAGE

Following radiolabeling, Ad5.tk.sst$_2$ viral proteins were separated and transferred onto a nitrocellulose membrane, which was incubated on a phosphor screen. Figure 1 shows the results of the phosphor screen. All major structural proteins of the adenoviral particles, such as hexon, penton, fiber and hexon associated I, II and III were shown to be radiolabeled. The 200 kDa hexon band disappears upon boiling (single hexon proteins migrate at 90-120 kDa, also shown by [29]).

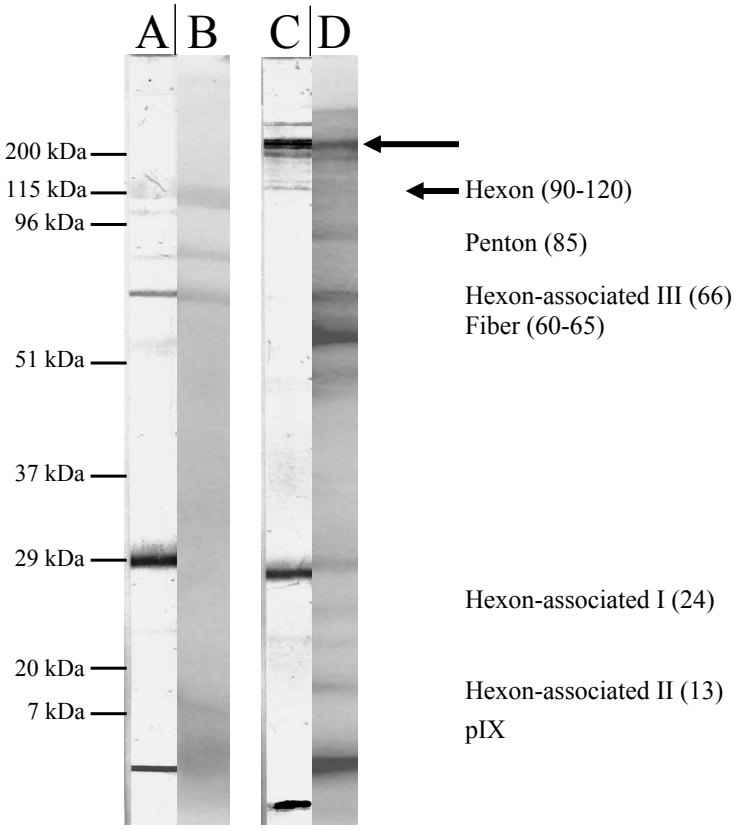

Figure 1. Anti-hexon immunostaining (A, C) and autoradiography (B, D) of boiled (A, B) and unboiled (C, D) ^{99m}Tc-Ad5.tk.sst$_2$ virus. Arrows indicate the positions of hexon. The expected height of the capsid proteins are also shown.

In Vitro Internalization and Expression Studies

Internalization studies were performed to investigate if radioactive viral particles loose their radioactivity during endocytosis. Figure 2 shows the results of ^{99m}Tc-Ad5.tk.sst$_2$ infection in three glioma cell lines with increasing moi. We found that radioactivity inside the tumor cells increases with increasing moi. The curves in figure 2 also show the uptake of radioactivity increases in time. In U251 and 9L cells, we also tested whether free, unbound ^{99m}Tc-[$(H_2O)_3(CO)_3^+$] particles could internalize or migrate into the cells when incubated for 1, 4 and 24 hours. We hardly found any uptake in cells incubated with ^{99m}Tc-Isolink; less than 0.1% of the total ^{99m}Tc dose was internalized into the cells.

In U87MG cells, infected seventy-two hours before with unlabeled, sham labeled or radiolabeled Ad5.tk.sst$_2$, we examined the expression of viral genes. In this case we incubated the cells with [^{111}In-DTPA^0]octreotide to show sst$_2$ gene expression *in vitro*, results of which are shown in figure 3. We found that uptake of the radiolabeled

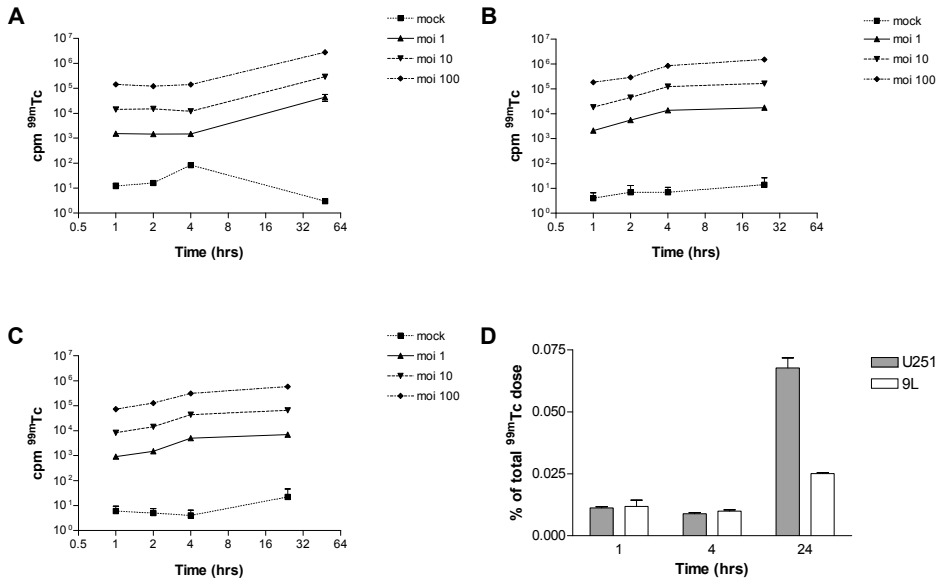

Figure 2. Time course of U87MG (A), U251 (B) and 9L cells (C) infected with ^{99m}Tc-Ad5.tk.sst$_2$ virus. Cells were incubated with either no virus (=mock infected), moi 1, 10 and 100 of ^{99m}Tc-Ad5.tk.sst$_2$ for several hours. Additionally, U251 and 9L cells were incubated with ^{99m}Tc-Isolink (D). After incubation, the amount of ^{99m}Tc radioactivity was measured inside the cells. Data are expressed as mean ± SEM counts per minute (cpm) of n=6 (A), n=12 (B and C). Data of (D) is expressed as % of total ^{99m}Tc dose of n=4 measurements.

tracer in all viral infected cells increased with increasing moi. However, the uptake of the tracer was significantly higher in the cells infected with the unlabeled viruses, especially at moi 10 and 100, compared to the radiolabeled and sham labeled viruses. At moi 100, the uptake of [^{111}In-DTPA^0]octreotide in cells infected with ^{99m}Tc-Ad5.tk.sst$_2$ was three times lower than in cells infected with unlabeled viruses.

Gamma Camera Imaging

Figure 4A shows the biodistribution data of rats bearing two 9L tumors injected with 9 MBq ^{99m}Tc-Ad5.tk.sst$_2$. We found a high uptake in the injected 9L tumors, a much lower uptake in kidneys and liver, and almost no uptake in blood and other organs at 4 hours post infection. At 24 hours post infection, the uptake in 9L tumors was lower than at 4 hours, while the uptake in kidneys and liver remained almost the same.

At 4 hours post injection, planar gamma camera images were made of three rats. These images are shown in figure 4B and visualize that almost all radioactivity is concentrated in the tumors. A minor uptake is shown in liver, kidneys and bladder. These results show that after injection of viral particles into a tumor, the gross part of the viral particles remain there.

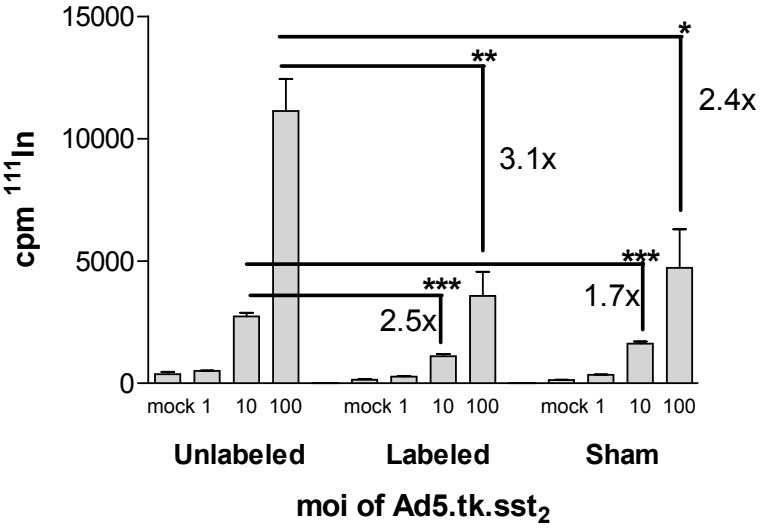

Figure 3. Internalized fraction of [^{111}In-DTPA^{0}]octreotide in U87MG cells infected 72 hours earlier with increasing moi of unlabeled, ^{99m}Tc-labeled or sham labeled Ad5.tk.sst$_2$ virus. Data are expressed as mean ± SEM cpm of n=4 measurements. * P<0.05; ** P<0.01; *** P<0.001

SPECT/CT Imaging

Figure 5A shows the SPECT/CT images from a representative mouse bearing two U87MG tumors injected with 19 MBq (2x10^9 PFU) ^{99m}Tc-Ad5.tk.sst$_2$. As was shown in the 9L-bearing rat images, most of the radioactivity after ^{99m}Tc-Ad5.tk.sst$_2$ injection remains in the tumor tissue. The images were quantified (see table 3) and we calculated that a mean of 2.39±0.28 MBq ^{99m}Tc was found in the tumors, while a small amount was found in bowel (0.24±0.12 MBq) after 4 hours. Sagittal, coronal and transversal slices in figure 5A show that the radioactivity in the tumor is not

Table 3: Quantified uptake in MBq after SPECT/CT imaging.

Activity (MBq)	^{99m}Tc-Ad5.tk.sst$_2$			[^{111}In-DTPA^{0}]octreotide		
	Mean	SD	n	Mean	SD	n
Tumor	2.39	0.28	6	0.83	0.47	4
Bowel	0.24	0.12	4	-	-	-
Kidneys	-	-	-	7.80	1.44	2
Bladder	0.99	0.24	4	-	-	-
Total body	4.99	1.53	4	36.55	17.04	2
Ratios						
Tumor/total body	0.48			0.02		
Tumor/bowel	9.77					
Tumor/kidney				0.11		
Tumor/bladder	2.41					

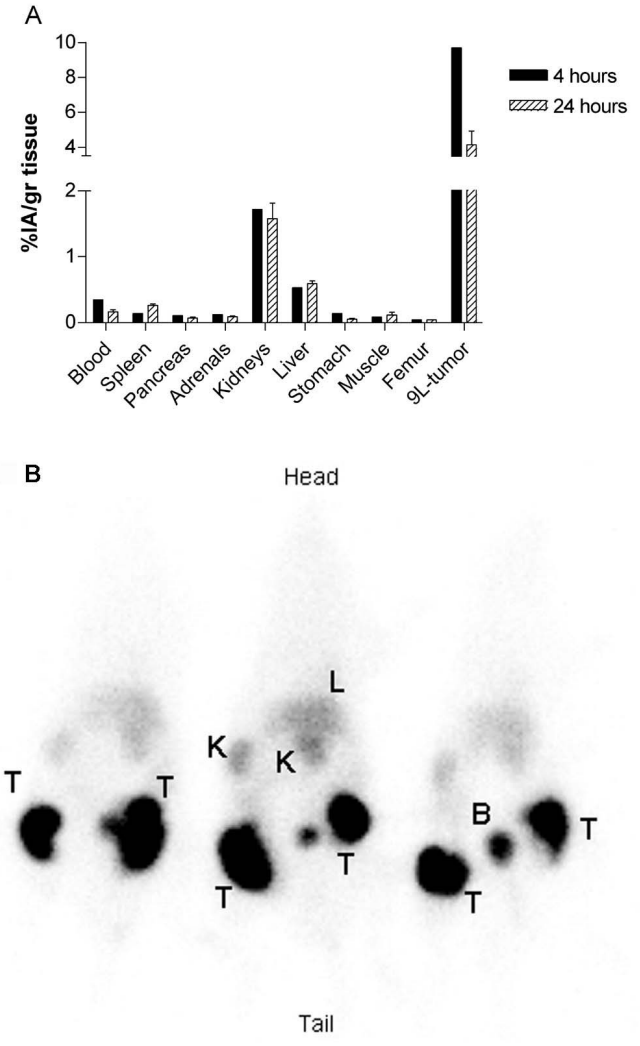

Figure 4. (A) Biodistribution at 4 and 24 hours post intra-tumoral injection of ^{99m}Tc-Ad5.tk.sst$_2$ in rats bearing two 9L tumors. Data is expressed as mean ± SEM % injected activity per gram tissue (%IA/g) n=3 animals (24 hours). Data at 4 hours post injection represents one animal. (B) Gamma camera images (maximum intensity projection) of three rats, each bearing two 9L tumors, following intra-tumoral injection of 9 MBq (10^8 plaque forming units) of ^{99m}Tc-Ad5.tk.sst$_2$ at 4 hours post injection.

homogeneous, but depict a striped and spotted pattern. In these images no uptake in liver and kidney was detected.

Three days after ^{99m}Tc-Ad5.tk.sst$_2$ injection and imaging, the same animals were scanned subsequent to a [^{111}In-DTPA^0]octreotide injection. Results of these images are shown in figure 5B; results of the image quantification can be found in table 3. Uptake of the tracer in both tumors is clearly visible in the SPECT images, indicating

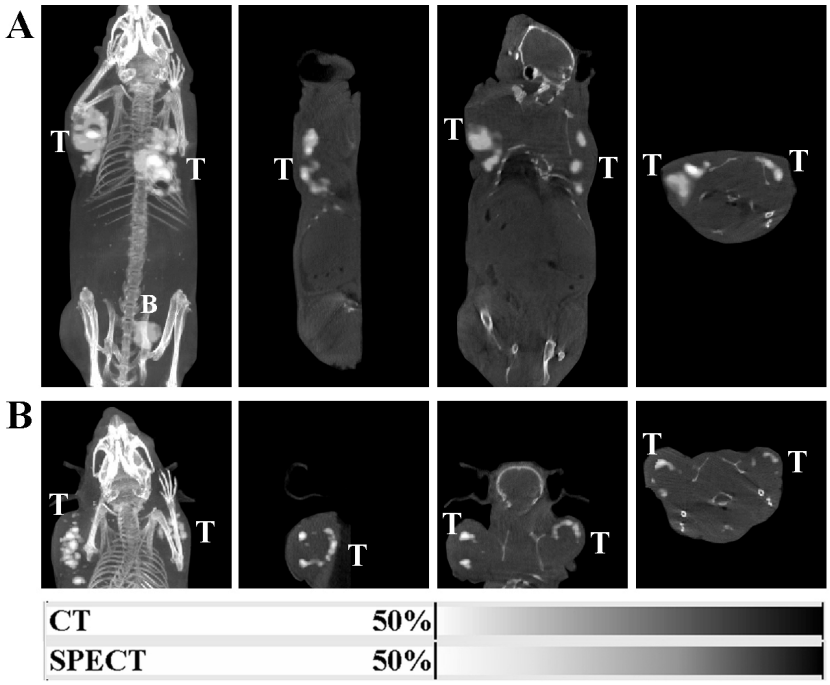

Figure 5. (A) SPECT/CT scans of a mouse bearing two U87MG tumors, injected with 19 MBq (2x10^9 PFU) of ^{99m}Tc-Ad5.tk.sst$_2$, taken at 4 hours post injection. Quantification: tumor left=2.37 MBq; tumor right=2.25 MBq; bladder=0.80 MBq, bowel=0.32 MBq. (B) Seventy-two hours thereafter, the same animal was injected with 200 MBq (2 µg) [^{111}In-DTPA^0]octreotide and scanned again at 4 hours post injection of the tracer. Quantification: tumor left=0.58 MBq; tumor right=0.30 MBq. Maximum intensity projection (1), sagittal (2), coronal (3) and transversal (4) slices are shown of the whole mouse at the height of the tumor. Images are examples and are representative for three animals in this group. Slice thickness=0.30 mm. (T=U87MG tumor infected with ^{99m}Tc-Ad5.tk.sst$_2$, B=bladder).
For color figure see page 243.

that these tumor cells express sst$_2$. We calculated a mean uptake of 0.83±0.47 MBq [^{111}In-DTPA^0]octreotide in the tumors. Radioactivity in kidneys and bladder is due to excretion of the radiolabeled peptide.

Figure 6A shows the results of the biodistribution data at 4 hours post injection of [^{111}In-DTPA^0]octreotide. No significant difference was found in biodistribution pattern between animals infected with virus or non-infected animals. Results depicted in figure 6B show that there is no significant difference between the uptake of [^{111}In-DTPA^0]octreotide in ^{99m}Tc-Ad5.tk.sst$_2$ or unlabeled Ad5.tk.sst$_2$ infected tumors. In both groups the uptake of the tracer was significantly higher than in the saline injected U87MG tumors, which confirms that expression of the transgenes is required for receptor mediated uptake of the tracer.

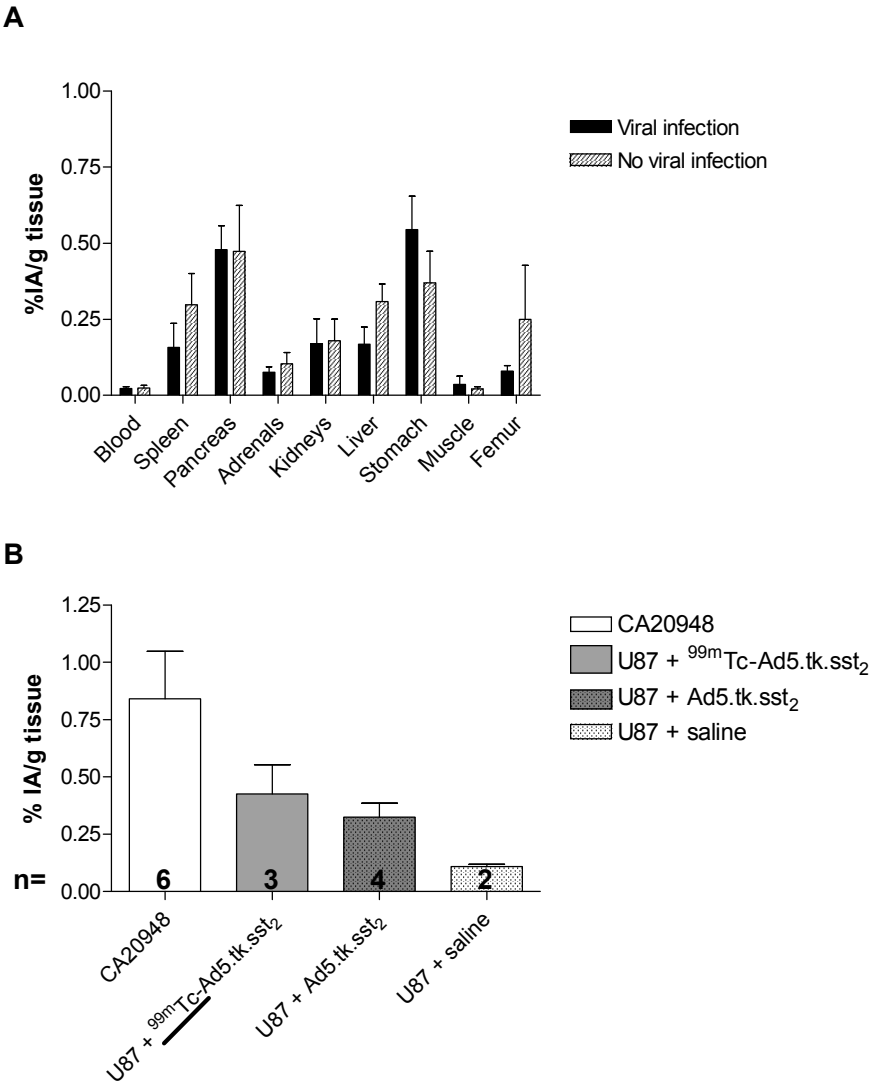

Figure 6. (A) Biodistribution of [^{111}In-DTPA^{0}]octreotide in organs of virally infected (n=4) and normal animals (no viral infection, n=5). (B) Uptake of [^{111}In-DTPA^{0}]octreotide in U87MG bearing mice infected with either ^{99m}Tc-labeled Ad5.tk.sst$_2$ (n=3), unlabeled Ad5.tk.sst$_2$ (n=4) or saline (n=2). CA20948 (n=6) is shown as positive control for sst$_2$ expression. Data are expressed as mean ± SEM % injected activity per gram tissue (%IA/g tissue).

Discussion

In this study, we aimed to radiolabel adenoviral particles with ^{99m}Tc for SPECT imaging purposes. Direct imaging of a viral vector is interesting for clinical application, since it was concluded from many clinical cancer gene therapy trials that non-invasive

imaging should be integrated in these modalities [6, 30]. Gene expression imaging following viral administration is essential in giving insight in the location, duration and extent of expression of the desired gene(s). So far, only a few research groups attempted to non-invasively follow the viral vector by radiolabeling the particle itself to show its location after administration, potential migration from the initial injection site, and whether non-target tissues are also infected [14-17, 31].

The Ad5.tk.sst_2 viral particle was radiolabeled with an excess of ^{99m}Tc-labeled molecules to show proof of concept. An excess of ^{99m}Tc-molecules in respect to PFU was used to ensure that all viruses would be radiolabeled. The results of this study show that adenoviruses can be radiolabeled using the Isolink™ kit. Retrospectively we calculated the radiation dose to the virus during and after labeling. We found that the dose rate to the viral particles is about 5.8 Gy/sec, which might be harmful to the viruses. However, in a clinical setting use only a small part of radiolabeled viruses; it is optional to add unlabeled viruses to the radiolabeled batch prior to injection, to achieve a higher infection rate *in vivo* and still be able to follow the viral distribution.

Despite the radiation dose, we found that the viability of the ^{99m}Tc-labeled viruses is still high enough to infect human and rat glioma tumor cells *in vitro* (figure 2) and *in vivo* (figure 4 and 5). In the *in vitro* internalization study we have shown that the uptake of ^{99m}Tc-activity inside the cells is dependent on the moi that is presented to these cells. Prerequisite to the internalization of ^{99m}Tc radioactivity is the stable binding to the Ad5.tk.sst_2 viral particles, since we found that almost no free ^{99m}Tc-molecules migrate into the cells (figure 2D). We can therefore conclude that the uptake of radioactivity shown in the *in vitro* studies is clearly mediated by the internalization of the adenovirus, and that stable radiolabeling was achieved in these studies.

We also found that after infection with ^{99m}Tc-Ad5.tk.sst_2 in cells *in vitro*, sst_2 gene expression could still be detected (figure 3), although a lower uptake of [^{111}In-DTPA^0] octreotide was detected in these U87MG cells, compared to the cells infected with unlabeled viruses, especially at moi 10 and 100. In our studies we only measured sst_2 expression, since we have recently found that the expression of both the sst_2 and HSV-tk genes are simultaneously expressed when using the Ad5.tk.sst_2 viral vector (manuscript in progress).

The results of the *in vivo* imaging studies (figure 4 and 5) show that only a small amount of radiolabeled viruses "escape" from the tumor to other organs after intra-tumoral injection. In rats, we found low ^{99m}Tc-activity in liver, kidneys and bladder. In mice, we also found some ^{99m}Tc-activity in the bladder, but not in liver and kidneys. Subbarayan et al. and Schellingerhout et al. reported on the intra-tumoral injection of radiolabeled viruses and the subsequent visualization of the radioactivity. They

both found that 24 hours after intra-tumoral injection the radioactivity remained at the site op injection [15, 17].

We could also image gene expression three days after *in vivo* infection with radiolabeled viruses, although a low uptake of [^{111}In-DTPA^{0}]octreotide was found in the infected tumors (see table 2 and figure 6). The uptake in the tumors could be improved when a tracer with higher sst_2-affinity would have been used, such as [DOTA,Tyr^{3}]octreotate [32] or [DOTA]-1-NaI_3-octreotide [33]. Additionally, a higher specific activity could improve the results. Here we used a relatively high amount of peptide to ensure visualization of gene expression since lower receptor expression was anticipated; partial saturation of the sst_2 receptors may have occurred in this experiment, leading to a lower uptake in the tumors.

As mentioned before, other groups have earlier performed direct labeling of viral particles for imaging purposes. Zinn and co-workers labeled a recombinant adenovirus serotype 5 knob with ^{99m}Tc (^{98m}Tc-Ad5K) and found that this did not change the trimeric structure or the specific binding of ^{98m}Tc-Ad5K to its cellular receptor [14]. They also imaged the ^{98m}Tc-Ad5K using a gamma camera after systemic injection *in vivo*. The ^{99m}Tc-Ad5K rapidly localized to the liver, with also specific binding to the heart, kidney and lungs. Regarding our imaging results, after intra-tumoral injection we did not see any uptake in heart and lungs, which indicates that the radiolabeled viral particles did not leak outside the tumor.

Simultaneously, Schellingerhout et al. described a method for radiolabeling Herpes Simplex Virus (HSV) with ^{111}In-oxine [16, 17]. They yielded 290 µCi/10^9 PFU with a labeling efficiency of 71%. The labeling yield was twice as high in our experiments (570 µCi/10^9 PFU), however Schellingerhout achieved a higher labeling efficiency. We calculated from the data of Schellingerhout that their experiments resulted in a similar dose rate compared to our studies; 7.7 Gy/sec and 5.8 Gy/sec to the viral particles was calculated, respectively. Moreover, they found that the infectivity of the virus was not significantly reduced, similar to what was found by Zinn et al. It is not clear why the infectivity of the HSV is not reduced in the study by Schellingerhout, compared to our results in Ad5 labeling. Both viruses should have similar radioresistance [34]. In relation to the lower titer of the radiolabeled virus and the lower expression of sst_2 in U87MG cells infected with radiolabeled viruses which we found, we believe that in part the radiolabeling procedure, but even more so the dose rate to the viral particles, influences the amount of viral particles after purification. It is therefore essential to further optimize the radiolabeling procedure, for example, by reducing the amount of radioactivity during the labeling procedure.

We provide here proof of concept for stable ^{99m}Tc labeling of adenoviral vectors, which encode genes for therapeutic purposes. The subsequent administration and imaging of the radiolabeled particles *in vivo* is feasible, as well as the *in vivo* gene

expression imaging in the same animals. Our data also indicates that the amount of radioactivity used to radiolabel the virus still gives room for optimization. After improving the radiolabeling, it would be interesting to test this application in a clinical trial, in addition to imaging of protein expression in the targeted tissue. The combination of these imaging results might give insight in the fate of viral vectors after administration *in vivo*. Compensation for viruses lost during the labeling procedure, by adding unlabeled viruses to the radiolabeled batch prior to the injection, is probably necessary for high-quality gene expression imaging in clinical trials.

Acknowledgements

The authors would like to thank Eric Brouwer and Esther Hulsenboom for technical assistance.

References

1. Klatzmann D., Valery C.A., Bensimon G., Marro B., Boyer O., Mokhtari K., *et al.* A phase I/II study of herpes simplex virus type 1 thymidine kinase "suicide" gene therapy for recurrent glioblastoma. Study Group on Gene Therapy for Glioblastoma. *Hum Gene Ther*, 1998 9(17): 2595-2604.
2. Rainov N.G. A phase III clinical evaluation of herpes simplex virus type 1 thymidine kinase and ganciclovir gene therapy as an adjuvant to surgical resection and radiation in adults with previously untreated glioblastoma multiforme. *Hum Gene Ther*, 2000 11(17): 2389-2401.
3. Prados M.D., McDermott M., Chang S.M., Wilson C.B., Fick J., Culver K.W., *et al.* Treatment of progressive or recurrent glioblastoma multiforme in adults with herpes simplex virus thymidine kinase gene vector-producer cells followed by intravenous ganciclovir administration: a phase I/II multi-institutional trial. *J Neurooncol*, 2003 65(3): 269-278.
4. Smitt P.S., Driesse M., Wolbers J., Kros M. and Avezaat C. Treatment of relapsed malignant glioma with an adenoviral vector containing the herpes simplex thymidine kinase gene followed by ganciclovir. *Mol Ther*, 2003 7(6): 851-858.
5. Immonen A., Vapalahti M., Tyynela K., Hurskainen H., Sandmair A., Vanninen R., *et al.* AdvHSV-tk gene therapy with intravenous ganciclovir improves survival in human malignant glioma: a randomised, controlled study. *Mol Ther*, 2004 10(5): 967-972.
6. Rainov N.G. and Ren H. Gene therapy for human malignant brain tumors. *Cancer J*, 2003 9(3): 180-188.
7. Jacobs A., Voges J., Reszka R., Lercher M., Gossmann A., Kracht L., *et al.* Positron-emission tomography of vector-mediated gene expression in gene therapy for gliomas. *Lancet*, 2001 358(9283): 727-729.
8. Bennett J.J., Tjuvajev J., Johnson P., Doubrovin M., Akhurst T., Malholtra S., *et al.* Positron emission tomography imaging for herpes virus infection: Implications for oncolytic viral treatments of cancer. *Nat Med*, 2001 7(7): 859-863.
9. Min J.J. and Gambhir S.S. Gene therapy progress and prospects: noninvasive imaging of gene therapy in living subjects. *Gene Ther*, 2004 11(2): 115-125.
10. Ray P., Bauer E., Iyer M., Barrio J.R., Satyamurthy N., Phelps M.E., *et al.* Monitoring gene therapy with reporter gene imaging. *Semin Nucl Med*, 2001 31(4): 312-320.
11. Massoud T.F. and Gambhir S.S. Molecular imaging in living subjects: seeing fundamental biological processes in a new light. *Genes Dev*, 2003 17(5): 545-580.
12. Liang Q., Gotts J., Satyamurthy N., Barrio J., Phelps M.E., Gambhir S.S., *et al.* Noninvasive, repetitive, quantitative measurement of gene expression from a bicistronic message by positron emission tomography, following gene transfer with adenovirus. *Mol Ther*, 2002 6(1): 73-82.
13. Honigman A., Zeira E., Ohana P., Abramovitz R., Tavor E., Bar I., *et al.* Imaging transgene expression in live animals. *Mol Ther*, 2001 4(3): 239-249.
14. Zinn K.R., Douglas J.T., Smyth C.A., Liu H.G., Wu Q., Krasnykh V.N., *et al.* Imaging and tissue biodistribution of ^{99m}Tc-labeled adenovirus knob (serotype 5). *Gene Ther*, 1998 5(6): 798-808.
15. Subbarayan M., Sundaresan G. and Gambhir S.S. *In vivo* imaging of ^{99m}Tc-adenovirus and reporter gene expression by different routes of administration in living subjects. *Molecular Imaging*, 2003 2(3): 259.
16. Schellingerhout D., Bogdanov A., Jr., Marecos E., Spear M., Breakefield X. and Weissleder R. Mapping the *in vivo* distribution of herpes simplex virions. *Hum Gene Ther*, 1998 9(11): 1543-1549.
17. Schellingerhout D., Rainov N.G., Breakefield X.O. and Weissleder R. Quantitation of HSV mass distribution in a rodent brain tumor model. *Gene Ther*, 2000 7(19): 1648-1655.

18. Zinn K.R., Chaudhuri T.R., Krasnykh V.N., Buchsbaum D.J., Belousova N., Grizzle W.E., *et al.* Gamma camera dual imaging with a somatostatin receptor and thymidine kinase after gene transfer with a bicistronic adenovirus in mice. *Radiology*, 2002 223(2): 417-425.
19. Hemminki A., Belousova N., Zinn K.R., Liu B., Wang M., Chaudhuri T.R., *et al.* An adenovirus with enhanced infectivity mediates molecular chemotherapy of ovarian cancer cells and allows imaging of gene expression. *Mol Ther*, 2001 4(3): 223-231.
20. Fallaux F.J., Bout A., van der Velde I., van den Wollenberg D.J., Hehir K.M., Keegan J., *et al.* New helper cells and matched early region 1-deleted adenovirus vectors prevent generation of replication-competent adenoviruses. *Hum Gene Ther*, 1998 9(13): 1909-1917.
21. Stabin M.G. and Konijnenberg M.W. Re-evaluation of absorbed fractions for photons and electrons in spheres of various sizes. *J Nucl Med*, 2000 41(1): 149-160.
22. (ICRU) I.C.o.R.U.M. Absorbed-dose specification in Nuclear Medicine (ICRU report 67). *Journal of the ICRU*, 2002.
23. San Martin C. and Burnett R.M. Structural studies on adenoviruses. *Curr Top Microbiol Immunol*, 2003 272: 57-94.
24. Howell R.W. Radiation spectra for Auger-electron emitting radionuclides: report No. 2 of AAPM Nuclear Medicine Task Group No. 6. *Med Phys*, 1992 19(6): 1371-1383.
25. De Jong M., Valkema R., Van Gameren A., Van Boven H., Bex A., Van De Weyer E.P., *et al.* Inhomogeneous Localization of Radioactivity in the Human Kidney After Injection of [^{111}In-DTPA^{0}]octreotide. *J Nucl Med*, 2004 45(7): 1168-1171.
26. Verwijnen S.M., Sillevis Smitt P.A.E., Hoeben R.C., Rabelink M.J., Wiebe L., Curiel D.T., *et al.* Molecular imaging and treatment of malignant gliomas following adenoviral transfer of the herpes simplex virus-thymidine kinase gene and the somatostatin receptor subtype 2 gene. *Cancer Biother Radiopharm*, 2004 19(1): 111-120.
27. Verwijnen S.M., ter Horst M., Sillevis Smitt P.A.E., Hoeben R.C., Forrer F., Mueller C., *et al.* Molecular imaging following adenoviral gene transfer visualizes sst_2 and HSV1-tk expression. *submitted*, 2007.
28. Forrer F., Valkema R., Bernard B., Schramm N.U., Hoppin J.W., Rolleman E., *et al. In vivo* radionuclide uptake quantification using a multi-pinhole SPECT system to predict renal function in small animals. *Eur J Nucl Med Mol Imaging*, 2006.
29. Wu H., Han T., Belousova N., Krasnykh V., Kashentseva E., Dmitriev I., *et al.* Identification of sites in adenovirus hexon for foreign peptide incorporation. *J Virol*, 2005 79(6): 3382-3390.
30. Pulkkanen K.J. and Yla-Herttuala S. Gene therapy for malignant glioma: current clinical status. *Mol Ther*, 2005 12(4): 585-598.
31. Sundaresan G., Murugesan S. and Gambhir S.S. MicroPET imaging of I-124 adenovirus biodistribution and optical imaging of reporter gene expression in living subjects. *Molecular Imaging*, 2003 2: 302.
32. De Jong M., Bernard B.F., De Bruin E., Van Gameren A., Bakker W.H., Visser T.J., *et al.* Internalization of radiolabelled [DTPA^{0}]octreotide and [DOTA^{0},Tyr^{3}]octreotide: peptides for somatostatin receptor-targeted scintigraphy and radionuclide therapy. *Nucl Med Commun*, 1998 19(3): 283-288.
33. Wild D., Schmitt J.S., Ginj M., Macke H.R., Bernard B.F., Krenning E., *et al.* DOTA-NOC, a high-affinity ligand of somatostatin receptor subtypes 2, 3 and 5 for labelling with various radiometals. *Eur J Nucl Med Mol Imaging*, 2003 30(10): 1338-1347.
34. Sullivan R., Fassolitis A.C., Larkin E.P., Read R.B., Jr. and Peeler J.T. Inactivation of thirty viruses by gamma radiation. *Appl Microbiol*, 1971 22(1): 61-65.

3

Receptor targeting using radiolabeled peptides

3.1 Peptide receptor expression on different human intracranial tumors

M. Verwijnen, M. Melis, J.M. Kros, E.P. Krenning, P.A.E. Sillevis Smitt, M. de Jong

Submitted

Abstract

Purpose: Peptide receptors are over-expressed in human malignant tissues and are excellent targets for non-invasive diagnostic imaging and treatment of cancer. Somatostatin analogs are most widely used for these purposes in neuroendocrine tumors; this principle may be interesting for other tumor types as well. Glioblastoma multiforme (GBM) is the most aggressive glioma subtype with high mortality rates. So far, treatment options (surgery, radiation and chemotherapy) have been marginally successful. Patients with GBM may therefore benefit from additional treatment options, such as peptide receptor radionuclide therapy (PRRT). In addition, other intracranial tumors, such as meningioma (MG) and also metastatic disease involving brain (MT), are interesting targets for PRRT. We therefore aimed to select a peptide receptor candidate for peptide receptor scintigraphy and PRRT for human intracranial tumors by determining receptor expression in GBM, MG, MT and normal human brain (NB) specimens using *in vitro* autoradiography, in addition to internalization of peptide analogs into established GBM cell lines.

Methods: Internalization studies were performed in primary and established GBM cell lines using radiolabeled peptides targeting the following receptors: somatostatin receptor subtype 2 (sst_2), neurokinine-1 receptor (NK-1), the integrin $\alpha_v\beta_3$, gastrin-releasing peptide receptor (GRP), vasoactive intestinal peptide receptor (VIP) and cholecystokinin-2 receptor (CCK_2). *In vitro* autoradiography studies were performed on human GBM, MG, MT and NB tissues using the same radiolabeled peptides except integrin $\alpha_v\beta_3$, supplemented with epidermal growth factor (EGF) receptor and neurotensin (NT) receptor analogs.

Results: VIP receptors were commonly expressed on the established GBM cells lines, GRP and NK-1 receptors were also expressed, although with a lower incidence. A high density and incidence of VIP receptors was found on almost all GBM, MG and MT tissues. Possible targets for GBM also include EGF and NK-1 receptors. In addition, sst_2 is a good target for MG patients since we detected sst_2 in all MG samples. We also found that the NK-1 receptor was expressed in high density and moderate incidence in MT tissues of the brain.

Conclusion: Analogs targeting VIP-, EGF- and NK-1 receptors can be used for PRS and PRRT of GBM patients, and sst_2 analogs in patients suffering from MG. A prerequisite is that the radiolabeled peptides are able to pass the blood-brain-barrier, can be locally injected or that the BBB is damaged at the site of the tumor.

Introduction

The finding that somatostatin receptors (sst) are over-expressed in various tumor tissues led to the application of peptide receptor scintigraphy (PRS) and peptide receptor radionuclide therapy (PRRT) using radiolabeled sst analogs [1-3]. PRS and PRRT with several sst analogs has been particularly successful in patients with neuroendocrine tumors [2, 4]. Studies in which patients suffering from other sst expressing tumors, such as differentiated thyroid carcinoma [5], paraganglioma and meningioma [6] are treated with these analogs are currently performed.

Patients with glioblastoma multiforme (GBM) would especially benefit from PRRT treatment with radiolabeled peptides, since current treatment options for these patients are very limited. In addition, PRS with these peptides would enable the visualization and monitoring of these intracranial tumors. GBM is a very aggressive and invasive tumor type, which is known for its very low median survival rate of 12 months or less after initial diagnosis [7], despite conventional treatment with surgery, radiation therapy and chemotherapy. GBMs characteristically diffusely infiltrate cerebral tissue by individual tumor cells without forming clear tumor margins. PRRT might be an interesting additional treatment modality, since radiolabeled peptides directly target the receptor expressing tumor cells following systemic injection. In patients with a disrupted blood-brain-barrier (BBB), the radiolabeled and chelated peptide analogs can reach the tumor cells while these molecules will hardly penetrate the BBB in normal brain [8, 9]. As an alternative, radiolabeled peptides may be locally administered. Importantly, these small molecules can reach even distant tumor cells that have infiltrated in healthy brain tissue.

The purpose of this study was to identify peptide receptors expressed in GBM tumors. In order to select one or several peptide candidates for PRS and PRRT of GBM, the receptor expression status of these tissues should be established. In addition, the receptor expression in normal brain tissue was assessed to compare receptor expression between healthy and diseased tissue. We performed internalization studies in primary and established cell lines of human glioblastoma multiforme. Additionally, eight glioblastoma tissues, eleven meningioma tissues, four metastatic tumors to the brain and three normal brain tissues were investigated for gastrin-releasing peptide (GRP), neurokinine-1 (NK-1), somatostatin subtype 2 (sst_2), cholecystokinin-2 (CCK_2), vasoactive intestinal peptide (VIP), epidermal growth factor (EGF) and neurotensin (NT) receptor expression using *in vitro* autoradiography.

Materials and methods

Cell culture

Cells were cultured as previously described [10]. We used three cell lines derived from primary human glioblastomas (VU86, 01-12941 and 02-1189) and six established human glioblastoma cell lines (U251, U118MG, U87MG, T98G, U373 and SNB-19). U251, U118MG, T98G, U373 and SNB-19 were cultured in Dulbecco's modified Eagle's medium (DMEM, Gibco, Life Technologies, Breda, The Netherlands), U87MG in minimum essential medium (MEM) and the primary glioblastomas were cultured in RPMI-1640. Medium was supplemented with 10% heat-inactivated fetal bovine serum (Gibco) and cells were maintained in a 37°C, 5% CO_2 atmosphere.

Radiolabeled peptides

For internalization studies the following peptides were used: the somatostatin subtype 2 targeting analog [^{111}In-DOTA^0,Tyr^3]octreotate [11], the NK-1 targeting peptide ^{125}I-Substance P (Amersham/GE Healthcare, Eindhoven, The Netherlands), the $\alpha_v\beta_3$ targeting peptide [^{111}In-DTPA]RGD [12], the GRP targeting peptide [^{111}In-DTPA-Pro^1,Tyr^4]bombesin [13], the VIP receptor targeting analog [^{111}In-DTPA]VIP and the CCK_2 targeting peptide [^{111}In]MG11 [14].

For autoradiographic studies the following peptides were used: [^{111}In-DOTA^0,Tyr^3] octreotate, [^{111}In-DTPA-Pro^1,Tyr^4]bombesin, [^{125}I]Substance P, [^{111}In]MG11 and the CCK_2 targeting peptide [^{111}In]MP2288 [15], [^{125}I]EGF (Amersham/GE Healthcare), the neurotensin targeting analog [^{111}In]MP2530 [16] and [^{125}I]VIP (Amersham/GE Healthcare).

Except for the ^{125}I-labeled analogs, all peptide analogs were radiolabeled with ^{111}In as previously described [17].

Internalization studies

Internalization studies were performed as previously described [16]. Uptake and internalization of a radiolabeled peptide was used as an indication for receptor expression. U251, U118MG, U87MG, T98G, U373, SNB-19 and the primary human glioblastoma cells VU86, 01-12941 and 02-1189 were incubated in triplicate for one hour with 1 ml of incubation medium (RPMI-HEPES with 1% BSA) containing 40-80 kBq of radiolabeled peptide in a concentration of 1-5x10^{-10} M, with or without excess (1 µmol) of unlabeled corresponding peptide to test the receptor specificity (competition assay). Medium was removed and the cells were washed with ice-cold PBS. Surface bound activity was removed by incubation with 20 mM sodium acetate in PBS and the cells were then lysed with 0.1 M sodium hydroxide. Internalized and surface bound activity was counted and the sum is defined as the uptake, which is

expressed as percentage of the applied dose per milligram cellular protein (%D/mg protein). The specific uptake was calculated by subtracting the uptake of the competition assay from the uptake of the normal internalization. Biorad protein assay was used to determine the amount of cellular protein as previously described [16].

Tissue sections and in vitro autoradiography

Human glioblastoma (GBM) samples (n=8), human meningioma (MG) samples (n=11), samples (n=3) of brain metastases (MT, see table 1) and normal brain (NB) tissue samples (n=3) were obtained from the archive of frozen samples of the neuropathological division of the department of Pathology of the Erasmus MC, Rotterdam. Ten μm sections were cut (Microm Cryo-Star HM 560 M, Walldorf, Germany) and mounted on glass slides (Superfrost Plus, Menzelgläser, Germany).

Table 1: Metastatic brain tumors used in autoradiographic studies.

Case nr	Origin/Primary tumor
99-4611	Small cell lung cancer
97-3313	Unknown origin
99-27	Breast cancer

In vitro autoradiography was performed as previously described [18] using the above mentioned peptides. Displacement, to determine receptor specific binding, was achieved with 1 μmol/l of octreotide (Novartis, Basel, Switzerland), [Tyr^4]BN (Sigma-Aldrich, Zwijndrecht, The Netherlands), gastrin (Bachem, Bubendorf, Switzerland), neurotensin (Sigma-Aldrich), RGD (Bachem), EGF (Sigma-Aldrich), substance P (Sigma-Aldrich) and VIP (Bachem) and was performed in a separate experiment. Frozen sections (10 μm) were incubated for 1 h at room temperature with 0.1 nmol/l radiolabeled peptide (= 5-20 kBq/ml) in 167 mmol/l Tris (pH 7.6, supplemented with 5 mmol/l $MgCl_2$, 1% bovine serum albumin, and 40 mg/ml bacitracin). After incubation, the sections were washed, dried and exposed to phosphor imaging screens (Perkin Elmer, Boston, USA). The imaging screens were read using a Cyclone Storage Phosphor System (Perkin Elmer), and the autoradiograms were quantified using Optiquant Software (Perkin Elmer), by drawing a region of interest around each section. Radioactivity was expressed in digital light units per millimeter square (DLU/mm^2). A tissue was defined as receptor-positive when the measured DLU/mm^2 in the total binding section was at least twice as high compared to the non-specific binding section, as defined by Reubi et al. [19]. Mean receptor density values were only calculated from the receptor-positive tissues. The incidence was calculated as the percentage of positive tissues from the total number of samples included per tumor group.

Results

Internalization studies

Internalizations studies using primary GBM tumor cells resulted in an extremely low uptake of all peptide analogs in the primary brain tumor cells (figure 1A). On the contrary, the uptake of radiolabeled peptides in the established human GBM cell lines was relatively high (figure 1B). We found a high and specific uptake of Substance P in U251 and SNB-19, while the other GBM cell lines showed a low uptake of Substance P. In all cell lines uptake of the VIP peptide could be measured (4-13%D/mg protein, 100% incidence). Uptake of DTPA-RGD was found in U251 (11.6%D/mg protein, 16% incidence), and uptake of the GRP analog [^{111}In-DTPA-Pro^{1},Tyr^{4}] bombesin was found in U251, U118MG, U373 and SNB-19 (19.2, 4.9, 6.9 and 2.1%D/mg protein, respectively), leading to 66% incidence.

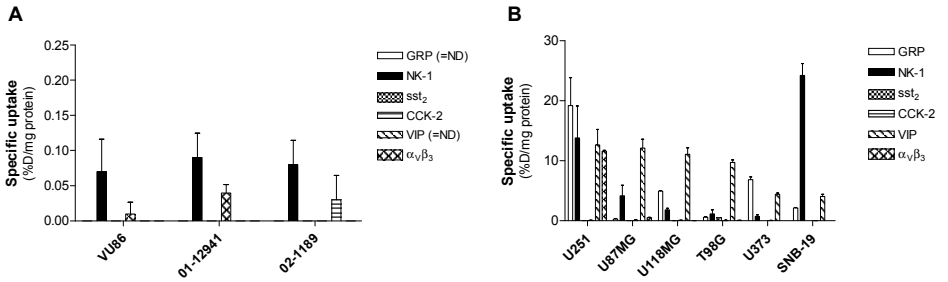

Figure 1: Specific uptake of radiolabelled peptides, as an indication for functional receptor expression in primary (A) and established GBM cell lines (B). Uptake was determined for the receptors of gastrin-releasing peptide (GRP), neurokinine-1 (NK-1), somatostatin subtype 2 (sst_2), cholecystokinin-2 (CCK_2), vasoactive intestinal peptide (VIP) and integrin $\alpha_v\beta_3$. Results are expressed as percentage dose/milligram cellular protein (%D/mg protein). Note the different scaling of the y-axis.

In vitro autoradiography

Figure 2 shows the results of the autoradiographic studies in human GBM, MG and MT tissues as well as of normal human brain tissues. Examples of autoradiographic images of these tissues after binding with several radiolabeled peptides are shown in figure 3.

Between 40 and 50 percent of the various intracranial tumors showed overexpression of the VIP receptor. Remarkably, no VIP receptor expression was found in NB tissues. Besides the VIP receptor, GBM tissues also overexpressed EGF and NK-1 receptors, in a rather high incidence of 75 and 63 percent, respectively (figures 2A and 3).

Our results showed that sst_2 expression was not detected in GBM tissues, however in 100% of the MGs a high sst_2 receptor density was found (figures 2B and 3). EGF

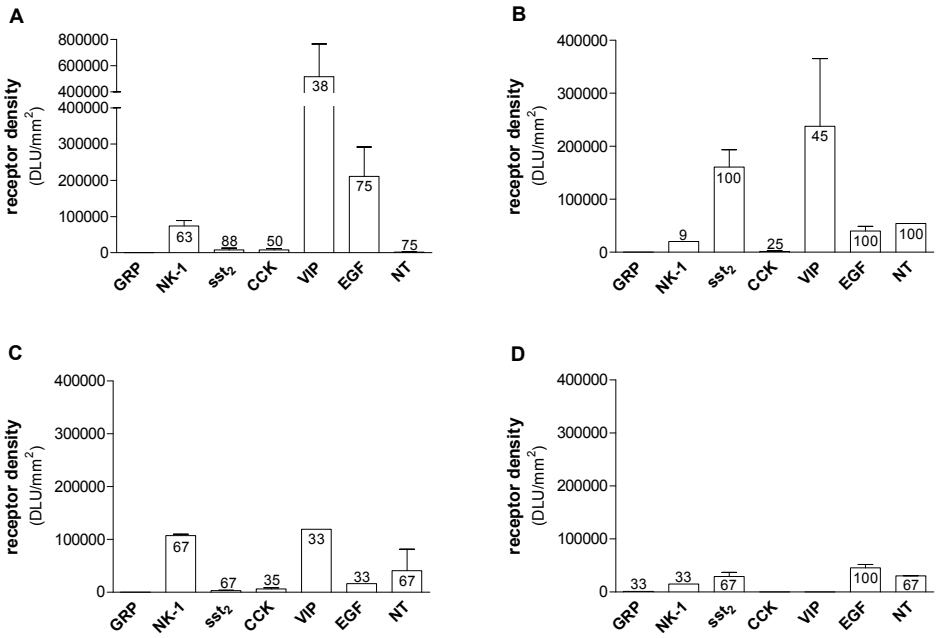

Figure 2: Results of autoradiography studies performed on (A) human glioblastoma (n=8), (B) meningioma (n=11), (C) metastases (n=3) and (D) normal brain (n=3) tissues. Expression was determined for the gastrin-releasing peptide receptor (GRP), neurokinin-1 receptor (NK-1), somatostatin receptor subtype 2 (sst_2), Cholecystokinin-2 receptor (CCK_2), vasoactive intestinal peptide receptor (VIP), epidermal growth factor receptor (EGF) and neurotensin receptor (NT). Numbers in the bars express the incidence (% receptor-positive of total tested tissues). The mean receptor density was calculated from the receptor-positive denoted tissues and was expressed as digital light units per millimeter square (DLU/mm^2). Note the aberrant y-axis scale in graph A.

and NT were expressed in high incidence but with rather low density in MG tissues. However these receptors were also expressed in NB (figures 2D and 3). Besides VIP expression on brain metastases, we also found a relatively high receptor density of NK-1 on these tissues (figures 2C and 3).

Discussion

In this pilot study the results of peptide receptor expression in human intracranial tumors are shown, and potential target receptors for PRS and PRRT in these tissues were detected. To the best of our knowledge, this is the first study determining a large number of peptide receptors in glioblastoma (GBM), meningioma (MG) and brain metastases (MT).

From the internalization studies in the established cell lines we can conclude that VIP, GRP and NK-1 are expressed with high incidences. However, we could

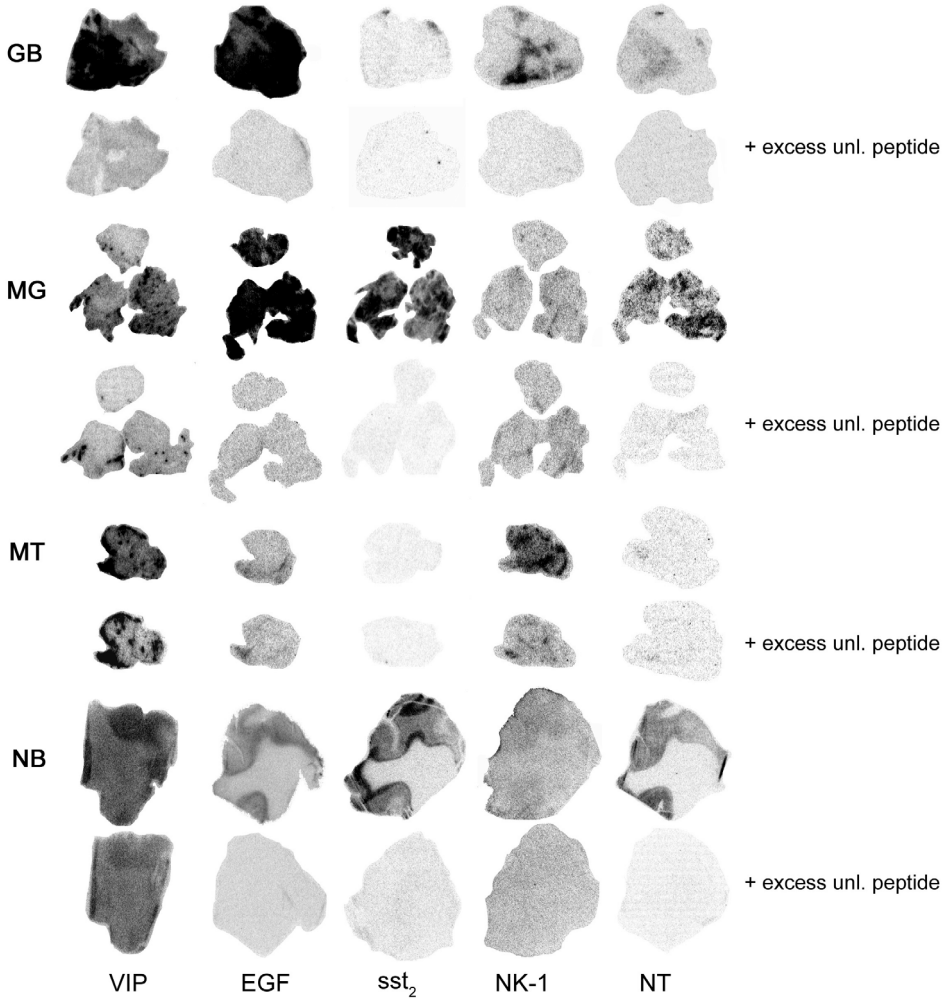

Figure 3: Examples of autoradiographic images of GB, MG, MT and NB tissues. The first row of images show binding of the radiolabeled peptide, while the second row of images show the displacement with an excess of their respective unlabelled receptor ligand.

not find any uptake of radiolabeled peptides in the primary cell lines. These results appeared not to be representative of the patient situation, which was demonstrated in the autoradiographic studies using pathological specimens from patients. In these studies, we found the following sequence in receptor expression density for GBM: VIP>EGF>NK-1>CCK>sst_2>NT>GRP; MG: VIP>sst_2>NT>EGF>NK-1>CCK>GRP; MT: NK-1>VIP>NT>EGF>CCK>sst_2>GRP; NB: EGF>NT>sst_2>NK-1>GRP>CCK/VIP. It appears that the VIP receptor is a highly interesting target for PRS and PRRT purposes in all human intracranial malignancies. We found a high receptor specific binding in GBM and MG tissues, while virtually no expression was found in normal brain tissue.

These findings confirm the results of studies on VIP expression in glioblastoma cell lines [20, 21], which we confirmed in these studies. Vertongen et al. showed that T98G human glioma cells express VIP receptors, mostly of the subtype 2 [20]. These authors also showed that VIP and PACAP incubation inhibits T98G cell proliferation. Sharma et al. described that a VIP receptor antagonist inhibits proliferation of several glioblastoma cells [21]. Although more investigations need to be performed, VIP as a candidate for scintigraphy and radionuclide therapy of brain tumors seems promising, provided that VIP receptor expression in normal tissues is low. We did not discriminate between the VPAC1 and VPAC2 receptors, the latter being rarely expressed in normal tissues unlike VPAC1 [8].

In addition to VIP, GBM can also be targeted with an EGF peptide analog or NK-1 binding peptide. Both EGF and NK-1 receptors are expressed at lower receptor densities than the VIP receptor but show a relatively high incidence. The up-regulation of EGF receptors in GBMs was also reported by other groups [22-25] and we were able to confirm this in a different set of human GBM samples. In addition, this study also includes a quantitative comparison of receptor expression in human GBMs. The effective use of EGF in brain tumors after systemic injection was questioned by Yang et al; since they found that only low amounts of this peptide passed the BBB into the tumor after systemic injection [26], probably due to the low transportation rate of EGF through the BBB [9]. EGF supposedly is transported across the BBB in brain tumors when it is conjugated to a BBB drug delivery system [9], making it an interesting target for scintigraphic and therapeutic purposes. Radiolabeled and BBB-passing EGF peptides were successfully used in an *in vivo* brain tumor model, in which it was shown that the unconjugated EGF did not penetrate the BBB [9].

From the present study and other studies in the literature it is clear that the NK-1 receptor is commonly overexpressed in glial neoplasms while NK-1 receptor expression in normal brain tissue is restricted to circumscribed areas [27]. Recently, Kneifel et al. reported on the targeted therapy with a NK-1 targeting substance P analog in patients with malignant gliomas [27]. In this study, patients were locally injected with DOTAGA-Substance P radiolabeled with either ^{90}Y, ^{213}Bi or ^{177}Lu and partial responses were observed in 4 out of 14 GBM cases. In addition, surgery after targeted therapy was found to be considerably facilitated due to a better demarcation of tumor margins as a result of radiation effects on the tumor.

We did not find evidence for high expression of GRP receptors, sst_2 receptors, CCK_2 receptors and NT receptors in these GBM tumors.

In our panel of MG tissues, however, we found 100% incidence of sst_2 expression with high receptor density, high density of VIP receptors in nearly half of the tested tissues and high incidence of EGF and NT receptor expression (both 100%), although with lower receptor density. Since sst_2 analogs are most widely used for PRS and

PRRT in a clinical setting, the use of these peptide analogs could be a good choice in these patients. In addition, MGs are extra-cerebral tumors without a functioning BBB while the sst_2 expressing regions of the normal brain are protected against sst_2 targeting peptides by the BBB. A sst_2-negative MG may well be targeted with one of the other above mentioned peptide analogs.

Several reports showed that the better differentiated gliomas expressed sst receptors while the poorly differentiated GBMs were usually free of these receptors [28, 29], and this was confirmed in the present study. Maini et al. reported that the uptake of radiolabeled octreotide varied among the sst positive central nervous system tumors: very intense uptake in meningioma, intermediate uptake in pituitary adenoma and low uptake in glioma [30]. Interestingly, Hennig et al. reported that the extent of sst expression was inversely correlated to that of the NK-1 receptors in glioblastomas, indicative for high NK-1 and low sst receptor expression in GBMs [31], also shown in this study.

We were unable to demonstrate high specific binding to CCK_2 receptors in the tumor tissues and in normal brain tissue. This correlates with the results reported by Reubi and co-workers, who showed that CCK_2/gastrin receptors were either not or rarely expressed in a number of tumor types, among which meningiomas and glioblastomas [32]. These results, however, did not overlap with the findings of Lefranc et al., who showed that 45% of the gliomas in their study expressed mRNA for CCK_2 receptors [33]. The discrepancy may indicate the unreliability of mRNA detection, and for that reason Reubi et al. recommended the use of a method that detects active proteins instead of mRNA [19]. In our study we used *in vitro* autoradiography for the determination of receptor expression in human tissues, as suggested by Reubi et al. [19]. We are currently testing various peptide receptor subtypes in a larger panel of tumor samples and try to relate results with glioma malignancy grade.

In conclusion, we found VIP receptor expression in virtually all brain neoplasms in addition to EGF and NK-1 binding in GBM, sst_2 binding in MG and NK-1 binding in tumors metastasized to the brain. Targeting the VIP, NK-1 and EGF receptors for scintigraphic and therapeutic purposes of GBM tumors might become increasingly interesting, provided that the radiolabeled peptides can pass the BBB in patients.

References

1. de Jong M., Kwekkeboom D., Valkema R. and Krenning E.P. Radiolabelled peptides for tumour therapy: current status and future directions. Plenary lecture at the EANM 2002. *Eur J Nucl Med Mol Imaging*, 2003 30(3): 463-469.
2. Kwekkeboom D.J., Mueller-Brand J., Paganelli G., Anthony L.B., Pauwels S., Kvols L.K., *et al.* Overview of results of peptide receptor radionuclide therapy with 3 radiolabeled somatostatin analogs. *J Nucl Med*, 2005 46 Suppl 1: 62S-66S.
3. Reubi J.C., Krenning E., Lamberts S.W. and Kvols L. Somatostatin receptors in malignant tissues. *J Steroid Biochem Mol Biol*, 1990 37(6): 1073-1077.
4. Virgolini I., Britton K., Buscombe J., Moncayo R., Paganelli G. and Riva P. In- and Y-DOTA-lanreotide: results and implications of the MAURITIUS trial. *Semin Nucl Med*, 2002 32(2): 148-155.
5. Teunissen J.J., Kwekkeboom D.J. and Krenning E.P. Staging and treatment of differentiated thyroid carcinoma with radiolabeled somatostatin analogs. *Trends Endocrinol Metab*, 2006 17(1): 19-25.
6. van Essen M., Krenning E.P., Kooij P.P., Bakker W.H., Feelders R.A., de Herder W.W., *et al.* Effects of therapy with [^{177}Lu-DOTA^{0},Tyr^{3}]octreotate in patients with paraganglioma, meningioma, small cell lung carcinoma, and melanoma. *J Nucl Med*, 2006 47(10): 1599-1606.
7. Surawicz T.S., Davis F., Freels S., Laws E.R., Jr. and Menck H.R. Brain tumor survival: results from the National Cancer Data Base. *J Neurooncol*, 1998 40(2): 151-160.
8. Reubi J.C., Macke H.R. and Krenning E.P. Candidates for peptide receptor radiotherapy today and in the future. *J Nucl Med*, 2005 46 Suppl 1: 67S-75S.
9. Kurihara A. and Pardridge W.M. Imaging brain tumors by targeting peptide radiopharmaceuticals through the blood-brain barrier. *Cancer Res*, 1999 59(24): 6159-6163.
10. de Leeuw B., Su M., ter Horst M., Iwata S., Rodijk M., Hoeben R.C., *et al.* Increased glia-specific transgene expression with glial fibrillary acidic protein promoters containing multiple enhancer elements. *J Neurosci Res*, 2006 83(5): 744-753.
11. Verwijnen S.M., Sillevis Smith P.A., Hoeben R.C., Rabelink M.J., Wiebe L., Curiel D.T., *et al.* Molecular imaging and treatment of malignant gliomas following adenoviral transfer of the herpes simplex virus-thymidine kinase gene and the somatostatin receptor subtype 2 gene. *Cancer Biother Radiopharm*, 2004 19(1): 111-120.
12. Capello A., Krenning E.P., Bernard B.F., Breeman W.A., van Hagen M.P. and de Jong M. Increased cell death after therapy with an Arg-Gly-Asp-linked somatostatin analog. *J Nucl Med*, 2004 45(10): 1716-1720.
13. de Visser M., Bernard H.F., Erion J.L., Schmidt M.A., Srinivasan A., Waser B., *et al.* Novel ^{111}In-labelled bombesin analogues for molecular imaging of prostate tumours. *Eur J Nucl Med Mol Imaging*, 2007.
14. Behe M. and Behr T.M. Cholecystokinin-B (CCK-B)/gastrin receptor targeting peptides for staging and therapy of medullary thyroid cancer and other CCK-B receptor expressing malignancies. *Biopolymers*, 2002 66(6): 399-418.
15. Reubi J.C., Waser B., Schaer J.C., Laederach U., Erion J., Srinivasan A., *et al.* Unsulfated DTPA- and DOTA-CCK analogs as specific high-affinity ligands for CCK-B receptor-expressing human and rat tissues *in vitro* and *in vivo*. *Eur J Nucl Med*, 1998 25(5): 481-490.
16. de Visser M., Janssen P.J., Srinivasan A., Reubi J.C., Waser B., Erion J.L., *et al.* Stabilised ^{111}In-labelled DTPA- and DOTA-conjugated neurotensin analogues for imaging and therapy of exocrine pancreatic cancer. *Eur J Nucl Med Mol Imaging*, 2003 30(8): 1134-1139.
17. Breeman W.A., De Jong M., Visser T.J., Erion J.L. and Krenning E.P. Optimising conditions for radiolabelling of DOTA-peptides with ^{90}Y, ^{111}In and ^{177}Lu at high specific activities. *Eur J Nucl Med Mol Imaging*, 2003 30(6): 917-920.

18. de Visser M., van Weerden W.M., de Ridder C.M., Reneman S., Melis M., Krenning E.P., *et al.* Androgen-dependent expression of the gastrin-releasing Peptide receptor in human prostate tumor xenografts. *J Nucl Med*, 2007 48(1): 88-93.
19. Reubi J.C. and Waser B. Concomitant expression of several peptide receptors in neuroendocrine tumours: molecular basis for *in vivo* multireceptor tumour targeting. *Eur J Nucl Med Mol Imaging*, 2003 30(5): 781-793.
20. Vertongen P., Camby I., Darro F., Kiss R. and Robberecht P. VIP and pituitary adenylate cyclase activating polypeptide (PACAP) have an antiproliferative effect on the T98G human glioblastoma cell line through interaction with VIP2 receptor. *Neuropeptides*, 1996 30(5): 491-496.
21. Sharma A., Walters J., Gozes Y., Fridkin M., Brenneman D., Gozes I., *et al.* A vasoactive intestinal peptide antagonist inhibits the growth of glioblastoma cells. *J Mol Neurosci*, 2001 17(3): 331-339.
22. Kurihara M., Tokunaga Y., Ochi A., Kawaguchi T., Tsutsumi K., Shigematsu K., *et al.* [Expression of insulin-like growth factor I receptors in human brain tumors: comparison with epidermal growth factor receptor by using quantitative autoradiography]. *No To Shinkei*, 1989 41(7): 719-725.
23. Eppenberger U. and Mueller H. Growth factor receptors and their ligands. *J Neurooncol*, 1994 22(3): 249-254.
24. Libermann T.A., Nusbaum H.R., Razon N., Kris R., Lax I., Soreq H., *et al.* Amplification, enhanced expression and possible rearrangement of EGF receptor gene in primary human brain tumours of glial origin. *Nature*, 1985 313(5998): 144-147.
25. Wong A.J., Bigner S.H., Bigner D.D., Kinzler K.W., Hamilton S.R. and Vogelstein B. Increased expression of the epidermal growth factor receptor gene in malignant gliomas is invariably associated with gene amplification. *Proc Natl Acad Sci U S A*, 1987 84(19): 6899-6903.
26. Yang W., Barth R.F., Leveille R., Adams D.M., Ciesielski M., Fenstermaker R.A., *et al.* Evaluation of systemically administered radiolabeled epidermal growth factor as a brain tumor targeting agent. *J Neurooncol*, 2001 55(1): 19-28.
27. Kneifel S., Cordier D., Good S., Ionescu M.C., Ghaffari A., Hofer S., *et al.* Local targeting of malignant gliomas by the diffusible peptidic vector 1,4,7,10-tetraazacyclododecane-1-glutaric acid-4,7,10-triacetic acid-substance p. *Clin Cancer Res*, 2006 12(12): 3843-3850.
28. Reubi J.C., Lang W., Maurer R., Koper J.W. and Lamberts S.W. Distribution and biochemical characterization of somatostatin receptors in tumors of the human central nervous system. *Cancer Res*, 1987 47(21): 5758-5764.
29. Lamszus K., Meyerhof W. and Westphal M. Somatostatin and somatostatin receptors in the diagnosis and treatment of gliomas. *J Neurooncol*, 1997 35(3): 353-364.
30. Maini C.L., Sciuto R., Tofani A., Ferraironi A., Carapella C.M., Occhipinti E., *et al.* Somatostatin receptor imaging in CNS tumours using ^{111}In-octreotide. *Nucl Med Commun*, 1995 16(9): 756-766.
31. Hennig I.M., Laissue J.A., Horisberger U. and Reubi J.C. Substance-P receptors in human primary neoplasms: tumoral and vascular localization. *Int J Cancer*, 1995 61(6): 786-792.
32. Reubi J.C., Schaer J.C. and Waser B. Cholecystokinin(CCK)-A and CCK-B/gastrin receptors in human tumors. *Cancer Res*, 1997 57(7): 1377-1386.
33. Lefranc F., Chaboteaux C., Belot N., Brotchi J., Salmon I. and Kiss R. Determination of RNA expression for cholecystokinin/gastrin receptors (CCKA, CCKB and CCKC) in human tumors of the central and peripheral nervous system. *Int J Oncol*, 2003 22(1): 213-219.

3.2 Oral versus intravenous administration of lysine: equal effectiveness in reduction of renal uptake of [^{111}In-DTPA^{0}]octreotide

S. M. Verwijnen, E.P. Krenning, R. Valkema, J.G.M. Huijmans, M. de Jong.

Journal of Nuclear Medicine, 2005; 46: 2057-2060

Abstract

Aim: During tumor therapy with radiolabeled somatostatin analogs, the kidneys are dose limiting. Renal uptake in patients can effectively be reduced by a 4- to 10-h intravenous infusion of a lysine/arginine solution, thereby increasing the maximum radiation dose to the tumor without renal side effects. Oral administration of amino acids could facilitate this labor-intensive procedure. Therefore, the effects of oral versus intravenous administration of D-lysine were compared in rats injected with [^{111}In-diethylenetriaminepentaacetic acid (DTPA^0)]octreotide.

Methods: Rats were intravenously injected with 3 MBq/0.5 μg [^{111}In-DTPA^0]octreotide and also received D-lysine intravenously or orally in various concentrations and following various time schedules. Twenty-four hours after injection, a biodistribution study and renal *ex vivo* autoradiography were performed.

Results: Renal uptake was reduced significantly—up to 40%—in all lysine-treated groups, without affecting the uptake in other organs.

Conclusion: Renal uptake of this radiolabeled peptide can be reduced up to 40% both by oral and by intravenous administration of lysine in rats.

Introduction

For years, stabilized somatostatin analogs have been used successfully in the clinic for peptide receptor scintigraphy of neuroendocrine tumors [1, 2]. These tumors overexpress somatostatin subtype 2 receptors on their cell membrane, to which somatostatin analogs (e.g., [diethylenetriaminepentaacetic acid ($DTPA^0$)]octreotide and [1,4,7,10-tetraazacyclododecane- *N',N'',N''',N''''*-tetraacetic acid ($DOTA^0$),Tyr^3] octreotate) bind with high affinity. [$DTPA^0$]octreotide also binds to somatostatin subtype 3 and somatostatin subtype 5 receptors, albeit with much lower affinity [3]. Somatostatin analogs radiolabeled with therapeutic radionuclides, such as ^{177}Lu and ^{90}Y, are being used for peptide receptor radionuclide therapy (PRRT). This new form of targeted therapy has proven to be promising in preclinical and clinical studies [4-6]. Other radiolabeled peptides frequently used in PRRT are [^{177}Lu $DOTA^0$,Tyr^3] octreotate [4], [^{90}Y-$DTPA^0$,Tyr^3]octreotide [3, 6], and ^{90}Y-lanreotide [4]. The results of these studies show high tumor response rates in patients.

However, the drawback of PRRT could be the total administered radioactivity to patients, which is limited by critical organs, such as the kidneys [3, 7-9]. The kidneys reabsorb part of the radiolabeled peptides in the proximal tubules after glomerular filtration [10]. The peptide itself is degraded in the lysosomes of these cells, whereas the radionuclide–chelator complex is trapped inside the proximal tubular cells [9, 10]. A high dose to the kidneys could lead to nephrotoxicity, which in turn could lead to kidney failure [9] When this high renal radiation dose can be reduced, a higher dose to the tumor can be given, possibly leading to a higher success rate for PRRT.

Several researchers have shown that intravenous co-administration of lysine to rats results in a 40%–50% reduction of renal uptake of these radiolabeled peptides [11-13]. In the clinic, the reduction of radioactivity in the kidneys is achieved by an infusion of lysine/arginine over a longer time [5, 9, 14-16]. Radiolabeled somatostatin analogs are positively charged, favoring binding to negatively charged proximal tubular cells. Lysine and arginine are also positively charged and can, at high-enough concentrations, partly inhibit the renal reabsorption of somatostatin analogs. Recently, our group has shown that megalin is involved in the renal retention of these analogs and that new strategies can be developed to further decrease renal uptake [17].

It is preferred that lysine/arginine infusions in the clinic take place over 10 h [16]; however, in practice most infusions are given in 4 h or less. Instead of this labor-intensive infusion method, a repeated oral administration of lysine/arginine solution could be more convenient both for the patients and for the hospital staff. Therefore, the aim of this work was to compare, in a rat model, oral versus intravenous administration of lysine with regard to reduction of renal uptake of [^{111}In-$DTPA^0$]octreotide.

Materials and methods

[^{111}In-DTPA^{0}]octreotide preparation

Commercially available kits of [DTPA^{0}]octreotide and $^{111}InCl_3$ were obtained from Tyco Health Care. The radiolabeling procedure was in accordance with standard procedures and previously published work [18].

Tissue distribution of [^{111}In-DTPA^{0}]octreotide in rats

Animal experiments were performed in compliance with the regulations of our institution and with generally accepted guidelines governing such work.

Adult male Lewis rats (Harlan) weighing 250–300 g were used for these experiments. All experimental groups are described in table 1. D-lysine (Sigma-Aldrich) was diluted to a concentration of 400 mg/ml in saline. Groups that were treated with D-lysine received a dose of 400 or 800 mg/kg of this solution.

At t = 0, [^{111}In-DTPA^{0}]octreotide (3 MBq; 0.5 µg of peptide) was administered to all rats intravenously into the dorsal vein of the penis. The control group had no D-lysine administered. The intravenous group received 400 mg/kg coinjected with the radiolabeled peptide. To the groups receiving D-lysine orally (using an oral needle), 400 mg/kg were administered 30, 60, or 120 min before the radiolabeled peptide. An additional group had food withheld for 6–8 h before receiving a 400 mg/kg oral dose of D-lysine 30 min before the peptide. A final group received an 800 mg/kg oral dose of D-lysine 30 min before the peptide.

Twenty-four hours after injection of [^{111}In-DTPA^{0}]octreotide, the following tissues were isolated: spleen, pancreas, adrenals, liver, stomach, muscle, femur, and one kidney. Radioactivity was measured in blood samples and in these isolated organs using a γ-counter (Wallac 1480 Wizard 3"; Perkin Elmer). The second kidney was immediately frozen using isopentane (Fluka Chemika) and liquid nitrogen and stored in a -80°C freezer, until processed for *ex vivo* autoradiography.

Table 1: Description of experimental groups. All rats received intravenous injection of [^{111}In-DTPA^{0}] octreotide

Group	n
Control	13
D-lysine, 400 mg/kg, intravenous, t=0 (co-injected with tracer)	12
D-lysine, 400 mg/kg, oral, t= -30 min, no food	10
D-lysine, 400 mg/kg, oral, t= -30 min	10
D-lysine, 800 mg/kg, oral, t= -30 min	10
D-lysine, 400 mg/kg, oral, t= -60 min	10
D-lysine, 400 mg/kg, oral, t= -120 min	7

Ex vivo autoradiography

Frozen tissues were embedded in TissueTek (Sakura) and processed for cryosectioning. Tissue sections of 10 µm were mounted on SuperFrostPlus glass slides (Menzel) and exposed to phosphor imaging screens (Perkin Elmer) overnight in x-ray cassettes (Kodak). The screens were analyzed using a Cyclone phosphor imager and a computer-assisted OptiQuant 03.00 image-processing system (Perkin Elmer). Thereafter, an adjacent tissue section was stained with conventional hematoxylin and eosin.

Statistical analysis

Data are expressed as mean ± SEM. Results were statistically analyzed using one-way ANOVA. Differences were considered statistically significant when P was <0.05. If significance was found, a Dunnett multiple-comparison test was performed to compare all groups with the control group. All statistical analyses were performed with the Prism 4.0 program (GraphPad).

Results

[^{111}In-DTPA]octreotide preparation

The labeling efficiency of [^{111}In-DTPA^{0}]octreotide was determined with instant thin-layer chromatography and was >95%.

Tissue distribution of [^{111}In-DTPA^{0}]octreotide in rats

Figure 1 shows the results for the tissue distribution of [^{111}In-DTPA^{0}]octreotide in blood and several somatostatin receptor–positive organs, such as pancreas and adrenals. No differences in these organs were seen between any treatment group and the control group. Slightly higher uptake in the adrenals was seen in the intravenous group and in the oral group from which food had been withheld; however, this increase was not statistically significant.

The uptake in the kidneys and the percentage reduction in kidney uptake are shown in figure 2. All treatments resulted in a lower renal uptake than that of the control group. A renal reduction of about 41% (39%–43%) was seen in the intravenous group, in the group that received 800 mg/kg orally, and in the group that received 400 mg/kg orally 60 min before the peptide. These results were confirmed by the *ex vivo* autoradiography data (fig. 3).

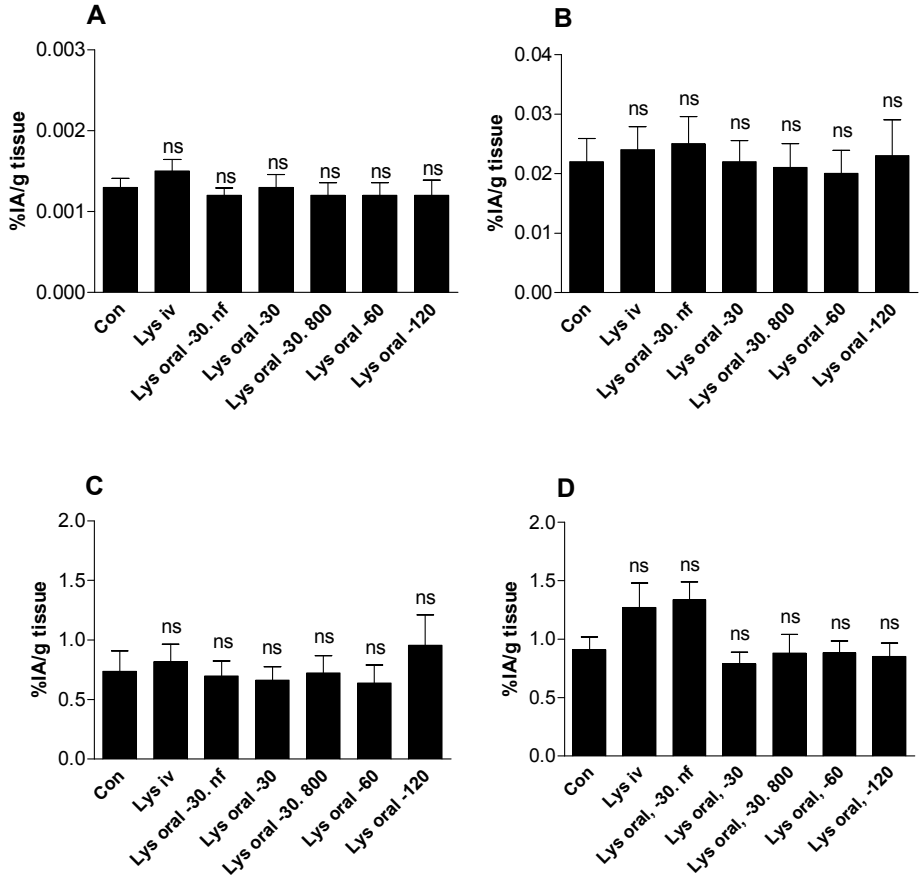

Figure 1: Radioactivity of [^{111}In-DTPA^{0}]octreotide in blood (A), spleen (B), and 2 somatostatin subtype 2 receptor–positive organs (pancreas (C) and adrenals (D)) 24 h after injection of peptide, 3 MBq/0.5 µg. Data are expressed as percentage injected activity (%IA) per gram of tissue (mean ± SEM). Statistical analysis showed no significance (ns) between control bar and any other bar. con = control; iv = intravenous; Lys = D-lysine; nf = no food.

Ex vivo autoradiography

Autoradiograms of the control group and 3 experimental groups are shown in figure 3. Histologic examination of hematoxylin- and eosin-stained sections adjacent to the autoradiography sections showed that radioactivity was taken up only in the cortex and outer medulla of the renal tissue.

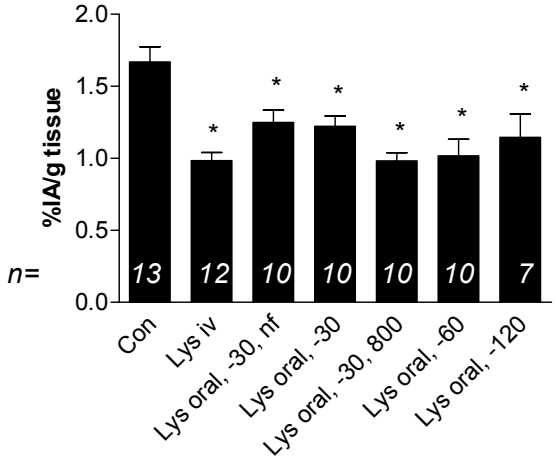

Treatment group	% reduction
Control	-
Lys iv	42.6 ± 8.9
Lys oral, -30, nf	30.8 ± 19.5
Lys oral, -30	31.2 ± 12.6
Lys oral, -30, 800	39.3 ± 11.9
Lys oral, -60	41.1 ± 9.9
Lys oral, -120	35.4 ± 12.0

Figure 2: Uptake of [^{111}In-DTPA^{0}]octreotide in kidney 24 h after injection of peptide, 3 MBq/0.5 µg, to all treatment groups. Data are expressed as percentage injected activity (%IA) per gram of tissue (mean ± SEM). Statistical analysis showed significant difference ($P < 0.01$) between control bar and each other treatment group. Also, percentage reduction of each treatment group is shown in adjacent table. Oral administration of lysine 30 min (800 mg/kg) or 60 min (400 mg/kg) before tracer produced renal reduction similar to that with intravenous administration. con = control; iv = intravenous; Lys = D-lysine; nf = no food.

Discussion

In PRRT, the kidneys are the dose-limiting organ because of retention of radioactivity in the proximal tubules of the renal cortex [10]. Based on external-beam radiation therapy data, an absorbed radiation dose to the kidneys of 23 Gy may lead to renal failure within 5 years in 5% of the patients. Therefore, the radiation dose limit to the kidneys in the various PRRT studies is mostly 23–27 Gy. By coinfusion of positively charged amino acids, such as lysine and arginine, the achieved radiation dose to the tumor can be higher without damaging the kidneys because of reduction of renal radioactivity [14]. These infusions of an amino acid solution should take place over a 10-h period [16]. Mostly, they are given within 4 h [14, 15, 19] because the procedure is highly labor-intensive. Repeated oral administration of lysine/arginine would be more convenient for patients and hospital staff. We therefore investigated the effect

of oral administration versus systemic administration of lysine on renal uptake of [^{111}In-DTPA^{0}]octreotide in a rat model.

In this study, we administered D-lysine, 400 and 800 mg/kg, intravenously and orally. The maximum tolerated dose of this amino acid in mice is approximately 1.4-fold higher than the maximum tolerated dose of L-lysine [20] and could therefore safely be used in this study. Previous studies showed that D-lysine, 400 mg/kg, intravenously injected in rats led to about a 40% reduction in renal uptake [12, 21] and that lysine/arginine combinations could not further the reduction of renal uptake in these rats (unpublished data). This study also confirmed this 40% renal reduction by comparing the control group and the intravenous group. Furthermore, this study showed that uptake of [^{111}In-DTPA^{0}]octreotide in blood, spleen, pancreas, and adrenals was not significantly affected in rats treated orally with D-lysine, in comparison with those treated intravenously; however, renal uptake was reduced in all treated groups. The group that received 800 mg/kg orally and the group that

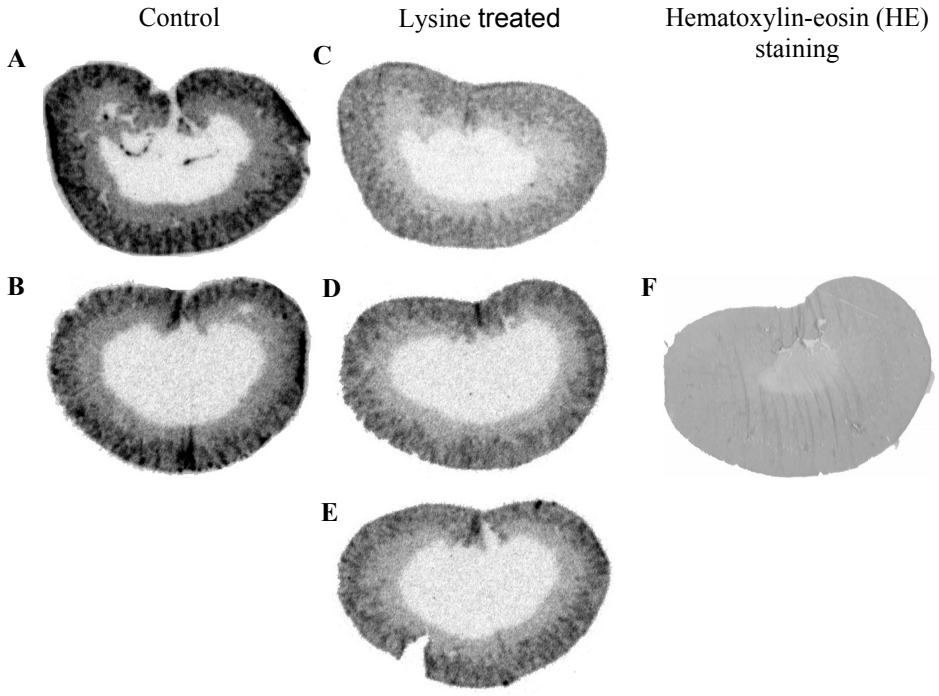

Figure 3: *Ex vivo* autoradiograms of renal tissue slices of control rats (A and B) and lysine-treated rats (C–E) 24 h after injection of [^{111}In-DTPA^{0}]octreotide, 3 MBq/ 0.5 µg. Greatest reduction of renal radioactivity was seen in rats treated with intravenous lysine coinjected with tracer (C) or lysine (400 mg/kg) orally 60 min before tracer (D). Increasing the interval between oral lysine (400 mg/kg) and tracer to 120 min (E) did not lead to greater renal reduction. (F) Hematoxylin- and eosin stained section adjacent to D shows high uptake of radioactivity in cortex and outer medulla but almost no uptake in inner medulla.
For color figure see page 244.

received 400 mg/kg orally 60 min before the peptide showed a reduction of renal uptake comparable with that in intravenously treated rats. These results are confirmed by the *ex vivo* autoradiography images shown in figure 3. The autoradiography data together with the hematoxylin- and eosin-stained sections showed that radioactivity was taken up only in the cortex and the outer medulla and that the reduction by lysine was therefore only in these sections of the kidney.

The group of Behr et al. [20] showed that lysine can effectively be used to reduce uptake of radioactivity in the kidneys when radiolabeled antibodies are applied and that this effect is not restricted to indium-labeled compounds. This group also showed that oral administration of L-lysine was as effective as intravenous administration at reducing renal uptake of these antibodies [20].

Several authors have reported that patients experienced nausea and vomiting when amino acids were infused [13, 15, 16, 22]. This adverse effect was related to the large amount of amino acids infused, the hyperosmolarity of the solution administered, and the rate of infusion [13].

Jamar et al. showed that infusion of amino acids over a period of up to 10 h could lead to a greater rate of reduction of renal uptake in patients [16] and that a large amount of amino acids could be given with relatively limited adverse effects [22]. When an amino acid solution is administered orally, ingestion over a longer time can be realized more easily and, therefore, a greater renal reduction might be achieved.

Conclusion

The standard intravenous and oral methods of administering D-lysine equally reduce renal uptake of [^{111}In-DTPA^{0}]octreotide in rats, with the oral administration preferably occurring 30–60 min before injection of the tracer. These results could offer a new clinical application for amino acid infusions before and during PRRT. The next step is to test this possibility in a clinical setting.

References

1. Reubi J.C. Peptide receptors as molecular targets for cancer diagnosis and therapy. *Endocr Rev*, 2003 24(4): 389-427.
2. Krenning E.P., Kwekkeboom D.J., Bakker W.H., Breeman W.A., Kooij P.P., Oei H.Y., *et al.* Somatostatin receptor scintigraphy with [^{111}In-DTPA-D-Phe^{1}]- and [^{123}I-Tyr^{3}]-octreotide: the Rotterdam experience with more than 1000 patients. *Eur J Nucl Med*, 1993 20(8): 716-731.
3. Paganelli G., Zoboli S., Cremonesi M., Macke H.R. and Chinol M. Receptor-mediated radionuclide therapy with ^{90}Y-DOTA-D-Phe^{1}-Tyr^{3}-Octreotide: preliminary report in cancer patients. *Cancer Biother Radiopharm*, 1999 14(6): 477-483.
4. Kwekkeboom D.J., Bakker W.H., Kam B.L., Teunissen J.J., Kooij P.P., de Herder W.W., *et al.* Treatment of patients with gastro-entero-pancreatic (GEP) tumours with the novel radiolabelled somatostatin analogue [^{177}Lu-DOTA^{0},Tyr^{3}]octreotate. *Eur J Nucl Med Mol Imaging*, 2003 30(3): 417-422.
5. de Jong M., Kwekkeboom D., Valkema R. and Krenning E.P. Radiolabelled peptides for tumour therapy: current status and future directions. Plenary lecture at the EANM 2002. *Eur J Nucl Med Mol Imaging*, 2003 30(3): 463-469.
6. Waldherr C., Pless M., Maecke H.R., Schumacher T., Crazzolara A., Nitzsche E.U., *et al.* Tumor response and clinical benefit in neuroendocrine tumors after 7.4 GBq ^{90}Y-DOTATOC. *J Nucl Med*, 2002 43(5): 610-616.
7. Otte A., Herrmann R., Heppeler A., Behe M., Jermann E., Powell P., *et al.* Yttrium-90 DOTATOC: first clinical results. *Eur J Nucl Med*, 1999 26(11): 1439-1447.
8. Waldherr C., Pless M., Maecke H.R., Haldemann A. and Mueller-Brand J. The clinical value of [^{90}Y-DOTA]-D-Phe^{1}-Tyr^{3}-octreotide (^{90}Y-DOTATOC) in the treatment of neuroendocrine tumours: a clinical phase II study. *Ann Oncol*, 2001 12(7): 941-945.
9. Lambert B., Cybulla M., Weiner S.M., Van De Wiele C., Ham H., Dierckx R.A., *et al.* Renal toxicity after radionuclide therapy. *Radiat Res*, 2004 161(5): 607-611.
10. De Jong M., Valkema R., Van Gameren A., Van Boven H., Bex A., Van De Weyer E.P., *et al.* Inhomogeneous localization of radioactivity in the human kidney after injection of [^{111}In-DTPA^{0}]octreotide. *J Nucl Med*, 2004 45(7): 1168-1171.
11. de Jong M., Breeman W.A., Bernard B.F., Rolleman E.J., Hofland L.J., Visser T.J., *et al.* Evaluation *in vitro* and in rats of ^{161}Tb-DTPA-octreotide, a somatostatin analogue with potential for intraoperative scanning and radiotherapy. *Eur J Nucl Med*, 1995 22(7): 608-616.
12. Bernard B.F., Krenning E.P., Breeman W.A., Rolleman E.J., Bakker W.H., Visser T.J., *et al.* D-lysine reduction of indium-111 octreotide and yttrium-90 octreotide renal uptake. *J Nucl Med*, 1997 38(12): 1929-1933.
13. Rolleman E.J., Valkema R., de Jong M., Kooij P.P. and Krenning E.P. Safe and effective inhibition of renal uptake of radiolabelled octreotide by a combination of lysine and arginine. *Eur J Nucl Med Mol Imaging*, 2003 30(1): 9-15.
14. Hammond P.J., Wade A.F., Gwilliam M.E., Peters A.M., Myers M.J., Gilbey S.G., *et al.* Amino acid infusion blocks renal tubular uptake of an indium-labelled somatostatin analogue. *Br J Cancer*, 1993 67(6): 1437-1439.
15. Bodei L., Cremonesi M., Zoboli S., Grana C., Bartolomei M., Rocca P., *et al.* Receptor-mediated radionuclide therapy with ^{90}Y-DOTATOC in association with amino acid infusion: a phase I study. *Eur J Nucl Med Mol Imaging*, 2003 30(2): 207-216.
16. Jamar F., Barone R., Mathieu I., Walrand S., Labar D., Carlier P., *et al.* ^{86}Y-DOTA^{0}-D-Phe^{1}-Tyr^{3}-octreotide (SMT487)--a phase 1 clinical study: pharmacokinetics, biodistribution and renal protective effect of different regimens of amino acid co-infusion. *Eur J Nucl Med Mol Imaging*, 2003 30(4): 510-518.

17. Melis M., Krenning E.P., Bernard B.F., Barone R., Visser T.J. and de Jong M. Localisation and mechanism of renal retention of radiolabelled somatostatin analogues. *Eur J Nucl Med Mol Imaging*, 2005.
18. Bakker W.H., Krenning E.P., Breeman W.A., Kooij P.P., Reubi J.C., Koper J.W., *et al. In vivo* use of a radioiodinated somatostatin analogue: dynamics, metabolism, and binding to somatostatin receptor-positive tumors in man. *J Nucl Med*, 1991 32(6): 1184-1189.
19. Valkema R., Pauwels S.A., Kvols L.K., Kwekkeboom D.J., Jamar F., de Jong M., *et al.* Long-Term Follow-Up of Renal Function After Peptide Receptor Radiation Therapy with ^{90}Y-DOTA^{0},Tyr^{3}-Octreotide and ^{177}Lu-DOTA^{0},Tyr^{3}-Octreotate. *J Nucl Med*, 2005 46(1 Suppl): 83S-91S.
20. Behr T.M., Becker W.S., Sharkey R.M., Juweid M.E., Dunn R.M., Bair H.J., *et al.* Reduction of renal uptake of monoclonal antibody fragments by amino acid infusion. *J Nucl Med*, 1996 37(5): 829-833.
21. de Jong M., Breeman W.A., Bernard B.F., Bakker W.H., Schaar M., van Gameren A., *et al.* [^{177}Lu-DOTA^{0},Tyr^{3}] octreotate for somatostatin receptor-targeted radionuclide therapy. *Int J Cancer*, 2001 92(5): 628-633.
22. Barone R., Pauwels S., De Camps J., Krenning E.P., Kvols L.K., Smith M.C., *et al.* Metabolic effects of amino acid solutions infused for renal protection during therapy with radiolabelled somatostatin analogues. *Nephrol Dial Transplant*, 2004 19(9): 2275-2281.

4

Radiation sensitivity of pancreatic tumor cells *in vitro*

4.1

Low dose rate irradiation by ^{131}I versus high dose rate external beam irradiation in the rat pancreatic tumor cell line CA20948

S.M. Verwijnen, A. Capello, H.F. Bernard, G.J.M.J. van den Aardweg, M.W. Konijnenberg, W.A.P. Breeman, E.P. Krenning, M. de Jong.

Cancer Biotherapy and Radiopharmaceuticals, 2004; 19(3), 285-292.

Abstract

Aim: The rat pancreatic CA20948 tumor cell line is widely used in receptor-targeted preclinical studies because many different peptide receptors are expressed on the cell membrane. The response of the tumor cells to peptide radionuclide therapy, however, is dependent on the cell line's radiosensitivity. Therefore, we measured the radiosensitivity of the CA20948 tumor cells by using clonogenic survival assays after high-energy external-beam radiotherapy (XRT*) in vitro*. It can, however, be expected that results of high-dose-rate XRT are not representative for those after low-dose-rate radionuclide therapy (RT), such as peptide-receptor radionuclide therapy. Therefore, we compared clonogenic survival *in vitro* in CA20948 tumor cells after increasing doses of XRT or RT, the latter using ^{131}I.

Methods: Survival of CA20948 cells was investigated using a clonogenic survival assay after RT by incubation with increasing amounts of ^{131}I, leading to doses of 1–10 Gy after 12 days of incubation (maximum dose rate, 0.92 mGy/min), or with doses of 1–10 Gy using an X-ray machine (dose rate, 0.66 Gy/min). Colonies were scored after a 12-day–incubation period. Also, the doubling time of this cell line was calculated.

Results: We observed a dose-dependent reduction in tumor-cell survival, which, at low doses, was similar for XRT and RT. For high-dose-rate XRT, the quadratic over linear component ratio (α/β) for CA20948 was 8.3 Gy, whereas that ratio for low-dose-rate RT was calculated to be 113 Gy. The calculated doubling time of CA20948 cells was 22 hours.

Conclusions: Despite the huge differences in dose rate, RT tumor cell–killing effects were approximately as effective as those of XRT at doses of 1 and 2 Gy, the latter being the common daily dose given in fractionated external-beam therapies. At higher doses, RT was less effective than XRT.

Introduction

Receptor-targeting peptides have been developed into a new generation of therapeutic radiopharmaceuticals. Peptide-receptor radionuclide therapy (PRRT) can be performed using these peptide analogs radiolabeled with therapeutic radionuclides, such as low linear energy transfer (LET) beta-particle emitters ^{177}Lu and ^{90}Y (1). This new application of peptide analogs—somatostatin analogs being the most commonly used—have shown to be most promising in preclinical studies (2) and in clinical patient treatment (3, 4).

However, until now, the emphasis of PRRT has been on efficacy in clinical and preclinical studies, and less consideration has been placed on the effect of radioactivity at the cellular level and to radiobiology in radionuclide therapy. Extrapolations have most often been made from external beam radiation effects, despite differences in the nature of the radiation—especially in the dose rate and irradiation period. These factors, as well as cell-growth kinetics, are important determinants of tumor-cell survival. They emphasize the need for further research on the effects, at the cellular level, of low-dose-rate irradiation over long periods delivered. We wanted to make a comparison between radionuclide therapy (RT) (without peptides) and external-beam radiotherapy (XRT) in CA20948 cells to establish the intrinsic radiosensitivity.

The authors and other colleagues have shown that the rat pancreatic tumor cell line CA20948 can be used as *in vitro* and *in vivo* models for research of different radiolabeled peptides for imaging and therapy (1, 5-12). This cell line expresses different kinds of high-affinity peptide receptors, such as somatostatin receptors, and also CCK/gastrin, NK-1, gastrin-releasing peptide (GRP) and $\alpha_v\beta_3$ receptors (5-9, 12-19). Therefore, this cell line is very interesting for testing newly developed peptide analogs and the effects of PRRT using these analogs.

For radiation-based therapy, tumor cure depends on several factors, such as the radiation dose absorbed in the tumor including the pattern of delivery (dose rate, fractionation), the number of clonogenic tumor cells that have to be sterilized in order to kill the tumor, and the response of the tumor cells to radiation, dependent on radiosensitivity and proliferation rate. We wanted to establish the intrinsic radiosensitivity of the CA20948 to interpret our *in vitro* and *in vivo* PRRT results. Therefore, we performed XRT therapy in a clonogenic survival assay to obtain radiation dose-survival curves, where clonogenicity is the ability of a tumor cell to undergo viable division and to proliferate. For many cell lines and for low LET irradiation, the logarithmic function of the survival fraction is characterized by an initial low-dose region starting with a shallow slope and followed by a shoulder region, and then an exponential survival decrease. This can be approximated by a linear-quadratic function of the dose, which is described in the linear-quadratic model (20); the cellular

survival (S) is in relation to the dose (D) as: Ln S = -(αD + βD^2). In this equation, the α and β parameters refer to different categories of lesions, namely lethal (α) versus repairable sublethal damage (β). The linear character of the model stems from the idea that a single hit can cause a lethal event. The α-component is indicative for the intrinsic radiosensitivity of the cells. The quadratic components stem from the idea that two hits on a single target are required for cell death. Close proximity of these two lesions can cause lethality, while further apart the lesions remain sublethal and repairable. The β-component is an estimate for the capacity of repairable damage. The α/β ratio is the dose where cell death is caused equally by irreparable and reparable lesions. For RT in our cell line, a different curve is expected than for XRT because of the difference in dose rate compared to XRT. The aim of our experiments was to further characterize the CA20948 rat pancreatic tumor cell line by comparing clonogenic survival and radiosensitivity *in vitro* using XRT and RT.

Materials and Methods

Cell culture

The rat pancreatic CA20948 tumor cells, which attach to a cell culture plate, were grown in Dulbecco's modified Eagle's medium (DMEM, Gibco Life Technologies, Breda, The Netherlands) supplemented with 10% heat-inactivated fetal bovine serum (FBS), 2 mmol/l of glutamine, 50 IU/ml penicillin/streptomycin (Gibco, Life Technologies, Breda, The Netherlands), 1 mmol/l sodium pyruvate, and 0.1 mg/l fungizone. The medium was changed two or three times per week. Cells were cultured in a 37°C incubator with a gas mixture of 95% air and 5% CO_2.

Cellular uptake Characteristics of ^{131}I

These experiments were performed to investigate whether or not ^{131}I (Mallinckrodt, Petten, The Netherlands) added to the medium would stick to the cells or the plastic of a 6-wells plate. We also determined whether the ^{131}I would stay homogeneously distributed in the medium. In these experiments, 400 and 800 cells were plated in 6-wells plates. After two days, these cells were incubated with 0.26 MBq ^{131}I in the medium. After an incubation time of 1, 2, 3, 20, 22, 23.5, 92, 94, 96, 98, and 116 hours, 10 different 10 µl samples were taken from the medium and counted in an LKB-1282-Compugammasystem (PerkinElmer, Oosterhout, The Netherlands) to determine the possible disappearance from the medium. Thereafter, the cells were lysed with 0.1 M NaOH and also counted in the LKB-gammasystem to exclude cellular uptake.

Calculations with a Monte Carlo model

The well-plate was modeled with the Monte Carlo code MCNP4C (21) to calculate the absorbed dose to the cells attached to the bottom on each well. The polyethylene well plate (density ρ = 0.92 g/cm^3) has a thickness of 4.118 mm, and each of the 6-wells has a surface area of 9.62cm^2 and a depth of 3.118 mm, resulting in a volume of 3 cm^3, evenly spaced over the whole plate. The well-plate cavities were filled with water (ρ = 1 g/cm^3) and only 1 cavity was assumed to be filled with a radioactivity source. The self-dose and cross-doses to the other wells could thereby be determined.

The radiation characteristics of ^{131}I ($T_{½}$ = 8.04 d) were taken from the ICRP38 database (22). Three separate calculations were performed for the beta emission (E_{max} = 806.9 keV), the gamma and X-rays (main γ line: 365.5 keV (81.2%/decay)) and the internal conversion and Auger electrons. The source distributions were modeled with a homogeneous distribution of the activity in the well. The thickness of the well cavity is too small to achieve electron equilibrium in the lateral direction. In the radial direction, there is electron equilibrium apart from a small region on the outer rim of the plate. To gain insight to the dose distribution in the lateral direction, scoring of the radiation dose in the bottom half of the well was done in 4 regions of 25 µm, 1 region of 59 µm and, consecutively, 14 regions of 100 µm. The top half of the well was not subdivided into scoring regions.

The Monte Carlo calculations were performed with 1 million starting particles, thus obtaining statistical variance in the scoring regions below 1%. Both the electron and photon minimum energy threshold was set at 1 keV. The deposited energy (in MeV) per starting particle was scored in all geometry elements. For an *in vitro* experiment with ^{131}I activity (of A MBq) load lasting T days, the cumulated activity (in MBq.d) is given by:

$$\tilde{A} = \int_0^T A\, e^{-\frac{\ln 2\, t}{T_{1/2}}}\, dt = \frac{A \times T_{1/2}}{\ln 2}\left(1 - e^{-\frac{\ln 2\, T}{T_{1/2}}}\right)$$

In vitro clonogenic survival assay

Single-cell suspensions of CA20948 cells were plated in 6-wells plates at 400 and 800 cells/well, with each concentration in triplicate and incubated for 24 hours. Cells were irradiated with either 200 kV X-rays (XRT) or with ^{131}I added to the medium (RT).

External X-irradiation was carried out at a dose rate of 0.66 Gy/min and with the machine operating at 20 mA. The X-ray machine contained a 1 mm Cu-filter, resulting in a half-value layer (HVL) of 1.6 mm Cu (23). Delivered doses were checked with thermoluminescent dosimetry (TLD), which indicated a <3% dose variation over

Table 1: Amount of ^{131}I activity in DMEM solutions, leading to a dose of 1 to 10 Gy in the clonogenic survival assay.

MBq/well	D (Gy)
0.00	0
0.17	1
0.35	2
0.53	3
0.70	4
0.87	5
1.05	6
1.22	7
1.40	8
1.57	9
1.75	10

the entire irradiation field. After irradiation, the cells were allowed to form colonies for 12 days in the above-mentioned incubator at 37°C. The cells irradiated with ^{131}I solutions were incubated with ^{131}I free in 3 ml of medium for 12 days in the 37°C incubator, leading to a dose of 1 to 10 Gray (Gy), with a maximum dose rate of 0.92 mGy/minute. ^{131}I was added as a sterile ^{131}I chloride solution, specific activity: 1–1.5 mCi/ml. The ^{131}I solutions were made according to table 1 (range: 0.17–1.75 MBq/well). After the colony-forming period, the cell colonies were fixated for 15 minutes with methanol:glacial acid (3:1), and then stained for 15 minutes with heamatoxylin. Colonies that contained ≥50 cells were counted and used to calculate the surviving fraction (19).

Data analysis

For each dose point, the number of colonies—as obtained from 3 wells with identical cell concentrations— was averaged and used to calculate the surviving fraction. Standard deviations were used as a weighing factor. Based on these surviving fractions, a cell-survival curve was computer-fitted to the LQ-model using a Curve Expert 3.1 program.

Sulforhodamine B (SRB) assay

The cell-doubling time was determined with the SRB-assay (24). This assay was adapted for *in vitro* cell cultures (van den Aardweg, in progress). In short, cells were grown at 37°C in 96-well plates with lanes of 8 wells containing cell concentrations of 100, 250, 500, 1000, 2500, or 5000 cells/ml and 200 µl medium per well. At intervals of 24 hours up to 6 days after plating, the cells were fixed with 10% trichloroactic acid solution for 1 hour at 4°C using 200 µl per well. After drying the plates, the cells were stained for 2 hours, adding 50 µl per well of a 0.4% SRB solution in 1% acetic

acid. Plates were washed and 150 µl Tris ([hydroxymethyl]aminomethane, 10 mmol/ml, Sigma-Aldrich, Zwijndrecht, The Netherlands) was added. The following day, the optical density was measured for each well at 540 nm using a spectrophotometer (Biorad, Veenendaal, The Netherlands). For each cell concentration, the logarithmic values for the mean optical densities plotted as a function of time gave straight lines. From the slopes of these lines, the cell-doubling time was calculated.

Results

Binding and cellular uptake of ^{131}I

The results of these experiments are shown in table 2. These results show that ^{131}I did not disappear from the medium, and did not bind to the cells plated in the 6-wells plate, but stayed homogeneously distributed in the medium.

Table 2: Percentage of the activity of ^{131}I in the medium and uptake of ^{131}I in CA20948 cells.

Hours	Activity in 400 cells % A ± SD	Activity in 800 cells % A ± SD	Mean activity in 400 and 800 cells % A ± SD
1	0.017 ± 0.005	0.009 ± 0.0002	0.013 ± 0.005
2	0.009 ± 0.003	0.012 ± 0.001	0.010 ± 0.003
3	0.016 ± 0.012	0.007 ± 0.001	0.011 ± 0.012
20	0.006 ± 0.001	0.005 ± 0.001	0.006 ± 0.001
22	0.009 ± 0.003	0.007 ± 0.001	0.008 ± 0.003
24	0.007 ± 0.001	0.010 ± 0.008	0.009 ± 0.008
92	0.007 ± 0.000	0.005 ± 0.001	0.006 ± 0.001
94	0.006 ± 0.001	0.005 ± 0.000	0.005 ± 0.001
96	0.013 ± 0.004	0.005 ± 0.001	0.009 ± 0.004
98	0.010 ± 0.004	0.005 ± 0.001	0.007 ± 0.004
116	0.008 ± 0.002	0.007 ± 0.001	0.008 ± 0.002

Monte Carlo calculations

The results for the dosimetry calculations inside the well with ^{131}I homogeneously distributed are given in table 3 as a function of the distance from the bottom of the well. The tumor cells are situated in the bottom layer of the well, and the dose is 5.51E-03 mGy/MBq.s. For a total activity load time of 12 days, the dose-per-unit activity is 3.56 Gy/MBq. The cross doses from the β- and γ-emissions from ^{131}I in neighboring wells are maximally 0.4 and 7 mGy/MBq, respectively, and are, therefore, neglected.

Table 3: Dose distribution in the 9.62 cm^2 well plate with ^{131}I distributed homogeneously inside the 3 ml well plate cavity volume.

	zmin- zmax		Absorbed dose per cum. act. (mGy/MBq·s)			
region	**(μm)**	**mass (g)**	**β-ray (E-03)**	**γ-ray (E-04)**	**IC+Auger (E-04)**	**total (E-03)**
1	0 - 25	0.0241	5.22	2.08	0.815	5.51
2	25 - 50	0.0241	5.92	2.20	0.948	6.24
3	50 - 75	0.0241	6.40	2.22	0.973	6.72
4	75 -100	0.0241	6.80	2.25	0.978	7.12
5	100 - 159	0.0568	7.26	2.23	1.02	7.58
6	159 - 259	0.0962	7.95	2.45	1.06	8.30
7	259 - 359	0.0962	8.58	2.63	1.10	8.96
8	359 - 459	0.0962	8.89	2.56	1.12	9.26
9	459 - 559	0.0962	9.11	2.62	1.15	9.48
10	559 - 659	0.0962	9.34	2.69	1.15	9.72
11	659 - 759	0.0962	9.45	2.76	1.18	9.85
12	759 - 859	0.0962	9.43	2.83	1.17	9.83
13	859 - 959	0.0962	9.52	2.89	1.17	9.93
14	959 - 1059	0.0962	9.54	2.91	1.19	9.94
15	1059 - 1159	0.0962	9.59	3.05	1.17	10.0
16	1159 - 1259	0.0962	9.61	2.91	1.17	10.0
17	1259 - 1359	0.0962	9.56	2.79	1.19	9.96
18	1359 - 1459	0.0962	9.60	2.76	1.18	9.99
19	1459 - 1559	0.0962	9.67	2.85	1.18	10.1
20	1559 - 3118	1.500	8.92	2.66	1.13	9.29
Total	0 - 3118	3.000	8.95	2.68	1.13	9.34

Clonogenic survival assay

We investigated the effects of two cell densities—400 and 800 cells/well—on cellular survival after incubation with ^{131}I (data not shown). The radiobiological parameters were calculated from the two curves, which showed that the α-and β-component were in the same range for the

two different cell densities. Therefore, for other experiments, we have used the cell density of 400 cells/well. Figure 1 shows the effects of external-beam therapy (XRT) and radionuclide therapy (RT) on the clonogenic survival of CA20948 cells. XRT was delivered in a single fraction by an X-ray machine in less than 30 minutes, while RT was delivered by using ^{131}I over a period of 12 days. For both therapies, we observed a dose-dependent reduction of tumor-cell survival. At low doses, the surviving fraction was almost identical for XRT and RT. The XRT curves exhibited a more rapid exponential decrease at higher doses. The radiobiological parameters were calculated and are presented in table 4. The α/β ratios for the CA20948 cell line was higher for RT than for XRT. These results indicate that the survival curve of the

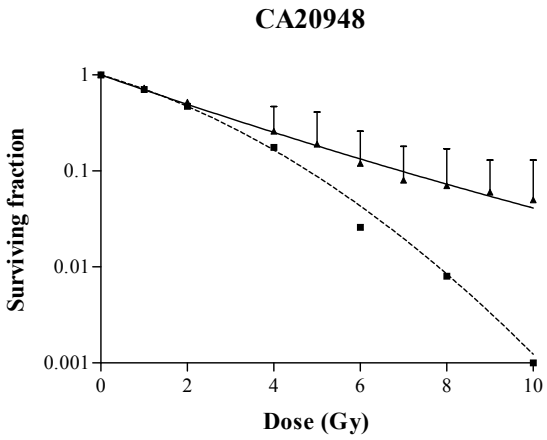

Figure 1: Clonogenic survival curve for CA20948 using two methods: (1) external-beam therapy (dashed line) and (2) radionuclide therapy (solid line). Data are expressed as the mean ± SD of at least three independent experiments.

Table 4. The radiobiological parameters α, β, α/β ratio and surviving fraction at 2 Gy (SF_2) calculated for CA20948. XRT = external-beam therapy; RT = radionuclide therapy.

Parameter	CA20948	
	XRT	RT
α	0.304	0.351
β	0.0366	0.0031
α/β ratio (Gy)	8.3	113
SF_2	0.47	0.49

RT-irradiated cells have a relatively flat slope at higher doses, compared to that after XRT. Therefore, RT resulted in less cell killing than XRT for this cell line at higher doses. The surviving fraction at 2 Gy (SF_2) was approximately 0.47 for CA20948 cells; this parameter was similar for both RT and XRT.

SRB assay

Figure 2 shows the results of the SRB assay for the CA20948, and a doubling time of 22 ± 1 hours was calculated.

Discussion

In this study, we compared the survival curves of the CA20948 cell line *in vitro* using both high-dose-rate XRT or exponentially decreasing low-dose-rate RT. The CA20948 cell line is widely used for radiolabeled peptide studies performed *in vitro* and *in vivo* in tumor-bearing rats (1, 2, 5-9, 12, 13, 19, 25-27). We performed *in*

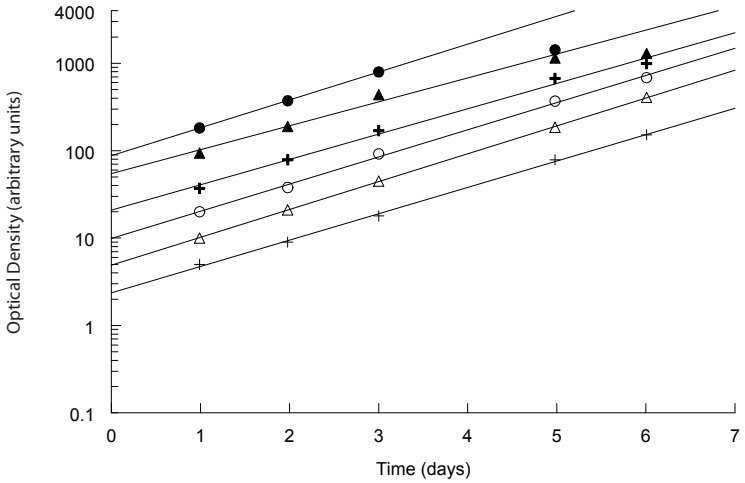

Figure 2: Growth curves for CA20498 cells obtained with the SRB assay. The slope of the curves is an estimate for the cell-doubling time. Increasing cell concentrations of 100 cells/ml (gray +), 250 cells/ml (Δ), 500 cells/ml (○), 1000 cells/ml (black +), 2500 cells/ml (▲), and 5000 cells/ml (●) were used.

vitro clonogenic survival assays using high-energy XRT to determine the radiation sensitivity. However, it can be expected that the results of XRT are not representative for the results of RT, because of the difference in, for instance, dose rate. RT has a continuously decreasing dose rate because of radionuclide decay, whereas XRT is given at a constant dose rate for a short period of time. Therefore, we also performed survival assays after RT using ^{131}I free in a culture medium. Damage to the cells is caused by the crossfire effect of ^{131}I. The radionuclide was not coupled to a peptide analog, because we wanted to exclude the effects of receptor affinity, as well as the internalization and externalization rate of the radiolabeled analog, which will influence the results.

To be able to compare the effects of RT and XRT, we shall describe here the development and validation of a RT clonogenic survival assay using incubation with the radionuclide ^{131}I present in its free form in a culture medium. The physical characteristics of this radionuclide are in the same range as those of ^{177}Lu, which is used in our clinical PRRT studies using [^{177}Lu-DOTA,Tyr^3]octreotate. The half-life of ^{177}Lu is 6.7 days, compared to 8.0 days for ^{131}I. Furthermore, the maximum energy of the beta particles of ^{177}Lu is 497 keV versus 807 keV for ^{131}I, and their maximum range in water or tissue is approximately 2–3 mm.

Several studies have been performed comparing XRT and radioimmunotherapy (RIT) in cell lines, such as the human colon carcinoma cell lines LS174T and WiDr (28-30). Experiments (28, 29) have shown that the LS174T human colon carcinoma cell line showed a comparable response to RIT and XRT. However, compared to XRT,

RIT was less effective in radioresistent cell lines, such as the human colon carcinoma cell line WiDr. A possible explanation would be a greater DNA-repair capacity of WiDr versus LS174T (28, 29). These studies conclude that the effectiveness of cell killing with RIT was lower than with XRT because of the dose-rate effect and dose heterogeneity in the tumor (28, 29).

The shape of any survival curve is dependent on different aspects, such as the type of cells, the kind of radiation, and the dose rate of the radiation used. In CA20948, RT caused a more linear than exponential decrease of cell survival. This can be explained by the lower dose rate of RT than of XRT; therefore, less damage occurs and there is more time to repair. We can, therefore, conclude from these results that a Gy of RT is not the same as a Gy of XRT. Table 4 also shows higher α/β ratios for RT compared to XRT for the CA20948, showing that this cell line is less sensitive to RT than to XRT at higher doses. Studies by Joiner et al. (31, 32) described a higher sensitivity in the radiation survival response of mammalian cells at doses below 0.5 Gy with low dose rates (0.02-1 $Gy \cdot h^{-1}$), the so-called hyper-radiosensitivity. We did not find this phenomenon in our studies with CA20948, because we did not use these low doses. In our further studies, possible hyper-radiosensitivity effects in our cell lines will be further investigated.

Cellular survival after exposure to radiation is a function of the detection and successful repair of double-stranded DNA breaks (33). A larger α than β component in the radiation survival curves, which was seen in our RT curves, suggests that the cell lines were more capable of repairing sublethal damage in RT than in XRT (34, 35). This was also seen in other studies, where the authors concluded that the differences between continuous low-dose-rate and acute high-dose-rate irradiation are caused by differences in the repair of sublethal and potentially lethal damage (36). Low-dose-rate irradiation (such as in RIT and also PRRT) has earlier been described to be less effective in cell killing than high-dose-rate irradiation (such as XRT) (35, 37). However, because in (PR)RT, and also in RIT, radiation is delivered selectively to the tumor(s) and metastases, the radiation dose to the tumor can be much higher than with XRT. This, however, is dependent on factors such as the affinity of the peptide to its receptor and the homogeneity of receptor distribution throughout the tumor. These factors have been excluded from this study.

The possible explanations for the differences in the effectiveness of RT versus XRT are dose rate and irradiation period. In RT, the damage to the cells will be lower because of the lower dose rate, and more repair time is allowed (28, 29, 36, 38). Despite the fact that RT is less efficient at higher doses than XRT, our PRRT results were very promising. When using [^{177}Lu-DOTA^{0},Tyr^{3}]octreotate in CA20948 tumor-bearing rats, a 100% cure rate could be reached (1). Also, in patients, this radiolabeled compound is very successful, because the effects of therapy showed

that 3% and 35% of the patients had a complete or partial response, respectively (39). This success of ^{177}Lu-octreotate can be explained by a high-receptor density on tumor cells and a very high affinity of the radiolabeled peptide to the receptor. Deacon et al. (34) published a report in which they compared the surviving fraction at 2 Gy (SF_2) of 51 human tumor cell lines. The mean SF_2 was calculated to discriminate between radioresistant and radiosensitive tumor cell lines. The cell lines were classified in categories A–E, according to their clinical radioresponsiveness—with category A being radiosensitive with a mean SF_2 of 0.187 and category E being radioresistant with a mean SF_2 of 0.518 (34). The latter SF_2 is similar to that calculated for the CA20948. Therefore, we can conclude that the CA20948 cell line we used in our *in vivo* PRRT studies was not radiosensitive. Also, Deacon et al. (34) concluded that a positive correlation exists between the steepness of the initial portion of the cell-survival curve after XRT *in vitro* and the clinical radioresponsiveness of the tumor.

Conclusion

In conclusion, we have shown that the CA20948 cell line is relatively radioresistant, and is more sensitive to XRT than to RT at high doses of 3–10 Gy in an *in vitro* clonogenic survival assay. However, RT and XRT are approximately equally toxic at lower doses.

References

1. de Jong, M., Breeman, W. A., Bernard, B. F., Bakker, W. H., Schaar, M., van Gameren, A., Bugaj, J. E., Erion, J., Schmidt, M., Srinivasan, A., and Krenning, E. P. [^{177}Lu-DOTA^{0},Tyr^{3}] octreotate for somatostatin receptor-targeted radionuclide therapy. Int J Cancer, *92:* 628-633, 2001.
2. de Jong, M., Breeman, W. A., Bernard, B. F., van Gameren, A., de Bruin, E., Bakker, W. H., van der Pluijm, M. E., Visser, T. J., Macke, H. R., and Krenning, E. P. Tumour uptake of the radiolabelled somatostatin analogue [DOTA^{0}, TYR^{3}]octreotide is dependent on the peptide amount. Eur J Nucl Med, *26:* 693-698, 1999.
3. De Jong, M., Valkema, R., Jamar, F., Kvols, L. K., Kwekkeboom, D. J., Breeman, W. A., Bakker, W. H., Smith, C., Pauwels, S., and Krenning, E. P. Somatostatin receptor-targeted radionuclide therapy of tumors: preclinical and clinical findings. Semin Nucl Med, *32:* 133-140, 2002.
4. Kwekkeboom, D., Krenning, E. P., and de Jong, M. Peptide receptor imaging and therapy. J Nucl Med, *41:* 1704-1713, 2000.
5. Achilefu, S., Dorshow, R. B., Bugaj, J. E., and Rajagopalan, R. Novel receptor-targeted fluorescent contrast agents for in vivo tumor imaging. Invest Radiol, *35:* 479-485., 2000.
6. Bernard, B. F., Krenning, E., Breeman, W. A., Visser, T. J., Bakker, W. H., Srinivasan, A., and de Jong, M. Use of the rat pancreatic CA20948 cell line for the comparison of radiolabelled peptides for receptor-targeted scintigraphy and radionuclide therapy. Nucl Med Commun, *21:* 1079-1085., 2000.
7. Bugaj, J. E., Erion, J. L., Johnson, M. A., Schmidt, M. A., and Srinivasan, A. Radiotherapeutic efficacy of ^{153}Sm-CMDTPA-Tyr^{3}-octreotate in tumor- bearing rats. Nucl Med Biol, *28:* 327-334., 2001.
8. de Jong, M., Breeman, W. A., Bernard, B. F., Bakker, W. H., Visser, T. J., Kooij, P. P., van Gameren, A., and Krenning, E. P. Tumor response after [^{90}Y-DOTA^{0},Tyr^{3}]octreotide radionuclide therapy in a transplantable rat tumor model is dependent on tumor size. J Nucl Med, *42:* 1841-1846, 2001.
9. Lewis, J. S., Laforest, R., Lewis, M. R., and Anderson, C. J. Comparative dosimetry of copper-64 and yttrium-90-labeled somatostatin analogs in a tumor-bearing rat model. Cancer Biother Radiopharm, *15:* 593-604., 2000.
10. Lewis, J. S., Wang, M., Laforest, R., Wang, F., Erion, J. L., Bugaj, J. E., Srinivasan, A., and Anderson, C. J. Toxicity and dosimetry of ^{177}Lu-DOTA-Y^{3}-octreotate in a rat model. Int J Cancer, *94:* 873-877., 2001.
11. Vallabhajosula, S., Moyer, B. R., Lister-James, J., McBride, B. J., Lipszyc, H., Lee, H., Bastidas, D., and Dean, R. T. Preclinical evaluation of technetium-99m-labeled somatostatin receptor-binding peptides. J Nucl Med, *37:* 1016-1022., 1996.
12. van Hagen, P. M., Breeman, W. A., Bernard, H. F., Schaar, M., Mooij, C. M., Srinivasan, A., Schmidt, M. A., Krenning, E. P., and de Jong, M. Evaluation of a radiolabelled cyclic DTPA-RGD analogue for tumour imaging and radionuclide therapy. Int J Cancer, *90:* 186-198, 2000.
13. Breeman, W. A., Hofland, L. J., de Jong, M., Bernard, B. F., Srinivasan, A., Kwekkeboom, D. J., Visser, T. J., and Krenning, E. P. Evaluation of radiolabelled bombesin analogues for receptor-targeted scintigraphy and radiotherapy. Int J Cancer, *81:* 658-665, 1999.
14. Behr, T. M. and Behe, M. P. Cholecystokinin-B/Gastrin receptor-targeting peptides for staging and therapy of medullary thyroid cancer and other cholecystokinin-B receptor-expressing malignancies. Semin Nucl Med, *32:* 97-109., 2002.
15. Markwalder, R. and Reubi, J. C. Gastrin-releasing peptide receptors in the human prostate: relation to neoplastic transformation. Cancer Res, *59:* 1152-1159., 1999.
16. Mantyh, C. R., Gates, T. S., Zimmerman, R. P., Welton, M. L., Passaro, E. P., Jr., Vigna, S. R., Maggio, J. E., Kruger, L., and Mantyh, P. W. Receptor binding sites for substance P, but not substance K or neuromedin K, are expressed in high concentrations by arterioles, venules, and

lymph nodules in surgical specimens obtained from patients with ulcerative colitis and Crohn disease. Proc Natl Acad Sci U S A, *85:* 3235-3239., 1988.
17. Haubner, R., Wester, H. J., Burkhart, F., Senekowitsch-Schmidtke, R., Weber, W., Goodman, S. L., Kessler, H., and Schwaiger, M. Glycosylated RGD-containing peptides: tracer for tumor targeting and angiogenesis imaging with improved biokinetics. J Nucl Med, *42:* 326-336., 2001.
18. DeNardo, S. J., Burke, P. A., Leigh, B. R., O'Donnell, R. T., Miers, L. A., Kroger, L. A., Goodman, S. L., Matzku, S., Jonczyk, A., Lamborn, K. R., and DeNardo, G. L. Neovascular targeting with cyclic RGD peptide (cRGDf-ACHA) to enhance delivery of radioimmunotherapy. Cancer Biother Radiopharm, *15:* 71-79., 2000.
19. Capello, A., Krenning, E. P., Breeman, W. A., Bernard, B. F., and de Jong, M. Peptide receptor radionuclide therapy *in vitro* using [^{111}In-DTPA^{0}]octreotide. J Nucl Med, *44:* 98-104, 2003.
20. Hall, E. J. Radiobiology for the radiologist, 5 edition, p. 478. Philadelphia: Lippincott Williams & Wilkins, 2000.
21. Briesmeister, J. F. MCNP - A General Monte Carlo N-Particle Transport Code, Version 4C, 2000.
22. Eckerman, K. F., Westfall, R. J., Ryman, J. C., and Cristy, M. Availability of nuclear decay data in electronic form, including beta spectra not previously published. Health Phys, *67:* 338-345., 1994.
23. van den Aardweg, G. J., Naus, N. C., Verhoeven, A. C., de Klein, A., and Luyten, G. P. Cellular radiosensitivity of primary and metastatic human uveal melanoma cell lines. Invest Ophthalmol Vis Sci, *43:* 2561-2565., 2002.
24. Skehan, P., Storeng, R., Scudiero, D., Monks, A., McMahon, J., Vistica, D., Warren, J. T., Bokesch, H., Kenney, S., and Boyd, M. R. New colorimetric cytotoxicity assay for anticancer-drug screening. J Natl Cancer Inst, *82:* 1107-1112., 1990.
25. Breeman, W. A., Hofland, L. J., van der Pluijm, M., van Koetsveld, P. M., de Jong, M., Setyono-Han, B., Bakker, W. H., Kwekkeboom, D. J., Visser, T. J., and Lamberts, S. W. A new radiolabelled somatostatin analogue [^{111}In-DTPA-D-Phe^{1}]RC-160: preparation, biological activity, receptor scintigraphy in rats and comparison with [^{111}In-DTPA-D-Phe^{1}]octreotide. Eur J Nucl Med, *21:* 328-335, 1994.
26. de Jong, M., Bakker, W. H., Bernard, B. F., Valkema, R., Kwekkeboom, D. J., Reubi, J. C., Srinivasan, A., Schmidt, M., and Krenning, E. P. Preclinical and initial clinical evaluation of ^{111}In-labeled nonsulfated CCK8 analog: a peptide for CCK-B receptor-targeted scintigraphy and radionuclide therapy. J Nucl Med, *40:* 2081-2087, 1999.
27. Lewis, J. S., Lewis, M. R., Srinivasan, A., Schmidt, M. A., Wang, J., and Anderson, C. J. Comparison of four ^{64}Cu-labeled somatostatin analogues *in vitro* and in a tumor-bearing rat model: evaluation of new derivatives for positron emission tomography imaging and targeted radiotherapy. J Med Chem, *42:* 1341-1347., 1999.
28. Langmuir, V. K., Fowler, J. F., Knox, S. J., Wessels, B. W., Sutherland, R. M., and Wong, J. Y. Radiobiology of radiolabeled antibody therapy as applied to tumor dosimetry. Med Phys, *20:* 601-610, 1993.
29. Buras, R. R., Wong, J. Y., Kuhn, J. A., Beatty, B. G., Williams, L. E., Wanek, P. M., and Beatty, J. D. Comparison of radioimmunotherapy and external beam radiotherapy in colon cancer xenografts. Int J Radiat Oncol Biol Phys, *25:* 473-479, 1993.
30. Roberson, P. L. and Buchsbaum, D. J. Reconciliation of tumor dose response to external beam radiotherapy versus radioimmunotherapy with 131iodine-labeled antibody for a colon cancer model. Cancer Res, *55:* 5811s-5816s, 1995.
31. Joiner, M. C., Marples, B., Lambin, P., Short, S. C., and Turesson, I. Low-dose hypersensitivity: current status and possible mechanisms. Int J Radiat Oncol Biol Phys, *49:* 379-389., 2001.
32. Mitchell, C. R., Folkard, M., and Joiner, M. C. Effects of exposure to low-dose-rate (60)co gamma rays on human tumor cells in vitro. Radiat Res, *158:* 311-318., 2002.

33. Collis, S. J., Sangar, V. K., Tighe, A., Roberts, S. A., Clarke, N. W., Hendry, J. H., and Margison, G. P. Development of a novel rapid assay to assess the fidelity of DNA double- strand-break repair in human tumour cells. Nucleic Acids Res, *30:* E1., 2002.
34. Deacon, J., Peckham, M. J., and Steel, G. G. The radioresponsiveness of human tumours and the initial slope of the cell survival curve. Radiother Oncol, *2:* 317-323., 1984.
35. Ning, S., Trisler, K., Wessels, B. W., and Knox, S. J. Radiobiologic studies of radioimmunotherapy and external beam radiotherapy in vitro and in vivo in human renal cell carcinoma xenografts. Cancer, *80:* 2519-2528. [pii], 1997.
36. Morton, J., Yabuki, H., Porter, E. A., Rockwell, S., and Nath, R. Relative biological effectiveness of ^{241}Am relative to ^{192}Ir for continuous low-dose-rate irradiation of BA1112 rat sarcomas. Radiat Res, *119:* 478-488., 1989.
37. Fowler, J. F. Radiobiological aspects of low dose rates in radioimmunotherapy. Int J Radiat Oncol Biol Phys, *18:* 1261-1269, 1990.
38. Dale, R. G. Dose-rate effects in targeted radiotherapy. Phys Med Biol, *41:* 1871-1884, 1996.
39. Kwekkeboom, D. J., Bakker, W. H., Kam, B. L., Teunissen, J. J., Kooij, P. P., de Herder, W. W., Feelders, R. A., van Eijck, C. H., de Jong, M., Srinivasan, A., Erion, J. L., and Krenning, E. P. Treatment of patients with gastro-entero-pancreatic (GEP) tumours with the novel radiolabelled somatostatin analogue [^{177}Lu-DOTA^{0},Tyr^{3}]octreotate. Eur J Nucl Med Mol Imaging, *30:* 417-422, 2003.

5

Summary, general discussion and conclusions

5.1 Summary, general discussion and conclusions

Almost two decades ago, it was found that somatostatin receptors (sst), mostly of the subtype 2 (sst_2), are being overexpressed on neuroendocrine tumors [1]. Since the native hormone is rapidly degraded following systemic injection, stable analogs of somatostatin (ss) were synthesized, of which octreotide is the most commonly applied ss peptide in patients nowadays [2, 3]. Stable peptide analogs bind sst on receptor-positive tissues after injection and they are subsequently internalized into the sst expressing (tumor) cells. This mechanism appeared to be most useful for the visualization and therapy of sst-positive tumors using radiolabeled ss analogs.

Hence, the stable ss analogs were radiolabeled in order to achieve visualization of the distribution of these peptides in patients. Compounds including [^{111}In-DTPA^0] octreotide (Octreoscan) [2, 4], ^{177}Lu labeled [DOTA^0,Tyr^3]octreotate (DOTAtate) [5, 6], [^{99m}Tc-N_4^{0-1},Asp^0,Tyr^3]octreotate (Demotate) [7, 8] and [^{90}Y-DOTA^0,Tyr^3]octreotide (DOTATOC) [4, 9, 10] are nowadays being used for clinical and preclinical evaluation of sst-positive tumors. The visualization of tumors using radiolabeled peptide analogs is referred to as peptide receptor scintigraphy (PRS). The use of α- or β-particle emitting radionuclides, e.g. ^{177}Lu, ^{213}Bi and ^{90}Y, coupled to sst peptides enable the targeted radiation of tumors, thereby decreasing the tumor size without invasive intervention. This concept is referred to as peptide receptor radionuclide therapy (PRRT) and is highly effective in the treatment of neuroendocrine tumors [11, 12].

In 1987, Reubi et al. showed that also malignant brain tumors, such as astrocytomas and oligodendrogliomas, express sst, while the poorly differentiated glioblastoma multiforme (GBM) tumors do not show sst expression [13]. GBM is the most aggressive tumor type of the brain and current treatments are not curative. The palliative treatment regimen includes surgery, radiation therapy and chemotherapy and leads to a median survival of less than a year [14-16]. Due to the infiltrative nature of GBM it is virtually impossible to remove every tumor cell; as a result all GBMs recur, usually within a 2-3 cm margin of the original tumor site.

Since sst were not found on GBM tumors, PRRT using radiolabeled ss analogs is not anticipated to result in an effective treatment of these patients. Experimental treatments for GBM patients at this moment include radioimmunotherapy [17-19], chemotherapy [20, 21], antiangiogenic therapy [22, 23] and gene therapy [24-26]. It is believed that gene therapy is an attractive treatment option for GBM patients, because of the confined location of the tumor in the skull and the low incidence of distant metastases. Unfortunately, the diffusely infiltrating nature of GBM might be a disadvantage for using gene therapy.

Results from clinical viral gene therapy studies in GBM patients showed that viral injection is safe and anti-tumor effects were sometimes observed [27-36]. Unfortunately, no complete responses were observed in these studies. Statistically significant survival advantage was only seen in two small randomized studies [28, 34]. From

these results it is evident that gene therapy strategies need to be improved in order to become more effective.

The aim of the studies described in chapter 2 of this thesis was to investigate the usefulness of the clinical application of the Ad5.tk.sst_2 adenoviral vector in GBM tumors, which was previously done for ovarian [37] and lung cancer [38]. This vector contains two heterologous genes: the sst_2 and herpes simplex virus enzyme thymidine kinase (HSV-tk) gene. Expression of sst_2 in the virally infected tumor cells can be visualized using radiolabeled peptide analogs as described above. In addition, the sst_2 gene can also be used for treatment, using therapeutic ss analogs. The HSV-tk gene in this vector can also be used both for imaging and therapeutic purposes: the expression of HSV-tk and the subsequent application of an antiviral prodrug, such as ganciclovir (GCV) leads to the phosphorylation of GCV into GCV-monophosphate and eventually into GCV-triphosphate. This latter compound is retained in the cell and is toxic for proliferating cells. In addition, nucleosides, such as FIAU [39] and FIRU [40, 41], are phosphorylated in the same manner as GCV and can be labeled with radioactive iodine (e.g. ^{123}I) for visualization purposes (see also chapter 1.1, figure 4 and 5).

In **chapter 2.1** we compared the uptake of [^{111}In-DOTA,Tyr^3]octreotate and [^{125}I] FIRU in several Ad5.tk.sst_2 infected glioblastoma cell lines *in vitro*. The cell lines used do not express sst_2 and HSV-tk prior to Ad5.tk.sst_2 infection. Internalization studies were performed two days after viral infection with Ad5.tk.sst_2 and we showed that uptake of the above-mentioned radiolabeled tracers was viral concentration dependent. Interestingly, uptake of [^{111}In-DOTA,Tyr^3]octreotate was higher than that of [^{125}I]FIRU in all cell lines indicating that sst_2 might be preferable over HSV-tk for gene expression imaging following viral infection. On the other hand, HSV-tk in combination with GCV for therapy was effective *in vitro* and in animal gene therapy studies with GBM models [42-44]. This strategy was also effective in combination with radiation therapy [45, 46]. We therefore propose Ad5.tk.sst_2 gene transfer with subsequent combination treatment using ^{177}Lu or ^{90}Y labeled ss analogs and GCV for a potential effective treatment in patients.

Viral infection and gene expression imaging efficacy was further investigated *in vivo* in **chapter 2.2**. Animals bearing subcutaneous U87MG tumors were infected with Ad5.tk.sst_2 via intratumoral injection, followed by gene expression imaging three days later, using the ss analog ^{99m}Tc-Demotate and the HSV-tk nucleoside ^{123}I-FIRU. We found that both tracers could non-invasively image the expression of their respective genes, sst_2 and HSV-tk, in Ad5.tk.sst_2 infected tumors. In addition, sst_2 expression was followed using SPECT for a week following infection showing that the uptake of the ss tracer was reduced over the course of that week. This

can be explained by the fact that the genetic material of an adenoviral vector does not integrate into the host genome. While the tumor grows during a week, the expression of the viral genes will be diluted over the daughter cells, leading to less gene expression per tumor volume. A possible second explanation could be that the immune system eliminates the viral gene expression, leading to less tracer uptake after a week. Although this was not tested in our model, we believe that this would also have been the case for HSV-tk imaging in this tumor model. In addition, we found that both genes were simultaneously, but non-homogeneously expressed in the infected tumor tissue. Unfortunately, this designates one of the problems in clinical gene therapy: the inhomogeneous expression will lead to an inefficient treatment of the tumor cells and consequently to a low response rate in patients.

It has been proposed that convection enhanced delivery (CED), i.e. the slow infusion of macromolecules, might improve the tissue penetration of adenoviral vectors in the brain. We therefore investigated in **chapter 2.3** whether CED is superior to single or multiple injections for intratumoral delivery of Ad5.tk.sst$_2$. The results of this study showed that after CED or single injection comparable tumor volumes and areas within the tumor were infected. Multiple injections of the virus, however, resulted in a higher tumor area and volume to be infected. Therefore, this delivery method is recommended for intratumoral injection of viral vectors in clinical gene therapy of GBMs.

The results presented in chapters 2.2 and 2.3 indicate that there is a need to improve the distribution of Ad5.tk.sst$_2$ in tumor tissue after injection. This can be achieved by using a (conditionally) replicating or oncolytic viral vector. More tumor cells might then be reached, as additional viral particles are formed during replication resulting in cell lysis and subsequent release of more viral particles into the tumor tissue. The non-homogeneous gene expression we found in these studies indicate that a combination treatment with GCV and ^{177}Lu-DOTA-tate will probably not achieve complete cure of the tumor. The use of ^{90}Y-labeled ss analogs might enhance the tumoricidal effect, compared to ^{177}Lu-labeled compounds, due to the longer particle range of ^{90}Y electrons [47]. Another approach to increase the therapeutic efficiency of the combination treatment is the use cytosine deaminase in combination with 5-FU. Some studies, conducted in hepatic and colorectal cancer cell lines, suggest that this is more effective in cell killing than the HSV-tk/GCV system [48, 49].

The above-described experiments all show expression of viral genes in tumor tissue several days after infection with Ad5.tk.sst$_2$. Unfortunately, viral gene expression does not show the viral distribution itself directly after injection into a tumor. We therefore aimed to radiolabel the adenovirus itself using ^{99m}Tc and a tricarbonyl-labeling agent. The results, described in **chapter 2.4**, show that Ad5.tk.sst$_2$ can indeed be radiolabeled with ^{99m}Tc; this allows the visualization of viral distribution

immediately after injection of the virus. Gamma camera and SPECT images show a high accumulation of radioactivity in the tumor in 9L bearing rats and U87MG bearing mice, respectively. *In vitro* infection with ^{99m}Tc-Ad5.tk.sst$_2$ showed the time dependent uptake of ^{99m}Tc radioactivity in U251, U87MG and 9L cells. This corresponded to the cellular infection of the virus, since we found that unbound ^{99m}Tc molecules did not enter the tumor cells. We found that both *in vitro* and *in vivo* gene expression could be detected when cells were infected with ^{99m}Tc-Ad5.tk.sst$_2$, although the expression was lower than in cells infected with unlabeled Ad5.tk.sst$_2$. We calculated a radiation dose of 5.8 Gy to the viral particles by ^{99m}Tc, which was given in an excess, to ensure radiolabeling of all viral particles. This may explain the discrepancy between the gene expression of radiolabeled and unlabeled viruses found in these experiments. Optimization of the radiolabeling, thereby most likely decreasing the radiation dose to the viral particles, is possible. Despite the loss of some viral particles due to the radiation dose, this method is still very interesting in a clinical setting to follow viruses upon injection, although further optimization studies are required.

In addition to gene therapy as potential therapeutic modality for GBM patients, we investigated whether PRS and PRRT using small peptides could also be used for patients with intracranial tumors. As mentioned before, it was found that GBMs do not, while differentiated glial tumors did express sst [13, 50]. In addition to sst, other peptide receptors, such as vasoactive intestinal peptide (VIP), neurokinine 1 (NK-1), gastrin-releasing peptide (GRP), cholecystokinin 2 (CCK$_2$), neurotensin (NT) and epidermal growth factor (EGF), could also be interesting for PRS and PRRT purposes. In **chapter 3.1**, we therefore examined the receptor expression status on brain tumor cell lines and on three groups of human intracranial tumors (GBMs, meningiomas (MG) and metastases (MT) originating from other organs than the brain) and normal human brain tissue (NB), using internalization and autoradiography techniques. We found that VIP receptors were expressed with high density and incidence on almost all GBM, MG and MT tumors, while NB tissues were usually free of VIP receptors, making this an interesting target for PRS and PRRT. In addition, EGF and NK-1 receptors were also highly expressed on GBM cells. The use of small radiolabeled peptides for scintigraphy and therapy would be of interest for the treatment of GBMs, since theoretically these small molecules can diffuse relatively easy through the whole brain targeting infiltrating tumor cells at a distance from the original tumor site. We also found that MG tissues expressed sst$_2$ with high density and incidence, confirming previous findings [13, 50]. Several publications have already showed that MG can be visualized using radiolabeled ss peptide analogs [51-55]. Recently, our institution performed PRRT studies using [^{177}Lu-DOTA,Tyr^3]octreotate in a small

group of patients with MG [6]. Five "end-stage" patients with a high tumor load were treated. Four patients had progressive disease at study entry and treatments resulted in stabilization in one of them, while the other three unfortunately progressed. The fifth MG patient was stable at the beginning of therapy and remained so after PRRT treatment. These results are encouraging for sst-based therapy in MG patients, especially when PRRT is performed earlier in the course of the disease or in combination with other therapies.

After systemic injection of ss analogs, a large amount of the radiation dose is excreted from the body within 24 hours. The radiolabeled peptides are filtered from the blood by the kidneys but part of the radioactivity remains in the proximal tubular cells of the kidneys after reabsorption, leading to a high radiation dose to these sensitive organs. Thus, when performing sst-based PRRT in patients, the kidney is one of the organs at risk and needs to be protected from a toxic radiation dose. It was found that positively charged amino acids, such as lysine and arginine, reduce the uptake of radiation in the kidneys by 40 to 50% in rats [56] as well as in humans [57-59]. Barone et al. found that a 10 hour infusion of amino acids in humans will give the highest reduction rate of radioactivity in patients [60]. However, this method is highly labor intensive and inconvenient for these patients. In **chapter 3.2**, we investigated whether orally administered lysine showed similar reduction rates in the kidneys compared to intravenously administered lysine in rats. We found that both intravenous and oral administration of lysine reduced the renal radioactivity in rats by 40%. This method might be a more convenient alternative for patients as well as for hospital staff, compared to the amino acid infusions performed nowadays.

In **chapter 4**, we studied the *in vitro* radiation sensitivity of the rat pancreatic tumor cell line CA20948, which is used in preclinical studies for PRS and PRRT due to the expression of many different peptide receptors, such as sst_2, GRP, CCK-2, $\alpha_v\beta_3$ and NK-1 [61-64]. The radiosensitivity was investigated using the most commonly used method with external beam radiation (XRT). XRT is however not representative for PRRT treatment due to the higher dose rate and short radiation period. We therefore performed radionuclide therapy (RT) using ^{131}I (this radionuclide has similar properties as ^{177}Lu, which is used in PRRT) to investigate radiosensitivity and compared this with the results of XRT. We found that the survival of CA20948 cells was similar for RT and XRT at low doses (1-2 Gy), however, when increasing the dose CA20948 cells showed to be more sensitive to XRT than to RT. Typically, in patients XRT is given in fractionated doses of 2 Gy and at this dose XRT and RT achieved an equal surviving fraction in CA20948 cells.

In conclusion, our studies show that Ad5.tk.sst_2 is an interesting new viral vector for gene therapy strategies in GBM patients. Both HSV-tk and sst_2 can be used as targets for non-invasive imaging, although sst_2 imaging has our preference. Imaging gene expression is highly desirable for monitoring gene transfer in clinical studies. In addition, these genes can be used for (combined) therapeutic purposes as well. In order to follow the distribution *in vivo*, adenoviral vectors can be radiolabeled, allowing more insight into the events following viral injection in patients. Unfortunately, the spatial distribution of this vector is still rather poor. Conditionally replicating viruses expressing these genes will hopefully lead to more transduced tumor cells. A new, and highly interesting approach is the use of radiolabeled peptides for therapy of GBM. Furthermore, we found that GBM tumors express VIP receptors in high density and incidence; also EGF and NK-1 receptors were found on these tumor tissues. These are all interesting targets for PRRT treatment in GBM patients.

References

1. Reubi J.C., Krenning E., Lamberts S.W. and Kvols L. Somatostatin receptors in malignant tissues. *J Steroid Biochem Mol Biol*, 1990 37(6): 1073-1077.
2. Krenning E.P., Kwekkeboom D.J., Bakker W.H., Breeman W.A., Kooij P.P., Oei H.Y., *et al.* Somatostatin receptor scintigraphy with [^{111}In-DTPA-D-Phe^{1}]- and [^{123}I-Tyr^{3}]-octreotide: the Rotterdam experience with more than 1000 patients. *Eur J Nucl Med*, 1993 20(8): 716-731.
3. Krenning E.P., Kwekkeboom D.J., Reubi J.C., van Hagen P.M., van Eijck C.H., Oei H.Y., *et al.* ^{111}In-octreotide scintigraphy in oncology. *Digestion*, 1993 54(Suppl 1): 84-87.
4. Valkema R., De Jong M., Bakker W.H., Breeman W.A., Kooij P.P., Lugtenburg P.J., *et al.* Phase I study of peptide receptor radionuclide therapy with [In-DTPA]octreotide: the Rotterdam experience. *Semin Nucl Med*, 2002 32(2): 110-122.
5. Kwekkeboom D.J., Bakker W.H., Kam B.L., Teunissen J.J., Kooij P.P., de Herder W.W., *et al.* Treatment of patients with gastro-entero-pancreatic (GEP) tumours with the novel radiolabelled somatostatin analogue [^{177}Lu-DOTA^{0},Tyr^{3}]octreotate. *Eur J Nucl Med Mol Imaging*, 2003 30(3): 417-422.
6. van Essen M., Krenning E.P., Kooij P.P., Bakker W.H., Feelders R.A., de Herder W.W., *et al.* Effects of therapy with [^{177}Lu-DOTA^{0},Tyr^{3}]octreotate in patients with paraganglioma, meningioma, small cell lung carcinoma, and melanoma. *J Nucl Med*, 2006 47(10): 1599-1606.
7. Maina T., Nock B., Nikolopoulou A., Sotiriou P., Loudos G., Maintas D., *et al.* [^{99m}Tc]Demotate, a new ^{99m}Tc-based [Tyr^{3}]octreotate analogue for the detection of somatostatin receptor-positive tumours: synthesis and preclinical results. *Eur J Nucl Med Mol Imaging*, 2002 29(6): 742-753.
8. Maina T., Nock B.A., Cordopatis P., Bernard B.F., Breeman W.A., van Gameren A., *et al.* [^{99m}Tc] Demotate 2 in the detection of sst$_2$-positive tumours: a preclinical comparison with [^{111}In] DOTA-tate. *Eur J Nucl Med Mol Imaging*, 2006 33(7): 831-840.
9. Otte A., Herrmann R., Heppeler A., Behe M., Jermann E., Powell P., *et al.* Yttrium-90 DOTATOC: first clinical results. *Eur J Nucl Med*, 1999 26(11): 1439-1447.
10. Chinol M., Bodei L., Cremonesi M. and Paganelli G. Receptor-mediated radiotherapy with Y-DOTA-DPhe-Tyr-octreotide: the experience of the European Institute of Oncology Group. *Semin Nucl Med*, 2002 32(2): 141-147.
11. Kwekkeboom D.J., Mueller-Brand J., Paganelli G., Anthony L.B., Pauwels S., Kvols L.K., *et al.* Overview of results of peptide receptor radionuclide therapy with 3 radiolabeled somatostatin analogs. *J Nucl Med*, 2005 46 Suppl 1: 62S-66S.
12. Teunissen J.J., Kwekkeboom D.J., de Jong M., Esser J.P., Valkema R. and Krenning E.P. Endocrine tumours of the gastrointestinal tract. Peptide receptor radionuclide therapy. *Best Pract Res Clin Gastroenterol*, 2005 19(4): 595-616.
13. Reubi J.C., Lang W., Maurer R., Koper J.W. and Lamberts S.W. Distribution and biochemical characterization of somatostatin receptors in tumors of the human central nervous system. *Cancer Res*, 1987 47(21): 5758-5764.
14. Salcman M. Survival in glioblastoma: historical perspective. *Neurosurgery*, 1980 7(5): 435-439.
15. Surawicz T.S., Davis F., Freels S., Laws E.R., Jr. and Menck H.R. Brain tumor survival: results from the National Cancer Data Base. *J Neurooncol*, 1998 40(2): 151-160.
16. Deorah S., Lynch C.F., Sibenaller Z.A. and Ryken T.C. Trends in brain cancer incidence and survival in the United States: Surveillance, Epidemiology, and End Results Program, 1973 to 2001. *Neurosurg Focus*, 2006 20(4): E1.
17. Zalutsky M.R. Targeted radiotherapy of brain tumours. *Br J Cancer*, 2004 90(8): 1469-1473.
18. Reardon D.A., Akabani G., Coleman R.E., Friedman A.H., Friedman H.S., Herndon J.E., 2nd, *et al.* Salvage radioimmunotherapy with murine iodine-131-labeled antitenascin monoclonal antibody 81C6 for patients with recurrent primary and metastatic malignant brain tumors: phase II study results. *J Clin Oncol*, 2006 24(1): 115-122.

19. Paganelli G., Bartolomei M., Grana C., Ferrari M., Rocca P. and Chinol M. Radioimmunotherapy of brain tumor. *Neurol Res*, 2006 28(5): 518-522.
20. Westphal M., Hilt D.C., Bortey E., Delavault P., Olivares R., Warnke P.C., *et al.* A phase 3 trial of local chemotherapy with biodegradable carmustine (BCNU) wafers (Gliadel wafers) in patients with primary malignant glioma. *Neuro-oncol*, 2003 5(2): 79-88.
21. Westphal M., Ram Z., Riddle V., Hilt D. and Bortey E. Gliadel wafer in initial surgery for malignant glioma: long-term follow-up of a multicenter controlled trial. *Acta Neurochir (Wien)*, 2006 148(3): 269-275; discussion 275.
22. Batchelor T.T., Sorensen A.G., di Tomaso E., Zhang W.T., Duda D.G., Cohen K.S., *et al.* AZD2171, a pan-VEGF receptor tyrosine kinase inhibitor, normalizes tumor vasculature and alleviates edema in glioblastoma patients. *Cancer Cell*, 2007 11(1): 83-95.
23. Mellinghoff I.K., Wang M.Y., Vivanco I., Haas-Kogan D.A., Zhu S., Dia E.Q., *et al.* Molecular determinants of the response of glioblastomas to EGFR kinase inhibitors. *N Engl J Med*, 2005 353(19): 2012-2024.
24. Simpson L. and Galanis E. Recurrent glioblastoma multiforme: advances in treatment and promising drug candidates. *Expert Rev Anticancer Ther*, 2006 6(11): 1593-1607.
25. Cutter J.L., Kurozumi K., Chiocca E.A. and Kaur B. Gene therapeutics: the future of brain tumor therapy? *Expert Rev Anticancer Ther*, 2006 6(7): 1053-1064.
26. Aghi M. and Chiocca E.A. Gene therapy for glioblastoma. *Neurosurg Focus*, 2006 20(4): E18.
27. Harrow S., Papanastassiou V., Harland J., Mabbs R., Petty R., Fraser M., *et al.* HSV1716 injection into the brain adjacent to tumour following surgical resection of high-grade glioma: safety data and long-term survival. *Gene Ther*, 2004 11(22): 1648-1658.
28. Immonen A., Vapalahti M., Tyynela K., Hurskainen H., Sandmair A., Vanninen R., *et al.* AdvHSV-tk gene therapy with intravenous ganciclovir improves survival in human malignant glioma: a randomised, controlled study. *Mol Ther*, 2004 10(5): 967-972.
29. Klatzmann D., Valery C.A., Bensimon G., Marro B., Boyer O., Mokhtari K., *et al.* A phase I/II study of herpes simplex virus type 1 thymidine kinase "suicide" gene therapy for recurrent glioblastoma. Study Group on Gene Therapy for Glioblastoma. *Hum Gene Ther*, 1998 9(17): 2595-2604.
30. Markert J.M., Medlock M.D., Rabkin S.D., Gillespie G.Y., Todo T., Hunter W.D., *et al.* Conditionally replicating herpes simplex virus mutant, G207 for the treatment of malignant glioma: results of a phase I trial. *Gene Ther*, 2000 7(10): 867-874.
31. Papanastassiou V., Rampling R., Fraser M., Petty R., Hadley D., Nicoll J., *et al.* The potential for efficacy of the modified (ICP 34.5(-)) herpes simplex virus HSV1716 following intratumoural injection into human malignant glioma: a proof of principle study. *Gene Ther*, 2002 9(6): 398-406.
32. Prados M.D., McDermott M., Chang S.M., Wilson C.B., Fick J., Culver K.W., *et al.* Treatment of progressive or recurrent glioblastoma multiforme in adults with herpes simplex virus thymidine kinase gene vector-producer cells followed by intravenous ganciclovir administration: a phase I/II multi-institutional trial. *J Neurooncol*, 2003 65(3): 269-278.
33. Ram Z., Culver K.W., Oshiro E.M., Viola J.J., DeVroom H.L., Otto E., *et al.* Therapy of malignant brain tumors by intratumoral implantation of retroviral vector-producing cells. *Nat Med*, 1997 3(12): 1354-1361.
34. Sandmair A.M., Loimas S., Puranen P., Immonen A., Kossila M., Puranen M., *et al.* Thymidine kinase gene therapy for human malignant glioma, using replication-deficient retroviruses or adenoviruses. *Hum Gene Ther*, 2000 11(16): 2197-2205.
35. Shand N., Weber F., Mariani L., Bernstein M., Gianella-Borradori A., Long Z., *et al.* A phase 1-2 clinical trial of gene therapy for recurrent glioblastoma multiforme by tumor transduction with the herpes simplex thymidine kinase gene followed by ganciclovir. GLI328 European-Canadian Study Group. *Hum Gene Ther*, 1999 10(14): 2325-2335.

36. Trask T.W., Trask R.P., Aguilar-Cordova E., Shine H.D., Wyde P.R., Goodman J.C., *et al.* Phase I study of adenoviral delivery of the HSV-tk gene and ganciclovir administration in patients with current malignant brain tumors. *Mol Ther*, 2000 1(2): 195-203.
37. Hemminki A., Belousova N., Zinn K.R., Liu B., Wang M., Chaudhuri T.R., *et al.* An adenovirus with enhanced infectivity mediates molecular chemotherapy of ovarian cancer cells and allows imaging of gene expression. *Mol Ther*, 2001 4(3): 223-231.
38. Zinn K.R., Chaudhuri T.R., Krasnykh V.N., Buchsbaum D.J., Belousova N., Grizzle W.E., *et al.* Gamma camera dual imaging with a somatostatin receptor and thymidine kinase after gene transfer with a bicistronic adenovirus in mice. *Radiology*, 2002 223(2): 417-425.
39. Dempsey M.F., Wyper D., Owens J., Pimlott S., Papanastassiou V., Patterson J., *et al.* Assessment of ^{123}I-FIAU imaging of herpes simplex viral gene expression in the treatment of glioma. *Nucl Med Commun*, 2006 27(8): 611-617.
40. Wiebe L.I., Knaus E.E. and Morin K.W. Radiolabelled pyrimidine nucleosides to monitor the expression of HSV-1 thymidine kinase in gene therapy. *Nucleosides Nucleotides*, 1999 18(4-5): 1065-1066.
41. Nanda D., de Jong M., Vogels R., Havenga M., Driesse M., Bakker W., *et al.* Imaging expression of adenoviral HSV1-tk suicide gene transfer using the nucleoside analogue FIRU. *Eur J Nucl Med Mol Imaging*, 2002 29(7): 939-947.
42. Vandier D., Rixe O., Besnard F., Kim M., Rikiyama T., Goldsmith M., *et al.* Inhibition of glioma cells *in vitro* and *in vivo* using a recombinant adenoviral vector containing an astrocyte-specific promoter. *Cancer Gene Ther*, 2000 7(8): 1120-1126.
43. Boviatsis E.J., Park J.S., Sena-Esteves M., Kramm C.M., Chase M., Efird J.T., *et al.* Long-term survival of rats harboring brain neoplasms treated with ganciclovir and a herpes simplex virus vector that retains an intact thymidine kinase gene. *Cancer Res*, 1994 54(22): 5745-5751.
44. Freeman S.M., Abboud C.N., Whartenby K.A., Packman C.H., Koeplin D.S., Moolten F.L., *et al.* The "bystander effect": tumor regression when a fraction of the tumor mass is genetically modified. *Cancer Res*, 1993 53(21): 5274-5283.
45. Nestler U., Wakimoto H., Siller-Lopez F., Aguilar L.K., Chakravarti A., Muzikansky A., *et al.* The combination of adenoviral HSV TK gene therapy and radiation is effective in athymic mouse glioblastoma xenografts without increasing toxic side effects. *J Neurooncol*, 2004 67(1-2): 177-188.
46. Kim J.H., Kolozsvary A., Rogulski K., Khil M.S., Brown S.L. and Freytag S.O. Selective radiosensitization of 9L glioma in the brain transduced with double suicide fusion gene. *Cancer J Sci Am*, 1998 4(6): 364-369.
47. de Jong M., Breeman W.A., Valkema R., Bernard B.F. and Krenning E.P. Combination radionuclide therapy using ^{177}Lu- and ^{90}Y-labeled somatostatin analogs. *J Nucl Med*, 2005 46 Suppl 1: 13S-17S.
48. Kuriyama S., Mitoro A., Yamazaki M., Tsujinoue H., Nakatani T., Akahane T., *et al.* Comparison of gene therapy with the herpes simplex virus thymidine kinase gene and the bacterial cytosine deaminase gene for the treatment of hepatocellular carcinoma. *Scand J Gastroenterol*, 1999 34(10): 1033-1041.
49. Trinh Q.T., Austin E.A., Murray D.M., Knick V.C. and Huber B.E. Enzyme/prodrug gene therapy: comparison of cytosine deaminase/5-fluorocytosine versus thymidine kinase/ganciclovir enzyme/prodrug systems in a human colorectal carcinoma cell line. *Cancer Res*, 1995 55(21): 4808-4812.
50. Maini C.L., Sciuto R., Tofani A., Ferraironi A., Carapella C.M., Occhipinti E., *et al.* Somatostatin receptor imaging in CNS tumours using ^{111}In-octreotide. *Nucl Med Commun*, 1995 16(9): 756-766.

51. Bohuslavizki K.H., Brenner W., Braunsdorf W.E., Behnke A., Tinnemeyer S., Hugo H.H., *et al.* Somatostatin receptor scintigraphy in the differential diagnosis of meningioma. *Nucl Med Commun*, 1996 17(4): 302-310.
52. Klutmann S., Bohuslavizki K.H., Brenner W., Behnke A., Tietje N., Kroger S., *et al.* Somatostatin receptor scintigraphy in postsurgical follow-up examinations of meningioma. *J Nucl Med*, 1998 39(11): 1913-1917.
53. Henze M., Schuhmacher J., Hipp P., Kowalski J., Becker D.W., Doll J., *et al.* PET imaging of somatostatin receptors using [^{68}GA]DOTA-D-Phe^{1}-Tyr^{3}-octreotide: first results in patients with meningiomas. *J Nucl Med*, 2001 42(7): 1053-1056.
54. Henze M., Dimitrakopoulou-Strauss A., Milker-Zabel S., Schuhmacher J., Strauss L.G., Doll J., *et al.* Characterization of ^{68}Ga-DOTA-D-Phe^{1}-Tyr^{3}-octreotide kinetics in patients with meningiomas. *J Nucl Med*, 2005 46(5): 763-769.
55. Nathoo N., Ugokwe K., Chang A.S., Li L., Ross J., Suh J.H., *et al.* The role of 111indium-octreotide brain scintigraphy in the diagnosis of cranial, dural-based meningiomas. *J Neurooncol*, 2007 81(2): 167-174.
56. de Jong M., Rolleman E.J., Bernard B.F., Visser T.J., Bakker W.H., Breeman W.A., *et al.* Inhibition of renal uptake of indium-111-DTPA-octreotide *in vivo*. *J Nucl Med*, 1996 37(8): 1388-1392.
57. Bodei L., Cremonesi M., Zoboli S., Grana C., Bartolomei M., Rocca P., *et al.* Receptor-mediated radionuclide therapy with ^{90}Y-DOTATOC in association with amino acid infusion: a phase I study. *Eur J Nucl Med Mol Imaging*, 2003 30(2): 207-216.
58. Jamar F., Barone R., Mathieu I., Walrand S., Labar D., Carlier P., *et al.* ^{86}Y-DOTA^{0}-D-Phe^{1}-Tyr^{3}-octreotide (SMT487)--a phase 1 clinical study: pharmacokinetics, biodistribution and renal protective effect of different regimens of amino acid co-infusion. *Eur J Nucl Med Mol Imaging*, 2003 30(4): 510-518.
59. Rolleman E.J., Valkema R., de Jong M., Kooij P.P. and Krenning E.P. Safe and effective inhibition of renal uptake of radiolabelled octreotide by a combination of lysine and arginine. *Eur J Nucl Med Mol Imaging*, 2003 30(1): 9-15.
60. Barone R., Pauwels S., De Camps J., Krenning E.P., Kvols L.K., Smith M.C., *et al.* Metabolic effects of amino acid solutions infused for renal protection during therapy with radiolabelled somatostatin analogues. *Nephrol Dial Transplant*, 2004 19(9): 2275-2281.
61. Bernard B.F., Krenning E., Breeman W.A., Visser T.J., Bakker W.H., Srinivasan A., *et al.* Use of the rat pancreatic CA20948 cell line for the comparison of radiolabelled peptides for receptor-targeted scintigraphy and radionuclide therapy. *Nucl Med Commun*, 2000 21(11): 1079-1085.
62. Behr T.M. and Behe M.P. Cholecystokinin-B/Gastrin receptor-targeting peptides for staging and therapy of medullary thyroid cancer and other cholecystokinin-B receptor-expressing malignancies. *Semin Nucl Med*, 2002 32(2): 97-109.
63. Breeman W.A., Hofland L.J., de Jong M., Bernard B.F., Srinivasan A., Kwekkeboom D.J., *et al.* Evaluation of radiolabelled bombesin analogues for receptor-targeted scintigraphy and radiotherapy. *Int J Cancer*, 1999 81(4): 658-665.
64. van Hagen P.M., Breeman W.A., Bernard H.F., Schaar M., Mooij C.M., Srinivasan A., *et al.* Evaluation of a radiolabelled cyclic DTPA-RGD analogue for tumour imaging and radionuclide therapy. *Int J Cancer*, 2000 90(4): 186-198.

5.2 Samenvatting en conclusies

Bijna twee decennia geleden werd ontdekt dat somatostatine receptoren (sst), voornamelijk van het subtype 2 (sst_2), tot overexpressie komen op neuro-endocriene tumoren [1]. Daar het humane somatostatine (ss) hormoon snel wordt afgebroken na injectie in de bloedbaan van een patiënt, werden er stabiele peptidenderivaten van somatostatine gemaakt, waarvan octreotide momenteel het meest gebruikte ss-peptide (eiwit) in patiënten is [2, 3]. Stabiele peptidederivaten binden, na injectie in de bloedbaan, aan sst op weefsels die receptor-positief zijn waarna ze worden geïnternaliseerd in (tumor)cellen die sst tot expressie brengen. Dit mechanisme bleek erg nuttig voor visualisatie en therapie van sst-positieve tumoren, waarbij gebruik wordt gemaakt van ss-peptidederivaten die gelabeld zijn met radioactiviteit.

Voor visualisatie van stabiele, radioactieve ss-peptidederivaten en hun distributie in patiënten worden momenteel verbindingen gebruikt als [^{111}In-DTPA^{0}]octreotide (Octreoscan) [2, 4], ^{177}Lu gelabeld [DOTA^{0},Tyr^{3}]octreotate (DOTAtate) [5, 6], [^{99m}Tc-N_4^{0-1},Asp^{0},Tyr^{3}]octreotate (Demotate) [7, 8] en [^{90}Y-DOTA^{0},Tyr^{3}]octreotide (DOTATOC) [4, 9, 10]. Deze radioactieve peptidederivaten worden gebruikt voor zowel klinische als preklinische evaluatie van sst-positieve tumoren. Visualisatie van tumoren met behulp van radiogelabelde peptidederivaten wordt "peptide receptor scintigrafie" (PRS) genoemd, waarbij gebruik wordt gemaakt van radionucliden (radioactiviteit) die γ-straling uitzenden (bijvoorbeeld ^{99m}Tc en ^{111}In). Wanneer ss-peptiden worden gekoppeld aan radionucliden die α- of β-straling uitzenden, zoals ^{177}Lu, ^{213}Bi of ^{90}Y, wordt het mogelijk om tumoren gericht te bestralen omdat de peptiden binden en internaliseren aan sst op tumorcellen. Deze manier van bestraling kan ervoor zorgen dat de tumor kleiner wordt zonder dat er invasief moet worden ingegrepen. Dit concept wordt "peptide receptor radionuclide therapie" (PRRT) genoemd en is erg effectief in de behandeling van neuro-endocriene tumoren [11, 12].

In 1987 vond Reubi et al. dat ook kwaadaardige hersentumoren, zoals astrocytoma's en oligodendroglioma's, sst tot expressie brengen, terwijl slecht gedifferentieerde tumoren, zoals glioblastoma multiforme (GBM), dat niet doen [13]. GBM is een erg agressieve tumor afkomstig uit de hersenen en de huidige behandelingen van dit type tumor is niet curatief. De palliatieve behandeling bestaat uit chirurgie, bestraling en chemotherapie en dit leidt tot een mediane overleving van minder dan een jaar [14-16]. Doordat GBM infiltratief groeit (d.w.z. tumorcellen groeien tussen gezond weefsel) is het bijna onmogelijk om elke tumorcel te verwijderen; daardoor zullen alle GBM's terugkeren, meestal binnen 2 tot 3 cm van de originele tumor locatie.

Aangezien sst-expressie niet werd gevonden bij GBM-tumoren is het niet waarschijnlijk dat PRRT met radiogelabelde sst peptidederivaten effectief zal zijn bij de behandeling van deze patiënten. Momenteel zijn radioimmunotherapie [17-19], chemotherapie [20, 21], anti-angiogenese-therapie [22, 23] en gentherapie [24-26] experimentele behandelingen voor GBM-patiënten. Gentherapie is een aantrekkelijke

behandelingsoptie voor patiënten met een GBM, omdat de tumoren groeien in de omsloten locatie van de schedel en vanwege de kleine kans op metastasen buiten de schedel. Helaas zou het infiltrerende karakter van een GBM een nadeel kunnen zijn voor het gebruik van gentherapie voor deze patiëntengroep.

De resultaten van klinische studies met virale gentherapie in GBM-patiënten lieten zien dat virale injectie in patiënten veilig is en dat er soms sprake was van een antitumor effect [27-36]. Helaas werden er in deze studies geen complete responsen geobserveerd. Statistisch significant langere overleving werd wel waargenomen in twee kleine gerandomiseerde studies [28, 34]. Hieruit blijkt dat gentherapie-strategieën voor GBM verbeterd moeten worden ten einde een effectievere therapie te verkrijgen.

Het doel van de studies die in hoofdstuk 2 van dit proefschrift zijn beschreven was te onderzoeken wat de bruikbaarheid van de Ad5.tk.sst_2 adenovirale vector is voor klinische toepassing in GBM-tumoren. Deze vector is eerder gebruikt in preklinische studies voor ovariumkanker (eierstokkanker) [37] en longkanker [38] en het bevat twee genen: het sst_2-gen en het Herpes Simplex Virus thymidine kinase (HSV-tk) gen. Expressie van sst_2 in viraal geïnfecteerde tumorcellen kan worden gevisualiseerd door gebruik te maken van radioactief gelabelde peptidederivaten zoals hiervoor beschreven. Daarnaast kan het sst_2-gen ook gebruikt worden voor behandeling van geïnfecteerde tumorcellen met behulp van ss-peptidederivaten gelabeld met β-straling voor therapie. Het HSV-tk-gen in deze vector kan ook gebruikt worden voor zowel visualisatie als therapeutische toepassing: na de expressie van HSV-tk wordt een antivirale "prodrug", zoals ganciclovir (GCV), toegediend en dit leidt tot de fosforylering van GCV in GCV-monofosfaat en uiteindelijk in GCV-trifosfaat. Deze laatst genoemde verbinding wordt vastgehouden in de cel en is toxisch voor delende cellen. In cellen waar HSV-tk niet tot expressie komt, vindt deze fosforylering niet plaats, waardoor GCV niet toxisch is voor deze cellen. Nucleosiden, zoals FIAU [39] en FIRU [40, 41], worden op een zelfde manier als GCV gefosforyleerd en kunnen gelabeld worden met radioactief jodium (bijvoorbeeld ^{123}I) voor visualisatie-doeleinden (zie ook hoofdstuk 1.1, figuur 4 en 5). Gefosforyleerde producten van FIAU en FIRU zijn niet toxisch voor cellen.

In **hoofdstuk 2.1** hebben we de *in vitro* opname van [^{111}In-DOTA,Tyr^3]octreotate (toont sst_2 expressie aan) en [^{125}I]FIRU (toont HSV-tk expressie aan) vergeleken in verschillende Ad5.tk.sst_2 geïnfecteerde GBM-cellijnen. De cellijnen die in deze experimenten zijn gebruikt, brengen onder normale omstandigheden geen sst_2 en HSV-tk tot expressie. Twee dagen na infectie met Ad5.tk.sst_2 werden internalisatie-studies gedaan en de resultaten lieten zien dat de opname van de bovengenoemde radioactieve verbindingen afhankelijk was van de concentratie virussen die gebruikt

zijn om de tumorcellen te infecteren. Wat opviel aan deze resultaten was dat de opname van [^{111}In-DOTA,Tyr^3]octreotate in alle gebruikte cellijnen hoger was dan de opname van [^{125}I]FIRU, wat een aanwijzing kan zijn dat visualisatie met behulp van peptidederivaten voor sst_2 de voorkeur heeft boven de visualisatie met nucleosiden voor HSV-tk. Zowel *in vitro* als in proefdierstudies is echter gebleken dat therapie waarbij HSV-tk-expressie in combinatie met GCV werd gebruikt effectief is in GBM tumormodellen [42-44]. Deze strategie is ook effectief gebleken in combinatie met externe bestraling [45, 46]. Voor GBM-patiënten zou een potentieel effectieve behandeling kunnen zijn: Ad5.tk.sst_2 infectie met daaropvolgend een combinatietherapie van GCV met ^{177}Lu of ^{90}Y gelabelde ss-peptidederivaten.

Virale infectie en visualisatie van genexpressie werd verder onderzocht *in vivo* in **hoofdstuk 2.2**. Proefdieren met een U87MG-tumor (een humane GBM-cellijn) onder de huid werden geïnfecteerd met Ad5.tk.sst_2 via een injectie in de tumor. Drie dagen later werd sst_2- en HSV-tk-genexpressie gevisualiseerd met het ss peptidederivaat ^{99m}Tc-Demotate en het HSV-tk nucleoside [^{123}I]FIRU. We hebben gevonden dat beide radioactieve tracers (verbindingen) gebruikt kunnen worden om sst_2 en HSV-tk genexpressie niet-invasief te visualiseren in Ad5.tk.sst_2 geïnfecteerde GBM-tumoren. Daarnaast is het mogelijk gebleken om sst_2-expressie in deze tumoren met behulp van SPECT-scans gedurende een week na virale infectie te volgen, waarbij de totale opname van de ss-tracer in de tumor gedurende die week afnam. Dit kan worden verklaard door het feit dat het genetisch materiaal van adenovirussen niet integreert in het genoom van de geïnfecteerde cel. Terwijl de tumor gedurende een week blijft groeien, wordt de expressie van virale genen verdeeld over de dochtercellen, wat leidt tot minder genexpressie per tumorvolume. Een mogelijk tweede verklaring kan zijn dat het immuunsysteem de virale genexpressie verwijdert, waardoor er na een week minder opname is van de radioactieve tracer. Ondanks dat we dit niet hebben onderzocht in dit tumormodel vermoeden we dat deze reductie in genexpressie ook geldt voor het HSV-tk-gen, omdat we hebben gevonden dat beide genen tegelijk tot expressie komen na virale infectie. Verder hebben we nog gevonden dat beide genen niet homogeen in het geïnfecteerde tumorweefsel tot expressie komen. Helaas is dit een aanwijzing voor één van de problemen in klinische gentherapie studies voor GBM-patiënten: inhomogene genexpressie leidt tot een inefficiënte behandeling van de tumorcellen (therapeutische stoffen komen niet bij elke tumorcel) en daardoor wordt een lage respons op de behandeling waargenomen bij deze patiënten.

Om de penetratie van adenovirale vectoren in tumorweefsel te verbeteren is eerder voorgesteld om een techniek als “convection enhanced delivery” (CED), oftewel het heel langzaam infunderen van macromoleculen, te gebruiken. In **hoofdstuk 2.3** hebben we onderzocht of CED beter is voor de intratumorale verspreiding van Ad5.tk.sst_2 dan een enkele injectie of meerdere injecties, terwijl het totale toegediende

aantal virussen gelijk bleef in alle behandelingen. De resultaten van deze experimenten lieten zien dat er vergelijkbare gedeelten van de tumor geïnfecteerd zijn met het virus na CED en een enkele virus-injectie. Echter, meerdere injecties van Ad5.tk.sst$_2$ resulteerden in een groter geïnfecteerd gebied in de tumor. Daarom zijn meerdere injecties de meest geschikte methode voor intratumorale toediening van virale vectoren in GBM's.

De resultaten in hoofdstukken 2.2 en 2.3 geven aan dat het nodig is om de distributie van Ad5.tk.sst$_2$ in het tumorweefsel na injectie te verbeteren. Dit kan bereikt worden door een (conditioneel) replicerende of oncolytische virale vector. Via deze methode is het mogelijk dat meer tumorcellen bereikt worden omdat meer virusdeeltjes worden gevormd tijdens replicatie. Dit resulteert in lysis van de tumorcel (de tumorcel barst open), wat leidt tot het vrijkomen van meer virusdeeltjes in het tumorweefsel. Vanwege de inhomogene genexpressie na virale infectie is het mogelijk dat een combinatietherapie van GCV en ^{177}Lu-DOTA-tate niet zal leiden tot een complete genezing van de tumor. Mogelijk kan het gebruik van ^{90}Y-gelabelde ss-peptidederivaten het therapeutisch effect verhogen in vergelijking met ^{177}Lu-gelabelde peptiden, vanwege de hogere energie van ^{90}Y-elektronen, waardoor een groter tumorgebied kan worden bestraald [47]. Een andere benadering is om de efficiëntie van de combinatietherapie te verhogen door gebruik te maken van het cytosine deaminase gen in combinatie met 5-FU (in plaats van de HSV-tk/GCV combinatie). Resultaten van studies in lever- en colorectale tumorcellijnen suggereren dat deze combinatie mogelijk effectiever is in het doden van tumorcellen dan het HSV-tk/GCV-systeem [48, 49].

In de hierboven beschreven experimenten werd aangetoond dat enkele dagen na infectie met Ad5.tk.sst$_2$ expressie van virale genen in het tumorweefsel aanwezig is. Helaas laten deze studies niet de distributie van het virus zelf, direct na injectie, zien. Om het virus zelf *in vivo* te visualiseren hebben we (**hoofdstuk 2.4**) de virusdeeltjes zelf gelabeld met radioactiviteit, waarbij we gebruik hebben gemaakt van ^{99m}Tc en een tricarbonyl-labeling agens. Uit de resultaten bleek dat Ad5.tk.sst$_2$ inderdaad gelabeld kan worden met ^{99m}Tc, wat de mogelijkheid biedt om de virusdeeltjes direct na injectie te volgen. Proefdieren met ofwel een 9L-tumor ofwel een U87MG-tumor (beide tumoren zijn modellen voor GBM) werden intratumoraal geïnjecteerd met ^{99m}Tc-gelabeld Ad5.tk.sst$_2$, waarna deze virussen werden gevolgd met behulp van een gamma camera of SPECT camera. Uit de resultaten bleek dat er een hoge opname van radioactiviteit in de tumor is na injectie met ^{99m}Tc-Ad5.tk.sst$_2$; er was nauwelijks radioactiviteit in andere organen te zien. *In vitro* infectie met ^{99m}Tc-Ad5.tk.sst$_2$ in U251-, U87MG- en 9L-tumorcellen resulteerde in een tijdsafhankelijke opname van ^{99m}Tc-activiteit. Dit komt overeen met de cellulaire infectie van het virus, omdat we ook hebben aangetoond dat ongebonden, vrije ^{99m}Tc-moleculen

vrijwel niet in de tumorcellen kunnen komen. Tevens vonden we dat de ^{99m}Tc-Ad5.tk.sst$_2$-virusdeeltjes nog in staat zijn om genexpressie te veroorzaken zowel *in vitro* als *in vivo*, ofschoon de expressie lager was dan in cellen die geïnfecteerd werden met ongelabelde virusdeeltjes. We hebben berekend dat de virusdeeltjes tijdens de labelingsprocedure een stralingsdosis van 5.8 Gy opdoen door de ^{99m}Tc-straling. Hierbij hebben we een overdosis ^{99m}Tc-activiteit toegevoegd om ervoor te zorgen dat alle virusdeeltjes zouden worden gelabeld. Dit zou een verklaring kunnen zijn voor het verschil in genexpressie in de cellen geïnfecteerd met radiogelabelde en ongelabelde virusdeeltjes. Het is mogelijk om de labeling van de virusdeeltjes te optimaliseren, waardoor de stralingsdosis voor de virusdeeltjes wordt gereduceerd. Ondanks de hoge stralingsdosis, waarbij mogelijk virusdeeltjes verloren gaan, is deze methode nog steeds erg interessant voor klinische studies om de virusdeeltjes na injectie in de patiënt te volgen. Verdere optimalisering van de radiolabeling is daarbij noodzakelijk.

Naast gentherapie als mogelijke behandelingsmethode voor GBM-patiënten hebben we ook onderzocht of PRS en PRRT met behulp van peptidederivaten gebruikt kan worden voor patiënten met tumoren die gelokaliseerd zijn in de schedel. Zoals al eerder genoemd, is er geen sst-expressie gevonden op GBM-tumorweefsel, maar wel in gedifferentieerd tumorweefsel van gliale afkomst [13, 50]. Daarnaast zouden andere peptide-receptoren, zoals vasoactive intestinal peptide (VIP) receptor, neurokinine 1 (NK-1) receptor, gastrin-releasing peptide (GRP) receptor, cholecystokinin 2 (CCK-2) receptor, neurotensine (NT) receptor en epidermal growth factor (EGF) receptor, ook interessant kunnen zijn voor visualisatie en therapie-doeleinden in deze patiënten. In **hoofdstuk 3.1** hebben we daarom de receptor-expressie-status bestudeerd van hersentumor-cellijnen en drie groepen humaan intra-craniaal tumorweefsel. De drie groepen waren: GBM's, meningioma's (MG, hersenvlies tumoren), en metastasen gelokaliseerd in de hersenen (MT, metastasen waarvan de oorspronkelijke tumor was gelokaliseerd in ander organen dan de hersenen). Daarnaast hebben we ook monsters van normale humane hersenen ("normal brain", NB) bestudeerd. Deze tumorcellijnen en -weefsels hebben we met behulp van internalisatie- en autoradiografie-studies getest op de aanwezigheid van de bovengenoemde receptoren. De resultaten van deze studies lieten zien dat VIP-receptoren in hoge densiteit en incidentie worden gevonden op bijna alle GBM-, MG- en MT-tumoren, terwijl NB-weefsels doorgaans geen VIP-expressie vertoonden. Deze receptor zou daarom een interessante target kunnen zijn voor PRS en PRRT. Bovendien werden in de onderzochte GBM-weefsels ook EGF- en NK-1-receptoren in grote mate tot expressie gebracht. Het gebruik van kleine radiogelabelde peptiden voor visualisatie en therapie is interessant voor de behandeling van GBM's, omdat deze kleine moleculen theoretisch door de

hersenen kunnen diffunderen, waardoor infiltrerende tumorcellen op een afstand van de primaire tumor ook "getarget" kunnen worden. Als bevestiging van eerdere resultaten hebben we gevonden dat MG-weefsels in hoge densiteit en incidentie sst_2 tot expressie brengen [13, 50]. Verschillende publicaties hebben al laten zien dat MG-tumoren kunnen worden gevisualiseerd met radiogelabelde ss-peptidederivaten [51-55]. Onlangs heeft het Erasmus MC PRRT studies gedaan in een kleine groep MG-patiënten, waarbij therapeutische doses van [^{177}Lu-DOTA,Tyr^3]octreotate werden geïnjecteerd [6]. Vijf "eindstadium"-patiënten met grote tumoren werden behandeld; vier patiënten hadden progressieve ziekte toen de studie begon en de behandeling resulteerde in een stabilisatie van de tumorgroei in één patiënt, terwijl de andere drie patiënten helaas progressief bleven. De vijfde patiënt was stabiel aan het begin van de therapie en dit bleef onveranderd na de PRRT-behandeling. Deze resultaten zijn bemoedigend voor PRRT met behulp van radiogelabelde ss-peptidederivaten als mogelijke therapie in MG-patiënten, zeker wanneer PRRT eerder in het verloop van de ziekte wordt gedaan of mogelijk in combinatie met andere therapieën.

Na intraveneuze injectie van radioactieve ss-peptiden wordt binnen 24 uur een groot gedeelte van de radioactiviteit uitgescheiden door het lichaam. De radiogelabelde peptiden worden uit het bloed gefilterd door de nieren, maar een deel van de radioactiviteit blijft na reabsorptie in de proximale tubulaire cellen van de nieren, wat leidt tot een hoge stralingdosis in deze stralingsgevoelige organen. In eerdere studies in ratten [56] en mensen [57-59] is ontdekt dat positief geladen aminozuren, zoals lysine en arginine, de opname van radioactiviteit in de nieren met 40-50% reduceert. In de studie van Barone et al. werd gevonden dat een tien uur durende infusie van aminozuren in patiënten de hoogste reductie van radioactiviteit in de nieren gaf [60]. Deze langdurige infusie is echter erg arbeidsintensief voor verplegend personeel en onaangenaam voor PRRT-patiënten. In **hoofdstuk 3.2** onderzochten we in gezonde ratten of oraal toegediende lysine een vergelijkbare reductie van radioactiviteit in de nieren geeft als intraveneus toegediende lysine. De resultaten tonen aan dat zowel intraveneus als oraal toegediende lysine de opname van radioactiviteit in de nieren met 40% reduceert. Deze methode van oraal toegediende aminozuren is mogelijk een patiëntvriendelijk alternatief voor de lange infusies die momenteel toegepast worden.

In **hoofdstuk 4** hebben we de *in vitro* stralingsgevoeligheid onderzocht van de tumorcellijn CA20948, afkomstig van de pancreas (alvleesklier) van de rat. Deze cellijn brengt verschillende peptide-receptoren tot expressie, waaronder sst_2, GRP, CCK-2, $\alpha_v\beta_3$ (integrine receptor) en NK-1 [61-64] en wordt daardoor veel gebruikt in preklinische studies voor PRS en PRRT. We onderzochten de radiosensitiviteit

van de CA20948-cellijn met behulp van externe bestraling (XRT), wat de meest gebruikte methode voor dit soort onderzoek is. Echter, XRT is niet representatief voor PRRT behandeling vanwege het hogere dosistempo (tijd waarin een radioactieve dosis wordt afgegeven) en korte bestralingstijd. Daarom hebben we daarnaast ook radionuclidentherapie (RT) gedaan, waarbij we gebruik hebben gemaakt van het radionuclide ^{131}I. Dit radionuclide heeft vergelijkbare eigenschappen heeft als ^{177}Lu, het radionuclide dat gebruikt wordt in veel PRRT-studies. De resultaten van XRT en RT hebben we vergeleken, waarbij we hebben gevonden dat de overleving van CA20948-cellen bij lage doses straling voor beide therapieën vergelijkbaar was. Wanneer de stralingsdosis verhoogd werd, vonden we dat CA20948-cellen gevoeliger waren voor XRT dan voor RT. In patiënten wordt XRT doorgaans gefractioneerd gegeven in doses van 2 Gy per dag en bij deze dosis werd een vergelijkbare celoverleving van CA20948 gevonden bij behandeling met RT.

Concluderend kunnen we stellen dat de studies uit dit proefschrift uitwijzen dat Ad5.tk.sst$_2$ een erg interessante, nieuwe vector is voor gentherapie in GBM-patiënten. Zowel HSV-tk als sst$_2$ kunnen worden gebruikt als "targets" voor niet-invasieve visualisatie van genexpressie, hoewel scintigrafie met behulp van sst$_2$ onze voorkeur heeft. Het visualiseren van genexpressie is erg wenselijk voor het vervolgen van de genoverdracht in klinische studies. Bovendien kunnen deze twee genen beide (afzonderlijk of gecombineerd) gebruikt worden voor therapeutische doeleinden. Ten einde de distributie van het virus *in vivo* direct na injectie te kunnen volgen, kunnen adenovirale deeltjes worden gelabeld met ^{99m}Tc, wat kan leiden tot meer inzicht in de gebeurtenissen die volgen op het injecteren van het virus. Helaas is gebleken dat de spatiële distributie van deze vector in tumorweefsel erg laag is. Het gebruik van conditioneel replicerende virussen die HSV-tk en sst$_2$ tot expressie brengen, zou mogelijk kunnen leiden tot meer geïnfecteerde tumorcellen en daardoor een betere behandeling. Een nieuwe en zeer aantrekkelijke methode voor de behandeling van GBM zou PRRT met radiogelabelde peptiden kunnen zijn. In humane GBM-tumorweefsels hebben we naast een hoge dichtheid en incidentie van VIP-receptoren ook expressie gevonden EGF- en NK-1-receptoren. Dit zijn allemaal interessante "targets" voor PRRT-behandelingen in GBM-patiënten.

Referenties

1. Reubi J.C., Krenning E., Lamberts S.W. and Kvols L. Somatostatin receptors in malignant tissues. *J Steroid Biochem Mol Biol*, 1990 37(6): 1073-1077.
2. Krenning E.P., Kwekkeboom D.J., Bakker W.H., Breeman W.A., Kooij P.P., Oei H.Y., *et al.* Somatostatin receptor scintigraphy with [^{111}In-DTPA-D-Phe^{1}]- and [^{123}I-Tyr^{3}]-octreotide: the Rotterdam experience with more than 1000 patients. *Eur J Nucl Med*, 1993 20(8): 716-731.
3. Krenning E.P., Kwekkeboom D.J., Reubi J.C., van Hagen P.M., van Eijck C.H., Oei H.Y., *et al.* ^{111}In-octreotide scintigraphy in oncology. *Digestion*, 1993 54(Suppl 1): 84-87.
4. Valkema R., De Jong M., Bakker W.H., Breeman W.A., Kooij P.P., Lugtenburg P.J., *et al.* Phase I study of peptide receptor radionuclide therapy with [In-DTPA]octreotide: the Rotterdam experience. *Semin Nucl Med*, 2002 32(2): 110-122.
5. Kwekkeboom D.J., Bakker W.H., Kam B.L., Teunissen J.J., Kooij P.P., de Herder W.W., *et al.* Treatment of patients with gastro-entero-pancreatic (GEP) tumours with the novel radiolabelled somatostatin analogue [^{177}Lu-DOTA^{0},Tyr^{3}]octreotate. *Eur J Nucl Med Mol Imaging*, 2003 30(3): 417-422.
6. van Essen M., Krenning E.P., Kooij P.P., Bakker W.H., Feelders R.A., de Herder W.W., *et al.* Effects of therapy with [^{177}Lu-DOTA^{0},Tyr^{3}]octreotate in patients with paraganglioma, meningioma, small cell lung carcinoma, and melanoma. *J Nucl Med*, 2006 47(10): 1599-1606.
7. Maina T., Nock B., Nikolopoulou A., Sotiriou P., Loudos G., Maintas D., *et al.* [^{99m}Tc]Demotate, a new ^{99m}Tc-based [Tyr^{3}]octreotate analogue for the detection of somatostatin receptor-positive tumours: synthesis and preclinical results. *Eur J Nucl Med Mol Imaging*, 2002 29(6): 742-753.
8. Maina T., Nock B.A., Cordopatis P., Bernard B.F., Breeman W.A., van Gameren A., *et al.* [^{99m}Tc] Demotate 2 in the detection of sst$_2$-positive tumours: a preclinical comparison with [^{111}In] DOTA-tate. *Eur J Nucl Med Mol Imaging*, 2006 33(7): 831-840.
9. Otte A., Herrmann R., Heppeler A., Behe M., Jermann E., Powell P., *et al.* Yttrium-90 DOTATOC: first clinical results. *Eur J Nucl Med*, 1999 26(11): 1439-1447.
10. Chinol M., Bodei L., Cremonesi M. and Paganelli G. Receptor-mediated radiotherapy with Y-DOTA-DPhe-Tyr-octreotide: the experience of the European Institute of Oncology Group. *Semin Nucl Med*, 2002 32(2): 141-147.
11. Kwekkeboom D.J., Mueller-Brand J., Paganelli G., Anthony L.B., Pauwels S., Kvols L.K., *et al.* Overview of results of peptide receptor radionuclide therapy with 3 radiolabeled somatostatin analogs. *J Nucl Med*, 2005 46 Suppl 1: 62S-66S.
12. Teunissen J.J., Kwekkeboom D.J., de Jong M., Esser J.P., Valkema R. and Krenning E.P. Endocrine tumours of the gastrointestinal tract. Peptide receptor radionuclide therapy. *Best Pract Res Clin Gastroenterol*, 2005 19(4): 595-616.
13. Reubi J.C., Lang W., Maurer R., Koper J.W. and Lamberts S.W. Distribution and biochemical characterization of somatostatin receptors in tumors of the human central nervous system. *Cancer Res*, 1987 47(21): 5758-5764.
14. Salcman M. Survival in glioblastoma: historical perspective. *Neurosurgery*, 1980 7(5): 435-439.
15. Surawicz T.S., Davis F., Freels S., Laws E.R., Jr. and Menck H.R. Brain tumor survival: results from the National Cancer Data Base. *J Neurooncol*, 1998 40(2): 151-160.
16. Deorah S., Lynch C.F., Sibenaller Z.A. and Ryken T.C. Trends in brain cancer incidence and survival in the United States: Surveillance, Epidemiology, and End Results Program, 1973 to 2001. *Neurosurg Focus*, 2006 20(4): E1.
17. Zalutsky M.R. Targeted radiotherapy of brain tumours. *Br J Cancer*, 2004 90(8): 1469-1473.
18. Reardon D.A., Akabani G., Coleman R.E., Friedman A.H., Friedman H.S., Herndon J.E., 2nd, *et al.* Salvage radioimmunotherapy with murine iodine-131-labeled antitenascin monoclonal antibody 81C6 for patients with recurrent primary and metastatic malignant brain tumors: phase II study results. *J Clin Oncol*, 2006 24(1): 115-122.

19. Paganelli G., Bartolomei M., Grana C., Ferrari M., Rocca P. and Chinol M. Radioimmunotherapy of brain tumor. *Neurol Res*, 2006 28(5): 518-522.
20. Westphal M., Hilt D.C., Bortey E., Delavault P., Olivares R., Warnke P.C., *et al.* A phase 3 trial of local chemotherapy with biodegradable carmustine (BCNU) wafers (Gliadel wafers) in patients with primary malignant glioma. *Neuro-oncol*, 2003 5(2): 79-88.
21. Westphal M., Ram Z., Riddle V., Hilt D. and Bortey E. Gliadel wafer in initial surgery for malignant glioma: long-term follow-up of a multicenter controlled trial. *Acta Neurochir (Wien)*, 2006 148(3): 269-275; discussion 275.
22. Batchelor T.T., Sorensen A.G., di Tomaso E., Zhang W.T., Duda D.G., Cohen K.S., *et al.* AZD2171, a pan-VEGF receptor tyrosine kinase inhibitor, normalizes tumor vasculature and alleviates edema in glioblastoma patients. *Cancer Cell*, 2007 11(1): 83-95.
23. Mellinghoff I.K., Wang M.Y., Vivanco I., Haas-Kogan D.A., Zhu S., Dia E.Q., *et al.* Molecular determinants of the response of glioblastomas to EGFR kinase inhibitors. *N Engl J Med*, 2005 353(19): 2012-2024.
24. Simpson L. and Galanis E. Recurrent glioblastoma multiforme: advances in treatment and promising drug candidates. *Expert Rev Anticancer Ther*, 2006 6(11): 1593-1607.
25. Cutter J.L., Kurozumi K., Chiocca E.A. and Kaur B. Gene therapeutics: the future of brain tumor therapy? *Expert Rev Anticancer Ther*, 2006 6(7): 1053-1064.
26. Aghi M. and Chiocca E.A. Gene therapy for glioblastoma. *Neurosurg Focus*, 2006 20(4): E18.
27. Harrow S., Papanastassiou V., Harland J., Mabbs R., Petty R., Fraser M., *et al.* HSV1716 injection into the brain adjacent to tumour following surgical resection of high-grade glioma: safety data and long-term survival. *Gene Ther*, 2004 11(22): 1648-1658.
28. Immonen A., Vapalahti M., Tyynela K., Hurskainen H., Sandmair A., Vanninen R., *et al.* AdvHSV-tk gene therapy with intravenous ganciclovir improves survival in human malignant glioma: a randomised, controlled study. *Mol Ther*, 2004 10(5): 967-972.
29. Klatzmann D., Valery C.A., Bensimon G., Marro B., Boyer O., Mokhtari K., *et al.* A phase I/II study of herpes simplex virus type 1 thymidine kinase "suicide" gene therapy for recurrent glioblastoma. Study Group on Gene Therapy for Glioblastoma. *Hum Gene Ther*, 1998 9(17): 2595-2604.
30. Markert J.M., Medlock M.D., Rabkin S.D., Gillespie G.Y., Todo T., Hunter W.D., *et al.* Conditionally replicating herpes simplex virus mutant, G207 for the treatment of malignant glioma: results of a phase I trial. *Gene Ther*, 2000 7(10): 867-874.
31. Papanastassiou V., Rampling R., Fraser M., Petty R., Hadley D., Nicoll J., *et al.* The potential for efficacy of the modified (ICP 34.5(-)) herpes simplex virus HSV1716 following intratumoural injection into human malignant glioma: a proof of principle study. *Gene Ther*, 2002 9(6): 398-406.
32. Prados M.D., McDermott M., Chang S.M., Wilson C.B., Fick J., Culver K.W., *et al.* Treatment of progressive or recurrent glioblastoma multiforme in adults with herpes simplex virus thymidine kinase gene vector-producer cells followed by intravenous ganciclovir administration: a phase I/II multi-institutional trial. *J Neurooncol*, 2003 65(3): 269-278.
33. Ram Z., Culver K.W., Oshiro E.M., Viola J.J., DeVroom H.L., Otto E., *et al.* Therapy of malignant brain tumors by intratumoral implantation of retroviral vector-producing cells. *Nat Med*, 1997 3(12): 1354-1361.
34. Sandmair A.M., Loimas S., Puranen P., Immonen A., Kossila M., Puranen M., *et al.* Thymidine kinase gene therapy for human malignant glioma, using replication-deficient retroviruses or adenoviruses. *Hum Gene Ther*, 2000 11(16): 2197-2205.
35. Shand N., Weber F., Mariani L., Bernstein M., Gianella-Borradori A., Long Z., *et al.* A phase 1-2 clinical trial of gene therapy for recurrent glioblastoma multiforme by tumor transduction with the herpes simplex thymidine kinase gene followed by ganciclovir. GLI328 European-Canadian Study Group. *Hum Gene Ther*, 1999 10(14): 2325-2335.

36. Trask T.W., Trask R.P., Aguilar-Cordova E., Shine H.D., Wyde P.R., Goodman J.C., *et al.* Phase I study of adenoviral delivery of the HSV-tk gene and ganciclovir administration in patients with current malignant brain tumors. *Mol Ther*, 2000 1(2): 195-203.
37. Hemminki A., Belousova N., Zinn K.R., Liu B., Wang M., Chaudhuri T.R., *et al.* An adenovirus with enhanced infectivity mediates molecular chemotherapy of ovarian cancer cells and allows imaging of gene expression. *Mol Ther*, 2001 4(3): 223-231.
38. Zinn K.R., Chaudhuri T.R., Krasnykh V.N., Buchsbaum D.J., Belousova N., Grizzle W.E., *et al.* Gamma camera dual imaging with a somatostatin receptor and thymidine kinase after gene transfer with a bicistronic adenovirus in mice. *Radiology*, 2002 223(2): 417-425.
39. Dempsey M.F., Wyper D., Owens J., Pimlott S., Papanastassiou V., Patterson J., *et al.* Assessment of ^{123}I-FIAU imaging of herpes simplex viral gene expression in the treatment of glioma. *Nucl Med Commun*, 2006 27(8): 611-617.
40. Wiebe L.I., Knaus E.E. and Morin K.W. Radiolabelled pyrimidine nucleosides to monitor the expression of HSV-1 thymidine kinase in gene therapy. *Nucleosides Nucleotides*, 1999 18(4-5): 1065-1066.
41. Nanda D., de Jong M., Vogels R., Havenga M., Driesse M., Bakker W., *et al.* Imaging expression of adenoviral HSV1-tk suicide gene transfer using the nucleoside analogue FIRU. *Eur J Nucl Med Mol Imaging*, 2002 29(7): 939-947.
42. Vandier D., Rixe O., Besnard F., Kim M., Rikiyama T., Goldsmith M., *et al.* Inhibition of glioma cells *in vitro* and *in vivo* using a recombinant adenoviral vector containing an astrocyte-specific promoter. *Cancer Gene Ther*, 2000 7(8): 1120-1126.
43. Boviatsis E.J., Park J.S., Sena-Esteves M., Kramm C.M., Chase M., Efird J.T., *et al.* Long-term survival of rats harboring brain neoplasms treated with ganciclovir and a herpes simplex virus vector that retains an intact thymidine kinase gene. *Cancer Res*, 1994 54(22): 5745-5751.
44. Freeman S.M., Abboud C.N., Whartenby K.A., Packman C.H., Koeplin D.S., Moolten F.L., *et al.* The "bystander effect": tumor regression when a fraction of the tumor mass is genetically modified. *Cancer Res*, 1993 53(21): 5274-5283.
45. Nestler U., Wakimoto H., Siller-Lopez F., Aguilar L.K., Chakravarti A., Muzikansky A., *et al.* The combination of adenoviral HSV TK gene therapy and radiation is effective in athymic mouse glioblastoma xenografts without increasing toxic side effects. *J Neurooncol*, 2004 67(1-2): 177-188.
46. Kim J.H., Kolozsvary A., Rogulski K., Khil M.S., Brown S.L. and Freytag S.O. Selective radiosensitization of 9L glioma in the brain transduced with double suicide fusion gene. *Cancer J Sci Am*, 1998 4(6): 364-369.
47. de Jong M., Breeman W.A., Valkema R., Bernard B.F. and Krenning E.P. Combination radionuclide therapy using ^{177}Lu- and ^{90}Y-labeled somatostatin analogs. *J Nucl Med*, 2005 46 Suppl 1: 13S-17S.
48. Kuriyama S., Mitoro A., Yamazaki M., Tsujinoue H., Nakatani T., Akahane T., *et al.* Comparison of gene therapy with the herpes simplex virus thymidine kinase gene and the bacterial cytosine deaminase gene for the treatment of hepatocellular carcinoma. *Scand J Gastroenterol*, 1999 34(10): 1033-1041.
49. Trinh Q.T., Austin E.A., Murray D.M., Knick V.C. and Huber B.E. Enzyme/prodrug gene therapy: comparison of cytosine deaminase/5-fluorocytosine versus thymidine kinase/ganciclovir enzyme/prodrug systems in a human colorectal carcinoma cell line. *Cancer Res*, 1995 55(21): 4808-4812.
50. Maini C.L., Sciuto R., Tofani A., Ferraironi A., Carapella C.M., Occhipinti E., *et al.* Somatostatin receptor imaging in CNS tumours using ^{111}In-octreotide. *Nucl Med Commun*, 1995 16(9): 756-766.
51. Bohuslavizki K.H., Brenner W., Braunsdorf W.E., Behnke A., Tinnemeyer S., Hugo H.H., *et al.* Somatostatin receptor scintigraphy in the differential diagnosis of meningioma. *Nucl Med Commun*, 1996 17(4): 302-310.

52. Klutmann S., Bohuslavizki K.H., Brenner W., Behnke A., Tietje N., Kroger S., *et al.* Somatostatin receptor scintigraphy in postsurgical follow-up examinations of meningioma. *J Nucl Med*, 1998 39(11): 1913-1917.
53. Henze M., Schuhmacher J., Hipp P., Kowalski J., Becker D.W., Doll J., *et al.* PET imaging of somatostatin receptors using [^{68}Ga]DOTA-D-Phe^{1}-Tyr^{3}-octreotide: first results in patients with meningiomas. *J Nucl Med*, 2001 42(7): 1053-1056.
54. Henze M., Dimitrakopoulou-Strauss A., Milker-Zabel S., Schuhmacher J., Strauss L.G., Doll J., *et al.* Characterization of ^{68}Ga-DOTA-D-Phe^{1}-Tyr^{3}-octreotide kinetics in patients with meningiomas. *J Nucl Med*, 2005 46(5): 763-769.
55. Nathoo N., Ugokwe K., Chang A.S., Li L., Ross J., Suh J.H., *et al.* The role of 111indium-octreotide brain scintigraphy in the diagnosis of cranial, dural-based meningiomas. *J Neurooncol*, 2007 81(2): 167-174.
56. de Jong M., Rolleman E.J., Bernard B.F., Visser T.J., Bakker W.H., Breeman W.A., *et al.* Inhibition of renal uptake of indium-111-DTPA-octreotide *in vivo*. *J Nucl Med*, 1996 37(8): 1388-1392.
57. Bodei L., Cremonesi M., Zoboli S., Grana C., Bartolomei M., Rocca P., *et al.* Receptor-mediated radionuclide therapy with ^{90}Y-DOTATOC in association with amino acid infusion: a phase I study. *Eur J Nucl Med Mol Imaging*, 2003 30(2): 207-216.
58. Jamar F., Barone R., Mathieu I., Walrand S., Labar D., Carlier P., *et al.* ^{86}Y-DOTA^{0}-D-Phe^{1}-Tyr^{3}-octreotide (SMT487)--a phase 1 clinical study: pharmacokinetics, biodistribution and renal protective effect of different regimens of amino acid co-infusion. *Eur J Nucl Med Mol Imaging*, 2003 30(4): 510-518.
59. Rolleman E.J., Valkema R., de Jong M., Kooij P.P. and Krenning E.P. Safe and effective inhibition of renal uptake of radiolabelled octreotide by a combination of lysine and arginine. *Eur J Nucl Med Mol Imaging*, 2003 30(1): 9-15.
60. Barone R., Pauwels S., De Camps J., Krenning E.P., Kvols L.K., Smith M.C., *et al.* Metabolic effects of amino acid solutions infused for renal protection during therapy with radiolabelled somatostatin analogues. *Nephrol Dial Transplant*, 2004 19(9): 2275-2281.
61. Bernard B.F., Krenning E., Breeman W.A., Visser T.J., Bakker W.H., Srinivasan A., *et al.* Use of the rat pancreatic CA20948 cell line for the comparison of radiolabelled peptides for receptor-targeted scintigraphy and radionuclide therapy. *Nucl Med Commun*, 2000 21(11): 1079-1085.
62. Behr T.M. and Behe M.P. Cholecystokinin-B/Gastrin receptor-targeting peptides for staging and therapy of medullary thyroid cancer and other cholecystokinin-B receptor-expressing malignancies. *Semin Nucl Med*, 2002 32(2): 97-109.
63. Breeman W.A., Hofland L.J., de Jong M., Bernard B.F., Srinivasan A., Kwekkeboom D.J., *et al.* Evaluation of radiolabelled bombesin analogues for receptor-targeted scintigraphy and radiotherapy. *Int J Cancer*, 1999 81(4): 658-665.
64. van Hagen P.M., Breeman W.A., Bernard H.F., Schaar M., Mooij C.M., Srinivasan A., *et al.* Evaluation of a radiolabelled cyclic DTPA-RGD analogue for tumour imaging and radionuclide therapy. *Int J Cancer*, 2000 90(4): 186-198.

List of abbreviations

%IA/g	percentage injected activity per gram tissue
^{18}FDG	[^{18}F]fluoro-2-deoxyglucose
5-FU	5-fluorocytosine
AAV	adeno-associated virus
ACV	acyclovir
Ad5	adenovirus serotype 5
Ad5.tk.sst$_2$	adenoviral vector encoding both HSV-tk and sst$_2$
Ad5K	adenoviral knob
Adtk	adenoviral vector encoding HSV-tk
AV	adenovirus
BBB	blood-brain-barrier
BN	bombesin
CAR	coxsackie adenovirus receptor
CCK	cholecystokinin receptor
CD	cytosine deaminase
CED	convection enhanced delivery
CMV	cytomegalovirus promoter
CNS	central nervous system
cpm (cps)	counts per minute (counts per second)
CRAd	conditionally replicative adenovirus
CS	cisplatinum
CT	computed tomography
DAB	diaminobenzidine
DC	docetaxel
Demotate	[N_4^{0-1},Asp^0,Tyr^3]octreotate
DLU	digital light units
DMEM	Dulbecco's modified Eagle's medium
DNA	Deoxyribonucleic acid
DOTA	1,4,7,10-tertraazacyclododecane-N',N'',N''',N''''-tetraacetic acid (chelator)
DOTAtate	[DOTA^0,Tyr^3]octreotate
DTPA	diethylenetriqaminepentaacetic acid (chelator)

DX	doxorubicin
EDDA	ethylenediamine-*N,N'*-diacetic acid
EGF	epidermal growth factor receptor
EMP	estramustine
FBS	fetal bovine serum´
FHBG	9-(4-fluoro-3-hydroxy-methyl-butyl)guanine
FIAU	2'-deoxy-2'-fluoro-β-D-arabinofuranosyl-5[*I]-iodouracil
FIRU	1-(2-fluoro-2-deoxy-β-D-ribofuranosyl)-5-[*I]iodouracil
FTBSRU	1-(2-fluoro-2-deoxy-β-D-ribofuranosyl)-5-tributyl-stannyl uracil (precursor compound of FIRU)
GBM	glioblastoma multiforme
GCV	ganciclovir
GLP-1	glucagon-like peptide-1
GRP	gastrin releasing peptide
Gy	Gray (measure for radiation dose)
HBSS	Hanks' Balanced Salt Solution
HE	hematoxillin-eosin staining
HPLC	High-performance liquid chromatography
HSV	herpes simplex virus
HSV1716	oncolytic HSV mutant
HSV-tk	Herpes Simplex Virus thymidine kinase
HYNIC	hydrazinonicotinamide
i.v.	intravenous administration
IL-2	interleukin 2
IU	infectious units
LET	linear energy transfer
LHRH	luteinizing hormone-releasing hormone
LV	lentivirus
MBq	megabecquerel
MEM	modified Eagle's medium
MeV	mega-electronvolt
MG	meningioma
MI	multiple injections
MIP	maximum intensity projection
moi	multiplicity of infection
MRI	magnetic resonance imaging
MT	metastasis in the brain
MTC	medullary thyroid cancer
NB	normal brain

NK-1	neurokinin 1 receptor
NT	neurotensin receptor
OI	optical imaging
ONYX-015	oncolytic adenovirus
p.i.	post injection
p.o.	oral administration
PBS	phosphate buffered saline
PET	positron emission tomography
PFU	plaque forming units
PRRT	peptide receptor radionuclide therapy
PRS	peptide receptor scintigraphy
RCA	replication competent adenovirus
RCP	radiochemical purity
RGD	arginine-glycine-aspartic acid
RIT	radioimmunotherapy
RLU	relative light units
RT	radionuclide therapy
RV	retrovirus
SA	specific activity
SF_2	surviving fraction at 2 Gy
SI	single injection
SPECT	single photon emission computed tomography
SRB	Sulforhodamine B
ss	somatostatin (hormone)
sst	somatostatin receptor
sst_2 / sst_5	somatostatin receptor subtype 2 / 5
$t_{½}$	half life of a radioisotope
tk	thymidine kinase (enzyme)
TLD	thermoluminescent dosimetry
US	ultrasonography
VIP	vasoactive intestinal peptide receptor
VP	viral particles
VPC	viral producer cells
WHO	world health organization
XRT	external beam radiotherapy

Dankwoord

"I get by with a little help from my friends"

Zoals de Beatles jaren geleden al zongen, was dit werk en het uiteindelijke proefschrift niet mogelijk geweest zonder de hulp van míjn "friends": begeleiders, collega's, vrienden en familie. Bij deze wil ik een ieder daarvoor danken. Een aantal mensen echter wil ik hierbij graag met een persoonlijk woord bedanken.

Allereerst de initiatoren achter dit proefschrift: Prof. Dr. Ir. M. de Jong, Prof. Dr. P.A.E. Sillevis Smitt en Prof. Dr. E.P. Krenning.

Beste Marion, toen ik op jouw lab begon als analiste had ik nooit gedacht dat dit zou leiden tot het schrijven van een proefschrift. Ik had ook nooit verwacht dat ik dat zou kunnen. Als jij niet in mij had geloofd, was ik dit werk waarschijnlijk nooit gaan doen. Ik ben blij dat ik de stap heb genomen en wil je graag bedanken voor alles wat je de afgelopen jaren voor me hebt gedaan. Mede dankzij dit gedeelde project heb ik mezelf kunnen ontpooien tot een zelfstandig onderzoeker. Ik heb ontzettend veel van je geleerd. Zaken die niet alleen van pas komen in mijn werk, maar soms ook in het dagelijks leven: positief blijven ook al zijn de resultaten niet altijd denderend, zelfverzekerd zijn (of in ieder geval lijken), het schrijven van manuscripten (wat af en toe nog steeds niet mee valt) en nog veel meer!!! Ik dank je daarvoor en ik hoop dat onze samenwerking nog lang vruchten blijft afwerpen…

Beste Peter, toen Marion begon over een mogelijke overstap van analist naar AIO, was je meteen enthousiast! En dat ben je altijd gebleven. Soms vond ik het lastig omdat ik een beetje tussen twee afdelingen, met ieder eigen ideeën en prioriteiten, "zweefde". Toch heb ik daar veel van geleerd en ik voel me daardoor nu zelfstandiger. De afgelopen maanden waren een race tegen de klok. Je mailbox zat vol met manuscripten (volgens mij wel een stuk of 6 tegelijk!!) en toch raakte je niet van je stuk! Mede dankzij jouw snelle nakijkwerk, is het me toch gelukt alles op tijd in te leveren. En natuurlijk bedankt voor de fijne samenwerking!

Beste professor Krenning, graag wil ik u bedanken voor de mogelijkheid die u me geboden hebt om dit proefschrift te schrijven. Als "minder-gelovige" op het gebied van gentherapie heeft u vaak kritische discussies op gang gebracht. Deze hebben mij enorm geholpen zelfstandig te leren denken en kritiek te accepteren!

Tevens wil ik hierbij ook Prof. Dr. R.C. Hoeben bedanken voor zijn hulp. Beste Rob, toen ik begon met dit gentherapie-project, heb ik een maand of twee in je lab mogen vertoeven. Ik heb toen erg veel geleerd over virussen, viruskweek en –zuivering: essentiële basisprincipes die mij hebben geholpen in mijn werk de jaren erna. Bedankt voor je gastvrijheid tijdens die maanden, en natuurlijk voor het snelle corrigeren van manuscripten (tja, wat wil je als "snelheid je handelsmerk is – als het zo uitkomt"?!)..!

Ook wil ik graag de commissieleden, Prof. Dr. G. Wagemaker, Prof. Dr. H.T. Wolterbeek en dr. Hofland bedanken voor het zitting nemen in de promotiecommissie op 12 december. Prof. Dr. P.H. Elsinga wil ik hierbij bedanken voor de snelle beoordeling van het proefschrift.

Daarnaast wil ik graag mijn dank uitspreken tot iedereen van de afdeling Nucleaire Geneeskunde: voor de gezelligheid en de prettige sfeer in de afgelopen jaren. Hoewel ik mij het afgelopen jaar heb "begraven" in dit proefschrift en ik door de drukte niet meer zoveel te zien was op de afdeling, merkte ik dat het toch altijd weer voelt als "thuiskomen" als ik de afdeling oploop. Hartelijk bedankt voor jullie interesse van de afgelopen jaren. Roelf Valkema: bedankt voor je tijd en hulp bij het lysinestuk. Linda de Jong: hoewel het "paarse graafwerk" niet je favoriete bezigheid was, was je toch altijd meer dan bereid me te helpen met de FIRU-labelingen. Hartstikke bedankt daarvoor!

Voor het werk in dit proefschrift was iedereen van de preklinische groep onmisbaar: Bert Bernard, Marleen Melis, Magda Bijster, Ria van den Berg, Ingrid Thuis, Edgar Rolleman, Cristina Müller, Flavio Forrer, Wout Breeman en Erik de Blois. Jullie hulp bij experimenten, de discussies die we konden voeren, de opbouwende kritiek: zoals gezegd onmisbaar voor een jonge onderzoeker! Bedankt allemaal voor jullie inzet…

Beste Bert, in mijn eerste NuGe jaren heb ik veel van je geleerd, vooral wat betreft het werken met proefdieren en radioactiviteit: twee onmisbare dingen in ons werk! De laatste jaren heb je zoveel voor onze groep gedaan, dat het nog moeilijk zal worden als je volgend jaar gaat vertrekken. Ik hoop dat je heel erg gaat genieten van je "vrije" tijd (ja, ja, jij kan toch niet stil zitten!).

Marleen, als de "nieuwe Arthur" heb jij heel snel je draai gevonden in onze groep en ben je nu gewoon Marleen. Ik bewonder je harde werk, je grote resultaatgerichtheid en je onvermoeibare inzet. Bedankt voor alle autoradiografieën die je voor me hebt gedaan!

Beste Magda, Ria, Ingrid en Edgar, bedankt voor alle discussies die we hebben gevoerd tijdens de thee, maar vooral ook voor de gezelligheid die ook niet mag ontbreken op een lab!

Dear Cristina, thank you for all the nice discussions we had in the past! And, of course, for your help with writing my manuscripts. You are a very devoted researcher, which I admire! I hope that your next job will give you as much fulfilment as you need.

Dear Flavio, thanks for all your help with the NanoSPECT acquisitions; they did not always go smoothly, but you were always there with a helping hand! I'm delighted that we have our defence on the same day (although it will be stressful for us all), and that we will be able to celebrate together! We will probably meet at EANM or SNM meetings in the future…

Wout en Erik, hartelijk bedankt voor jullie altijd accurate, vlotte labelingen die het werk in dit proefschrift mogelijk hebben gemaakt. Met een vrolijke lach zijn jullie altijd bereid om weer iets nieuws te labellen! Wout, hierbij wil ik je ook bedanken voor de discussies die we gevoerd hebben. Je hebt me geleerd om kritisch naar mezelf en anderen te kijken. Ik hoop dat ik, met een beetje "Wout-begeleiding", ook het "provoceren" onder de knie krijg… Erik, succes met de laatste loodjes van je opleiding. Ik heb veel bewondering voor je doorzettingsvermogen. En dan daarna toch een proefschrift schrijven…?

Veel van het *in-vitro*-werk heb ik samen met MLO-stagiaire Patrick Sluiter gedaan. Patrick, samen hebben we heel wat cellen en medium voorbij zien komen! Hopelijk komen we elkaar nog eens tegen op het professionele vlak!

Misschien is het raar om de paranimfen van je collega te bedanken, maar ik ben ze zeker veel dank verschuldigd: Arthur van Gameren en Maria van der Sluis.

Lieve Arthur, al vanaf het moment dat ik bij NuGe kwam werken zijn we meer vrienden dan collega's. Nu je ex-preklinieker bent, merk ik dat ik toch nog steeds wel op je kennis terugval. De afgelopen tijd heb je me veel kunnen steunen tijdens het schrijven en dat ik je soms wel eens wegstuurde, vond je dan niet erg! Ik vind het erg prettig dat je nog steeds zo dicht bij mijn werk staat. Jij helpt me altijd dingen te relativeren. En … bedankt voor de haastklus "drukker-zoeken"!

Lieve Maria, niet mijn paranimf, maar toch zoveel werk verzet voor de promotie van mij en Monique. Dat we dadelijk een heerlijke dag gaan hebben, waarbij we aan niets hoeven te denken, is ook aan jou te danken.

Hierbij nog een woord van dank aan de neuro-oncologie groep: Erik Brouwer, Bertie de Leeuw, Esther Hulsenboom, Mark Rodijk en Maarten ter Horst.

Eric, bedankt voor alle hulp en hand- en spandiensten tijdens mijn experimenten. Je staat altijd klaar om te helpen, helemaal super!

Bertie, de afgelopen jaren zijn voor jou ook niet makkelijk geweest. Toch nam je altijd de tijd om mij te helpen, te overleggen, dingen uit te leggen en te helpen zoeken naar een stofje hier of daar, wat ik heel erg heb gewaardeerd! Ik hoop dat de nieuwe weg die je bent ingeslagen je veel goeds gaat brengen. Ik duim voor je!

Esther, hartelijk bedankt voor alle hulp met de SDS-PAGE experimenten. Ik kon op elk moment bouwen op jouw expertise en dat is ontzettend prettig geweest. Het leidde tot onmisbare data voor het artikel!

Mark, bedankt voor alle gezellige praatjes tijdens het eindeloze pipetteren! Ik heb altijd erg veel lol gehad. Sorry dat onze lunch-dates zijn gestaakt: zullen we dat weer oppakken?

Maarten, veel van mijn experimenten waren niet mogelijk geweest zonder jouw hulp. Je was altijd bereid langer te blijven, soms tot het onvermoeibare toe! Ik vond het heel prettig om met jou samen te werken. Nog maar heel even wachten en dan heb je ook je titel! Dat wil ik niet missen!!!

Natuurlijk wil ik hierbij ook Martijn Rabelink hartelijk bedanken voor alle virussen (een ruwe schatting: 10^{50} virusdeeltjes?!) die hij voor mij heeft opgekweekt, zodat deze studies mogelijk waren. Wetende dat dit een heel karwei is, ben ik erg dankbaar dat je het voor me hebt willen doen.

Van Mallinckrodt wil ik graag Mark Konijnenberg en Hector Knight bedanken. Mark, jouw berekeningen, vaak binnen recordtempo gedaan, waren erg belangrijk voor twee van de artikelen in dit proefschrift. Ik heb erg veel waardering voor je expertise op het gebied van dosimetrie. Hector, ook jouw kennis bleek onmisbaar bij de voorbereiding, uitvoering en beoordeling van het werk met gelabeld virus. Voor mij was het een nieuwe weg in het onderzoek, die heel uitdagend bleek! Je uitnodiging voor Helsinki was voor mij een unieke ervaring in mijn, toen nog, korte AIO-bestaan! Beiden bedankt voor alle hulp in de afgelopen jaren.

Natuurlijk ook een woord van dank aan mijn vriendin, collega en mede-promovenda: lieve Monique, toen ik twee maanden na jou bij NuGe kwam werken had ik nooit durven denken dat één van mijn collega's, één van mijn beste vriendinnen zou worden! Op de afdeling worden we altijd in één adem genoemd, als een soort Siamese tweeling, en als je objectief kijkt, is dat ook wel logisch: we zijn bijna tegelijk AIO geworden, getrouwd, moeder geworden en (dadelijk) gepromoveerd. Toch weten we allebei dat we ook in veel opzichten verschillen (gelukkig maar!)… We hebben zoveel meegemaakt de afgelopen jaren waarbij we elkaar echt hebben kunnen steunen (samen experimenten doen, er voor elkaar zijn wanneer die experimenten fout dreigden te gaan, elkaar steunen bij onze presentaties tijdens congressen, schrijf-

leed, (be)vallen en weer doorgaan!). Je weet het: ik ga je ontzettend missen nu we, professioneel gezien, ieder een eigen kant uit gaan. Maar ik weet ook dat we beiden de richting opgaan waar ons hart ligt, dus dan is het goed. Dit einde is een begin: voor ons samen en voor ieder van ons apart. Bedankt voor je vriendschap!

Lieve Suzanne en Rogier, ik ben zo superblij met de omslag van het boekje dat dankzij jullie grote inzet tot stand is gekomen! Ontzettend bedankt. En heel veel geluk met jullie nieuwe avontuur: Cas!

Vanzelfsprekend wil ik ook mijn eigen paranimfen ontzettend bedanken voor de steun gedurende de afgelopen jaren. Lieve Astrid en Cindy, bedankt dat jullie mij willen steunen en helpen in dit traject naar de promotie. Astrid, jij als "professionele" paranimf kent ondertussen wel het klappen van de zweep (figuurlijk dan!). Hoewel je het promoveren nooit zelf zult gaan doen, weet je wat het inhoudt en heb ik dus aan een half woord genoeg om je te vertellen dat het soms ook echt (PIEP) is! Cindy, op deze manier kun je het promoveren eens rustig van dichtbij bekijken, maar ik kan je bij deze alvast vertellen: het gaat nooit zoals je het je voorstelt of zoals je hoopt. Samen met Marije en Jolanda hebben we het vaak gehad over dit traject en konden jullie me echt helpen alles te relativeren. Maar wat me nog het meest heeft geholpen: het kletsen over ándere dingen dan onderzoek! Meiden, bedankt voor jullie vriendschap!

Uiteraard wil ik ook mijn familie en schoonfamilie niet vergeten! Lieve pa en ma, dit is het dan: het proefschrift van jullie dochter! Het heeft heel wat voeten in aarde gehad en zonder jullie begrip en steun was het vast nooit zover gekomen… In de afgelopen jaren hebben jullie geprobeerd om mijn werk te begrijpen, ondanks dat het zo lastig is! Bedankt dat we altijd zo openhartig met elkaar kunnen praten. De laatste jaren is jullie steun uitgegroeid tot de broodnodige hulp. Ik weet niet hoe ik jullie moet bedanken voor de ontelbare keren dat jullie op Bram hebben gepast, zodat ik aan dit boek kon werken. Het is fijn om te weten dat jullie het graag doen en dat Bram zich bij jullie thuis voelt. En…bedankt voor het vele corrigeerwerk: het is toch wel fijn om wat leraren in de familie te hebben (nooit gedacht dat ik dat nog eens zou zeggen!!).

Lieve Marc, Kim, Irma en Willy, hoewel het voor jullie misschien toch een soort "ver-van-mijn-bed-show" was de afgelopen jaren, wil ik jullie bedanken voor alle mentale steun. Ik vind het ontzettend fijn dat jullie zo met mij mee hebben geleefd!

Lieve Margo, Frans en Hanh, Erik, Roland en Tanja: bedankt voor jullie steun en vrolijke noot in de afgelopen jaren. Nu het proefschrift dan eindelijk af is, hebben we weer tijd voor leuke dingen…! Margo, fijn dat Bram, vaak onverwachts, bij je

kon komen spelen of logeren. Het is onmisbaar geweest in de laatste fase van dit proefschrift…

En dan als laatste “mijn mannen”:

Lieve Bram, hoewel je niet letterlijk hebt meegeholpen aan dit proefschrift (pipetteren en tumoren injecteren is nog niet echt een karweitje voor jou…), ben ik zo ontzettend blij dat je bij ons bent. Als ik een drukke dag heb gehad en het werk nog in mijn hoofd zit, kijk jij mij altijd met een heerlijke glimlach aan, waardoor alles weer van me afglijdt. Jij bent mijn kostbaarste “bezit” en ik zou je nooit willen missen!

Lieve Jeroen, toen ik aan deze AIO-baan begon, wisten we allebei dat het druk zou worden, maar ik denk dat we geen van beiden dít hadden verwacht. Zeker het afgelopen (anderhalf)jaar is het erg zwaar geweest. Een proefschrift schrijven, de zolder verbouwen en een zoontje hebben rondlopen, is een combinatie die verre van ideaal is voor een rustig gezinsleven (en dat is echt een “understatement”)!!! Toch bleef jij altijd mijn rots in de branding. Één ding weet ik zeker: zonder jou had ik het nooit willen, maar ook niet kúnnen doen. Nu het voorbij is, komt eindelijk een mooie tijd: samen genieten van ons gezin... Bedankt dat je in mijn leven bent!

Suzanne

Sponsoring

De uitgave van dit proefschrift werd financieel ondersteund door de volgende bedrijven:

Mallinckrodt Medical B.V. / Tyco Health Care
J. E. Jurriaanse Stichting
Bioscan Europe Ltd.
Siemens Nederland N.V.
Uno Roestvaststaal B.V.
Veenstra Instruments
Harlan Netherlands B.V.
Beun-de Ronde

Op deze plaats wil ik deze bedrijven hartelijk danken voor hun bijdrage.

Curriculum Vitae

Suzanne Martine Verwijnen werd geboren op 27 maart 1978 te Dordrecht. Na het behalen van haar HAVO-diploma in 1995 aan de Goudse Scholengemeenschap te Gouda vervolgde ze haar algemene opleiding aan de C.S.G. Oude Hoven te Gorinchem, wat in 1997 resulteerde in een VWO-diploma. In september van datzelfde jaar startte ze aan de Hogeschool van Utrecht met de Hogere Laboratorium Opleiding, afstudeerrichting Dierkunde. Na een stage- en afstudeeropdracht bij de afdelingen Biotechnologie en Farmacologie van Solvay Pharmaceuticals B.V. te Weesp (begeleiders: Dr. J. Venema en Dr. A. Herremans) studeerde ze in 2001 af, waarna ze werkzaam werd als research-analist in de groep van Prof. Dr. Ir. M. de Jong bij de afdeling Nucleaire Geneeskunde aan het Erasmus MC te Rotterdam (hoofd: Prof. Dr. E.P. Krenning).

Vanaf september 2002 werkte ze bij dezelfde groep als assistent in opleiding (AIO) waarbij ze onderzoek deed naar potentiële therapiemethoden voor patiënten met een glioblastoom. Mede dankzij de nauwe samenwerking tussen de afdelingen Neurologie (hoofd: Prof. Dr. P.A.E. Sillevis Smitt) en Nucleaire Geneeskunde is dit proefschrift tot stand gekomen.

Publicatielijst

1. Verwijnen S.M., Capello A., Bernard H.F., van den Aardweg G., Konijnenberg M., Breeman W.A.P., *et al.* Low-dose-rate irradiation by ^{131}I versus high-dose-rate external-beam irradiation in the rat pancreatic tumor cell line CA20948. *Cancer Biother Radiopharm*, 2004 19(3): 285-292.

2. Verwijnen S.M., Sillevis Smitt P.A.E., Hoeben R.C., Rabelink M.J., Wiebe L., Curiel D.T., *et al.* Molecular imaging and treatment of malignant gliomas following adenoviral transfer of the herpes simplex virus-thymidine kinase gene and the somatostatin receptor subtype 2 gene. *Cancer Biother Radiopharm*, 2004 19(1): 111-120.

3. Verwijnen S.M. and Bonthuis F. Orbitapunctie misschien niet meer nodig? *Biotechniek*, 2005 44(1): 20-21.

4. Verwijnen S.M., Krenning E.P., Valkema R., Huijmans J.G. and de Jong M. Oral versus intravenous administration of lysine: equal effectiveness in reduction of renal uptake of [^{111}In-DTPA^{0}]octreotide. *J Nucl Med*, 2005 46(12): 2057-2060.

5. ter Horst M., Verwijnen S.M., Brouwer E., Hoeben R.C., de Jong M., de Leeuw H.C.G.M., *et al.* Locoregional delivery of adenoviral vectors. *J Nucl Med*, 2006 47(9): 1483-1489.

6. de Visser M., Verwijnen S.M. and de Jong M. Improvement Strategies for Peptide Receptor Scintigraphy and Radionuclide Therapy. *Cancer Biother Radiopharm*, 2007 in press.

7. ter Horst M., Brouwer E., Verwijnen S.M., Rodijk M., de Jong M., Hoeben R.C., *et al.* Targeting Malignant Gliomas with a GFAP-Selective Oncolytic Adenovirus. *J Gene Med*, 2007 in press.

8. Verwijnen S.M., Melis M., Kros J.M., Krenning E.P., Sillevis Smitt P.A.E. and de Jong M. Peptide receptor expression on different human intracranial tumors. *Semin Nucl Med*, 2007: submitted.

9. Verwijnen S.M., Sillevis Smitt P.A.E., Knight H., Konijnenberg M., Hoeben R.C., de Leeuw H.C.G.M., *et al.* Directly radiolabeled adenoviruses show viral distribution *in vivo* following intra-tumoral injection. *J Gene Med*, 2007: submitted.

10. Verwijnen S.M., ter Horst M., Sillevis Smitt P.A.E., Hoeben R.C., Forrer F., Mueller C., *et al.* Molecular imaging following adenoviral gene transfer visualizes sst_2 and HSV1-tk expression. *Nucl Med Biol*, 2007: submitted.

Color figures

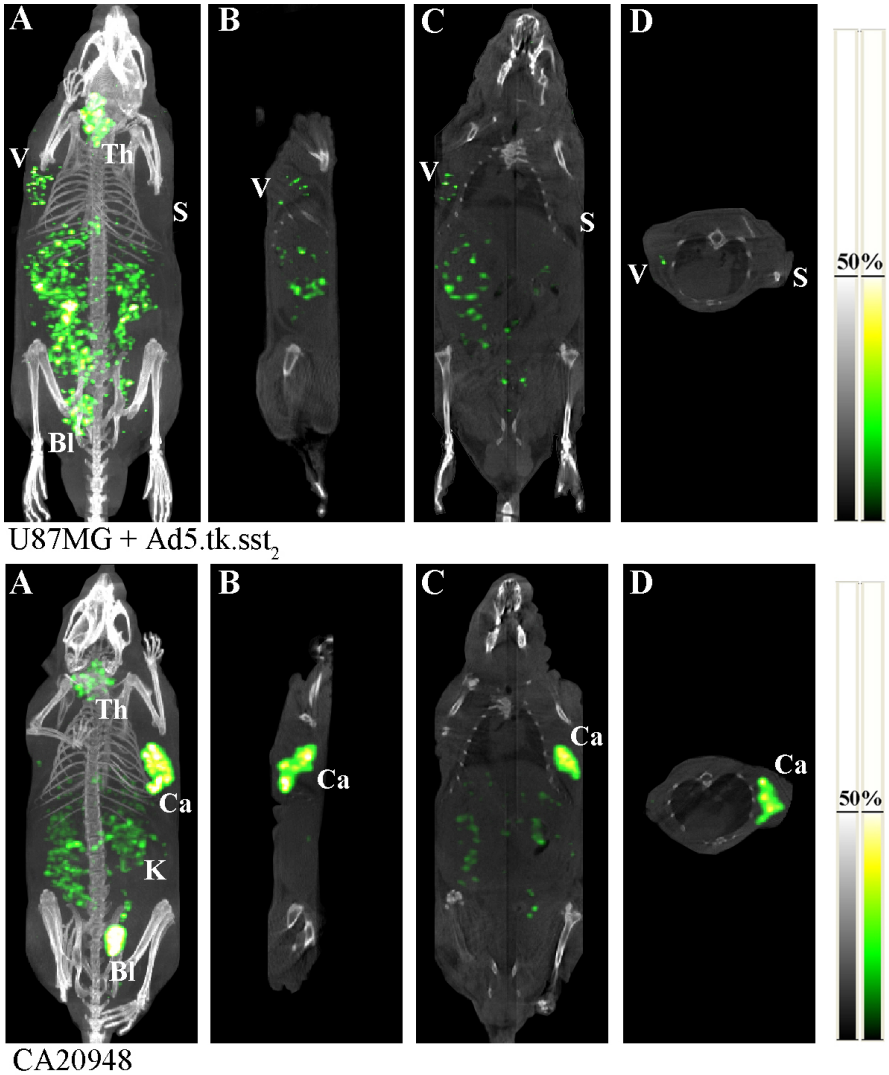

	U87MG + Ad5.tk.sst$_2$	U87MG + saline	CA20948
^{99m}Tc activity (kBq)	0.0275	0.0002	0.1295
measured volume (mm^3)	104	137	158
Uptake (kBq/mm^3)	0.2637	0.00113	0.8189

Figure 1: Animal SPECT/CT scans. The upper panel shows a mouse bearing one Ad5.tk.sst$_2$ infected U87MG tumor and one saline-injected U87MG tumor. The lower panel shows a sst$_2$-positive CA20948 tumour-bearing mouse. Both where scanned 4 hours p.i. of 100 MBq (1 µg) [^{99m}Tc]Demotate 2. Maximum intensity projection images (A), sagittal (B), coronal (C) and transversal (D) slices are shown at the height of the tumor. Images are representative examples of n=3 animals per group. Grey scale = CT image, Color scale = SPECT image, slice thickness=0.30 mm. (Th=thyroid, Bl=bladder, K=kidney, V=viral-infected U87MG tumor, S=saline-injected U87MG tumor, Ca=CA20948 tumor). The table shows quantification results of these images.

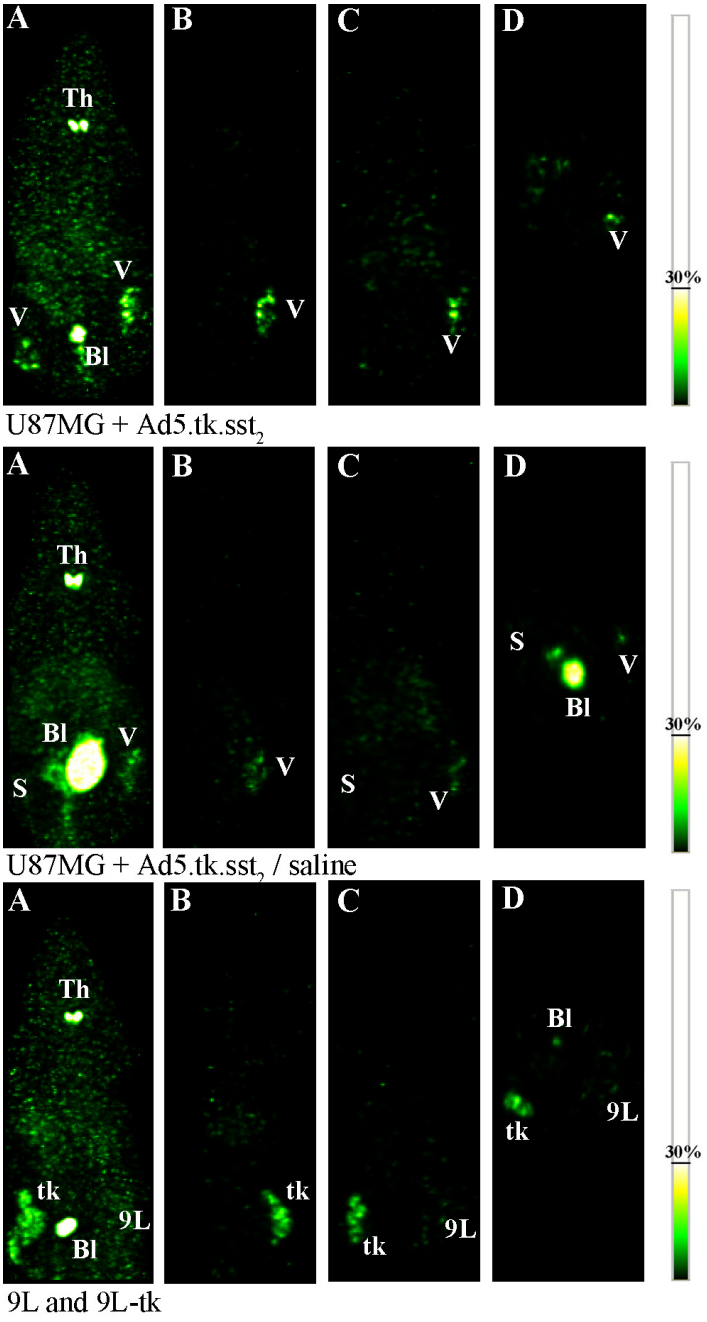

Figure 2: Animal SPECT scans of Ad5.tk.sst$_2$ infected or saline injected U87MG and 9L-tk/9L tumor bearing mice injected with 40 MBq/0.6 µg [^{123}I]FIRU, 4 hours p.i. of the radiolabelled tracer. Whole body images (A), coronal (B), sagittal (C) and transversal (D) slices are shown at the height of the tumor, slice thickness=0.30 mm. Images are examples of n=3 animals per group. (Th=thyroid, Bl=bladder, V=viral-infected U87MG tumor, S=saline injected U87MG tumor, tk=9L-tk tumor, 9L=9L tumor)

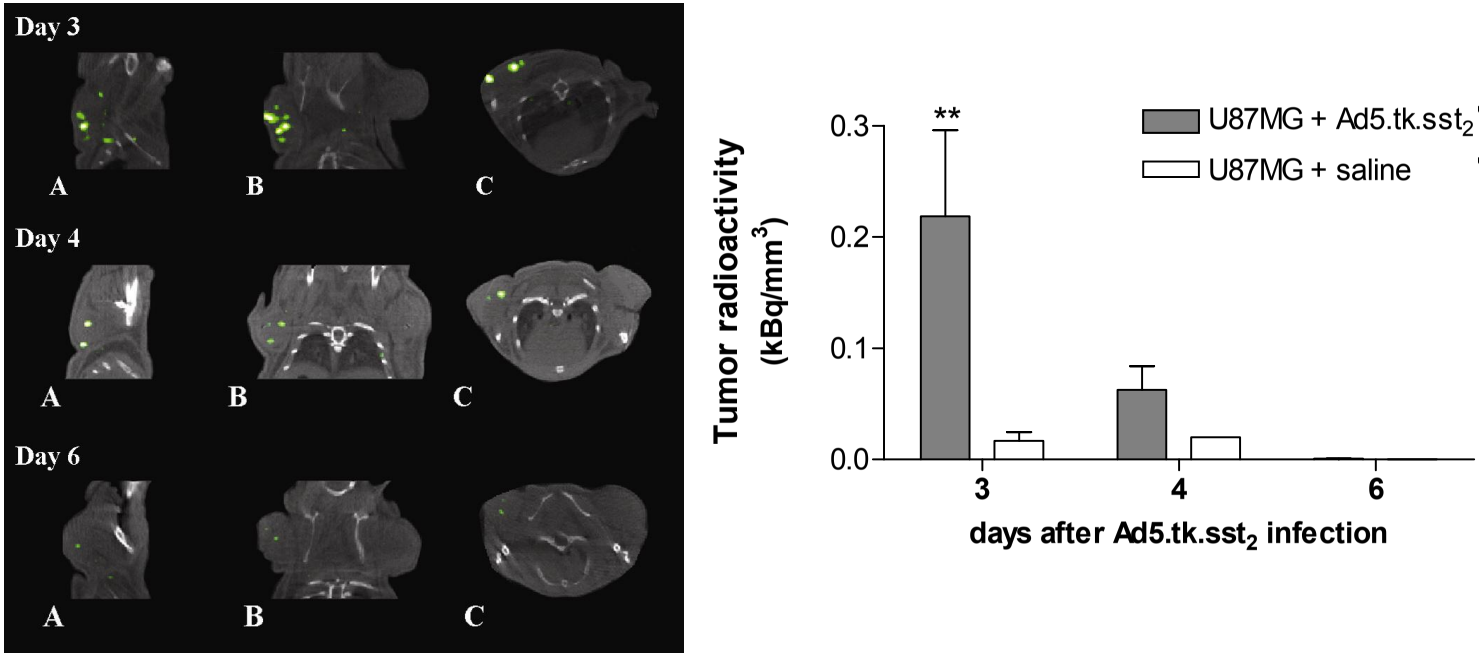

Figure 3: Longitudinal study in a mouse bearing one Ad5.tk.sst$_2$ infected and one saline injected U87MG tumor. On day 3, 4 and 6 after infection the mouse was injected with either 100 MBq/1 µg [^{99m}Tc]Demotate 2 (on day 3) or [^{111}In-DTPA^0]octreotide (on days 4 and 6); SPECT and CT images were made. SPECT images are shown at the height of the tumor, slice thickness=0.30 mm. The graph shows the quantification results of at least n=2 animals. (sagittal (A), coronal (B) and transversal (C) slices are shown). Data is expressed as mean ± SEM kBq/mm^3. ** P<0.01.

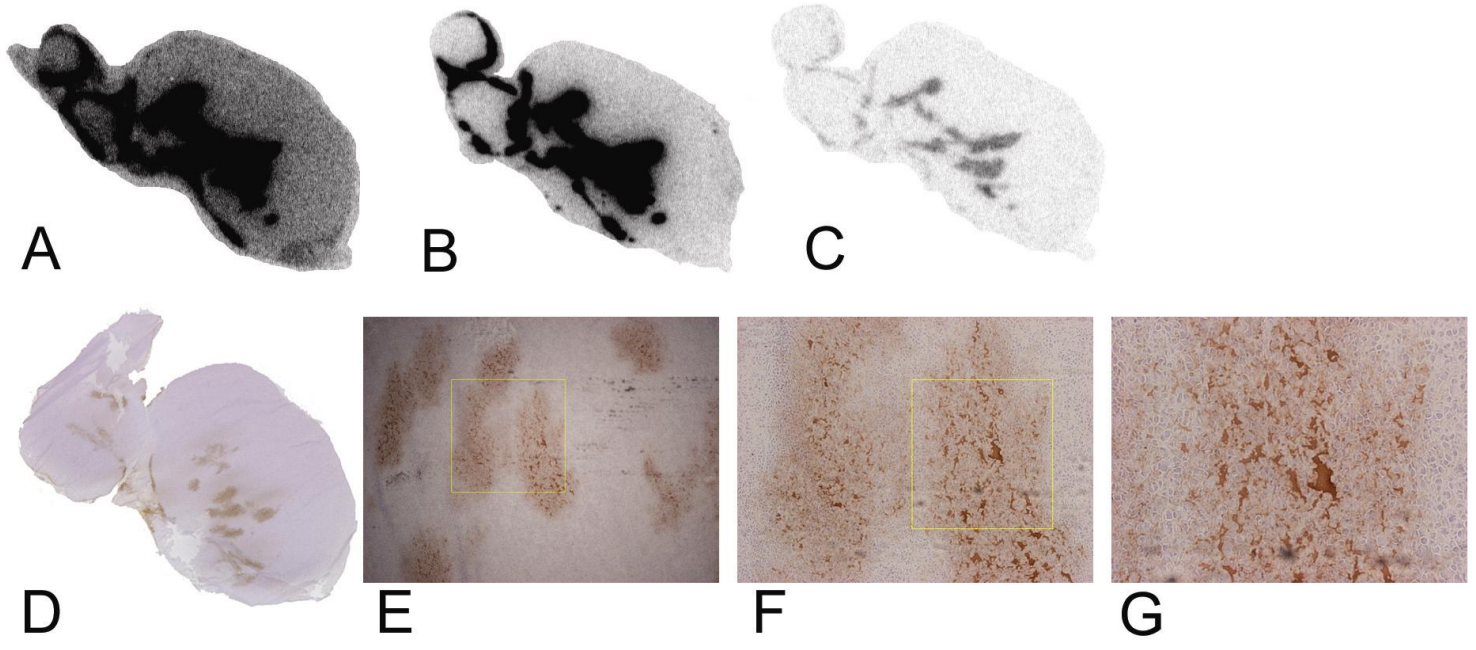

Figure 7: *Ex vivo* autoradiography 4 hours after injection of 3 MBq of [^{123}I]FIRU (A), *in vitro* autoradiography using 10^{-10} M [^{111}In-DOTA^{0},Tyr^{3}]octreotate (B), or [^{111}In-DOTA^{0},Tyr^{3}]octreotate plus an excess of octreotide (C) and immunohistochemistry (D-G) staining using rabbit-anti-HSV-tk primary antibody, at different magnifications; D: section overview (no magnification), E: 40x, F: 100x, G: 200x.

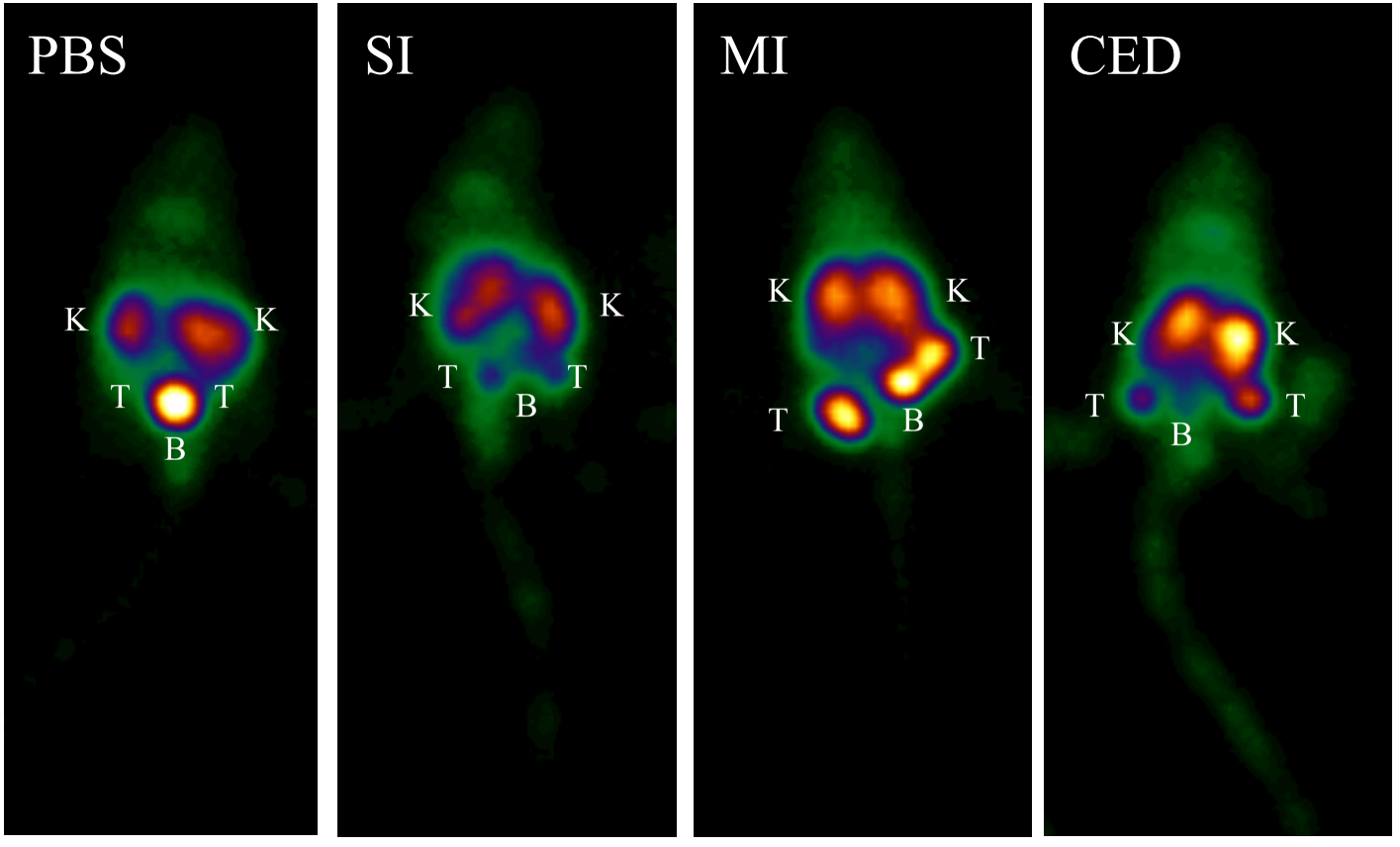

Figure 2: γ-Camera images of NMRI nu/nu mice. Mice bearing U87MG xenografts 3.5 h after intravenous administration of 0.5 µg ^{99m}Tc-Demotate 2 (100 MBq). Three days before imaging, tumors had been injected with PBS (left) or 1.5x10^{9} PFU of Ad5.tk.sst$_{2}$ administered with CED, SI, or MI (4x, MI). Both tumors in each animal received the same treatment. Images are representative and demonstrate that MI results in better tracer uptake than CED and SI. B = bladder; K = kidney; T = tumor.

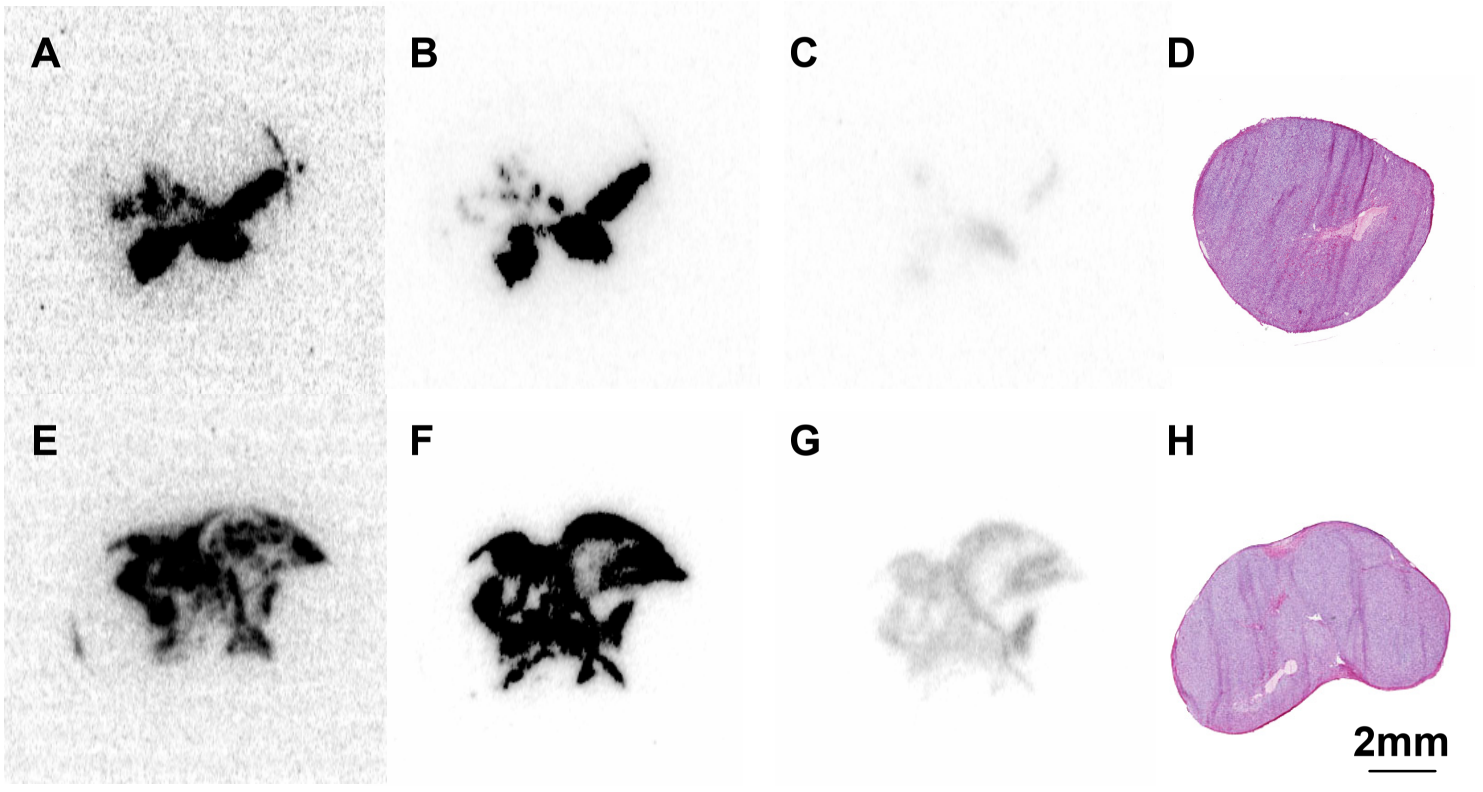

Figure 3: Autoradiographs of Ad5.tk.sst_2–injected U87MG xenografts by single injection (A–D) or by multiple injection (E–H). *Ex vivo* autoradiographs were performed 4 h after injection of ^{99m}Tc-Demotate 2 (A and E). *In vitro* autoradiographs were performed on adjacent slides with [DOTA-^{125}I-Tyr^3]octreotate (B and F). Binding was displaced by excess unlabeled octreotide (C and G). Adjacent tumor sections were visualized with hematoxylin–eosin staining (D and H). Representative sections demonstrate that the area of viral distribution is larger in sections from tumors injected with MI compared with SI.

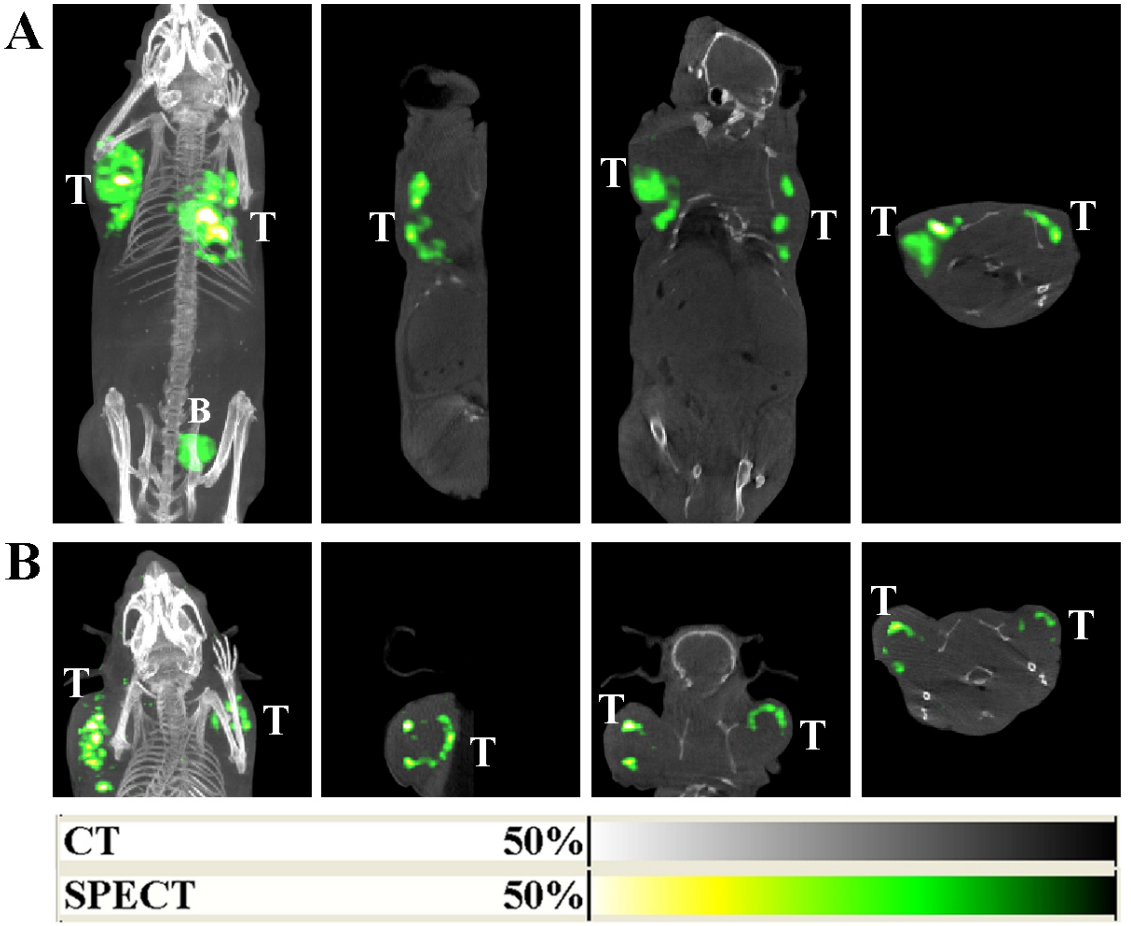

Figure 5. (A) SPECT/CT scans of a mouse bearing two U87MG tumors, injected with 19 MBq ($2x10^9$ PFU) of ^{99m}Tc-Ad5.tk.sst$_2$, taken at 4 hours post injection. Quantification: tumor left=2.37 MBq; tumor right=2.25 MBq; bladder=0.80 MBq, bowel=0.32 MBq. (B) Seventy-two hours thereafter, the same animal was injected with 200 MBq (2 µg) [^{111}In-DTPA^0]octreotide and scanned again at 4 hours post injection of the tracer. Quantification: tumor left=0.58 MBq; tumor right=0.30 MBq. Maximum intensity projection (1), sagittal (2), coronal (3) and transversal (4) slices are shown of the whole mouse at the height of the tumor. Images are examples and are representative for three animals in this group. Slice thickness=0.30 mm. (T=U87MG tumor infected with ^{99m}Tc-Ad5.tk.sst$_2$, B=bladder).

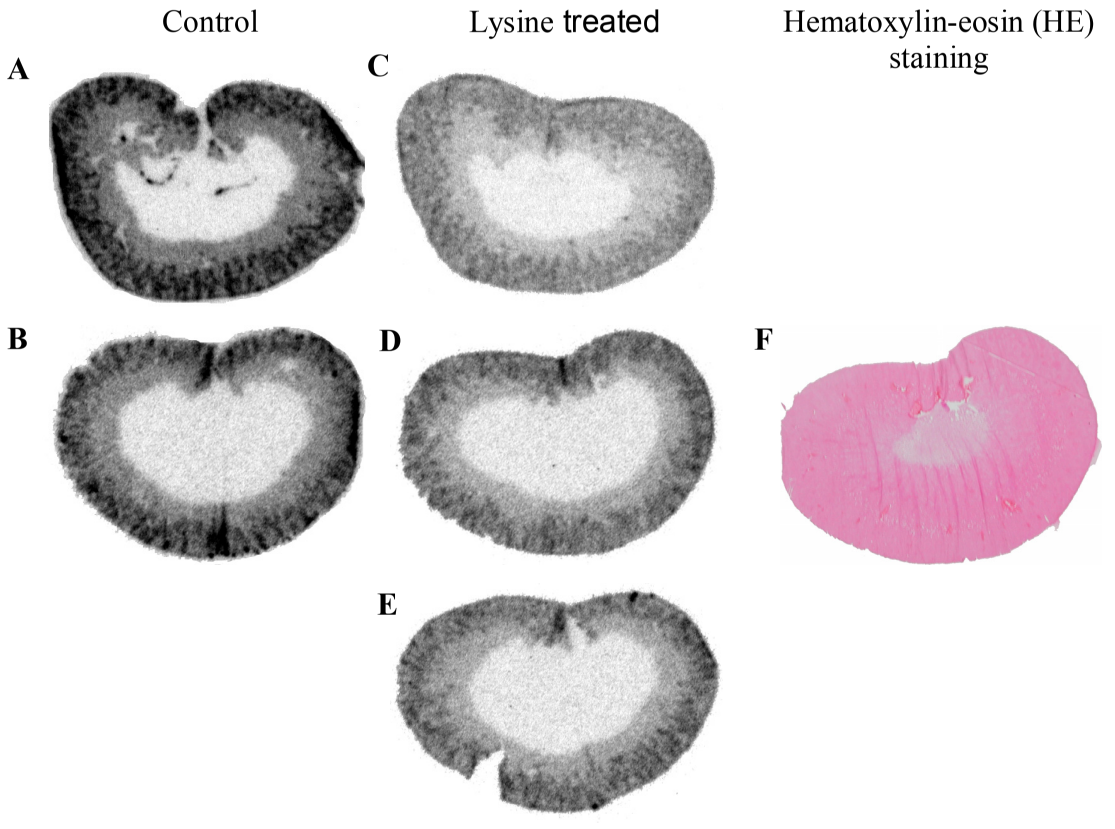

Figure 3: *Ex vivo* autoradiograms of renal tissue slices of control rats (A and B) and lysine-treated rats (C–E) 24 h after injection of [^{111}In-DTPA^{0}]octreotide, 3 MBq/ 0.5 µg. Greatest reduction of renal radioactivity was seen in rats treated with intravenous lysine coinjected with tracer (C) or lysine (400 mg/kg) orally 60 min before tracer (D). Increasing the interval between oral lysine (400 mg/kg) and tracer to 120 min (E) did not lead to greater renal reduction. (F) Hematoxylin- and eosin stained section adjacent to D shows high uptake of radioactivity in cortex and outer medulla but almost no uptake in inner medulla.